



Grant, Jennifer S. (2014) *The role of microRNA in the development of pulmonary arterial hypertension: studies in cell culture and animal models*. PhD thesis.

<http://theses.gla.ac.uk/5261/>

Copyright and moral rights for this work are retained by the author

A copy can be downloaded for personal non-commercial research or study, without prior permission or charge

This work cannot be reproduced or quoted extensively from without first obtaining permission in writing from the author

The content must not be changed in any way or sold commercially in any format or medium without the formal permission of the author

When referring to this work, full bibliographic details including the author, title, awarding institution and date of the thesis must be given

Enlighten:Theses
<http://theses.gla.ac.uk/>
theses@gl.a.ac.uk

The role of microRNA in the development of pulmonary arterial hypertension: studies in cell culture and animal models

**Jennifer S. Grant
B.Sc. (Hons)**

Submitted in the fulfilment of the requirements for the degree of Doctor of Philosophy (Ph.D.) in the Institute of Cardiovascular and Medical Sciences, University of Glasgow.

Institute of Cardiovascular and Medical Sciences
College of Medical, Veterinary and Life Sciences
University of Glasgow.



May 2014

© J.S. Grant 2014

Authors Declaration

I declare that this thesis has been written entirely by myself and is a record of research performed by myself with the exception of elastic van gieson staining for the antimiR-451 rat study (Margaret Nilson), hypoxia/SU5416 mouse model of PH including SAP, RVP and RVH measurements (Dr Loredana Ciucan), hypoxia/SU5416 fourteen week rat model of PH including RVP measurements (Olivier Bonneau), RVP and SAP measurements in the antimiR-145 rat study (Nicholas Duggan) and α -SMA and von Willebrand Factor staining for the antimiR-145 rat study (histology department at Novartis). This work has not been submitted previously for a higher degree. The research was carried out at the Institute of Cardiovascular and Medical Sciences, University of Glasgow under the supervision of Professor Andrew H. Baker and Professor Margaret R. MacLean, with the exception of the hypoxia/SU5416 model of PH and echocardiography which was performed at Novartis Pharmaceuticals UK Limited under the supervision of Dr Matthew Thomas.

Jennifer S. Grant

May 2014

Acknowledgements

First and foremost, I would like to thank my supervisors Professor Andrew Baker, Professor Mandy MacLean and Dr Matthew Thomas for their excellent advice, support, help and guidance throughout my studies. In particular, I would like to thank Professor Baker for the wonderful opportunities which have been afforded to me during the last three years. Additionally, I would like to thank the Medical Research Council for the support and funding of this work.

I greatly appreciate the support received through the collaborative work undertaken with Novartis Pharmaceuticals. Thanks to Dr Matthew Thomas for his scientific advice and insightful discussions and to Dr Loredana Ciucan for taking me under her wing and guiding me through my time at Novartis. I'd like to thank all the members of team 'Remodelling' down at Novartis, in particular Oli, Nick, Sonia, Christine, Martin and David for welcoming me into the lab and providing exceptional technical expertise. A big thank you also to the Barber family who put up with me for three months and made me feel like part of the family.

Thanks to everyone who I have been fortunate enough to work with in the BHF GCRC. Special thanks to Dr Laura Denby, Dr Robert McDonald, Dr Hannah Stevens, Ruifang Lu, Nicola Britton and Gregor Aitchison for their first-class knowledge and support in the lab. I'd also like to thank the members of the MacLean Research Group, in particular Dr Yvonne Dempsie and Dr Ian Morecroft, whose knowledge of *in vivo* techniques has been invaluable.

To Akiko Hata and the members of the Hata Research Lab at the University of California San Francisco, I am grateful for the chance to visit and be part of their lab and learn new techniques.

Massive thanks go out to the girls who helped me through every day. Hollie, Lesley, Clare, Erin, Liz and Hannah, I couldn't have got through the last three years without all the laughter, tears, pub trips and general fun we had in and out of the lab! Also thanks to my friends outside of work for reminding me that there is a life outside of the lab.

I would like to say a heartfelt thank you to my Mum, Dad and Gordon for always believing in me and encouraging me even when the going gets tough. Without your love and support I could never have achieved this and for that I will be eternally grateful.

And last but not least, thanks to Connor who has been by my side and supported me throughout this PhD. Thank you for your unconditional love and always being there.

Table of Contents

Authors Declaration	ii
Acknowledgements.....	iii
List of Figures.....	x
List of Tables.....	xiii
List of Publications, Presentations and Awards	xiv
Definitions/Abbreviations	xv
Abstract.....	xxii
1 Introduction	1
1.1 Pulmonary vasculature.....	2
1.1.1 Structure of the pulmonary vessels	4
1.1.2 Function of the pulmonary circulation.....	4
1.2 Pulmonary arterial hypertension	5
1.2.1 Classification.....	5
1.2.2 Cellular components of PAH.....	10
1.2.2.1 Fibroblasts	11
1.2.2.2 Smooth muscle cells.....	12
1.2.2.3 Endothelial cells	13
1.2.2.4 Inflammatory Cells	13
1.2.2.5 Plexiform lesion formation.....	14
1.2.3 BMPR2 mutations in PAH	17
1.2.4 Current treatment for PAH	20
1.2.4.1 Endothelin receptor antagonists	22
1.2.4.2 Prostacyclin analogues.....	23
1.2.4.3 Phosphodiesterase type 5 inhibitors	24
1.2.4.4 Combination therapy.....	25
1.2.5 Future treatment for PAH	26
1.2.5.1 Guanylate cyclase activators	26
1.2.5.2 Tyrosine kinase inhibitors	26
1.2.6 Traditional animal models of PH.....	27
1.2.6.1 Chronic hypoxia	27
1.2.6.2 Monocrotaline injury	29
1.2.7 Other animal models of PH	30
1.2.7.1 Hypoxia/SU5416 model	30
1.2.7.2 S100A4/Mts1 over-expression in mice	30
1.2.7.3 Interleukin-6 over-expression in mice	31

1.2.7.4	BMPR2 mutant mice	32
1.3	MicroRNAs.....	33
1.3.1	Biogenesis of microRNAs	33
1.3.2	Regulation of miRNA function	35
1.3.3	MiRNAs involved in PAH	38
1.3.3.1	MiR-204.....	40
1.3.3.2	MiR-17/92	41
1.3.3.3	MiR-21	43
1.3.3.4	MiRNAs as biomarkers	45
1.3.4	MiRNAs as therapeutic targets	47
1.4	Aims	51
2	Materials & Methods	52
2.1	Chemicals	53
2.2	Generation of Ad-miR-451.....	53
2.2.1	Generation of Ad5 vector containing miRNA insert	53
2.2.2	Generation of crude adenovirus stock	57
2.2.3	Adenovirus purification	57
2.2.4	Calculation of total viral particle titre	58
2.2.5	Titration of adenovirus by end-point dilution	58
2.3	Cell culture	59
2.3.1	Transduction of Ad-miR-451	60
2.3.1.1	Visualisation of control Ad5-lacZ virus	60
2.3.2	miR mimics.....	61
2.3.2.1	Visualisation of cy3 labelled miR mimic.....	61
2.3.3	Migration of hPASCs.....	61
2.3.4	Proliferation of hPASCs.....	62
2.3.4.1	Thymidine incorporation assay	62
2.3.4.2	MTS assay	63
2.3.5	MicroRNA pull-down assay	63
2.4	Hypoxic model of PH	64
2.4.1	Knockout mice	64
2.4.1.1	MiR-145 knockout mice	65
2.4.1.2	MiR-451 knockout mice	65
2.4.2	AntimiR-451 administration in rat hypoxic model.....	66
2.4.3	Assessment of PH.....	67
2.4.3.1	Hypoxic mouse hemodynamic measurements	67
2.4.3.2	Hypoxic rat hemodynamic measurements	67

2.4.3.3	Right ventricular hypertrophy	68
2.4.3.4	Pulmonary remodelling	68
2.5	Hypoxia/SU5416 model of PH.....	69
2.5.1	Mouse 3 week model.....	69
2.5.2	Rat 14 week model	70
2.5.3	AntimiR-145 administration	71
2.5.3.1	Prophylactic study	71
2.5.3.2	Therapeutic study	72
2.5.4	Assessment of PH.....	73
2.5.4.1	RVH	73
2.5.4.2	Pulmonary remodelling	73
2.5.4.3	Occluded vessel quantitative analysis	73
2.5.4.4	Echocardiography.....	74
2.6	RNA extraction, purification and quantification	74
2.6.1	Cells.....	74
2.6.2	Tissue	75
2.6.3	Streptavidin bead samples.....	76
2.6.4	Paraffin embedded tissues.....	76
2.6.5	Agilent testing RNA quality	77
2.7	RNA expression by qRT-PCR.....	77
2.7.1	cDNA synthesis.....	77
2.7.1.1	miRNA expression.....	77
2.7.1.2	mRNA expression	78
2.7.2	Quantitative real-time polymerase chain reaction	78
2.8	Target prediction	79
2.9	Northern blotting	79
2.10	Protein extraction and quantification	80
2.11	Western blotting.....	81
2.12	Alpha-smooth muscle actin staining	82
2.13	Statistical analysis.....	82
3	The role of miRNA-451 in PAH.....	84
3.1	Introduction	85
3.1.1	Aim	87
3.2	Results.....	88
3.2.1	<i>In vitro</i> modulation of miR-451 using Ad-miR-451.....	88
3.2.2	Modulation of miR-451 in hPASMCs by miR-451 mimic	93
3.2.3	Over-expression of miR-451 has no effect on hPASMC proliferation	96

3.2.4	Over-expression of miR-451 promotes hPASMC migration in the absence of serum	96
3.2.5	Target gene analysis on hPASMCs over-expressing miR-451	99
3.2.6	Transient knockdown of miR-451 <i>in vivo</i> attenuates the development of PH in the rat hypoxic model.....	101
3.2.7	Target gene analysis in antimiR-451 treated rats	109
3.2.8	Genetic ablation of miR-451 in mice has no protective effect in hypoxia	111
3.2.9	Target gene analysis in miR-451 knockout mice.....	114
3.3	Discussion	116
4	MicroRNA analysis in hypoxia/SU5416 model of PH	123
4.1	Introduction	124
4.1.1	Aim	126
4.2	Results.....	127
4.2.1	Development of PH in hypoxia/SU5416 mouse model of PH.....	127
4.2.2	Lung miRNA expression profile in hypoxia/SU5416 mouse model of PH	129
4.2.3	Lung miRNA expression profile in hypoxia/SU5416 rat model of PH	134
4.2.4	Cardiac signature in hypoxia/SU5416 model of PH	139
4.3	Discussion	144
5	The role of miR-145 in PAH	150
5.1	Introduction	151
5.1.1	Aim	154
5.2	Results.....	155
5.2.1	Prophylactic modulation of miR-145 in hypoxia/SU5416 model of PH	155
5.2.2	Effect of prophylactic silencing of miR-145 on the development of PH in the hypoxia/SU5416 model.....	159
5.2.3	Target gene analysis in prophylactic antimiR-145 study	164
5.2.4	Therapeutic modulation of miR-145 in hypoxia/SU5416 model of PH	168
5.2.5	Effect of therapeutic silencing of miR-145 in established PH	172
5.2.6	Target gene analysis in therapeutic antimiR-145 study	172
5.2.7	Genetic ablation of miR-145 has no beneficial effect on the development of PH in male hypoxic mice	180
5.2.8	<i>In vitro</i> analysis of miR-145 targets in hPASMCs.....	185
5.3	Discussion	189
6	General Discussion	196
6.1	Future Perspective	203
	List of References	204

Appendices238

List of Figures

Figure 1.1 - Schematic of the pulmonary circulation.	3
Figure 1.2 - Pathogenesis of PAH.....	10
Figure 1.3 - Vascular pruning and remodelling observed in PAH.	16
Figure 1.4 - Smad-dependent BMP signalling under normal physiological conditions.....	19
Figure 1.5 - Current therapies for PAH patients.	21
Figure 1.6 - MicroRNA biogenesis pathway.	36
Figure 1.7 - MiRNA targeted treatment.	49
Figure 2.1 - Schematic diagram illustrating the production of recombinant adenovirus containing precursor miR-451.....	56
Figure 2.2 - AntimiR-451 <i>in vivo</i> study design.	66
Figure 2.3 - Mouse 3 week hypoxia/SU5416 <i>in vivo</i> study design.	69
Figure 2.4 - Rat 14 week hypoxia/SU5416 <i>in vivo</i> study design.	70
Figure 2.5 - Prophylactic antimiR-145 <i>in vivo</i> study design.	71
Figure 2.6 - Therapeutic antimiR-145 <i>in vivo</i> study design.....	72
Figure 3.1 - miR-451 expression in HeLa cells transduced with adenovirus to over-express human or rat pre-miR-451.	90
Figure 3.2 - β -galactosidase expression in hPASCs transduced with Ad5 lacZ control virus.	91
Figure 3.3 - MiR-451 expression in hPASCs transduced with adenovirus to over-express human or rat pre-miR-451.....	92
Figure 3.4 - Visualisation of cy3 labelled miR mimics in hPASCs.	94
Figure 3.5 - miR-451 expression in hPASCs over-expressing miR-451.	95
Figure 3.6 - Effect of over-expressing miR-451 on hPASC proliferation.	97
Figure 3.7 - Effect of over-expressing miR-451 on hPASC migration.....	98
Figure 3.8 - Target gene mRNA expression in hPASCs over-expressing miR-451.	100
Figure 3.9 - MiR-451 expression in antimiR-451 treated rats as detected by qRT-PCR.	102
Figure 3.10 - MiR-451 expression in antimiR-451 treated animals, as detected by northern blot.....	103
Figure 3.11 - MiR-144 expression in antimiR-451 treated animals.	104

Figure 3.12 - Effect of antimiR-451 treatment on systemic arterial pressure and heart rate.....	106
Figure 3.13 - Effect of antimiR-451 treatment on systolic right ventricular pressure.	107
Figure 3.14 - Effect of antimiR-451 treatment on right ventricular hypertrophy and pulmonary vascular remodelling.	108
Figure 3.15 - Target gene mRNA expression in lung from antimiR-451 treated animals.	110
Figure 3.16 - MiR-451 and miR-144 expression in female miR-451 knockout mice.	112
Figure 3.17 - Quantification of PH indices in female miR-451 knockout mice. .	113
Figure 3.18 - Target gene mRNA expression in lung from female miR-451 knockout mice.	115
Figure 4.1 - Quantification of PH indices in hypoxia/SU5416 mouse model of PH.	128
Figure 4.2 - MiR-21 expression in lung from hypoxia/SU5416 mouse model of PH.	130
Figure 4.3 - MiR-143 expression in lung from hypoxia/SU5416 mouse model of PH.	131
Figure 4.4 - MiR-145 expression in lung from hypoxia/SU5416 mouse model of PH.	132
Figure 4.5 - MiR-451 expression in lung from hypoxia/SU5416 mouse mode of PH.	133
Figure 4.6 - Systolic RVP in hypoxia/SU5416 rat model of PH.	136
Figure 4.7 - Localisation of α -SMA in rat lung from hypoxia/SU5416 model of PH.	137
Figure 4.8 - Time course analysis of miRNA expression in lung from hypoxia/SU5416 model of PH.	138
Figure 4.9 - Cardiac miRNA signature from hypoxia/SU5416 mouse model of PH.	141
Figure 4.10 - MiR-27a and miR-27b expression in cardiac tissue from hypoxia/SU5416 rat model of PH.....	142
Figure 4.11 - MiR-27a and miR-27b expression in lung tissue from hypoxia/SU5416 model of PH.	143
Figure 5.1 - Prophylactic antimiR-145 <i>in vivo</i> study design.	156

Figure 5.2 - MiR-145 expression in lung from prophylactic antimiR-145 study. .	157
Figure 5.3 - MiR-143 expression in lung from prophylactic antimiR-145 study. .	158
Figure 5.4 - Quantification of PH indices in prophylactic antimiR-145 study....	160
Figure 5.5 - Pulmonary remodelling in prophylactic antimiR-145 study.....	161
Figure 5.6 - Pulmonary occluded vessel analysis in prophylactic antimiR-145 study.....	162
Figure 5.7 - Cardiac function parameters from prophylactic antimiR-145 study.	163
Figure 5.8 - Target gene mRNA expression from prophylactic antimiR-145 study.	165
Figure 5.9 - Klf4 protein expression in lung from prophylactic antimiR-145 study.	167
Figure 5.10 - Therapeutic antimiR-145 <i>in vivo</i> study design.	169
Figure 5.11 - MiR-145 expression in lung from therapeutic antimiR-145 study..	170
Figure 5.12 - MiR-143 expression in lung from therapeutic antimiR-145 study..	171
Figure 5.13 - Quantification of PH indices in therapeutic antimiR-145 study. ..	173
Figure 5.14 - Pulmonary remodelling in therapeutic antimiR-145 study.	174
Figure 5.15 - Pulmonary occluded vessel analysis in therapeutic antimiR-145 study.....	175
Figure 5.16 - Cardiac function parameters from therapeutic antimiR-145 study.	176
Figure 5.17 - Target gene mRNA expression from therapeutic antimiR-145 study.	177
Figure 5.18 - Klf4 protein expression in lung from therapeutic antimiR-145 study.	179
Figure 5.19 - MiR-145 and miR-143 expression in male miR-145 knockout mice.	182
Figure 5.20 - Quantification of PH indices in male miR-145 knockout mice.	183
Figure 5.21 - Target gene mRNA expression in lung from male miR-145 knockout mice.	184
Figure 5.22 - Schematic diagram of miRNA pull down experimental set up.	187
Figure 5.23 - MiR-145 and target gene mRNA expression in hPASCs transfected with miR-145 mimic in miRNA pull-down assay.	188

List of Tables

Table 1-1 - WHO classification of pulmonary hypertension.	8
Table 1-2 - New York Heart Association/ World Health Organisation (NYHA/WHO) functional classification of pulmonary hypertension.	9
Table 2-1 - In-Fusion primers used to add the start/kozak, stop and restriction site sequences to the precursor miRNA and for amplification of miR- 451 stem loop in human and rat.	55

List of Publications, Presentations and Awards

J.S. Grant, K. White, M.R. MacLean & A.H. Baker (2013). MicroRNAs in pulmonary arterial remodelling. *Cell Mol Life Sci*, **70**, 4479-94. [Appendix 1]

J.S. Grant, I. Morecroft, Y. Dempsie, E. van Rooij, M.R. MacLean & A.H. Baker. Transient but not genetic loss of miR-451 is protective in the development of pulmonary arterial hypertension. *Pulm Circ*, accepted for publication November 2013. [Appendix 2]

L. Denby, V. Ramdas, R. Lu, B.R. Conway, J.S. Grant, B. Dickinson, A.B. Aurora, J.D. McClure, D. Kipgen, C. Delles, E. van Rooij & A.H. Baker (2014). MicroRNA-214 antagonism protects against renal fibrosis. *J Am Soc Nephrol*, **25**, 65-80.

Presentations:

J.S. Grieve, L. Ciucan, O. Bonneau, N. Duggan, D. Rowlands, M. Thomas, M.R. MacLean & A.H. Baker. MicroRNA expression in a novel model of pulmonary arterial hypertension (PAH). MRC Postgraduate Day, University of Glasgow, 1st June 2012. [Poster communication]

J.S. Grieve, I. Morecroft, Y. Dempsie, E. van Rooij, M.R. MacLean & A.H. Baker. The role of miR-451 in the development of pulmonary arterial hypertension (PAH). Pulmonary vascular disease and right ventricular dysfunction: Current concepts and future therapies (Keystone Symposia), Monterey, California, September 2012. [Oral and poster communication]

Awards:

MRC Centenary Award, awarded September 2012.

Definitions/Abbreviations

14-3-3 ζ	Ywhaz
3'-UTR	3'-untranslated region
5'-UTR	5'-untranslated region
α -SMA	Alpha smooth muscle actin
AAV	Adeno-associated virus
AccT	Acceleration time
Ad5 lacZ	Control adenovirus containing lacZ gene
Ad-miR-451	Adenovirus containing the pre-miR-451 sequence
Ago	Argonaute
ANOVA	Analysis of variance
APAH	Associated pulmonary arterial hypertension
AT ₁ R	Angiotensin II receptor type 1
B2M	Beta-2-microglobulin
BCA	Bicinchonic Acid
BMP	Bone morphogenetic protein
BMPR2	Bone morphogenetic protein type 2 receptor
BMPR2 ^{+/-}	BMPR2 heterozygous
bp	Base pair
BSA	Bovine serum albumin
Ca ²⁺	Calcium ion
cAMP	Cyclic adenosine monophosphate
CAR	Coxsackie and adenovirus receptor

cGMP	Cyclic guanosine monophosphate
CML	Chronic myelogenous leukaemia
CNV	Choroidal neovascularisation
CO	Cardiac output
CO ₂	Carbon dioxide
COX	Cyclooxygenase
cpm	Counts per minute
CsCl	Caesium chloride
CTEPH	Chronic thromboembolic pulmonary hypertension
DGCR8	DiGeorge syndrome critical region gene 8
DIG	Digoxigenin
DMEM	Dulbecco's Modified Eagle Medium
DOCK	Dedicator of cytokinesis
EC	Endothelial cell
ECL	Enhanced Chemiluminescence
EDTA	Ethylene diamine tetraacetic acid
EGTA	Ethylene glycol tetraacetic acid
ER α	Oestrogen receptor alpha
ET-1	Endothelin-1
ET _A	Endothelin receptor type A
ET _B	Endothelin receptor type B
FCS	Fetal calf serum
FGF	Fibroblast growth factor

FOSL1	Fos-like antigen 1
Gleevec	Imatinib mesylate
HDL	High density lipoprotein
HEK293	Human embryonic kidney 293 cells
HIF-1 α	Hypoxia-inducible factor 1 α
hnRNP	Heterogeneous nuclear ribonucleoproteins
hPAEC	Human pulmonary artery endothelial cell
HPAH	Heritable pulmonary arterial hypertension
hPASMC	Human pulmonary artery smooth muscle cell
HPV	Hypoxic pulmonary vasoconstriction
HRP	Horse radish peroxidase
HUVEC	Human umbilical vein endothelial cell
ICAM-1	Intracellular cell adhesion molecule
IL-6	Interleukin-6
IPAH	Idiopathic pulmonary arterial hypertension
IRAK1	Interleukin-1 associated kinase 1
IV	Intravenous
K ⁺	Potassium ion
KHSRP	KH-type splicing regulatory protein
KO	Knockout
Kv	Voltage gated potassium channel
LNA	Locked nucleic acid
LV+S	Left ventricle plus septum

MAPK	Mitogen activated protein kinase
MCT	Monocrotaline
MCTP	Monocrotaline pyrrole
MHC	Myosin heavy chain
MIF	Macrophage migration inhibitory factor
miR	MicroRNA
miRNA	MicroRNA
MMP	Matrix metalloproteinase
mRNA	Messenger RNA
MRTF	Myocardin related transcription factor
Myocd	Myocardin
NF	Nuclear factor
NFAT	Nuclear factor of activated T-cells
NIH	National Institutes of Health
NO	Nitric oxide
NOS	Nitric oxide synthase
NSCLC	Non-small cell lung carcinoma
nt	Nucleotide
NYHA	New York Heart Association
O ₂	Oxygen
PA	Pulmonary artery
PAEC	Pulmonary artery endothelial cell
PAH	Pulmonary arterial hypertension

PAP	Pulmonary artery pressure
PASMC	Pulmonary artery smooth muscle cell
PBS	Phosphate buffered saline
PCR	Polymerase chain reaction
PDE5	Phosphodiesterase type 5
PDGF	Platelet derived growth factor
PDK	Pyruvate dehydrogenase kinase
PFA	Paraformaldehyde
pfu	Plaque forming unit
PGI ₂	Prostacyclin
PH	Pulmonary hypertension
PI3K	Phosphoinositide-3-kinase
PMS	Phenazine methosulfate
PMSF	Phenylmethanesulfonyl fluoride
PPH	Primary pulmonary hypertension
pre-miRNA	Precursor microRNA
pri-miRNA	Primary microRNA
PVR	Pulmonary vascular resistance
qRT-PCR	Quantitative real-time polymerase chain reaction
RAS	Renin angiotensin system
RBC	Red blood cell
RISC	RNA-induced silencing complex
ROS	Reactive oxygen species

RV	Right ventricle
RVH	Right ventricular hypertrophy
RVP	Right ventricular pressure
SAP	Systemic arterial pressure
SDS-PAGE	Sodium dodecyl sulphate polyacrylamide gel electrophoresis
SEM	Standard error of the mean
SILAC	Stable-isotope labelling by amino acids in cell culture
SMC	Smooth muscle cell
SRF	Serum response factor
STAT3	Signal transducer and activator of transcription 3
SU5416	Sugen-5416; a VEGF receptor inhibitor
TAK-1	TGF- β -activated kinase 1
T-ALL	T-cell lymphoblastic leukaemia
TCA	Trichloroacetic acid
TGF- β	Transforming growth factor beta
TMEM49	Transmembrane protein 49
TNF- α	Tumour necrosis factor alpha
TRAF6	TNF receptor-associated factor 6
TRBP	Trans-activating response RNA binding protein
TRPM3	Transient receptor potential melastatin 3
UTR	Untranslated region
VEGF	Vascular endothelial growth factor
VEGFR	Vascular endothelial growth factor receptor

V_{\max}	Maximal flow velocity
vp	Viral particle
VTI	Velocity time integral
vWF	von Willebrand Factor
WHO	World Health Organisation
WT	Wild type

Abstract

Pulmonary arterial hypertension (PAH) is a complex disease characterised by narrowing and remodelling of the small pulmonary arteries. This process involves all cell types within the vessel wall and results in an increase in pulmonary artery pressure, right heart failure and can eventually lead to premature death. Diagnosis of PAH occurs late in disease progression with patients already displaying severe hemodynamic compromise and mortality rates remain unacceptably high despite current treatment. Therefore the development of new therapies is required to manage the symptoms and treat the underlying causes of this multifaceted disease. Recent studies have highlighted a role for microRNAs (miRNAs) in the initiation, development and progression of PAH. MiRNAs are small non-coding RNA molecules ~22 nucleotides long that negatively regulate gene expression. Previous work from our laboratory has shown that miRNAs are dysregulated within the lung during the development of experimental pulmonary hypertension (PH). Consequently, the aim of this study was to assess the involvement of specific miRNAs in the development of PAH using cell culture and experimental models of PH.

The first miRNA focused on was miR-451 which is up-regulated in the lungs from animal models of PH. In human pulmonary artery smooth muscle cells (hPASMCs), miR-451 over-expression promoted migration in the absence of serum but had no effect on cellular proliferation. Silencing of miR-451 was performed *in vivo* using antimiR-451 and miR-451 knockout mice. Indices of PAH were assessed after exposure to hypoxia via measurement of right ventricular pressure (RVP), right ventricular hypertrophy (RVH) and pulmonary vascular remodelling. There was a reduction in systolic RVP in hypoxic rats pre-treated with antimiR-451 compared to control antimiR (47.7 ± 1.36 mmHg and 56.0 ± 2.03 mmHg respectively, $p < 0.01$). MiR-451 knockout mice exposed to chronic hypoxia displayed no significant differences for PAH indices compared to wild type hypoxic mice. Thus illustrating that transient inhibition of miR-451 attenuates the development of PH in hypoxic rats however, genetic deletion of miR-451 has no beneficial effect on the development of PH. This may be due to compensatory mechanisms present in the miR-451 knockout mice.

Previous work has also shown that miR-145 is up-regulated in the lungs and pulmonary arteries from animal models of PH as well as PAH patients. Therefore miR-145 expression was modulated in rats using anti-miR-145 both prior to and post exposure to hypoxia and SU5416 administration. Prophylactic silencing of miR-145 in the hypoxia/SU5416 model of PH showed no beneficial effect on the development of PH compared to control anti-miR treated rats exposed to hypoxia. Therapeutic modulation of miR-145 also demonstrated no protective effect on RVP, RVH or muscularisation of pulmonary arteries in the rat hypoxia/SU5416 model. There was however a significant reduction in the number of occluded vessels in rats with established PH treated with anti-miR-145. This reduction in occluded vessel count is interesting as it was not observed in the prevention study. Further work is required to pinpoint the exact mechanisms through which anti-miR-145 is producing this positive effect on pulmonary vessels with therapeutic silencing of miR-145.

The role of miR-145 on PAH development was further investigated with the use of miR-145 knockout mice. Recent studies show that genetic ablation of miR-145 protects female mice from developing hypoxia-induced PH. We therefore sought to establish whether this beneficial response was also observed in male miR-145 knockout mice. Hypoxic male miR-145 knockout mice showed similar indices of PAH as hypoxic miR-145 wild type mice, with increased RVP and RVH compared with normoxic mice. Pulmonary vascular remodelling analysis indicates that miR-145 knockout mice exposed to hypoxia may have a reduction in remodelling compared to wild type hypoxic mice however this does not reach significance. Thus it appears from this study that male miR-145 knockout mice are not protected against developing PAH as the female knockout mice are. The results from this study on male miR-145 knockout mice demonstrate that the effects of silencing miR-145 *in vivo* are indeed gender specific.

As well as affecting the pulmonary arteries, PAH also induces changes within the right ventricle culminating in right ventricular dysfunction and failure. Therefore a miRNA profile was established for the PAH diseased right ventricle. MiR-27a and miR-27b were up-regulated within the right ventricle of hypoxia/SU5416 mice and rats, respectively. This response appears to be cardiac specific and may help to establish therapies to maintain and stabilise RV function.

In summary of these findings, we have confirmed that miRNAs are dysregulated within the lung and right ventricle during PH development. Results suggest that there are complex mechanisms regulating miRNA processing within the lung during the development of PAH and that these pathways may be gender specific. Further work is required to understand the genes targeted, and therefore the pathways modulated, by miRNAs during PAH development to enhance our understanding of the intricate systems involved in disease progression. MiRNAs represent a potential therapeutic target for the treatment of PAH with further work required to pinpoint the exact mechanistic pathways through which they exert their effects.

1 Introduction

1.1 Pulmonary vasculature

Under normal physiological conditions, the pulmonary circulation is a low pressure, high flow system where gaseous exchange takes place between the pulmonary capillaries and the air filled alveolar sacs. Deoxygenated blood enters the right atrium of the heart via the superior and inferior vena cava. From here, blood enters the right ventricle through the tricuspid valve. Upon contraction, blood is forced out of the right ventricle, through the pulmonary semilunar valve and into the pulmonary artery (PA). The PA splits to form the right and left pulmonary arteries, each one entering the corresponding lung hilum. The right PA enters the right lung which is divided into three lung lobes (superior, middle and inferior), separated by the oblique and horizontal fissures. In a similar manner, the left PA enters the left lung which is divided into only two lobes (superior and inferior) (Ding et al., 2009). All five lobes of the lung are further divided into lobules, which contain bronchi and further division and branching results in a large network of small air filled alveoli. The pulmonary artery follows and indeed lies adjacent to the airways, with subsequent branching of the pulmonary artery until pulmonary capillaries surround the alveoli allowing gaseous exchange to occur. From here, the oxygenated blood is carried back to the heart via the venules and pulmonary vein into the left atria. Blood then passes through the bicuspid valve into the left ventricle. Contraction of the heart forces the blood through the aortic semilunar valve into the aorta where oxygenated blood is delivered throughout the body via the systemic circulation (Figure 1.1).

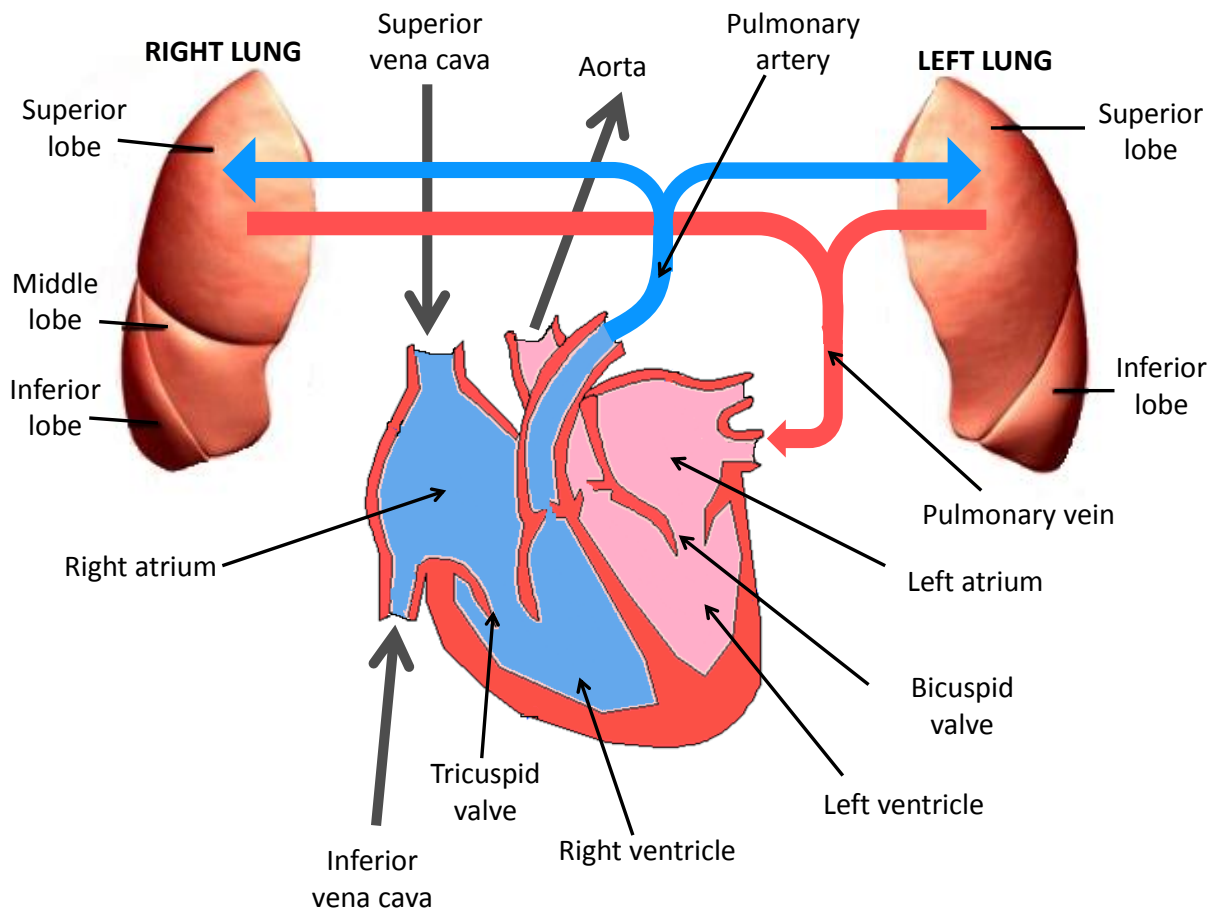


Figure 1.1 – Schematic of the pulmonary circulation.

Deoxygenated blood enters the right atrium, flows through the tricuspid valve and into the right ventricle. During contraction, blood is forced into the pulmonary artery which bifurcates into the right and left lung where gaseous exchange takes place. Oxygenated blood is then returned to the heart via the pulmonary vein and enters the left atrium. Blood enters the left ventricle through the bicuspid valve and upon contraction, oxygenated blood is pushed into the aorta and distributed throughout the body.

1.1.1 Structure of the pulmonary vessels

The pulmonary artery and vein branch into the lung in a tree-like structure and the pulmonary vessels can be categorized according to their size and composition. There are 15 orders of pulmonary arteries between the main pulmonary artery and the capillaries and a total of 15 orders of veins between the capillaries and the main pulmonary vein (Huang et al., 1996). The large proximal pulmonary vessel is defined as of order 15, with the smallest distal non-capillary blood vessel of order 1. The large pulmonary arteries of order 15-13 are generally $>1000\ \mu\text{m}$ in diameter and the media consists primarily of a thick elastic lamina. Branching of the pulmonary artery (order 12-4) causes a reduction in the diameter of the arteries ($100 - 1000\ \mu\text{m}$) and a progressive increase in smooth muscle within the media, with few elastic fibrils present. The most distal PAs (order 3-1) are $<100\ \mu\text{m}$ in diameter and surrounded by a thin layer of endothelium with absence of smooth muscle (Brenner, 1935, Hislop and Reid, 1973, Yen and Sobin, 1988). Pulmonary arteries of order 1 connect to the pulmonary capillaries which form capillary plexuses at the alveolar ducts to aid blood-gas exchange. Pulmonary capillaries are $<10\ \mu\text{m}$ in diameter and are composed of a very thin layer of endothelium (approximately $0.15\ \mu\text{m}$ thick). The alveolar epithelial layer (also approximately $0.15\ \mu\text{m}$ thick) is in contact with the capillary and this forms an extremely thin blood-gas barrier to facilitate the diffusion of gases (Low, 1953). At rest, the pulmonary capillary bed can accommodate the stroke volume.

1.1.2 Function of the pulmonary circulation

The main function of the pulmonary circulation is to enable the oxygenation of deoxygenated blood. The pulmonary circulation needs to accommodate the entire stroke volume of blood at each heart beat and is a low resistance and pressure system which is normally fully dilated. Blood arriving at the alveoli has a high carbon dioxide (CO_2) content produced from cellular respiration within the body. This produces a concentration gradient with the air in the alveoli causing diffusion of CO_2 out of the blood. In the same way, oxygen (O_2) concentrations are significantly higher in the alveoli compared to the blood resulting in diffusion of O_2 into the blood. In the blood, O_2 binds to a protein present in red blood cells called haemoglobin. Haemoglobin is composed of four

subunits each containing a heme group with a ferrous iron atom which can reversibly bind to O₂ (Pittman, 2011). This CO₂/O₂ exchange within the lung allows the re-oxygenation of blood and is vital for the functioning of many processes throughout the body.

As mentioned above, the pulmonary circulation is a high flow, low resistance and low pressure system due to the lungs receiving 100% of the cardiac output. This is in contrast to the systemic circulation which is a high pressure circuit. In a healthy individual, the mean pulmonary artery pressure (PAP) is approximately 10-20 mmHg while the mean systemic arterial pressure (SAP) is approximately 70-105 mmHg (Kuhr et al., 2012). The pulmonary vascular resistance (PVR) is calculated as a function of cardiac output and PAP. PVR is the resistance in the pulmonary arteries against which the right ventricle must eject blood and according to Poiseuille's Law, PVR is inversely related to the fourth power of pulmonary arterial radius (Chemla et al., 2002). All orders of pulmonary arteries are involved in defining PVR however, the small and medium arteries contribute significantly more than the large vessels. Therefore even small changes in lumen diameter, as a result of vasoconstriction or vessel wall hypertrophy, can result in large changes in PVR.

1.2 Pulmonary arterial hypertension

1.2.1 Classification

In 1951, Dresdale coined the term primary pulmonary hypertension (PPH) to describe a condition which displays an elevated pulmonary pressure without demonstrable cause (Dresdale et al., 1951). The term primary pulmonary hypertension has now been replaced with the term idiopathic pulmonary arterial hypertension (IPAH). Clinical classification of pulmonary hypertension (PH) is based on guidelines established by the fifth World Symposium on Pulmonary Hypertension held in Nice, France in 2013 and modified previous guidelines based on the current knowledge of the disease (Simonneau et al., 2013). There are five categories of pulmonary hypertension (Table 1.1) with each separate group sharing pathological and clinical features.

This study will focus on group 1 pulmonary arterial hypertension, which includes idiopathic PAH (IPAH), heritable PAH (HPAH) and PAH associated with other diseases (APAH). IPAH describes the development of the disease without any known cause or risk factors. In contrast, HPAH characterises the condition when there is a genetic aspect involved and heterozygous mutations within the gene encoding for bone morphogenetic protein receptor II (BMP2) are present in 50-90% of patients diagnosed with HPAH (McLaughlin and McGoon, 2006). APAH can manifest as a result or alongside other conditions, such as HIV infection, collagen vascular diseases, congenital heart disease and drug related PAH (e.g. anorexigenic drugs) (Simonneau et al., 2009).

Pulmonary arterial hypertension is an increasingly prevalent disease with an adult prevalence of 48.7 - 51.8 cases/million of the population in Scotland, England and Wales (NAPH, 2013). PAH is established by elevation of pulmonary vascular resistance and pulmonary arterial pressure, leading to right ventricular failure and eventual death. Clinically, PAH is defined as a mean pulmonary artery pressure of >25 mmHg. Group 1 PAH is distinguished from other groups of pulmonary hypertension with a pulmonary capillary wedge pressure of ≤ 15 mmHg and pulmonary vascular resistance of >240 dynes/sec/cm⁵ (Rich et al., 1987, Rubin, 2004). Diagnosis of PAH is confirmed by right heart catheterisation (Barst et al., 2004). Clinical symptoms of PAH include dyspnea, chest pain, syncope and fatigue however, symptoms are not specific for PAH and do not usually arise until later stages of disease development. In addition to this, studies have reported a delay of approximately 2 years from onset of symptoms to diagnosis (Humbert et al., 2006, Badesch et al., 2009, Rich et al., 1987) and so detection of PAH occurs late in the progression of the disease with the majority of patients displaying severe hemodynamic compromise (Humbert et al., 2006). As a result, PAH has a poor prognosis with patient survival 1 and 3 years after diagnosis at 88% and 68%, respectively, with current therapies (Hurdman et al., 2012).

Based on the severity of the symptoms and the ability to perform daily tasks, PAH patients are further classified into groups using the New York Heart Association/World Health Organisation (NYHA/WHO) functional classification (Table 1.2). Functional classification describes the physical limitations which are placed on the patient, with early stage PAH patients in class I and late stage

patients with right heart failure in class IV. The NYHA/WHO classification system is also a strong predictor of patient mortality. NYHA/WHO class I and II patients have a median survival time of almost 6 years, class III survival time is 2.5 years while survival time for class IV patients drops dramatically to 6 months (D'Alonzo et al., 1991).

Table 1-1 – WHO classification of pulmonary hypertension.

Reproduced from (Simonneau et al., 2013).

1	Pulmonary arterial hypertension (PAH)
1.1	Idiopathic PAH
1.2	Heritable PAH
1.2.1	BMPR2
1.2.2	ALK-1, ENG, SMAD9, CAV1, KCNK3
1.2.3	Unknown
1.3	Drug and toxin induced
1.4	PAH associated with:
1.4.1	Connective tissue disease
1.4.2	HIV infection
1.4.3	Portal hypertension
1.4.4	Congenital heart diseases
1.4.5	Schistosomiasis
1'	Pulmonary veno-occlusive disease and/or pulmonary capillary hemangiomatosis
1''	Persistent pulmonary hypertension of the new born (PPHN)
2	Pulmonary hypertension due to left heart disease
2.1	Left ventricular systolic dysfunction
2.2	Left ventricular diastolic dysfunction
2.3	Valvular disease
2.4	Congenital/acquired left heart inflow/outflow tract obstruction and congenital cardiomyopathies
3	Pulmonary hypertension due to lung diseases and/or hypoxia
3.1	Chronic obstructive pulmonary disease
3.2	Interstitial lung disease
3.3	Other pulmonary diseases with mixed restrictive and obstructive pattern
3.4	Sleep-disordered breathing
3.5	Alveolar hypoventilation disorders
3.6	Chronic exposure to high altitude
3.7	Developmental lung diseases
4	Chronic thromboembolic pulmonary hypertension (CTEPH)
5	Pulmonary hypertension with unclear multifactorial mechanisms
5.1	Hematological disorders: chronic haemolytic anemia, myeloproliferative disorders, splenectomy
5.2	Systemic disorders: sarcoidosis, pulmonary histiocytosis, lymphangioleiomyomatosis
5.3	Metabolic disorders: glycogen storage disease, Gaucher disease, thyroid disorders
5.4	Others: tumoral obstruction, fibrosing mediastinitis, chronic renal failure, segmental PH

The first registry of primary pulmonary hypertension was carried out in the early 1980s by the National Institutes of Health (NIH) (Rich et al., 1987, D'Alonzo et al., 1991) and further registries have been conducted to provide more up to date information on the patient population. The incidence of PAH varies from 1.1, 2.3 and 2.4 cases per million of adult population per year in the UK and Ireland, USA and France, respectively (Ling et al., 2012, Frost et al., 2011, Humbert et al., 2006). The median age of PAH diagnosis is 56 years of age (Ling et al., 2012, Badesch et al., 2010). Females are more susceptible to developing PAH with a female to male ratio of 4.3:1 in PAH (Walker et al., 2006) and 4.1:1 in IPAH (Badesch et al., 2010). However although females have a higher preponderance of PAH, severity and survival rates are worse in males who have developed the disease (Humbert et al., 2010).

Table 1-2 – New York Heart Association/ World Health Organisation (NYHA/WHO) functional classification of pulmonary hypertension.

Class	Description
I	Patients with PH in whom there is no limitation of usual physical activity. Ordinary physical activity does not cause increased dyspnea, fatigue, chest pain or presyncope.
II	Patients with PH who have mild limitation of physical activity. There is no discomfort at rest, but normal physical activity causes increased dyspnea, fatigue, chest pain or presyncope.
III	Patients with PH who have a marked limitation of physical activity. There is no discomfort at rest but less than ordinary activity causes dyspnea, fatigue, chest pain or presyncope.
IV	Patients with PH who are unable to perform any physical activity at rest and who may have signs of right ventricular failure. Dyspnea and/or fatigue may be present at rest and symptoms are increased by almost any physical activity.

1.2.2 Cellular components of PAH

Within the pulmonary vessels, interaction occurs between all cell types present in the three distinct layers of the pulmonary vessel in response to various stimuli and can often result in pathobiological changes to the pulmonary wall (Abe et al., 2010, Pietra et al., 2004). Vascular stress, such as injury, inflammation or hypoxic exposure, can result in remodelling of the pulmonary vessels and primarily within the small pulmonary arteries (Stenmark et al., 2006b) (Figure 1.2).

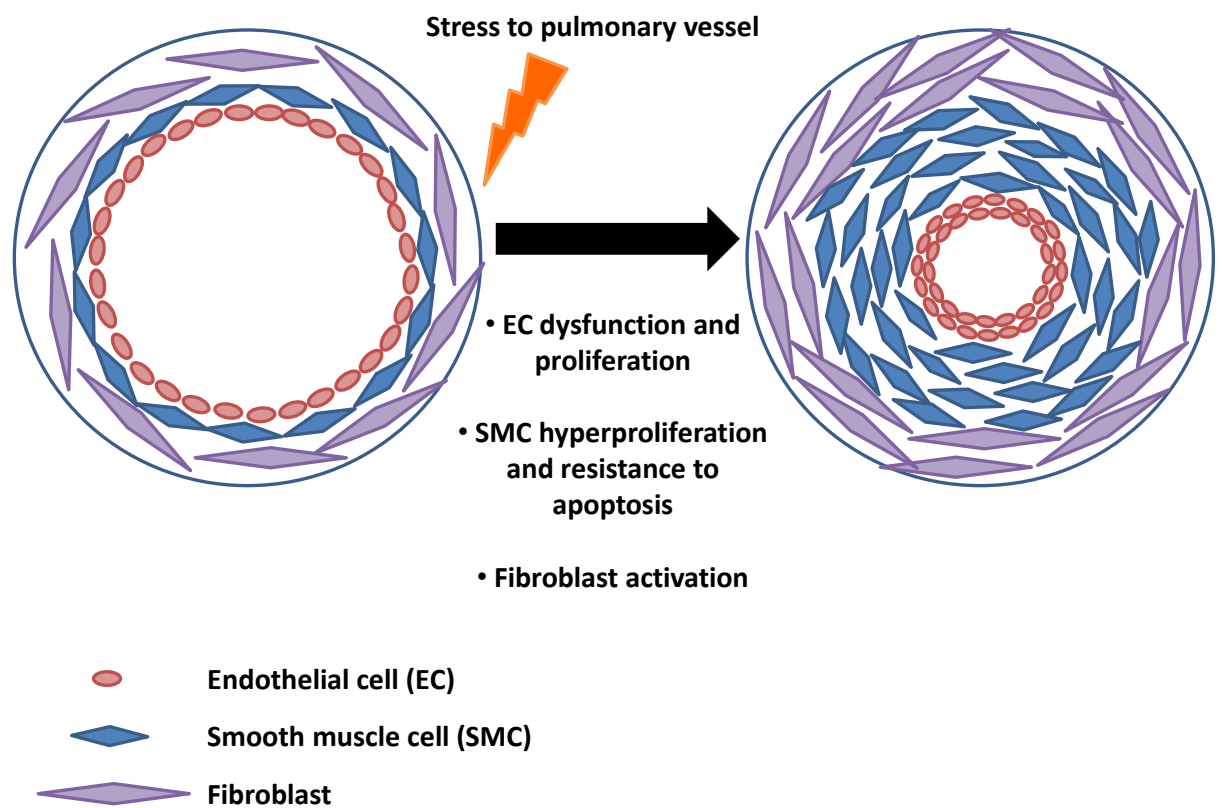


Figure 1.2 – Pathogenesis of PAH.

Vascular stress to the distal pulmonary arteries results in adventitial fibroblast activation along with smooth muscle and endothelial cell proliferation and resistance to apoptosis resulting in hypertrophy of the medial and intimal layers of the vessel wall. Vasoconstriction and pulmonary vascular remodelling ensues together with endothelial dysfunction to form plexiform lesions in human PAH. Reproduced from (Grant et al., 2013).

1.2.2.1 Fibroblasts

The outermost layer of the vessel wall is the adventitia and is predominantly comprised of fibroblasts. Adventitial remodelling appears to precede intima and medial remodelling, with early fibroblast hyperplasia in response to vascular stress (Meyrick and Reid, 1979). Within the lung, the fibroblast population is heterogeneous and subpopulations differ in shape, proliferation rate and protein synthesis rate (Jelaska et al., 1999). In conditions of vascular stress fibroblasts release reactive oxygen species (ROS), in particular the superoxide radical $O_2^{\cdot-}$, through the NADPH oxidase pathway (Meier et al., 1989). Increased ROS production within the adventitia results in a release of growth factors such as endothelin-1 (ET-1), serotonin and platelet derived growth factor (PDGF) (Liao et al., 2000) causing migration, proliferation and contraction of fibroblasts and smooth muscle cells (SMC) (Stenmark et al., 2006a). From the activated adventitial fibroblasts, a subset population differentiates into myofibroblasts (Stenmark et al., 2002). Myofibroblasts are specialised mesenchymal cells which are characterised by the expression of α -SMA and several studies have reported a possible source for myofibroblasts. Transdifferentiation of fibroblasts or fibrocytes into myofibroblasts via induction with TGF- β 1, thrombin or ET-1 contributes to muscularisation of previously non-muscular distal pulmonary arteries (Jiang et al., 2006, Bogatkevich et al., 2003, Shi-Wen et al., 2004). Reports have also shown the presence of vascular progenitor cells within the adventitia which can differentiate into SM-expressing myofibroblasts in response to vascular injury (Hu et al., 2004). In addition, circulating fibrocytes can enter the adventitia via the vasa vasorum where they can then go on to form myofibroblasts and contribute to neovascular growth (Frid et al., 2006). Myofibroblasts produce extracellular matrix proteins, such as collagen, fibronectin, tenascin-C and elastin which can induce SMC proliferation and migration within the media (Stenmark et al., 2006a, Chiang et al., 2009, Rabinovitch, 2007). In addition to this, myofibroblasts produce matrix metalloproteinases (MMPs) and excessive MMP expression enhances the migration of myofibroblasts from the adventitia into the medial or intimal regions (Shi et al., 1999), increasing the thickness of the vessel wall and contributing to lesion formation.

1.2.2.2 Smooth muscle cells

The medial layer within the vessel wall contains SMCs which are regulated under the control of many growth factors and cytokines, such as the transforming growth factor beta (TGF- β) superfamily, tumour necrosis factor alpha (TNF- α) and interleukin-6 (IL-6). Medial thickening, as well as neo-intimal formation, as is observed in PAH is thought to be due to a combination of factors including SMC hypertrophy, SMC hyperplasia and accumulation of extracellular matrix proteins such as collagen and elastin (Stenmark et al., 2006b). SMCs produce MMPs (in particular MMP-2) which degrade the extracellular matrix and release matrix bound growth factors, such as basic fibroblast growth factor (FGF) to induce SMC proliferation (Thompson and Rabinovitch, 1996). As well as this, MMP-2 induces the expression of tenascin-C, a large glycoprotein which promotes SMC proliferation and survival and thus further elevates SMC hyperplasia (Cowan et al., 2000). Another aspect involving pulmonary artery SMCs (PASMCs) in PAH development is the down-regulation of voltage-sensitive potassium channels (Kv). Decreased activity of Kv in PASMCs results in an increase in K^+ ions in the cell and therefore depolarisation of the cell membrane. Membrane depolarisation activates voltage-dependent L-type calcium (Ca^{2+}) channels to cause an influx of Ca^{2+} into the cell. Ca^{2+} levels may be further increased via Ca^{2+} -dependent Ca^{2+} -release from intracellular stores (Platoshyn et al., 2000, Firth et al., 2009). When Ca^{2+} concentrations are high, binding of Ca^{2+} to calmodulin occurs to activate myosin light chain kinase resulting in phosphorylation of myosin light chain and subsequent activation of myosin ATPase. This leads to cross-bridge cycling between actin and myosin filaments and PASMC contraction (Somlyo and Somlyo, 1994, Wang et al., 2007). Furthermore, elevated cytosolic Ca^{2+} activates Ca^{2+} dependent kinases and other transcription factors (e.g. NFAT) to promote PASMC proliferation (Kuhr et al., 2012, Bonnet et al., 2007). PASMCs from IPAH patients display reduced levels of Kv1.5 (Yuan et al., 1998) and this down-regulation of Kv channels is also well reported in response to hypoxia (Post et al., 1992, Platoshyn et al., 2001) resulting in hypoxic pulmonary vasoconstriction (HPV).

1.2.2.3 Endothelial cells

Endothelial cells (EC) are the predominant cell type within the intimal layer of pulmonary arteries and regulate the levels of vasodilators (e.g. nitric oxide (NO) and prostacyclin) and vasoconstrictors (ET-1 and thromboxane) (Archer and Rich, 2000). Imbalance between these vasoactive peptides results in dysregulation of vascular tone. Vascular stress also results in excessive production of growth factors by pulmonary artery endothelial cells (PAECs) which can act in both an autocrine and paracrine manner to contribute to pulmonary remodelling. Increased production of FGF2, serotonin and ET-1 from pulmonary ECs stimulates SMC proliferation (Izikki et al., 2009). Endothelial release of FGF2 also promotes EC proliferation via activation of ERK1/2 and inhibits apoptosis by increasing anti-apoptotic molecules BCL2 and BCL-xL (Tu et al., 2011). This increase in EC hyperplasia is typical of late stage PAH however, the early stage of disease is characterised by initial EC apoptosis. Loss of BMPR2 (as is observed in many PAH patients) results in vascular leakage (Burton et al., 2011) and increased rate of apoptosis in PAECs (Teichert-Kuliszewska et al., 2006).

ECs are activated via numerous stimuli, including shear stress, inflammation, TNF- α and ROS, resulting in the release of endothelial microparticles from the plasma membrane. These microparticles carry proteins such as intercellular cell adhesion molecule (ICAM-1) and vascular endothelial cadherin (Dignat-George and Boulanger, 2011). Endothelial microparticles contain DNA, RNA and microRNA (miRNA) which can be transferred to target cells to control cell phenotype. An example of this is the regulation of SMC phenotype by endothelial microparticles containing elevated levels of miR-143/miR-145 (Hergenreider et al., 2012).

1.2.2.4 Inflammatory Cells

In addition to the cell types mentioned above, it is clear that inflammatory processes also play an important role in the pathogenesis of pulmonary arterial hypertension. Patients with severe IPAH display elevated levels of inflammatory cells within the adventitial layer of the pulmonary vasculature and in vascular lesions, in particular macrophages, T cells, B cells and mast cells (Savai et al., 2012). Circulating levels of pro-inflammatory cytokines, such as IL-1 β and IL-6,

are also increased in IPAH patients compared to control subjects (Humbert et al., 1995). Macrophages and mast cells secrete MMPs, thus allowing a subset of circulating mesenchymal precursors from a monocyte/macrophage lineage (fibrocytes) to enter the adventitia where they can transdifferentiate into myofibroblasts (Frid et al., 2006). Activated macrophages also release cytokines such as IL-6 (Martin and Dorf, 1991). IL-6 is a pro-inflammatory cytokine which activates pro-angiogenic vascular endothelial growth factor (VEGF), pro-proliferative transcription factors c-MYC and MAX and anti-apoptotic proteins survivin and Bcl-2 (Steiner et al., 2009). IL-6 also stimulates PASMC migration (Savale et al., 2009), therefore further contributing to pulmonary vascular remodelling. Macrophage migration inhibitory factor (MIF) is another pro-inflammatory cytokine secreted from numerous cell types, including T cells and monocytes/macrophages. MIF can induce PASMC proliferation through activation of the ERK1/2 and JNK pathway (Zhang et al., 2012), thus enhancing the vascular remodelling process.

1.2.2.5 Plexiform lesion formation

As mentioned above, the development of PAH involves all cell types in the multiple layers of the vessel wall. Pulmonary artery remodelling and vasoconstriction result from increased proliferation and resistance to apoptosis of ECs and SMCs as well as distal extension of smooth muscle into previously non-muscular pulmonary arteries. The increase in medial hypertrophy can lead to occlusion and eventual loss of the small pulmonary arteries; an effect known as vascular pruning and results in reduced perfusion of the lung (Figure 1.3A) (Ryan et al., 2012b, Moledina et al., 2011). Hyperproliferation of ECs produces a thick neointima and can result in plexiform lesion formation (Figure 1.3B). The plexiform lesion is a disorganised proliferative lesion of endothelial channels lined with myofibroblasts, SMCs and connective tissue matrix (Pietra et al., 2004). High expression of VEGF and VEGF receptors, key regulators of EC angiogenesis, are observed in the endothelial cells from plexiform lesions (Cool et al., 1999) along with increased CD44 expression, a cell adhesion molecule reported to play a role in EC proliferation, migration and angiogenesis (Ohta-Ogo et al., 2012). Inflammatory cells are also present in these plexiform lesions with increased macrophage and T-cell infiltration thought to further promote the development of vascular lesions (Tuder et al., 1994). Furthermore, it has been

reported that lungs from IPAH patients contain perivascular tertiary lymphoid tissue connected to remodelled vessels. They are composed of T-lymphocytes and B-lymphocytes which express lymphocyte survival factors such as IL-17 and PDGF-A (Perros et al., 2012). Plexiform lesions are most commonly located downstream of the obliterated distal arteries (Archer et al., 2010) and at, or distal to, branch points of the small pulmonary arteries (Cool et al., 1999). As well as affecting the distal pulmonary arteries, PAH also affects the large pulmonary artery. Medial and adventitial hypertrophy occurs in the large proximal pulmonary arteries causing vessel stiffness, a decrease in vessel compliance and increase in pulmonary artery impedance (Huez et al., 2004). Together, this elevates the right ventricular afterload and contributes to the development of right ventricular hypertrophy (RVH). RVH is characterised by increased RV wall thickness, cardiomyocyte proliferation and results in a decrease in cardiac contraction. A shift to glycolytic metabolism is observed in RVH where the RV cannot support increased energy demands and can lead to RV failure (Voelkel et al., 2012).

Although PAH is a relatively well-studied condition, the exact cellular and molecular processes that lead to initiation and progression of the disease are still under investigation. It is most likely due to complex interactions between transcriptional and signalling pathways within the layers of the vessel leading to the severe phenotype observed in patients with PAH, characterised by the formation of plexiform lesions.

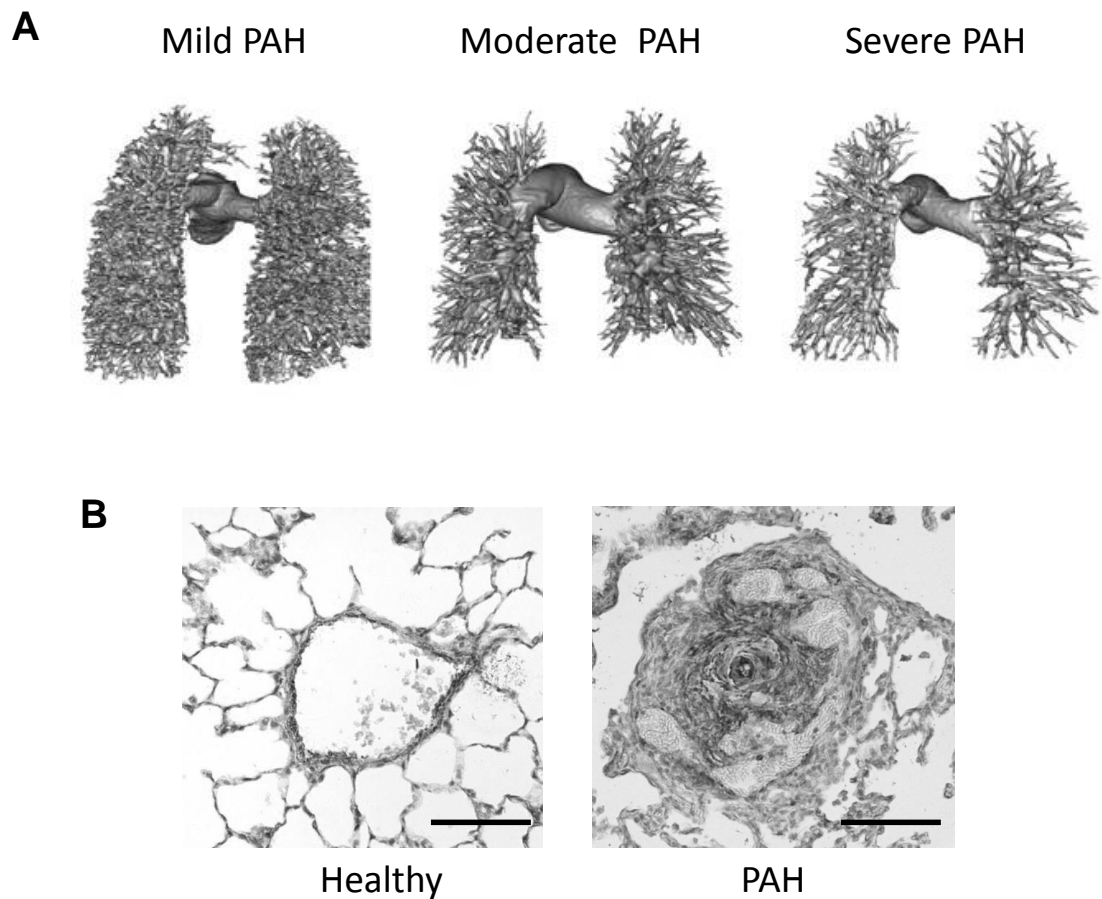


Figure 1.3 – Vascular pruning and remodelling observed in PAH.

A) Pulmonary angiogram from patients with mild, moderate and severe PAH shows evident vascular pruning as the disease progresses. This is characterised by loss of distal pulmonary arteries and the sparse arterial tree. Adapted from (Moledina et al., 2011). B) Histological analysis of pulmonary arteries shows obliteration of the lumen by hypertrophy of the medial and intimal layers in diseased vessels. Scale bar = 100 μ m.

1.2.3 BMPR2 mutations in PAH

There is a large cohort of data implicating the BMP pathway in the etiology of PAH as heterozygous mutations within the gene encoding bone morphogenetic protein type 2 receptor (BMPR2) have been reported in ~70% of HPAH (Lane et al., 2000, Machado et al., 2006) and ~26% of IPAH cases (Thomson et al., 2000). BMPR2 is a serine/threonine receptor kinase which binds the TGF- β superfamily of ligands. The BMPR2 gene is located on chromosome 2q33 with exons 1-3 encoding an extracellular domain, exon 4 encoding the transmembrane domain, exons 5-11 encoding the serine/threonine kinase domain and exons 12-13 encoding a large intracellular C-terminus (Newman et al., 2004). Within the pulmonary circulation, BMPR2 expression is primarily localised in endothelial cells with lower expression detected in vascular smooth muscle cells (Atkinson et al., 2002). BMPR2 activates intracellular signalling in a ligand-specific manner and the resulting outcome is cell and site specific.

Under normal conditions, BMP4 signals via a Smad-dependent pathway to inhibit proliferation of PSMCs (Yang et al., 2005). Binding of the BMP4 ligand causes heterodimerization of BMP type 1 and type 2 receptors, inducing phosphorylation of the intracellular section of the type 1 receptor (Wrana et al., 1994). Activated BMPR type 1 phosphorylates BMP-specific receptor regulated Smad (R-Smad) proteins (Smad1/5/8) at serine residues at the carboxy terminal ends. This promotes the formation of a heteromeric complex between the R-Smad and the common mediator Smad, Smad4, to allow nuclear translocation (Kretzschmar et al., 1997). Once in the nucleus, the Smad complex associates with DNA-binding cofactors (either co-activators or co-repressors) to control the transcription of target genes (Figure 1.4) (Massague and Chen, 2000). TGF- β signalling is similar to that of BMP however, TGF- β signals via Smad2/3 (Morrell, 2006). Evidence also suggests that BMPs can signal in a Smad-independent manner. When Smad signalling is repressed, as in the case with BMPR2 mutations, BMP and TGF- β signal through mitogen-activated protein kinase (MAPK) pathways via activation of TGF- β -activated kinase 1 (TAK1), a member of the MAPKKK family (Yang et al., 2005). Under basal conditions TAK1 is bound to BMPR2 however, this interaction is reduced with BMPR2 mutations therefore making TAK1 accessible for TGF- β signalling. In addition to this, TAK1 reduces Smad-dependent BMP signalling by inhibiting the phosphorylation of Smad1

(Nasim et al., 2012). The Smad and MAPK signalling pathways appear to exert opposing effects in PASMCs and conditions favouring the Smad-independent pathway result in a pro-proliferative and anti-apoptotic response (Nasim et al., 2012, Yang et al., 2005).

The BMP signalling pathway is tightly controlled by regulatory molecules. Smad6 and Smad7 are inhibitory Smads which have been shown to block TGF- β and BMP signalling in two ways. Inhibitory Smads can either bind to the activated type I receptor therefore preventing the association, phosphorylation and activation of R-Smads (Hayashi et al., 1997, Imamura et al., 1997) or by binding to the activated R-Smad thereby preventing heteromerization of R-Smad with Smad4 and inhibiting subsequent nuclear translocation (Hata et al., 1998). It has also been reported that Smad6 and Smad7 are induced in response to BMP or TGF- β signalling suggesting that these inhibitory Smads provide negative feedback to control the signalling response to these ligands (Afrakhte et al., 1998, Nakao et al., 1997). Another factor involved in negatively regulating BMP signalling is Smad-ubiquitin regulatory factor 1 (Smurf1). Smurf1 is an E3 ubiquitin ligase which binds specifically to the BMP specific Smads, resulting in degradation of Smad1 and Smad5 (Figure 1.4) (Zhu et al., 1999, Shi et al., 2004). It has been reported that specific proteins interact with the tail domain of BMPR2, in particular Tribbles like protein 3 (Trb3). Upon BMP4 stimulation, Trb3 dissociates from the tail domain of BMPR2 and binds to Smurf1 inducing degradation of Smurf1. This increases signalling through the BMP-specific Smad pathway and promotes the contractile phenotype in vascular SMCs (Chan et al., 2007).

Many different mutations have been discovered within the BMPR2 gene encoding region from patients diagnosed with PAH (Machado et al., 2006). However, kindred studies have shown that only ~20% of people with these mutations go on to develop PAH (Newman et al., 2001), thus indicating that there may be environmental or additional genetic risk factors involved. It is proposed that mutations in the BMPR2 gene predispose individuals to develop PAH and multiple 'hits' are required for disease development (Yuan and Rubin, 2005). PAH patients harbouring a heterozygous mutation in the gene encoding BMPR2 display reduced levels of BMPR2 protein (Atkinson et al., 2002). PASMCs from these patients are deficient in Smad signalling (Yuan and Rubin, 2005), initiate an

altered response to BMP growth factors (Morrell et al., 2001) and BMP-induced apoptosis is inhibited (Zhang et al., 2003). Similarly, animal models of PH show a reduction in BMPR2 protein levels in the lungs (Takahashi et al., 2006).

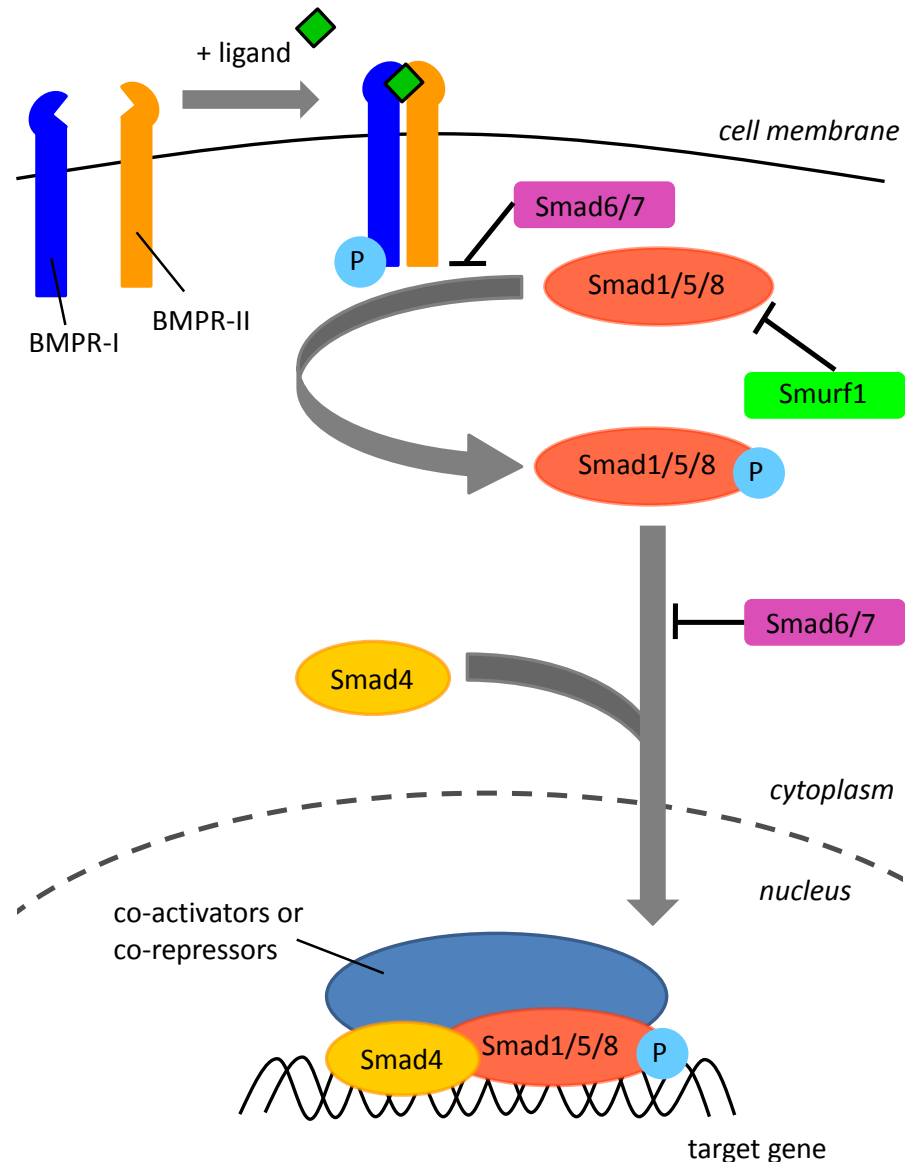


Figure 1.4 – Smad-dependent BMP signalling under normal physiological conditions.

Binding of ligand BMP4 causes heterodimerisation of BMP receptor type 1 (BMPR-I) and BMP receptor type 2 (BMPR-II) inducing phosphorylation of BMPR-I by BMPR-II. Activated BMPR-I stimulates the phosphorylation of Smad1/5/8 promoting the formation of a complex with Smad4. The resulting Smad complex is translocated into the nucleus and binds to DNA-binding co-factors to control the transcriptional regulation of target genes.

1.2.4 Current treatment for PAH

As mentioned above there are many diverse systems and cell types involved in the pathobiology of PAH and as a result, finding an effective treatment for the condition is challenging. The fundamental aim in the treatment of PAH is to reduce pulmonary arterial pressure and decrease the pressure in the right ventricle therefore preventing right ventricular failure. Under normal circumstances the endothelium produces a balance between vasodilators such as nitric oxide (NO) and prostacyclin, and vasoconstrictors such as ET-1. Endothelial dysfunction however results in a decrease in the production of NO as a result of reduced expression of nitric oxide synthase and prostacyclin and elevated levels of ET-1 culminating in constriction of the pulmonary arteries (Humbert et al., 2004b, Badesch et al., 2004). Current therapies aim to restore endothelial function by inhibiting the actions of ET-1 or increasing NO and prostacyclin levels (Archer et al., 2010) (Figure 1.5). Current treatments relieve the symptoms of PAH and provide a survival benefit, with increased survival rates of 83%, 67% and 58% at 1, 2 and 3 years, respectively (Humbert et al., 2010). Treatment also causes a reduction in mortality of 38% compared to placebo treated groups (Galie et al., 2009) however, mortality rates remain high and treatment does not prevent the aggressive progression of the disease (Macchia et al., 2007).

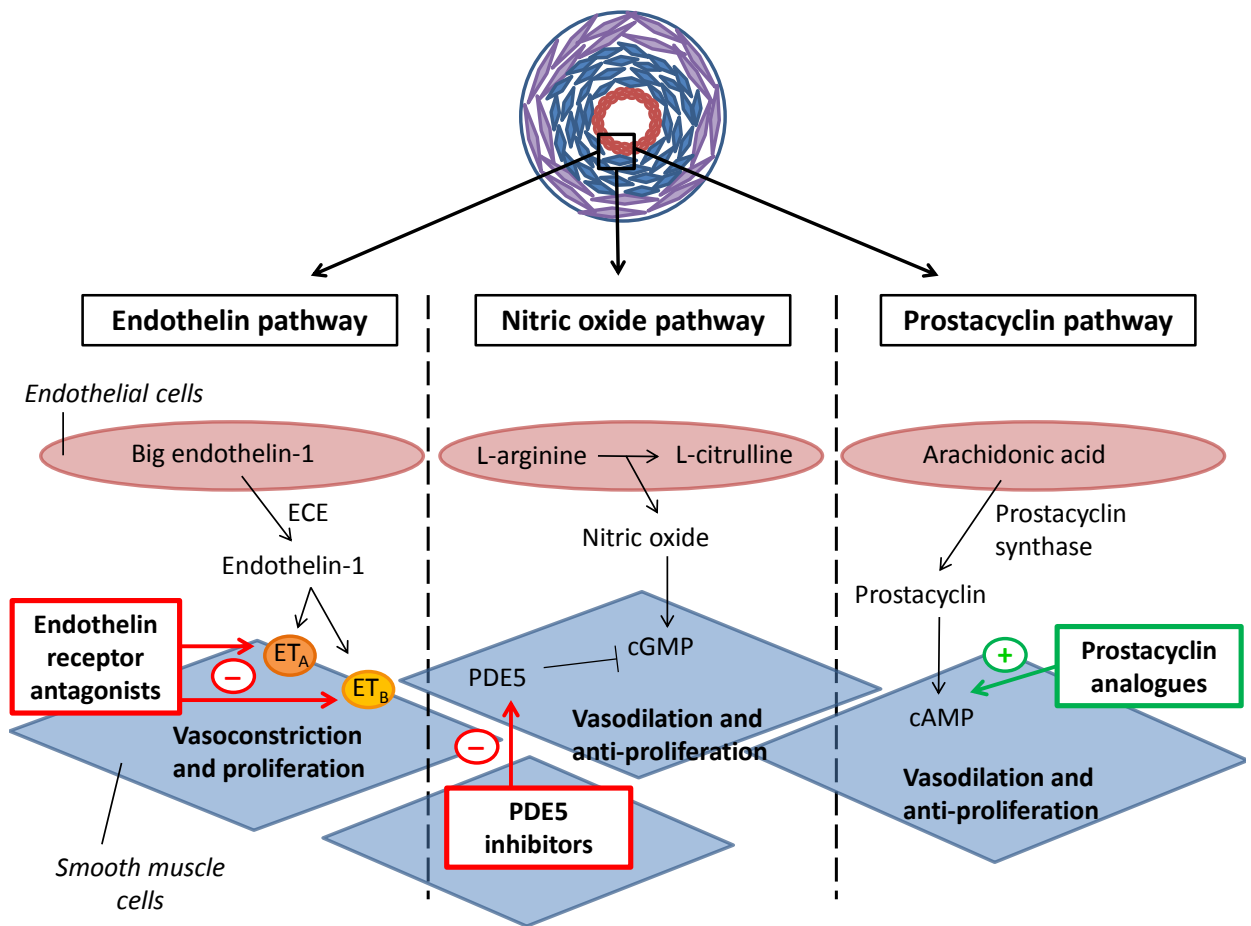


Figure 1.5 – Current therapies for PAH patients.

Therapies for PAH patients target three distinct signalling pathways; endothelin pathway (endothelin receptor antagonists), nitric oxide pathway (phosphodiesterase type 5 inhibitors) and the prostacyclin pathway (prostacyclin analogues) to induce vasodilation and reduce smooth muscle cell proliferation. ECE = endothelin converting enzyme, ET_A = endothelin receptor type A, ET_B = endothelin receptor type B, PDE5 = phosphodiesterase type 5. Adapted from (Humbert et al., 2004b).

1.2.4.1 Endothelin receptor antagonists

Endothelins are produced primarily by endothelial cells. Endothelin-1 (ET-1) is the predominant isoform found within the pulmonary vasculature (Matsumoto et al., 1989). ET-1 is formed through cleavage of big endothelin-1 by endothelin converting enzyme 1 (ECE-1) to form a 21 amino acid vasoactive peptide (Shimada et al., 1994) which is a potent vasoconstrictor and induces SMC proliferation (Yanagisawa et al., 1988, McCulloch et al., 1996). Lung tissue and plasma from patients diagnosed with PAH have increased levels of ET-1 and this expression level is correlated with disease severity (Stewart et al., 1991, Giaid et al., 1993, Galie et al., 1996). Two endothelin receptors have been identified; the ET_A receptor is localised on SMCs while the ET_B receptor is present on both SMCs and ECs (Seo et al., 1994). Both receptors are G-protein coupled receptors (Arai et al., 1990, Sakurai et al., 1990) and activation of smooth muscle ET_A or ET_B receptors by ET-1 activates the phospholipase C signal transduction pathway leading to increased inositol triphosphate and diacylglycerol production. These second messengers are then able to trigger release of calcium from intracellular stores, resulting in prolonged vasoconstriction (Pollock et al., 1995). Conversely, binding of ET-1 to endothelial ET_B receptor promotes the release of NO and prostacyclin to induce endothelial dependent vasodilation (Hirata et al., 1993, Liu et al., 2003). Due to the actions of ET-1 on smooth muscle cells within the pulmonary vessels, endothelin receptor antagonists are currently used as treatment for PAH patients.

Bosentan, an orally active dual endothelin receptor antagonist, is FDA approved for the treatment of class III and IV PAH patients (Galie et al., 2004). The first clinical trial to assess the efficacy of bosentan in PAH patients assessed 32 patients for 12 weeks (Channick et al., 2001) and was followed up by a larger multicentre study assessing 213 PAH patients for 16 weeks (BREATHE-1 trial; (Rubin et al., 2002)). In both studies, bosentan treatment improved exercise capacity (as measured by the 6 minute walk distance), pulmonary hemodynamics and increased time to clinical worsening compared to placebo treated PAH patients. One of the drawbacks of bosentan therapy is hepatic toxicity and liver function tests are performed prior to commencing bosentan treatment and on a monthly basis during treatment (McLaughlin and McGoon, 2006).

Another orally active dual endothelin receptor antagonist is Macitentan, which was developed via modification of bosentan to enhance oral efficacy and safety (Bolli et al., 2012). In a Phase 3 clinical trial, long term treatment with Macitentan reduced morbidity and mortality in patients with PAH (SERAPHIN; (Pulido et al., 2013)). This was the first PAH clinical trial where clinical events were used as a primary end point.

In order to preserve the vasodilatory effect of ET-1 acting on endothelial ET_B receptors, the specific ET_A receptor antagonist Ambrisentan was developed for treatment of PAH. Clinical trials (ARIES-1 and ARIES-2; (Galie et al., 2008)) revealed that oral once daily treatment with Ambrisentan improved exercise capacity, time to clinical worsening and WHO functional class in PAH patients following treatment. To date, there are no clinical trials which compare the efficacy of selective ET_A receptor antagonists with dual endothelin receptor antagonists. However there have been reports suggesting cross talk between the endothelin receptors to provide compensation when only one receptor is antagonised (Clozel and Gray, 1995).

1.2.4.2 Prostacyclin analogues

Prostacyclin (PGI₂) is produced by pulmonary artery endothelial cells. Arachidonic acid is metabolised by cyclooxygenase (COX) into prostaglandin H₂ which is converted into prostacyclin by prostacyclin synthase. Prostacyclin production activates cyclic adenosine monophosphate (cAMP) to cause vasodilation, decrease platelet aggregation and inhibit smooth muscle cell proliferation (Moncada and Vane, 1981, Owen, 1985). Thromboxane A₂ is another metabolite of arachidonic acid produced by thromboxane synthase and is antagonistic in action to prostacyclin. Thromboxane A₂ is a potent vasoconstrictor and stimulates platelet aggregation. Imbalance between these two vasoactive prostanoids results in endothelial dysfunction. There is a reduction in prostacyclin synthase and its metabolites in PAH patients while thromboxane A₂ production is increased (Tuder et al., 1999, Christman et al., 1992). In addition to this, PGI₂ receptor knockout (KO) mice exposed to hypoxic conditions develop an exaggerated PH phenotype (Hoshikawa et al., 2001) while mice over-expressing prostacyclin synthase selectively in the pulmonary vasculature are protected against hypoxia-induced PH (Geraci et al., 1999).

Thus, synthetic analogues of prostacyclins are used as treatment for PAH due to the vasodilatory effects and inhibition of platelet aggregation by prostacyclin.

Epoprostenol is a prostacyclin analogue which must be administered continuously via intravenous (IV) infusion due to its short half-life (<5 mins) (Badesch et al., 2004). Clinical trials on functional class III and IV PAH patients found that continuous IV infusion of epoprostenol improved exercise capacity, hemodynamic measurements and survival rates (Barst et al., 2006, Sitbon et al., 2002, McLaughlin et al., 2002). Although prostacyclin analogues are generally well tolerated, common side effects can result from systemic vasodilation, including headaches, flushing, diarrhoea and jaw pain (Badesch et al., 2004). There are however problems with epoprostenol treatment, the main complication being the need for continuous intravenous infusion. Because of the problems and inconvenience of IV infusion, epoprostenol is often used only for very severe cases of PAH. As a result, other prostacyclin analogues have been investigated which are chemically more stable and can be administered by more appropriate methods.

Trepostinil is a stable prostacyclin analogue with a longer half-life (up to 3 hours) (Badesch et al., 2004) than epoprostenol. Trepostinil can be administered subcutaneously via a microinfusion pump (Seferian and Simonneau, 2013) and increases exercise capacity, symptoms of PH and hemodynamics to a similar extent to that observed with epoprostenol treatment (Simonneau et al., 2002, McLaughlin et al., 2003). An oral formulation of trepostinil has been developed with preliminary data from clinical trials showing increased exercise tolerance with oral trepostinil treatment (FREEDOM-M study; (Jing et al., 2013)). Functional class and time to clinical worsening however were not improved. Further longitudinal studies are required to assess the long term effects of oral trepostinil treatment.

1.2.4.3 Phosphodiesterase type 5 inhibitors

Within the pulmonary endothelium, NO is released and activates soluble guanylate cyclase to increase cyclic guanosine monophosphate (cGMP) levels leading to relaxation of the smooth muscle (Lucas et al., 2000). One of the key enzymes involved in depleting cGMP levels is phosphodiesterase type 5 (PDE5),

which hydrolyses cGMP in smooth muscle cells and primarily works in the lung (Corbin et al., 2005). This reduction in cGMP augments intracellular Ca^{2+} and K^{+} levels resulting in proliferation of pulmonary SMCs, reduction in SMC apoptosis and vasoconstriction (Chiche et al., 1998, Archer and Michelakis, 2009). Expression and activity of PDE5 is significantly higher in neonate lungs compared to adult lungs (Sanchez et al., 1998). However, it has been reported that PDE5 levels are increased in PASMCs from IPAH patients with high expression located within the remodelled vessels (Wharton et al., 2005). In addition to this, PDE5 gene and protein expression is increased in human hypertrophied RV compared to healthy RV tissue (Nagendran et al., 2007).

Sildenafil is a highly potent and selective PDE5 inhibitor which prevents the hydrolysis of cGMP therefore allowing accumulation of NO-mediated cGMP and subsequent vasodilation (Michelakis et al., 2002a). Sildenafil has been shown to reduce PASMC proliferation (Wharton et al., 2005) while oral sildenafil treatment attenuates hypoxia-induced PH in mice (Zhao et al., 2001) and monocrotaline (MCT) induced PH in rats (Schermuly et al., 2004). Sildenafil was FDA approved for treatment of PAH in patients in NYAH/WHO functional class II or III with mild to moderate disease in 2005. Improvements in exercise capacity, mean pulmonary arterial pressure and functional class have been observed in PAH patients treated with oral sildenafil with common side effects including headaches, flushing and dyspepsia (SUPER trial; (Galie et al., 2005)). As well as having beneficial effects on the pulmonary artery, PDE5 inhibition has a positive response within the myocardium. Sildenafil significantly increased contractility within cardiomyocytes isolated from MCT rats with significant RVH but had no effect on healthy RV tissue (Nagendran et al., 2007), thus increasing RV function selectively within diseased myocardium. The improvements observed in PAH patients treated with sildenafil are most likely due to a combination of both the pulmonary and cardiac effects.

1.2.4.4 Combination therapy

In many cases, monotherapy is inadequate to control PAH and therefore combination therapy is an attractive option to target multiple pathways simultaneously. Combination therapy has been shown to be safe and well tolerated in PAH patients (Buckley et al., 2013). Several studies have shown

combination therapy to be efficacious with an increase in exercise capacity and reduction in mean pulmonary artery pressure (McLaughlin et al., 2006). Further studies are required to determine the most effective drug combinations and optimise the timings for when additional therapies should be administered.

1.2.5 Future treatment for PAH

1.2.5.1 Guanylate cyclase activators

In addition to PDE5 inhibitors, cGMP levels can be increased through activation of soluble guanylate cyclase, the enzyme responsible for cGMP synthesis. Riociguat has a dual action by synergistically acting with nitric oxide to stimulate soluble guanylate cyclase as well as activating guanylate cyclase directly in the absence of nitric oxide (Grimminger et al., 2009). Phase III clinical trials show promise for use of riociguat in the treatment of PAH, with improvements observed in exercise capacity, functional class, pulmonary vascular resistance and time to clinical worsening (PATENT-1 trial; (Ghofrani et al., 2013)). Results from a long-term extension study (PATENT-2) led to approval of Riociguat for patients with PAH in the USA and the EU and is the first drug to be approved for patients with chronic thromboembolic pulmonary hypertension (CTEPH).

1.2.5.2 Tyrosine kinase inhibitors

PDGF has recently been implicated in the development of PAH. There are four isoforms of PDGF (A-D) and isoform A and B combine to form homodimers or heterodimers which bind to the two PDGF receptors, α and β (Fredriksson et al., 2004). Expression of PDGF-A and PDGF-B and the phosphorylated cell surface receptors are increased in small pulmonary arteries from patients with IPAH (Perros et al., 2008). PDGF is a potent mitogen and activation of PDGF receptors within the pulmonary vasculature induces SMC proliferation and migration (Yu et al., 2003). Imatinib mesylate (imatinib) is a tyrosine kinase inhibitor which targets, for example, BCR/ABL kinase, c-kit and PDGF receptor α and β (Buchdunger et al., 2000) and due to the inhibition of BCR/ABL, imatinib is currently in use for the treatment of chronic myelogenous leukaemia (CML) (Cohen et al., 2002, Gambacorti-Passerini et al., 2011). Imatinib inhibits PDGF-induced proliferation and migration of PSMCs (Perros et al., 2008), induces apoptosis in PDGF-induced PSMCs taken from IPAH patients (Nakamura et al.,

2012) and causes pulmonary vasodilation (Abe et al., 2011). *In vivo*, imatinib treatment reduced experimental PH in various models of the disease (Abe et al., 2011, Schermuly et al., 2005, Ciucan et al., 2013). A phase III clinical trial, involving 202 PAH patients in NYAH/WHO functional class II-IV, recently evaluated the efficacy and safety of imatinib as an add-on therapy for PAH (IMPRES study; (Hoepfer et al., 2013)). Results from this 24 week randomised study showed an increase in exercise capacity and improved hemodynamics compared to placebo treated patients. However, severe adverse effects (subdural hematoma) were observed in this trial and the marketing application for the use of imatinib in the treatment of PAH was withdrawn in 2013. Recent reports have shown the tyrosine kinase inhibitor dasatinib to induce PAH in patients taking the drug as treatment for CML (Montani et al., 2012). Although PDGF inhibition modulates many pathways involved in PAH development, the broad actions of these tyrosine kinase inhibitors suggests that it will be hard to design effective therapeutic agents with minimal adverse effects in this patient population.

1.2.6 Traditional animal models of PH

In order to fully understand the molecular mechanisms underlying PAH, appropriate animal models are required which mimic the pathophysiology of human PAH. The use of these animal models will allow more effective therapeutic treatments to be designed which target the underlying mechanisms of PAH, rather than just treating the symptoms of the disease. The classic rodent models most commonly used to study PAH are exposure to chronic hypoxia and monocrotaline insult.

1.2.6.1 Chronic hypoxia

Initially it was noted that both humans and cattle living at high altitudes had increased PAP and RVH indicating mild PH (Peñaloza et al., 1963, Arias-Stella and Saldana, 1963). Further to this, placing subjects at high altitude or simulated high altitude resulted in a similar phenotype (Stenmark et al., 1987) and this is thought to be due to the effects of hypoxia. Chronic exposure of rodents to hypoxia can be achieved in a laboratory setting using a normobaric or hypobaric hypoxic chamber, where animals are exposed to 10% O₂ for 2-4 weeks.

Rats exposed to hypoxia for 14 days display increased mean pulmonary arterial pressure, right ventricular hypertrophy, muscularisation of peripheral distal arteries, medial hypertrophy and a loss of peripheral arteries (Rabinovitch et al., 1979).

Acute hypoxia induces HPV in SMCs through hypoxia-induced down-regulation of Kv channels in PASMCs and the subsequent increases in cytosolic Ca^{2+} (Firth et al., 2009). This hypoxic vasoconstriction attributes to the increase in PAP observed in hypoxic animals. In addition to this, increases in cytosolic Ca^{2+} in PASMCs results in proliferation and medial hypertrophy contributing to pulmonary vascular remodelling (Platoshyn et al., 2001). Under hypoxic conditions, proliferation of medial SMCs and adventitial fibroblasts is increased (Voelkel and Tuder, 2000). Endothelial cells show very little proliferation in response to hypoxia and the hypoxic model of PH displays minimal changes in morphology in the intimal layer (Meyrick and Reid, 1980).

The effects of hypoxic exposure are more severe in younger subjects as the lungs are still developing (Stenmark et al., 2006b). Also, the effects of hypoxia differ between strains of animal and indeed species. The hypoxic mouse model of PH displays a similar response to the rat hypoxic model however, vascular remodelling within the mouse lung is minimal (Dempsey et al., 2009, Frank et al., 2008). Microarray analysis of lung tissue illustrates a difference in gene expression induced by hypoxia in mice and rats (Hoshikawa et al., 2003).

One of the benefits of the chronic hypoxic model of PH is that it does not involve administration of any compounds which may have pleiotropic effects. However there is minimal vascular remodelling, particularly within the mouse model, and plexogenic lesions, which are characteristic of the human disease, are not observed even when hypoxic exposure is extended (Herget et al., 1978). Right ventricular hypertrophy occurs in the hypoxic model but there is little evidence of right ventricular failure (Stenmark et al., 2009). Thus, hypoxic exposure is an acute model for PH and studies have shown the effects of chronic hypoxia are slowly reversed with return to normoxia (Herget et al., 1978, Peñaloza et al., 1963).

1.2.6.2 Monocrotaline injury

Monocrotaline is a pyrrolizidine alkaloid extracted from the seeds of the *Crotalaria spectabilis* plant (Lalich and Ehrhart, 1962). The active and pneumotoxic metabolite monocrotaline pyrrole (MCTP) is formed by dehydrogenation of MCT by cytochrome P-450 CYP3A in the liver (Reid et al., 1998). Administration of MCT results in a pulmonary hypertensive phenotype characterised by right ventricular hypertrophy and pulmonary remodelling due to medial hypertrophy in the small pulmonary vessels (Kay et al., 1967, Roth et al., 1981). The development of PH in the rat MCT model is not observed until 7-14 days after the initial MCT dose, after which mean pulmonary arterial pressure and RVH progressively worsen over time (Meyrick et al., 1980). MCT induces an early inflammatory response with a significant increase in mononuclear inflammatory cells within the adventitia of small pulmonary arteries 8-16 hours after MCT injection (Wilson et al., 1989). Moreover, neutrophil activation and infiltration is increased in the right ventricle during early RVH development and levels remain high throughout disease progression (Campian et al., 2010). The pulmonary inflammatory response induced by MCT disrupts the endothelial cell membrane with the extensive loss of membrane proteins such as caveolin-1, leading to the release of proliferative and anti-apoptotic signals and dysregulation of the nitric oxide signalling pathway (Huang et al., 2010). Thus culminating in medial hypertrophy, vascular remodelling and experimental PH (Todorovich-Hunter et al., 1988).

The use of MCT as a model to study PH is appealing as the procedure is relatively simple involving one sub-cutaneous injection of MCT. However, the resulting PH phenotype is an acute inflammatory response in which no complex lesions are formed. In addition to this, in house observations have shown that mortality rates are ~10% in rats treated with 40 mg/kg MCT. This may be due to the fact that MCT treatment can cause liver toxicity by inducing hepatic parenchymal cell injury (Copple et al., 2003) which can lead to hepatic veno-occlusive disease. Another drawback with the MCT model is the lack of efficacy in mice. This is due to the differences in hepatic metabolism by cytochrome P-450 between the species. To get around this problem, Dumitrascu and colleagues administered the active compound MCTP to mice. Although an early inflammatory stage similar to that observed in the rat was displayed in the mice,

MCTP injection resulted in lung fibrosis with no PH observed (Dumitrascu et al., 2008).

1.2.7 Other animal models of PH

Traditional models of PAH have provided a vast amount of knowledge regarding the development of PAH. However, both the monocrotaline and hypoxic models of PAH lack the plexogenic arteriopathy which characterises the human disease. As a result, newer models have been developed which modify the classic models to include a second “hit” to produce more severe PH and occlusive lesions like those observed in human PAH. In addition to this, genetically modified mice have been used to investigate PH and give an indication as to the role of specific molecules and pathways in the pathobiology of this complex disease.

1.2.7.1 Hypoxia/SU5416 model

The hypoxia/SU5416 model of PH was developed by Taraseviciene-Stewart and colleagues in an attempt to better model the human disease. The model involves exposure to chronic hypoxia along with administration of the VEGF receptor inhibitor Sugen-5416 (SU5416) (Taraseviciene-Stewart et al., 2001). VEGF is a key regulatory factor involved in the maintenance and survival of endothelial cells (Lee et al., 2007). The hypoxia/SU5416 model of PH displays a more severe PH phenotype than hypoxia alone and produces lesions in the rat which are indistinguishable from the plexiform lesions observed in human PAH (Abe et al., 2010). See section 4.1 for a more comprehensive overview of the hypoxia/SU5416 model of PAH.

1.2.7.2 S100A4/Mts1 over-expression in mice

The S100A4/Mts1 gene is a calcium binding protein which confers a metastatic phenotype (Grigorian et al., 1993). Ambartsumian and colleagues produced transgenic mice over-expressing S100A4/Mts1 in all tissues and found that a small proportion of the mice (~5% of the transgenic mice) developed plexiform like lesions in the pulmonary arteries (Ambartsumian et al., 1998), similar to the lesions observed in human PAH. Histologically, the lesions formed in S100A4/Mts1 transgenic mice displayed intimal hypertrophy, occlusion of the lumen and considerable inflammation surrounding the damaged vessels

(Greenway et al., 2004). It was also reported that the development of these lesions in S100A4/Mts1 transgenic mice was absolute; the mice were either completely lesion free or developed these severe plexogenic lesions. In a similar manner, analysis of human pulmonary arteries found S100A4/Mts1 expression was absent in lungs from healthy individuals and patients with early stage PAH, while there was a significant increase of S100A4/Mts1 in lungs from patients with late stage PAH (Greenway et al., 2004). Thus suggesting that S100A4/Mts1 expression may not be involved in the initiation of PH but the gene may have an important role in the development of severe pulmonary lesions. Under hypoxic conditions, S100A4/Mts1 transgenic mice displayed significantly increased RVP, RVH and decreased cardiac output compared to wild type (WT) mice. Interestingly, these parameters persisted in the transgenic mice, even after 3 months recovery in normoxic conditions. Both wild type and S100A4/Mts1 transgenic mice developed similar degrees of pulmonary vascular disease however, arterial changes displayed in the transgenic mice did not regress on exposure to normoxia and the authors suggest that Fibulin-5, a matrix component required for elastin fibre assembly, may play a role (Merklinger et al., 2005).

1.2.7.3 Interleukin-6 over-expression in mice

Interleukin 6 (IL-6) is an inflammatory cytokine (Scheller et al., 2011). Patients with severe PAH have increased levels of IL-6 in the serum and lung expression of IL-6 is increased in the hypoxic rat model of PH (Humbert et al., 1995). In order to assess the role of IL-6 in the development of PH, Steiner and colleagues used transgenic mice specifically over-expressing IL-6 in the lung. The IL-6 transgenic mice displayed elevated RVP, RVH and muscularisation of distal pulmonary vessels, which were further increased by chronic hypoxia. Increased intimal thickness was observed in the transgenic IL-6 mice comprising of pulmonary artery endothelial cells and inflammatory T-cells, leading to a higher number of occluded vessels. This is thought to be due to IL-6 activating pro-angiogenic, pro-proliferative and anti-apoptotic pathways (Steiner et al., 2009). Supporting this data, IL-6 knockout mice exposed to chronic hypoxia displayed reduced RVP, RVH and a decrease in distal pulmonary vessel muscularisation compared to hypoxic wild type mice. Inflammation was also significantly reduced in lungs from IL-6 knockout mice (Savale et al., 2009).

1.2.7.4 BMPR2 mutant mice

As mentioned in Section 1.2.3, mutations within the gene encoding BMPR2 are present in numerous patients with HPAH and IPAH. Many different BMPR2 mutations have been reported from patients with PAH (Nishihara et al., 2002), with the majority predicted to result in a premature termination codon of the BMPR2 transcript (Machado et al., 2001). Due to the human data available, studies have been looking into the effect of BMPR2 deficiency in mice.

Genetic ablation of BMPR2 proves lethal due to epiblast undifferentiation and lack of mesoderm (Beppu et al., 2000). Therefore mice heterozygous for BMPR2 (BMPR2^{+/-}) were studied and one study reported that a 50% reduction in BMPR2 gene expression in the lung caused a mild increase in pulmonary arterial pressure and pulmonary vascular resistance (Beppu et al., 2004). On the contrary, other studies have shown that heterozygous BMPR2 mutant mice do not develop spontaneous PH (Frank et al., 2008, Song et al., 2005). However, it was reported that exposure of BMPR2^{+/-} mice to a secondary insult (e.g. serotonin or inflammation), increased pulmonary artery pressure and pulmonary vascular remodelling (Song et al., 2005, Long et al., 2006). Research then focused on investigating the effect of reducing BMPR2 levels in specific cell types on the development of PH. Mice harbouring a smooth muscle-specific loss of function BMPR2 mutation were found to develop PH with elevated pulmonary artery pressure, RVH and muscularisation of pulmonary arteries at 8 weeks of age compared to wild type mice. There were however no indication of lesions in these mice (West et al., 2004). West and colleagues then went on to generate transgenic mice expressing the inducible BMPR2 mutation R899X (arginine to termination mutation at amino acid 899 in the tail domain) specifically in smooth muscle cells. The R899X nonsense mutation is derived from a human patient family and has been identified in both idiopathic and heritable PAH (Thomson et al., 2000). After 9 weeks of induction, all transgenic mice displayed vascular pruning within the lung. A proportion of the transgenic mice had increased right ventricular pressures along with occlusive lesions comprised of endothelial cells, smooth muscle cells and surrounded by large numbers of macrophages and T-cells (West et al., 2008). High expression of BMPR2 was found in pulmonary endothelial cells and this expression was significantly reduced in plexiform lesions from HPAH patients with a BMPR2 mutation

(Atkinson et al., 2002). As a result, conditional knockout mice were created where the *BMPR2* gene was deleted in pulmonary endothelial cells. A subset of the mice with endothelial *BMPR2* deficiency developed spontaneous PH with increased RVP, RVH and muscularisation of distal pulmonary arteries (Hong et al., 2008).

These data show that a reduction in functional *BMPR2* in either SMCs or ECs is sufficient to induce PH within a subsection of mice. The evidence shown here strengthens the idea that *BMPR2* mutations predispose patients to develop PAH and that other factors are involved in developing PAH. Models of PH using *BMPR2* mutations provide us with a tool for extending our knowledge for studying the genetic aspect of the disease and understanding how these genetic mutations contribute to the pathogenesis of PAH.

Taken together, a great deal of knowledge has been gained from the various animal models of PH, including both the traditional and newly developed models, to provide insight into the complex pathology of PAH. Researchers are slowly moving away from the classic models of PH onto the newer models which incorporate multiple stimuli in order to produce a PH pathology similar to that observed in the human disease. There are of course drawbacks to each experimental model and careful consideration must be given when planning future studies. At present, there is no perfect experimental model of PH which recapitulates all aspects of the human disease. However, use of the current models allows discovery of signalling pathways involved in disease development as well as preclinical evaluation of new therapeutic agents.

1.3 MicroRNAs

1.3.1 Biogenesis of microRNAs

MicroRNAs are small non-coding RNA molecules ~22 nucleotides long that regulate gene expression post-transcriptionally by binding to complementary target messenger RNA (mRNA) (Figure 1.6) (Bartel, 2004, van Rooij and Olson, 2007). MicroRNA biogenesis begins with the transcription of the primary miRNA (pri-miRNA) in the nucleus by RNA polymerase II. The primary transcripts can be over 1kb in length and often contain the sequences for multiple mature miRNAs.

The pri-miRNA is then cleaved by Drosha, a nuclear RNase III enzyme, in a complex along with DiGeorge syndrome critical region gene 8 (DGCR8). DGCR8 is a double stranded RNA-binding domain protein thought to be involved in binding the pri-miRNA to Drosha, allowing cleavage to occur and the formation of an ~70 nucleotide stem loop molecule; the precursor miRNA (pre-miRNA) (Gregory et al., 2004, Han et al., 2004). The pre-miRNA is characterised by a two nucleotide single stranded overhang on the 3' end which is recognised by Exportin 5 and Dicer for further processing (Du and Zamore, 2005). Exportin 5 is a nucleocytoplasmic transport factor which binds pre-miRNA in the presence of RanGTP and exports the precursor molecule into the cytoplasm. Once in the cytoplasm, hydrolysis occurs converting RanGTP into RanGDP and therefore releasing the pre-miRNA from the Exportin 5/RanGTP complex (Yi et al., 2003). From here, the stem loop pre-miRNA can be processed by the cytoplasmic RNase III endonuclease Dicer. Along with the cofactor trans-activating response RNA binding protein (TRBP), Dicer cleaves the pre-miRNA into an ~22 nucleotide miRNA duplex. Subsequently, TRBP mediates binding of this duplex to the argonaute (Ago) protein (Chendrimada et al., 2005) where the mature miRNA is formed by stabilisation of the guide strand (identified by the suffix 5p) while the passenger strand (identified by the suffix 3p) is either degraded or incorporated into the RNA-induced silencing complex (RISC).

The argonaute protein is the principle component of the RISC. The 3'-end of the mature miRNA binds to the PAZ domain of argonaute and directs the silencing complex to target mRNA where one of two fates can be adopted: if complementarity between the miRNA 'seed' sequence and mRNA is complete, mRNA degradation occurs, however, incomplete complementarity results in translational repression. The miRNA 'seed' sequence is defined as nucleotides 2-8 on the 5' end of the miRNA and complementarity and binding of this region to the mRNA target via Watson-Crick base pairing can result in effective regulation of mRNA. In plants, perfect or near-perfect complementarity is usually achieved between miRNA and mRNA targets resulting in mRNA degradation (Rhoades et al., 2002). However in animals the majority of miRNA binding with target mRNA is imperfect with G:U base pair interruptions and single nucleotide bulges commonly observed (Brennecke et al., 2005). As a result of non-complimentary binding, other factors (in addition to seed sequence binding) are thought to play

a role in determining miRNA target recognition, including proximity to sites for co-expressed miRNAs and positioning at least 15 nucleotides from the stop codon in the 3'-untranslated region (3'-UTR) of mRNA (Grimson et al., 2007). One of these key factors is complementary interaction between the miRNA 3' end with target mRNA. This is thought to modulate miRNA binding and is particularly important in distinguishing target genes for miRNA family members (Brennecke et al., 2005). This would explain how miRNAs with identical seed sequences can target independent mRNAs.

1.3.2 Regulation of miRNA function

The 'slicer' activity of the RISC, responsible for cleavage of mRNA when complementarity between miRNA and mRNA is complete, is due to the carboxy terminal PIWI domain of the argonaute protein. This is an RNase H enzyme domain which is involved in cleaving the target RNA providing RISC with nuclease function (Song et al., 2004). Of the four argonaute proteins expressed in humans, only Ago2 appears to have nuclease activity and can directly cleave mRNA as part of the RISC (Meister et al., 2004, Liu et al., 2004). Studies have shown that protein expression can be inhibited *in vitro* in a miRNA-independent manner by tethering argonaute proteins to the 3'-UTR of mRNA. Thus illustrating the importance of the Ago protein in mediating gene silencing and highlighting the principal role of miRNAs within the RISC is directing the silencing complex to the mRNA (Pillai et al., 2004). Another protein, GW182, has been found to bind to the argonaute protein within the RISC and the interaction between Ago and GW182 is essential for miRNA mediated repression and gene silencing (Eulalio et al., 2008). In addition to the pathway described above, specific miRNAs are processed independent of Dicer activity. In particular, miR-451 has a short hairpin precursor molecule of ~42 nucleotides and is directly loaded into Ago2, bypassing the step involving cleavage by Dicer. Pre-miR-451 specifically binds to Ago2 where it is cleaved into the mature miRNA via the endonuclease activity of Ago2 (Cifuentes et al., 2010, Yang et al., 2010).

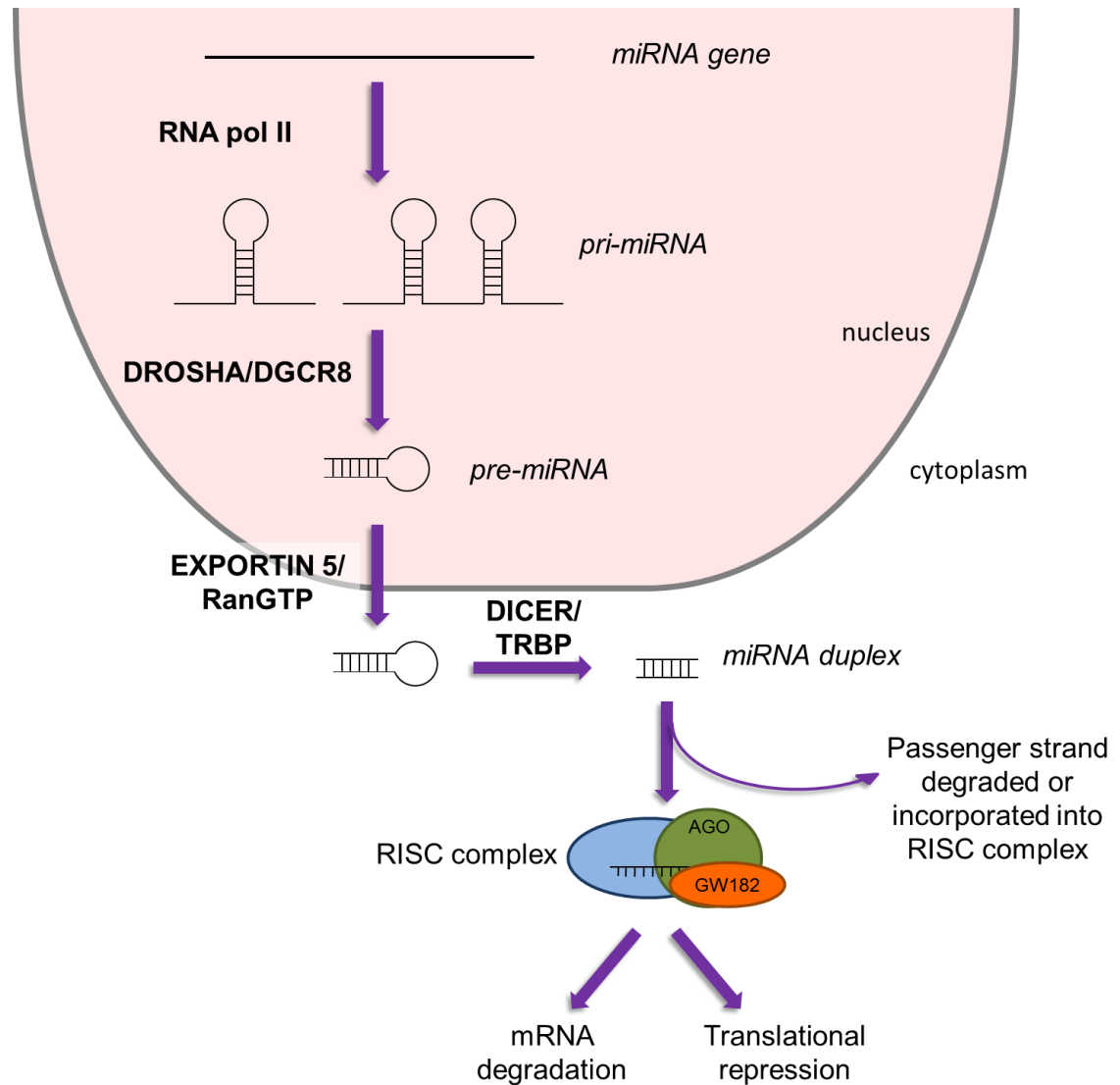


Figure 1.6 – MicroRNA biogenesis pathway.

The primary miRNA (*pri-miRNA*) is transcribed in the nucleus by RNA polymerase II (RNA pol II). This is cleaved by Drosha and cofactor DGCR8 to form the stem loop precursor structure (*pre-miRNA*), which is exported out of the nucleus by Exportin 5 in the presence of RanGTP. Processing by Dicer and TRBP gives rise to a miRNA duplex of approximately 22 nucleotides in length. The mature miRNA is incorporated into the argonaute protein to form the RNA-induced silencing complex (RISC) which targets mRNA to induce mRNA degradation or translational repression. Adapted from (Grant et al., 2013).

Originally it was thought that only the mature guide strand was incorporated into the RISC to exert an effect however, new evidence suggests that there is also a role for the passenger strand (Eulalio et al., 2012, Kos et al., 2012). *In vitro* over-expression of miR-590-3p or miR-199a-3p induced post-natal cardiomyocyte proliferation and re-entry in to the cell cycle therefore elevating the number of cardiomyocytes. Ectopic expression of these miRNA *in vivo* post myocardial infarction caused cardiac regeneration and improved cardiac function (Eulalio et al., 2012). Thus, although a great deal of knowledge is known about the role of the guide miRNA strand, it would appear that both strands of the miRNA duplex have biologically functional roles via regulation of signalling pathways.

The majority of miRNAs regulate gene expression through binding to the 3'-UTR of target mRNA. However, some miRNAs have recently been shown to modulate mRNA targets through binding sites in the 5'-untranslated region (5'-UTR) or coding sequences of the mRNA. *In vitro* studies have shown that introduction of a miRNA binding site at any position along the length of the mRNA (3'-UTR, coding sequences or 5'-UTR) can result in translational repression at a stage downstream of initiation (Lytle et al., 2007, Kloosterman et al., 2004). Within the 5'-UTR of mRNA, there are endogenous sequences complementary to the 3'-end of miRNA and it has been proposed that certain miRNAs are able to target both the 5'-UTR and 3'-UTR binding sites simultaneously (Lee et al., 2009). With regards to the modulation of miRNA in a disease setting, Jin and colleagues reported that miR-138 directly targeted proto-oncogene Fos-like antigen 1 (FOSL1) mRNA in squamous cell carcinoma cell lines through 6 targeting sites; one present in the 5'-UTR, three overlapping in the coding regions and two overlapping sites in the 3'-UTR (Jin et al., 2011). In addition to causing translational repression, some reports indicate that binding of miRNA to 5'-UTR mRNA may in fact cause translational activation. MiR-10a binds to the 5'-UTR of ribosomal protein mRNA and promotes translation. As a result, this miRNA:mRNA interaction may increase global protein synthesis (Orom et al., 2008). Although targeting sites have been found to exist within all areas of the mRNA molecule, the exact mechanism of regulation of miRNA binding to the 5'-UTR or coding sequences of target mRNA is still relatively unknown and requires further investigation.

In addition to the molecules mentioned previously, there are many regulatory proteins which aid or impede the formation of the mature miRNA. The ratio between pre-miRNA and mature miRNA differs between miRNA type and tissue/cell type, therefore indicating that there are different rates of processing and this may be due to the presence or absence of accessory molecules. The Drosha/DGCR8 complex is associated with other proteins, including members of the heterogeneous nuclear ribonucleoproteins (hnRNP). Two of these proteins, hnRNPH1 and hnRNPR, bind directly to the pri-miRNA and elicit opposing effects. Knockdown and over-expression studies in HeLa cells suggest that hnRNPH1 promotes miRNA processing while hnRNPR inhibits miRNA maturation (Volk and Shomron, 2011). Another protein involved in the regulation of miRNA biogenesis is KH-type splicing regulatory protein (KHSRP). KHSRP is a component of both Drosha and Dicer and binds to the terminal stem loop of specific pre-miRNAs with high affinity to facilitate maturation (Trabucchi et al., 2009). On the contrary, the heterodimerisation of nuclear factor 90 (NF90) and NF45 binds directly to the pri-miRNA and prevents Drosha/DGCR8 to access the pri-miRNA, thereby inhibiting the conversion into pre-miRNA and resulting in a reduction in mature miRNA (Sakamoto et al., 2009).

1.3.3 MiRNAs involved in PAH

MiRNAs are essential in the normal development of the lung and maintenance of lung homeostasis. Evidence for this comes from Dicer knockout mice. Global loss of Dicer is embryonically lethal (Bernstein et al., 2003) while conditional knockout of Dicer in lung epithelial cells results in a lack of normal branching (Harris et al., 2006). Thus illustrating that Dicer is critical for lung epithelial morphogenesis. MiRNA expression is regulated differentially in the fetal and adult lung, with a fetal miRNA profile which assists in development of the lung. A subset of miRNAs (miR-134, miR-154, miR-214, miR-296, miR-299, miR-323, miR-337 and miR-370) are of higher abundance in the fetal human lung compared with the adult lung. In a similar manner, the adult lung shows up-regulation of miR-26b, miR-29a, miR-29b, miR-146-3p and miR-187. This miRNA profile is comparable between mice and humans demonstrating that miRNA expression is conserved during lung development (Williams et al., 2007).

MiRNAs are known for their pleiotropic effects and many PAH-relevant stimuli, such as hypoxia and inflammation, can modulate miRNA expression in vascular cells. In response to vascular injury, low oxygen concentrations can result at site-specific regions of the pulmonary vasculature, leading to activation of the transcription factor hypoxia-inducible factor 1 α (HIF-1 α). HIF-1 α promotes the transcription of genes responsible for mediating the adaptive response to hypoxia and a number of miRNAs are induced in this manner (Kulshreshtha et al., 2007). Inflammation is another factor responsible for miRNA dysregulation, with miRNAs being activated as well as targeting inflammatory cytokines and chemokines. One such miRNA is miR-146a, which is transcribed through NF- κ B binding to the promoter region. Mature miR-146a targets TNF receptor-associated factor 6 (TRAF6) and IL-1 associated kinase 1 (IRAK1) which then trigger downstream signalling to activate transcription factors essential to the inflammatory response, including NF- κ B. Thus, miR-146a provides a negative feedback system to tightly regulate the immune response (Taganov et al., 2006). MiRNA regulation is involved in many cellular processes, including migration, proliferation, cell fate and metabolism. The pathology of PAH is extremely complex and through the use of bioinformatics and knockout/over-expression studies, the role and regulation of miRNAs in this disease is slowly being revealed.

MiRNA screening is an effective way in which to study miRNA expression within a tissue under various conditions and allows a miRNA profile to be established for a particular disease. Caruso and colleagues studied the miRNA profile in lung tissue during the development of PH using two rat models of PH. From the microarray, miR-222, miR-30 and let-7f were down-regulated while miR-322 and miR-451 were up-regulated in both the hypoxic and monocrotaline rat models of PH. A similar pattern of miRNA expression was reproduced *in vitro* when pulmonary artery fibroblasts and SMCs were stimulated with PAH-related growth factors or hypoxia (Caruso et al., 2010). Another group reported that miR-450a, miR-145, miR-302b, miR-27b, miR-367 and miR-138 were up-regulated while miR-204 was down-regulated in PASMCs from patients with PAH compared to healthy PASMCs (Courboulin et al., 2011). In contrast, others have used a candidate approach where a specific miRNA is focused on and bioinformatics is used to identify all possible target genes and pathway interactions (Parikh et al.,

2012). These critical studies demonstrate that miRNAs are dysregulated during PAH development and highlight molecules which can be targeted to increase our understanding of the disease and as possible therapeutic targets.

1.3.3.1 MiR-204

One of the first studies to establish a mechanistic link between miRNA expression and signalling pathways involved in PH was performed by Courboulin and colleagues and focused on miR-204. The coding sequence for miR-204 is intronic and located within the human transient receptor potential melastatin 3 (TRPM3) cation channel (Deo et al., 2006). MiR-204 has been shown to act in a pro-apoptotic manner in many types of cancer with down-regulation of miR-204 reported in gastric cancer (Sacconi et al., 2012). In the setting of cancer, miR-204 directly targets the 3'-UTR of anti-apoptotic gene Bcl2 and oncogene Ntrk2. MiR-204 expression also increases the responsiveness of cancer cells to treatment by promoting apoptosis in response to anticancer drugs such as cisplatin and oxaliplatin (Ryan et al., 2012a, Sacconi et al., 2012).

In the pulmonary circulation miR-204 is localised primarily within the smooth muscle layer (Courboulin et al., 2011). Experimental models of PH have shown that miR-204 expression is repressed in the hypoxic and MCT rat models of PH (Caruso et al., 2010) as well as the hypoxic mouse model of PH. Lung tissue and PASMCs from PAH patients show similar down-regulation of miR-204 along with increased PASMC proliferation and resistance to apoptosis. *In vivo* therapeutic modulation of miR-204 was investigated specifically within the lung via intratracheal nebulisation of synthetic miR-204. Elevation of pulmonary miR-204 expression in established PH lowered pulmonary artery pressure, right ventricular wall thickness and reduced medial hypertrophy of pulmonary arteries (Courboulin et al., 2011).

The beneficial effect miR-204 exerts on PASMC proliferation and apoptosis is thought to be via the Src-STAT3-NFAT activation pathway. Within the layers of the pulmonary vessels, release of PAH-induced growth factors such as angiotensin II, ET-1 and PDGF stimulate activation of the transcription factor signal transducer and activator of transcription 3 (STAT3). STAT3 is responsible for the down-regulation of miR-204 observed during PAH. MiR-204 has been

shown to directly bind to the Src activator, SHP2. Without miR-204 repression, Src kinase activation via SHP2 leads to STAT3 activation (Couboulin et al., 2011). This positive feedback of STAT3 on miR-204 expression may explain why the development and progression of PAH is so severe and results in a sustained phenotype. Once STAT3 activation reaches a maximal level, increased expression of nuclear factor of activated T-cells (NFATc2) and oncogene Pim1 are observed, both of which stimulate activation and nuclear translocation of NFATc2 (Paulin et al., 2011a). Activated NFATc2 can contribute to the PH phenotype via two separate and well-described pathways. Bonnet and colleagues discovered that activation of NFATc2 down-regulates the expression of voltage-sensitive potassium channel Kv1.5, leading to membrane depolarisation, an increase in intracellular calcium (Bonnet et al., 2007) and subsequent PASM C proliferation (Platoshyn et al., 2000). In addition to increased cellular proliferation, PAH is also characterised with decreased PASM C apoptosis. Apoptosis is most commonly instigated by a decrease in mitochondrial membrane potential and increase in pro-apoptotic mediators. NFATc2 activation increases levels of anti-apoptotic Bcl2 causing hyperpolarisation of PASM C mitochondrial membrane potential to confer resistance to apoptosis and contributing to the PH phenotype (Bonnet et al., 2007). Activation of the miR-204-Src-STAT3-NFAT pathway in PH development has been confirmed in experimental models of MCT-induced PH with inhibition of STAT3 activity (using DHEA), Pim1 or NFAT activity (using the indirect NFAT inhibitor, cyclosporine A) reducing indices of PH (Paulin et al., 2011a, Paulin et al., 2011b, Bonnet et al., 2007). These critical studies show a clear role for miR-204 in regulating PASM C proliferation and apoptosis through activation of the STAT3/NFAT pathway. The complex nature of this signalling pathway provides a plethora of molecules which could be targeted as future therapy for pulmonary arterial hypertension.

1.3.3.2 MiR-17/92

Another miRNA which mediates its effects in a STAT3 dependent manner is miR-17/92. MiR-17/92 is a polycistronic miRNA cluster located on human chromosome 13 with the primary transcript yielding six mature miRNAs; miR-17, miR-18a, miR-19a, miR-20a, miR-19b-1 and miR-92-1 (Tanzer and Stadler, 2004). With regards to PAH, the inflammatory cytokine IL-6 activates STAT3 in human PAECs, which can bind directly to a highly conserved STAT3 binding site in the promoter

region of miR-17/92. Two specific members of the cluster, miR-17-5p and miR-20a target the 3'-UTR of BMP2 leading to down-regulation of BMP2 protein and pulmonary vascular remodelling (Brock et al., 2009). This illustrates a possible mechanism to explain the loss of BMP2 during PAH development. In addition to this, miR-204 has been reported to regulate IL-6 secretion and therefore may in turn regulate BMP2 expression (Couboulin et al., 2011). Both miR-17/92 and miR-204 are activated via distinct mechanisms however, both pathways involve common mediators and this highlights the importance of interconnectivity between miRNA systems to affect cellular processes.

Activation of the miR-17/92 cluster is through the oncogene c-Myc which controls cellular proliferation and apoptosis. Members of the miR-17/92 cluster (specifically miR-17-5p and miR-20a) directly target transcription factor E2F1, which is involved in G1 to S cell cycle progression. The E2F transcription family have also been shown to induce c-Myc and activate transcription of the miR-17/92 promoter region, therefore providing a feedback mechanism for strict regulation of proliferation (Brock et al., 2009, Woods et al., 2007). Increased expression of the miR-17/92 cluster has been reported in numerous cancers, including human B-cell lymphoma (He et al., 2005) and this up-regulation of miR-17/92 is thought to contribute to the pro-proliferative and anti-apoptotic phenotype observed in tumour cells. Other targets of miR-17-5p include the cell cycle regulator cyclin dependent kinase inhibitor (p21) and pro-apoptotic protein BIM (Bcl2-interacting mediator of cell death). Over-expression of miR-17 in PASMCs resulted in down-regulation of target gene p21 accompanied with increased proliferation (Pullamsetti et al., 2012) while conversely, knockdown of miR-17 in neuroblastoma cells increased BIM expression at both the mRNA and protein level (Fontana et al., 2008). Knockdown of miR-17 *in vivo* using antagomiR-17 reduced right ventricular pressure, pulmonary artery remodelling and expression of p21 in both the mouse hypoxic and rat MCT model of PH (Pullamsetti et al., 2012).

The exact mechanism of action of miRNA clusters is still relatively unknown as although they are transcribed together, each miRNA has the capability to target many different genes and indeed be regulated individually by post-transcriptional mechanisms. The modulation of specific miRNAs within the miR-

17/92 cluster requires further investigation before we can fully elucidate the role of these miRNAs within the pulmonary vasculature.

1.3.3.3 MiR-21

MiR-21 is an intronic miRNA with the primary transcript located within the transmembrane protein 49 (TMEM49) gene on human chromosome 17 with its own promoter region and termination sequence (Kumarswamy et al., 2011). Up-regulation of miR-21 has been observed in many pathological conditions, including heart failure (Thum et al., 2008), cardiac remodelling (Patrick et al., 2010a) and breast cancer (Yan et al., 2008). Considerable research has been carried out regarding the role of miR-21 in pulmonary arterial hypertension using both cell culture and *in vivo* models. MiR-21 expression is elevated in hypoxia exposed hPAECs (Parikh et al., 2012), hPASMCs (Sarkar et al., 2010) and lung tissue from experimental models of PH (Yang et al., 2012). *In situ* hybridisation also shows increased miR-21 staining in small pulmonary arteries (<200 μ m) from human PAH patients (Parikh et al., 2012).

MiR-21 has been shown to modulate PASMC proliferation, migration and contractility and it is through these mechanisms that miR-21 is thought to contribute to the PH phenotype. Over-expression of miR-21 in PASMCs (as observed in hypoxic hPASMCs and diseased PASMCs) caused a reduction in target genes SPRY2, PDCD4 and PPAR α to stimulate proliferation, migration and prevent apoptosis (Sarkar et al., 2010, Cheng et al., 2010). MiR-21 is also modulated by BMP signalling pathways in a post-transcriptional and ligand dependent manner. TGF- β and BMP signalling activates R-Smads (Smad2/3 in response to TGF- β , Smad1/5 in response to BMP) initiating binding of R-Smads to pri-miR-21 via RNA helicase p68, a component of Drosha. This stabilises the pri-miR-21/Drosha complex and promotes the processing of pri-miR-21 into pre-miR-21, therefore increasing expression of pre-miR-21 and mature miR-21 without altering pri-miR-21 levels (Davis et al., 2008). Within hPASMCs, miR-21 then directly targets members of the dedicator of cytokinesis (DOCK) 180-related protein superfamily, in particular DOCK4, DOCK5 and DOCK7, to modulate cell migration and contractility (Kang et al., 2012). As well as being modulated by BMP signalling, BMPR2 is also targeted by miR-21 thereby adding another

regulatory mechanism into this complex pathway (Yang et al., 2012, Parikh et al., 2012).

Due to the increase in miR-21 expression during PH development, the effect of silencing miR-21 on PH progression and development was investigated. However, results from these studies produced conflicting results. Yang and colleagues silenced miR-21 *in vivo* using an LNA-modified antimiR both prior to and post hypoxic exposure and reported a decrease in hypoxia-induced PH. A reduction in muscularisation of small pulmonary arteries was accompanied by a decrease in ET-1, α -SMA and SM22 α (Yang et al., 2012). Use of antagomiR-21 in hypoxia-induced PH showed similar results with a reduction in pulmonary artery pressure and vascular remodelling (Pullamsetti et al., 2012). Contrary to this, Parikh and colleagues exposed miR-21 null mice to hypoxia/SU5416 insult and reported an exaggerated PH phenotype, with increased RVP, RVH and pulmonary remodelling evident. One explanation for this augmented phenotype is due to RhoB kinase activation. MiR-21 directly targets RhoB, a small GTPase which is critical in actin-dependent processes. Inhibition of miR-21 in hPAECs results in an increase in RhoB protein, therefore increased Rho kinase activation and phosphorylation of myosin phosphatase culminating in vasoconstriction. Furthermore, Rho kinase activation down-regulates endothelial nitric oxide synthase leading to pulmonary vasoconstriction (Parikh et al., 2012). Use of RhoB knockout mice support this theory with mice genetically void of RhoB displaying a diminished PH phenotype in response to chronic hypoxia (Wojciak-Stothard et al., 2012).

From the studies mentioned here, there is a lot of controversy surrounding the role of miR-21 in the pulmonary vasculature and how best to therapeutically target this miRNA. The variation between study conditions may provide a possible explanation as to the opposing results obtained. For example, strain and species differences as well as gender are important factors which can influence biological outcomes. Different methods were also used to modulate miR-21 levels *in vivo* and therefore must be considered. Nevertheless, it is clear that miR-21 does indeed play an integral part in both PAEC and PASMC proliferation, migration and contractility and is an essential miRNA involved in PH development.

1.3.3.4 MiRNAs as biomarkers

MiRNA expression is altered within tissues during disease pathology and it has recently been reported that circulating miRNAs can be detected in the plasma, making them ideal candidates for use as biomarkers. Circulating miRNAs are highly stable and resistant to harsh experimental conditions, including extremes of pH and boiling. In addition to this, plasma miRNAs are resistant to nuclease activity (Chen et al., 2008), suggesting that miRNAs are transported in the plasma in a form to prevent degradation. Originally it was thought that plasma miRNAs were encapsulated in vesicles derived from the plasma membrane, such as exosomes, microparticles and apoptotic bodies. These vesicles protect the miRNA from RNase degradation and have been found to have biologically functional roles in intercellular communication (Skog et al., 2008, Valadi et al., 2007, Zerneck et al., 2009). Vesicular transfer of miRNAs is important to regulate paracrine signalling of neighbouring cells. Reports have shown that tumour cells release exosomes during disease and miRNA expression within these vesicles correlates with the tumour profile (Skog et al., 2008). More recently, circulating miRNAs have been separated into two classes; vesicle associated miRNAs and non-vesicle associated miRNAs. Arroyo and colleagues found that almost 90% of circulating miRNAs exist in protein complexes, rather than within vesicles. Using differential ultracentrifugation and size-exclusion chromatography, it was found that the majority of plasma miRNAs form a complex with the RNA binding protein Ago2 (an essential component of the miRNA maturation pathway) (Arroyo et al., 2011). Circulating miRNAs have also been shown to form complexes with high density lipoprotein (HDL) for transport in the circulation (Vickers et al., 2011). The exact mechanisms which release Ago2-miRNA complexes from the cell or allow HDL to load miRNAs are currently unknown however, it is clear that association of circulating miRNAs with these proteins provides protection against degradation and may confer a biological role.

A reliable biomarker is defined as a characteristic that is objectively measured and evaluated as an indicator of normal biological processes, pathogenic processes or pharmacological responses to a therapeutic intervention (FDA, 2008). Biomarkers must be easily accessible and circulating miRNAs are stable and can be readily detected in plasma therefore a blood sample is all that is

required. This also has the advantage that plasma miRNA expression can be tested periodically. Measurement of the candidate biomarker must also be highly sensitive and specific and miRNA levels are quantified easily by quantitative real time polymerase chain reaction (qRT-PCR) and microarray analysis. Another key aspect required for biomarkers is that the molecule must be detected early on in disease pathology and changes in circulating miRNA levels have been reported early after tissue injury (Wang et al., 2010). There are of course difficulties which arise when analysing miRNAs from serum or plasma samples. One of the major challenges is the lack of a standard reference molecule, as expression of the normal standard molecules often changes in plasma samples under diseased conditions (Zampetaki and Mayr, 2012). Without a standard to compare all samples to, precision and accuracy of results can be reduced. In order to overcome this problem, synthetic miRNAs are often used in a spike-in normalisation method, using miRNAs from *C.elegans*. However, these exogenous miRNAs are not protected from the nuclease activity present in the plasma and therefore may not be as stable as endogenous miRNAs.

Circulating miRNAs have already been proposed as biomarkers for a number of diseases. Expression of miR-423-5p is significantly up-regulated in the plasma of patients with heart failure and levels are correlated to the NYHA classification (Tijssen et al., 2010) while miR-208a is undetected in healthy volunteer plasma but is elevated following an acute myocardial infarction (Wang et al., 2010). A plasma miRNA signature has also been determined for patients suffering from type 2 diabetes mellitus, characterised by loss of endothelial miR-126 (Zampetaki et al., 2010). Wang and colleagues studied the potential for using circulating miRNAs as biomarkers for toxin-induced liver injury. Plasma expression of miR-122 and miR-192 (levels of which are elevated in the liver) correlated to the stage of liver degeneration and showed a dose and time dependent change which was detected earlier than currently used biomarkers (Wang et al., 2009). With regards to PAH, miR-150 expression is significantly reduced in total plasma as well as in circulating microvesicles from PAH patients. Furthermore, miR-150 plasma expression is correlated with 2 year survival and is a significant predictor of survival in patients with PAH (Rhodes et al., 2013).

Once the plasma miRNA profile is determined for specific diseases, this may improve the diagnostic procedure and help detect changes earlier than the current methods in use. It may also allow clinicians to follow disease progression more closely due to the ease of sampling and sensitivity of detection of plasma miRNA and monitor the effects of the treatment administered. Of course, questions still need to be answered on the exact role of these circulating miRNAs, whether they play a role in disease or are simply novel diagnostic markers. Further work is also required to establish how early the plasma miRNA profiles arise.

1.3.4 MiRNAs as therapeutic targets

From the studies described above, miRNAs play an important role in tissue homeostasis and miRNA expression is often dysregulated during disease pathogenesis. Therefore, research has focused on potential therapeutic approaches which could be adopted to target the miRNA pathway. MiRNAs are small molecules of known sequence and well conserved making them ideal targets for drug development.

One method used to therapeutically modulated miRNA expression is through miRNA mimics, which enhance endogenous miRNA function and are used to re-express miRNAs which are down-regulated during disease (Figure 1.7). Mature miRNA mimics are synthetic molecules where the passenger strand is chemically modified to promote uptake into the cell (e.g. conjugating the miRNA duplex to cholesterol) while the guide strand is left unmodified (van Rooij and Olson, 2012). Of course, modification must be limited so that the synthetic miRNA is still biologically functional in the cell. Precursor miRNA mimics can also be used to stimulate miRNA biogenesis and increase mature miRNA expression by binding to the miRNA processing complexes within the cell. One of the most effective methods for increasing miRNA expression is using adeno-associated virus (AAV). AAVs are appealing viral vectors to use as there are numerous AAV serotypes which display varying tropism for different organs (Zincarelli et al., 2008) allowing targeting of the therapeutic effect to specific tissues. AAV vectors can be modified with tissue-specific promoters to limit exposure to particular cell types and AAVs also provide continuous transgene expression. Systemic administration of AAVs to over-express miR-26a, a miRNA which is down-

regulated in hepatocellular carcinoma cells, reduced cancer cell proliferation, promoted tumour cell apoptosis and prevented further liver cancer progression (Kota et al., 2009).

Another key approach used to therapeutically modulate miRNA expression *in vivo* is by using antimiRs to reduce endogenous miRNA levels. AntimiRs are single-stranded, chemically modified oligonucleotides which are complementary to miRNA. AntimiRs bind to mature miRNA to form a duplex and prevent the miRNA binding to target mRNAs (Figure 1.7). There are different chemistries used to design antimiRs, with the majority including modifications to enhance RNA binding, increase stability and facilitate cellular uptake. Phosphorothioate backbone linkages are included to increase stability of the antimiR. High affinity 2' sugar modifications, such as 2'-*O*-methylation, promote nuclease resistance and increase antimiR:miRNA duplex melting temperature, therefore preventing dissociation of the duplex at lower temperatures and ensuring miRNA inhibition. Locked nucleic acid (LNA) is another 2' sugar modification which contains an extra bridge between the 2' oxygen and 4' carbon which "locks" the ribose in the 3'-endo conformation. This conformation change increases the binding for complementary RNA and significantly increases duplex melting temperature (van Rooij and Olson, 2012). AntimiRs which are cholesterol conjugated and contain 2'-*O*-methylation with phosphorothioate backbone linkages are called antagomiRs. These antagomiRs are efficient, long lasting and specific in silencing miRNAs *in vivo* (Krutzfeldt et al., 2007). The first miRNA targeted treatment to enter clinical trials is miravirsen, a LNA-modified antimiR which targets miR-122, a miRNA which is highly expressed in the liver and involved in the replication of hepatitis C viral RNA (Jopling et al., 2005). The phase 2a clinical study, funded by Santaris Pharma, showed that miravirsen was both safe and efficacious in patients with hepatitis C virus and provided prolonged antiviral activity (Janssen et al., 2013).

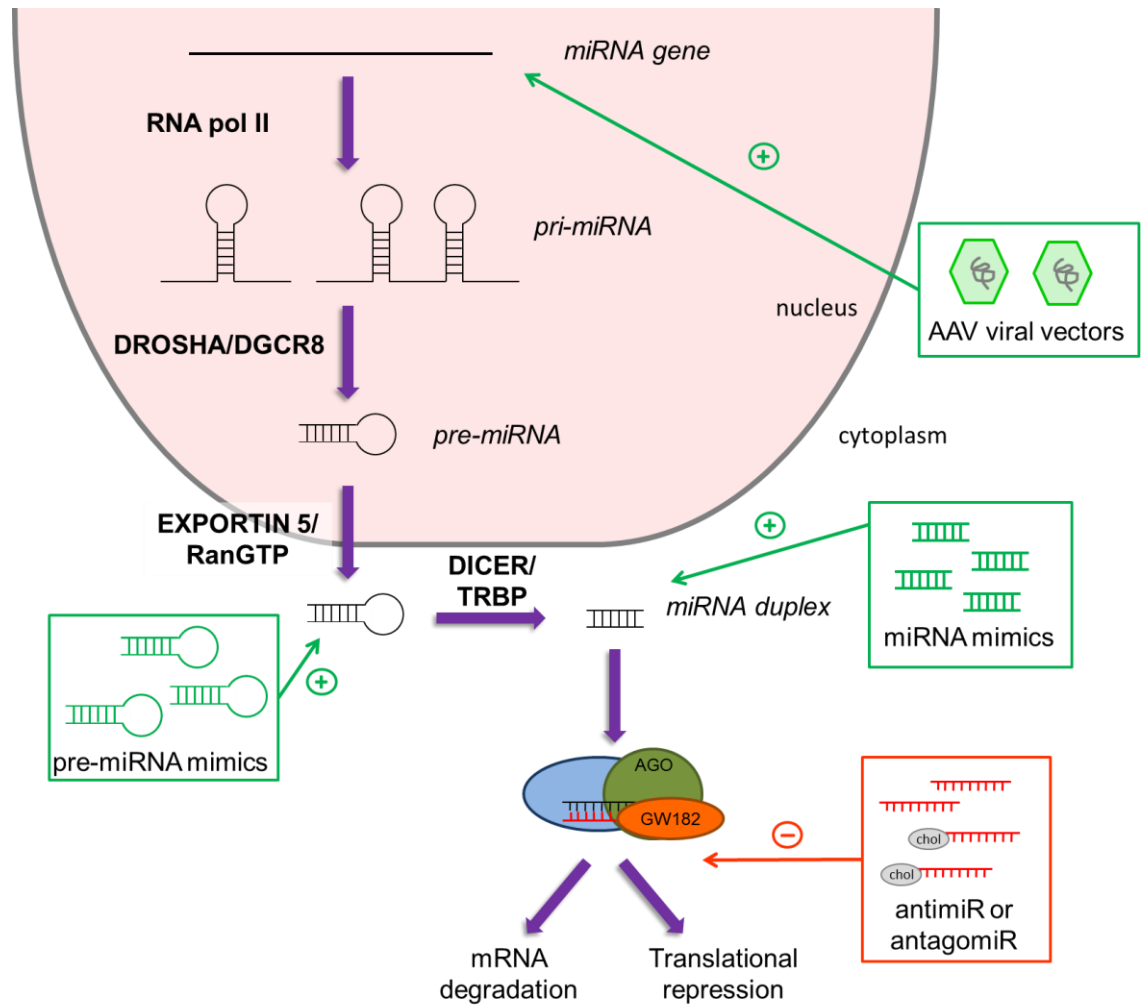


Figure 1.7 – MiRNA targeted treatment.

MiRNA function can be modulated *in vivo* to re-express or inhibit miRNAs which are dysregulated during disease development. MiRNA biogenesis can be enhanced with the use of AAV viral vectors or pre-miRNA or mature miRNA mimics which are recognised in the same manner as endogenous miRNAs. MiRNA function is inhibited by the use of antimiRs, which are antisense oligonucleotides complementary in sequence to the mature miRNA and prevent binding of miRNA to target mRNA. AntagomiRs are cholesterol conjugated antimiRs and work in a similar manner to antimiRs. Adapted from (Grant et al., 2013).

The most significant advantage of therapeutically targeting miRNAs is their broad spectrum of action. MiRNAs can target hundreds of genes (Doench and Sharp, 2004) and this would allow modulation of a multitude of different pathways involved in disease initiation and progression. However, this can also be a drawback with targeting miRNAs directly and may result in off-target effects. For use in PAH, direct targeting of the miRNA therapy via local delivery to the lung is essential to minimise off target effects. One way this can be achieved is through intratracheal delivery which will deliver the miRNA therapy directly into the pulmonary system. Another way to target treatment to the lung is through complexing the miRNA therapy with a lipopolyamine (such as Staramine) which can then be administered intravenously. MiRNA delivery via Staramine is distributed across all organs however, the clearance rate from the lung is much slower than in other tissues leading to an accumulation of drug within the lung (Polach et al., 2012).

MiRNA modulation in a cell type or tissue distinct from the target cell can result in deleterious off-target effects via regulation of biological pathways not involved in the disease process. This effect can be limited through use of tissue-specific promoters to reduce unwanted effects. Alternatively, targeting of specific miRNA genes may overcome this problem and result in a more selective response and reduce disease severity. The potential to target miRNAs therapeutically is great and further research will hopefully generate novel therapeutic agents selective and specific in action.

1.4 Aims

Previously, studies within this laboratory have shown that miRNAs are dysregulated within the lung during the development of PH using the hypoxic and monocrotaline rodent models of PH (Caruso et al., 2010). Therefore the principle research aim of this study was to determine the role of specific miRNAs within the pulmonary vasculature using cell culture and rodent models of PH. The specific aims of this project were:

- To establish a role for miR-451 in the development of PH using both *in vitro* and *in vivo* techniques.
- To evaluate the miRNA profile within pulmonary and cardiac tissue during the development of PH using the mouse and rat hypoxia/SU5416 model of PH.
- To determine the role of miR-145 in the development of PH in the rat hypoxia/SU5416 model of PH.

2 Materials & Methods

All experimental procedures conform with the United Kingdom Animal Procedures Act (1986) and to the 'Guide for the Care and Use of Laboratory Animals' published by the US National Institutes of Health (NIH publication No. 85-23, revised 1996). All transgenic mice were bred under the project licence 60/3752 held by Professor A.H. Baker (University of Glasgow, UK). *In vivo* procedures using the hypoxic model of PH were conducted under project licence 60/3773 held by Professor M.R. MacLean (University of Glasgow, UK) while all *in vivo* procedures using the hypoxia/SU5416 model of PH were performed under project licence 70/7182 held by Dr Matthew Thomas (Novartis Pharmaceuticals Ltd, Horsham, UK). Experimental procedures using human pulmonary artery smooth muscle cells conform to the principles outlined in the declaration of Helsinki.

2.1 Chemicals

All chemicals unless otherwise indicated were obtained from Sigma-Aldrich (Dorset, UK). All tissue culture reagents were obtained from Gibco (Paisley, UK) unless otherwise stated. All transfection reagents were purchased from Life Technologies (Paisley, UK) unless stated otherwise.

2.2 Generation of Ad-miR-451

Recombinant adenoviruses targeting human or rat miR-451 were created and used to over-express miR-451 *in vitro*. The stem loop precursor sequence of human miR-451 or rat miR-451 was cloned into the pAdEasy-1 vector using the pAdEasyTM Adenoviral Vector System (Agilent Technologies, Berkshire, UK).

2.2.1 Generation of Ad5 vector containing miRNA insert

The first step in the cloning procedure was to ligate the pre-miR-451 sequence into the pcDNA3.1(+) vector using In-Fusion technology (Clontech, Mountain View, USA) (Figure 2.1). The stem loop miRNA precursor sequence (GeneArt, Paisley, UK) had a start/kozak and stop sequence added as well as restriction sites and 15 nucleotides homologous to pcDNA3.1(+) using In-Fusion primers (Table 2.1) and amplified by polymerase chain reaction (PCR). The PCR product was run on a 1% agarose gel and purified by gel extraction (Wizard[®] SV Gel and

PCR Clean-Up System; Promega, Madison, USA). The pcDNA3.1(+) vector was linearized by double restriction digest with *EcoRV* and *HindIII* and purified by gel extraction. Ligation of miRNA insert with vector followed by transformation into Top10 competent cells (Invitrogen, Paisley, UK) was performed as detailed in the In-Fusion protocol. The transformation process propagates the vector (containing the insert) in bacterial cells and the transformation product was grown on Ampicillin agar plates. Colonies were chosen and small scale preparation of plasmid DNA was performed using QIAprep Spin Miniprep Kit (Qiagen, Crawley, UK) followed by large scale preparation of plasmid DNA using QIAGEN Plasmid Maxi Kit.

The miRNA insert was then cloned into a shuttle plasmid, pShuttleCMV (Agilent Technologies) (Figure 2.1). This plasmid was linearized by restriction digest with *EcoRV* and *HindIII*, followed by gel extraction purification. In the same way, the miRNA insert was prepared by digesting the DNA product from the ligated pcDNA3.1(+) and insert with *EcoRV* and *HindIII*. The digestion product was separated on a 2% agarose gel and small miRNA insert was purified by gel extraction. Ligation of pShuttleCMV vector and the miRNA insert was performed using Rapid Ligation Kit (Roche Applied Science, West Sussex, UK) according to manufacturer's instructions and transformed into Top10 competent cells. Transformation products were streaked on Kanamycin agar plates. Colonies were picked and miniprep DNA was prepared, followed by maxiprep DNA.

The next step in the cloning procedure was to insert the miRNA sequence into the large pAdEasy-1 vector (Figure 2.1). The pAdEasy-1 vector contains the Ad5 genome and has the E1 and E3 regions deleted. These are the regions required for viral replication and escaping host immunity, respectively. The pShuttleCMV vector (containing miRNA insert) was linearized by restriction digest with *EcoRI* and electroporated into BJ5183-Ad1 electrocompetent cells (Stratagene, La Jolla, USA). These bacterial cells express active recombination genes and are pre-transformed with the pAdEasy-1 viral plasmid, therefore allowing homologous recombination to occur between the pShuttleCMV and pAdEasy-1 plasmid. Recombinant products were grown on kanamycin agar plates and small colonies were picked. Positive recombinants were retransformed into Top10

competent cells to increase the yield of DNA. DNA was isolated by miniprep and then maxiprep extractions.

Table 2-1 - In-Fusion primers used to add the start/kozak, stop and restriction site sequences to the precursor miRNA and for amplification of miR-451 stem loop in human and rat.

Primer	Sequence
Human miR-451 Forward	5'CTAGCGTTTAAACTTAAGCTTGGATCCACGCGTACCATG GCTTGGGAATGGCAAGGAAAC 3'
Human miR-451 Reverse	5'GCCGCCACTGTGCTGGATATCCTCGAGATCGATAAAAAA CTATATGGGTATAGCAAGAGAACC 3'
Rat miR-451 Forward	5'CTAGCGTTTAAACTTAAGCTTGGATCCACGCGTACCATG GTTTGGGAATGGCGAGGAAAC 3'
Rat miR-451 Reverse	5'GCCGCCACTGTGCTGGATATCCTCGAGATCGATAAAAAA CTATGTGGGAGCAGCAAGAGAAC 3'

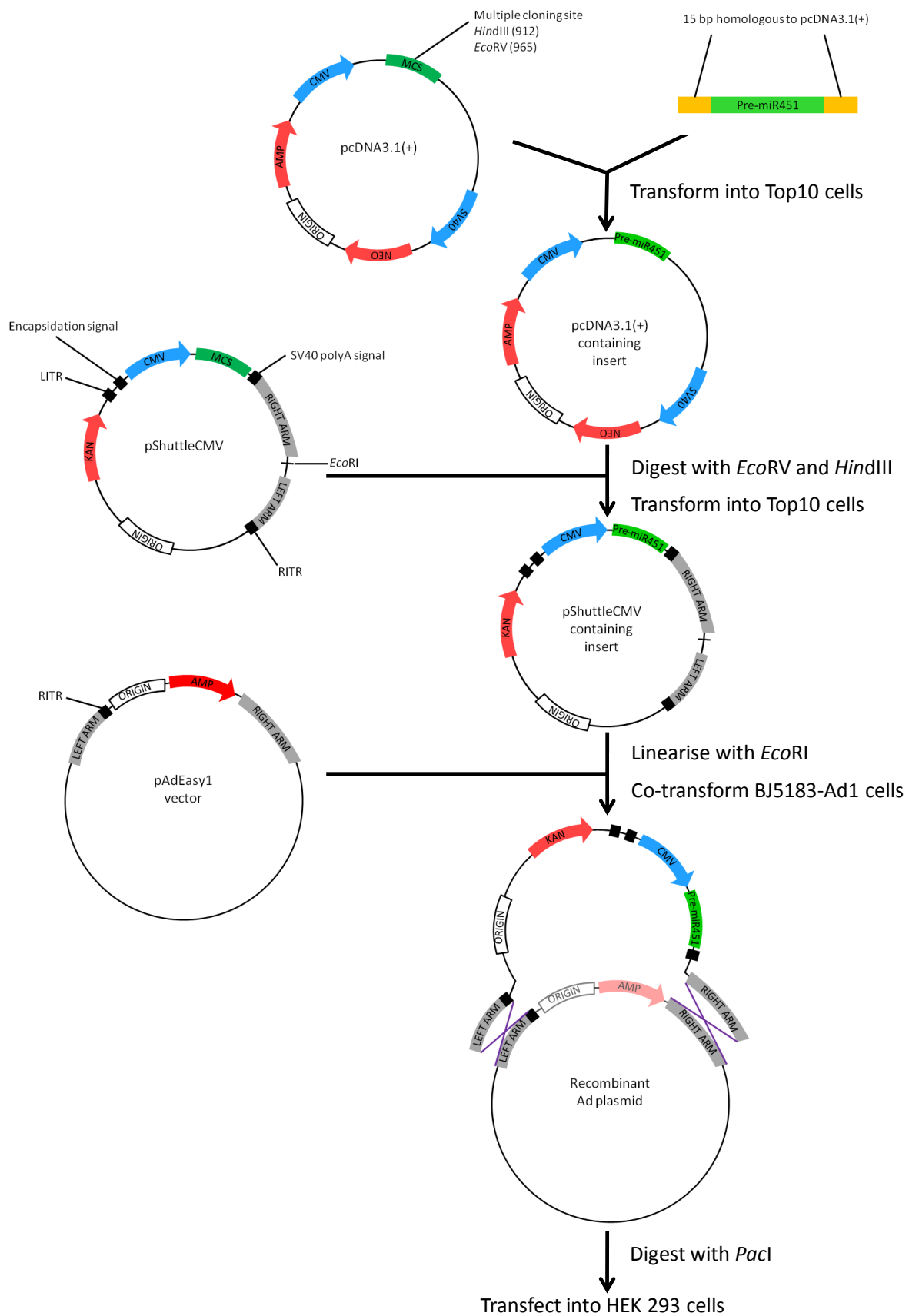


Figure 2.1 – Schematic diagram illustrating the production of recombinant adenovirus containing precursor miR-451.

2.2.2 Generation of crude adenovirus stock

Recombinant adenoviral plasmid DNA was then digested with Pac1 to linearize the plasmid and expose the inverted terminal repeats, which is necessary before transfection into cells. Human embryonic kidney (HEK) 293 cells produce the adenoviral E1 viral assembly gene in *trans*, therefore allowing production of infectious virus particles. Transfection of *PacI* digested plasmid DNA into 80% confluent HEK293 cells was performed in 6-well plates using Lipofectamine[®] 2000 Transfection Reagent following manufacturer's instructions. Transfected cells were monitored for cytopathic effects and the formation of viral plaques. Once plaques had formed, cells were harvested and exposed to three freeze/thaw cycles (-80°C and 37°C, respectively) in order to release the adenovirus from the cells. Centrifugation was performed at 4,500 x g for 5 min to pellet cellular debris and the supernatant was added to two T150 flasks of HEK293 cells to expand the viral population. Once the majority of the cells were infected, cells were harvested, exposed to three freeze/thaw cycles and centrifuged as before. The supernatant was then added to twenty-five T150 flasks in order to further expand the virus. Once cells were infected, cells were collected, centrifuged at 800 x g for 10 min and the pellet was resuspended in phosphate buffered saline (PBS). Equal volume of Arklone P was added and the cells were inverted 10 times. Cells were centrifuged for 10 min at 1,500 x g and then the top adenoviral layer was isolated.

2.2.3 Adenovirus purification

This crude adenovirus stock was then further concentrated and purified by centrifugation on caesium chloride (CsCl) density gradients. The adenoviral stock was placed above layered caesium chloride densities (1.40 g/ml and 1.25 g/ml) and spun by ultracentrifugation at 100,000 x g for 1.5 h at 18°C (Beckman Coulter Optima L-80 XP Ultracentrifuge). The adenovirus purifies in a white band between the two CsCl layers and was removed carefully. The adenovirus was then purified in a second CsCl gradient, where the adenovirus was placed on top of 1.34 g/ml CsCl and spun by ultracentrifugation at 100,000 x g at 18°C for 18 h. The adenovirus band was once again removed and dialysed in a Slide-A-Lyzer (ThermoScientific, Pittsburgh, USA) cassette for 2 h in 1 x TE. Further dialysis was then performed overnight in 1 X TE with 10% glycerol to remove any CsCl

contamination. The virus was then removed from the Slide-A-Lyzer cassette and stored at -80°C.

Sequencing and restriction digests were performed throughout the cloning procedure and virus production to confirm that the adenovirus contained the correct precursor sequence.

2.2.4 Calculation of total viral particle titre

Viral particle titre (vp/ml) was assessed using a microBCA assay (MicroBCA™ Protein Assay Kit, ThermoScientific) following manufacturer's instructions. Protein standards of bovine serum albumin (BSA) were prepared at concentrations ranging from 0.5 µg/ml to 200 µg/ml. These reference samples were used to generate a standard curve. A working reagent was prepared by mixing reagent A, reagent B and reagent C at a ratio of 25:24:1, respectively. Protein standards (150 µl) or dilutions of the adenovirus stock (1 µl, 3 µl or 5 µl made up to 150 µl with PBS) were then added to the working reagent (150 µl) in a 96-well plate, mixed thoroughly, protected from light and incubated at 37°C for 2 h. Absorbance was measured at 570 nm using the Wallac 1420 Victor²™ plate reader (Perkin Elmer, Waltham, USA). Samples and standards were measured in duplicate with average values taken. Protein concentration of the virus was determined using the standard curve generated by the BSA protein standards. Protein concentration was converted to viral particle/ml (vp/ml) using the formula: 1 µg protein = 1×10^9 vp (Von Seggern et al., 1998).

2.2.5 Titration of adenovirus by end-point dilution

The number of infective particles was determined by titration of adenovirus using end-point dilution in HEK293 cells and expressed as plaque forming units (pfu/ml). Serial dilutions of adenovirus were made in full media, ranging from 1×10^{-2} to 1×10^{-11} dilution. These adenoviral dilutions were added to 50-60% confluent HEK293 cells in a 96 well plate (100 µl per well) and incubated at 37°C for 18 h. After this incubation, adenovirus containing media was removed and replaced with fresh media every 2-3 days. Cells were checked daily for the appearance of plaques. Once cytopathic effects were observed within a well, the media was no longer replaced with fresh media. After 8 days incubation the

number of wells containing plaques was determined and the titre of the adenovirus stock was calculated using the equations below.

$$\text{Proportionate distance} = \frac{(\% \text{ positive above } 50\% - 50\%)}{(\% \text{ positive above } 50\% - \% \text{ positive below } 50\%)}$$

$$\text{LogID}_{50} = \log \text{ dilution above } 50\% + (\text{dilution factor} \times \text{proportionate distance})$$

$$\text{Hence, ID}_{50} = 10^x$$

$$\text{TCID}_{50} \text{ per } 100 \mu\text{l} = 1/10^x$$

$$\text{TCID}_{50} \text{ per } 1 \text{ ml} = (1/10^x) \times 10$$

Note: 1 TCID₅₀ is ~ 0.7 pfu

$$\text{Therefore, pfu/ml} = (\text{TCID}_{50} \text{ per } 1 \text{ ml}) \times 0.7$$

2.3 Cell culture

All cells were handled under sterile conditions using class II biological safety cabinets (Holten Safe 2010). Cabinets were cleaned before and after use with dH₂O and 70% ethanol. All cells were cultured in a humidified incubator with a constant supply of 5% CO₂ at 37°C.

HeLa cells were cultured in Dulbecco's Modified Eagle Medium (DMEM) supplemented with 10% (v/v) fetal calf serum (FCS), 100 U/ml penicillin, 100 µg/ml streptomycin, 2 mM L-glutamine and 1 mM sodium pyruvate. Proximal human pulmonary artery smooth muscle cells (hPASMCs; Lonza, Slough, UK) from control patients were cultured in smooth muscle cell medium 2 (Promocell, Heidelberg, Germany) containing 15% FCS, 0.5 ng/ml epidermal growth factor, 2 ng/ml basic fibroblast growth factor, 5 µg/ml insulin, 100 U/ml penicillin, 100 µg/ml streptomycin, 2 mM L-glutamine and 1 mM sodium pyruvate.

Cell cultures were grown in 75 cm² flasks and routinely passaged using trypsin-EDTA (0.05% trypsin, 0.02% EDTA) when cells reached 80-90% confluency. Cells were washed twice with sterile Dulbecco's calcium and magnesium free

phosphate buffered saline (PBS) and incubated at 37°C with trypsin-EDTA until cells had detached from the flask. Trypsinisation was stopped with the addition of growth medium containing 10-15% (v/v) FCS as this neutralises the trypsin. Cells were pelleted by centrifugation at 1,500 x g for 5 min, resuspended in fresh growth medium and counted using a haemocytometer before being plated.

2.3.1 Transduction of Ad-miR-451

HeLa cells were seeded at 4×10^4 cells/well in a 24 well plate. Once cells were ~80% confluent, cells were transduced with human Ad-miR-451, rat Ad-miR-451 or Ad5-lacZ control virus at a concentration of 10, 50 or 100 plaque forming units (pfu)/cell. Twenty four hours later, media was replaced with fresh media for a further 24 h, after which cells were lysed for RNA extraction.

Human PSMCs were seeded at 4×10^4 cells/well in a 24 well plate. Once cells were ~80% confluent, cells were transduced with human Ad-miR-451, rat Ad-miR-451 or Ad5-lacZ control virus at a concentration of 5,000, 10,000 or 20,000 viral particles (vp)/cell. Twenty four hours later, media was removed and replaced with 0.1% (v/v) serum containing media for a further 48 h. Cells were then lysed for RNA extraction.

2.3.1.1 Visualisation of control Ad5-lacZ virus

Transduction efficacy of the adenovirus was visualised using the Ad5-lacZ control virus. Ad5-lacZ is an adenovirus which contains the *lacZ* gene that results in over-expression of β -galactosidase. In the presence of x-gal stain (containing an analog of lactose), cells successfully transduced with the Ad5-lacZ virus produce β -galactosidase which hydrolyses lactose to form 5-bromo-4-chloro-3-hydroxyindole. This is then oxidised to form 5,5'-dibromo-4,4'-dichloro-indigo which is blue in colour. Human PSMCs seeded at 4×10^4 cells/well in a 24 well format were transduced with Ad5-lacZ control virus at 5,000, 10,000 or 20,000 vp/cell. Twenty four hours later, media was replaced with 0.1% or 15% (v/v) serum containing media for a further 48 h. Cells were then washed in PBS and fixed in 2% paraformaldehyde (PFA) for 10 min. X-gal stain (77 mM Na_2HPO_4 , 23 mM NaH_2PO_4 , 1.3 mM MgCl_2 , 3 mM $\text{K}_3\text{Fe}(\text{CN})_6$, 3 mM $\text{K}_4\text{Fe}(\text{CN})_6$, 1 mg/ml x-gal stain dissolved in dimethyl formamide) was added to each well and wells were

incubated at 37°C. The following day, cells were imaged using the QImaging QICAM Fast 1394 camera.

2.3.2 miR mimics

Synthetic miR-451 mimic or negative control cy3 labelled mimic was transfected into hPASCs using the siPORT™ neoFX™ transfection protocol. To assess miRNA and gene expression, hPASCs were transfected with miR mimics at a concentration of 10 nM, 25 nM or 50 nM using the reverse transfection protocol where cells are simultaneously transfected and plated. Briefly, 3 µl siPORT™ neoFX™ transfection agent was diluted in 50 µl opti-MEM® I media for each well and incubated at room temperature for 10 min. MiR mimics were then diluted in opti-MEM® I media to the desired concentration, mixed with the diluted siPORT™ neoFX™ transfection agent and incubated at room temperature for 10 min. The RNA/siPORT™ neoFX™ transfection agent complexes were then dispensed into a 24 well plate and cell suspension was added to give 4×10^4 cells/well. Twenty-four hours after transfection, cells were quiesced in 0.1% (v/v) serum containing media for 48 h and then lysed for RNA isolation. A mock transfection control was included in each independent experiment where cells were treated with siPORT™ neoFX™ transfection agent but not exposed to miR mimic.

2.3.2.1 Visualisation of cy3 labelled miR mimic

Human PASCs were reverse transfected with negative control cy3 labelled mimic at concentrations of 10 nM, 25 nM or 50 nM and plated at 4×10^4 cells/well on chamber slides using the protocol detailed in section 2.3.2. Cells were then incubated in 0.1% (v/v) serum containing medium for 48 h followed by fixation. Briefly, cells were washed twice with PBS, fixed with 4% (v/v) PFA for 10 min, washed with PBS and ProLong® Gold reagent (containing DAPI nuclear stain; Invitrogen) was added before mounting the chamber slide. Slides were left to cure for 24 h and then visualised using an Olympus IX70 fluorescent microscope (Olympus, Southend-on-Sea, UK).

2.3.3 Migration of hPASCs

Migration of hPASCs was analysed using the scratch wound assay. Human PASCs were reverse transfected with 10 nM miR-451 mimic, control mimic or

mock transfected using the protocol detailed in section 2.3.2 but using the 6 well plate format with 4×10^5 cells/well. Following 48 h serum starvation, vertical scratches were drawn through the confluent monolayer of cells using a P200 pipette tip. Cells were washed with PBS to remove any cell debris caused by induction of the wound and fresh 0.1% (v/v) or 15% (v/v) serum containing media was added. Scratches were imaged at 0, 6, 12 and 24 h post scratch using the Nikon Eclipse TS100 microscope and imaged on QICAM Fast 1394 camera (QImaging, Burnaby, Canada). Image analysis was performed using ImageJ software where a grid composed of 10 horizontal lines was placed over the image. The distance between the edges of the wound were measured along the grid lines and distance migrated was expressed as a percentage of the 0 h time point. Independent experiments were performed three times, with two wells per condition and four scratches per well.

2.3.4 Proliferation of hPASCs

2.3.4.1 Thymidine incorporation assay

DNA synthesis of hPASCs was assessed using a thymidine incorporation assay. This technique utilises the radioactive nucleoside ^3H -thymidine, which is incorporated into new strands of chromosomal DNA during DNA synthesis. The traditional siPORTTM neoFXTM transfection protocol was used where cells are plated prior to transfection. Cells were plated in a 24 well plate at a density of 2×10^4 cells/well and grown to ~50% confluency. Cells were quiesced in 0.1% (v/v) serum containing media for 48 h and then transfected with 10 nM miR-451 mimic, control mimic or mock transfected. Four hours post transfection, media was removed and fresh media was added to the cells containing differing serum concentrations (0.1%, 2.5% or 10% (v/v) serum). Cells were incubated for 72 h and 1 μCi ^3H -thymidine (Perkin Elmer) added for the last 24 h. The experiment was stopped by aspirating the media from each well and rinsing wells twice with cold PBS. DNA was precipitated by washing three times with 5% (w/v) trichloroacetic acid (TCA) followed by a 30 min incubation with 500 μl of 0.3 M NaOH at room temperature. The contents of each well were transferred to individual tubes and 1ml Ecosint XR scintillation fluid (National Diagnostics, Atlanta, USA) was added. Samples were then stored overnight, protected from light and radioactivity levels were measured using a liquid scintillation counter

(Tri-Carb 2800 TR Liquid Scintillation Analyser; Perkin Elmer) and results expressed as counts per minute (cpm).

2.3.4.2 MTS assay

The CellTiter96® AQueous Non-Radioactive Cell Proliferation Assay (also known as the MTS assay; Promega) was also used to measure hPASC proliferation. The MTS assay is a colorimetric technique used to determine the number of viable cells in a proliferation assay. Cells were transfected with 10 nM mimic in 96 well plates and exposed to fresh media with differing concentration of serum (0.1%, 2.5% or 10% (v/v) serum) for 72 h as described in section 2.3.4.1. A working solution containing MTS (3-(4,5-dimethylthiazol-2-yl)-5-(3-carboxymethoxyphenyl)-2-(4-sulfophenyl)-2H-tetrazolium, inner salt) and phenazine methosulfate (PMS, an electron coupling reagent) was prepared at a ratio of 20:1, respectively. Media was removed from the hPASCs and 100 µl fresh media (of the same serum concentration as before) was added along with 20 µl of the MTS working solution. Cells were incubated at 37° for 3 h, after which absorbance was read at 490 nm using the Wallac 1420 Victor2™ plate reader.

2.3.5 MicroRNA pull-down assay

Human PASCs were plated in 10 cm plates at 7×10^5 cells/plate. Once cells were 70-80% confluent, cells were transfected with 3'-biotinylated miR-145 mimic (Dharmacon, Pittsburgh, USA) or a control miR mimic (directed against *C.elegans* miR-67) with twelve plates per condition. Transfection was performed using Lipofectamine® RNAiMax transfection reagent. Briefly, 30 µl Lipofectamine® RNAiMax transfection reagent was diluted in 470 µl opti-MEM® I media per plate. The biotinylated mimics were also diluted in opti-MEM® I media to a final concentration of 30 nM in 500 µl per plate. Diluted lipofectamine and mimics were added together and incubated at room temperature for 5 min. Media was removed from the hPASCs and 1 ml of the lipofectamine/mimic complex was added to the cells along with fresh media. Twenty four hours later, cells were trypsinised using trypsin-EDTA and pelleted at 200 x g for 5 min. The cell pellet was washed twice in PBS, resuspended in 250 µl lysis buffer (20 mM Tris pH 7.5, 100 mM KCl, 5 mM MgCl₂, 0.3% NP-40, 50 U of RNase OUT, 1x

protease inhibitor cocktail (Roche Applied Sciences)) and incubated at 4°C for 20 min with shaking. Samples were centrifuged at 9,000 x g for 10 min and the cytoplasmic lysate was removed to a clean tube. At this point, 10% of the lysate was taken and stored at -80°C as the 'input' sample. Streptavidin coated magnetic beads (1.25 mg/ml, Dynabeads[®] M-280 Streptavidin; Invitrogen) were blocked for 2 h at 4°C in lysis buffer containing 1 mg/ml yeast tRNA and 1 mg/ml BSA. Tubes containing the beads were then placed in a magnetic holder (Dyna bead separator) for 2 min, supernatant removed and washed in this way twice with 1 ml lysis buffer. Lysates were then added to the beads and incubated at 4°C for 4 h. Following this, the beads were washed five times in 1 ml lysis buffer and RNA was extracted using TRIzol[®] LS reagent (described in section 2.6.3).

2.4 Hypoxic model of PH

Hypoxia-induced PH was achieved using a hypobaric hypoxic chamber. The hypoxic chamber was depressurised over the course of two days to 550 mbar (equivalent to 10% O₂) to allow acclimatisation. Chamber temperature was maintained at 21-22°C and the chamber was ventilated with air at 45 lmin⁻¹. Normoxic mice were exposed to atmospheric pressure of ~1000 mbar (equivalent to 21% O₂). Cages were changed and cleaned every five days and food and water were accessible *ad libitum*.

2.4.1 Knockout mice

MiR-145 knockout mice and miR-451 KO mice were kindly supplied by Eric Olson (University of Texas Southwestern).

KO mice were generated at University of Texas, Southwestern using Cre-recombinase technology. Briefly, targeting vectors were created which contained fragments upstream and downstream of the pre-miRNA of interest along with a neomycin resistant gene flanked by loxP sites. The target vector was then linearised and electroporated into embryonic stem cells where homologous recombination took place, knocking out the miRNA of interest and replacing it with the neomycin cassette. Positive clones were then selected and injected into blastocysts and crossed with C57Bl/6 mice to achieve germline transmission of the targeted allele and form chimeric mice. These chimeric mice

were then bred with mice ubiquitously expressing the CAG-Cre transgene. Breeding of these heterozygous mice produced global knockout of the miRNA of interest. All genetic mice were generated at the University of Texas, Southwestern and kindly gifted to the University of Glasgow where colonies of knockout and wild-type mice were established. Genotyping was performed to ensure knockout mice did not contain the miRNA of interest. Mice were housed with littermates and subjected to a continuous 12 h light/dark cycle. Food and water were accessible *ad libitum*.

2.4.1.1 MiR-145 knockout mice

Targeting vectors used to knock out miR-145 removed the 70 bp sequence of pre-miR-145 as described in section 2.4.1 above and in more detail by Xin and colleagues (Xin et al., 2009).

Eight week old male miR-145 KO mice or age matched wild type controls were exposed to chronic hypoxia for 14 days or maintained in normoxic conditions and assessment of PH indices was performed at 10 weeks of age. Previously our lab has reported that female miR-145 KO mice were protected from the development of hypoxia-induced PH (Caruso et al., 2012). Hence, male mice were used in this study to assess whether the same protective effect was observed in male mice.

2.4.1.2 MiR-451 knockout mice

Targeting vectors used to knock out miR-451 removed the 76 bp sequence of pre-miR-451 as described in section 2.4.1 above and in more detail by Patrick and colleagues (Patrick et al., 2010b).

Eight week old female miR-451 KO mice or age matched wild type controls were exposed to chronic hypoxia for 14 days or maintained in normoxic conditions and assessment of PH indices was performed at 10 weeks of age. Female mice were used for this study as previous work from our laboratory has shown that PH is more prominent in female transgenic mice compared to male mice (White et al., 2011a, White et al., 2011b, Dempsey et al., 2011).

2.4.2 AntimiR-451 administration in rat hypoxic model

An antimiR targeting mature miR-451 (antimiR-451) was used to silence miR-451 *in vivo*. AntimiR-451 (miRagen Therapeutics Ltd, Boulder, Colorado) consisted of LNA and DNA bases of the complementary reverse sequence bases 2-17 of miR-451 and was suspended in PBS. Male Wistar rats (aged 8 weeks) were administered antimiR-451 or control antimiR (similar composition to the antimiR but directed against a miRNA in *C.elegans*) intravenously via the femoral vein at a dose of 10 mg/kg. Anaesthesia was induced at 3% (v/v) isoflurane and then maintained at 2.5% (v/v) isoflurane via a face mask throughout the procedure. Rats were housed individually in heated cages until they came around and were closely observed to ensure full recovery after the surgery. After three days recovery, rats were placed in normoxic or hypoxic conditions for 7 days. Hemodynamic pressures were taken on day 10 and tissues harvested (Figure 2.2).

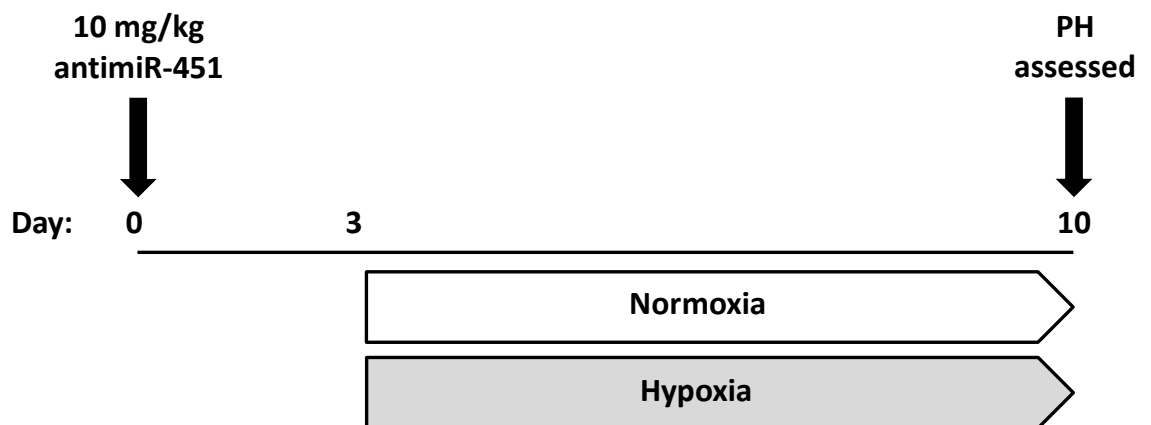


Figure 2.2 – AntimiR-451 in vivo study design.

Male 8 week old Wistar rats were administered 10 mg/kg antimiR-451 or control antimiR intravenously. After three days recovery, animals were placed in normoxic or hypoxic conditions for 7 days, after which hemodynamic measurements were taken along with right ventricular hypertrophy assessment and tissues harvested.

2.4.3 Assessment of PH

2.4.3.1 Hypoxic mouse hemodynamic measurements

Anaesthesia was induced using 3% (v/v) isoflurane supplemented with O₂. Mice were then maintained on 1.5-2% (v/v) isoflurane via a face mask. Hind limb and tail reflexes were checked before and throughout surgery to confirm mice were fully anaesthetised.

Systemic arterial blood pressure (SAP) was measured via cannulation of the left carotid artery. The micro-cannula (Harvard Apparatus, Massachusetts, USA) was attached to a Biopac pressure transducer connected to MP35 data acquisition system (Biopac, Goleta, USA) allowing SAP to be recorded. Systolic right ventricular pressure (RVP) was measured via cardiac puncture. A calibrated 25 gauge needle connected to a Biopac pressure transducer was advanced directly into the right ventricle trans-diaphragmatically to record RVP. The transducer was connected to the MP35 data acquisition system. Both SAP and RVP were analysed using the MP35 data analysis software and pressure traces were used to derive heart rate.

2.4.3.2 Hypoxic rat hemodynamic measurements

Anaesthesia was induced using 3% (v/v) isoflurane supplemented with O₂. Rats were maintained on 2.5% (v/v) isoflurane via a face mask and placed on a thermostatically controlled pad and fitted with a rectal thermometer to monitor body temperature. Hind limb and tail reflexes were checked before and throughout surgery to confirm rats were fully anaesthetised.

SAP was measured in rats as described for mice in section 2.4.3.1. RVP was measured in rats via cannulation of the right jugular vein. The cannula was inserted into the jugular vein, advanced forward through the right atrium and into the right ventricle. The catheter was curved at the end to easily manoeuvre the catheter into the right ventricle. The catheter was attached to the Biopac pressure transducer and recorded using the MP35 data acquisition system. Both SAP and RVP were analysed using the MP35 data analysis software and pressure traces were used to derive heart rate.

2.4.3.3 Right ventricular hypertrophy

Right ventricular hypertrophy (RVH) was assessed by dissection of the heart. The atria and fat surrounding the heart was discarded and the right ventricle (RV) was separated from the left ventricle plus septum (LV+S). The ratio of right ventricular weight to left ventricular weight plus septum (RV/LV+S) was used as an index of PH.

2.4.3.4 Pulmonary remodelling

Muscularisation of the pulmonary arteries was assessed by staining lung sections with Miller's Elastic Stain and counterstained with Elastic van Gieson. The left lung lobe was fixed in 10% formalin overnight and then paraffin embedded. Single tissue sections of 5 μm were mounted onto silane coated slides and incubated at 60°C overnight. Sections were deparaffinised by incubation for 1 h in histoclear and rehydrated by passing the slides through decreasing strengths of alcohol for 5 min each. Sections were incubated for 5 min in 0.5% (w/v) potassium permanganate to increase the contrast of the final staining, rinsed in running water for a few minutes then decolourised in 1% (v/v) oxalic acid for 2 min. Sections were then rinsed in 95% (v/v) ethanol and incubated with Miller's Elastic Stain (VWR chemicals, Leicestershire, UK) for 2 h at room temperature. Following this, sections were placed in 95% ethanol to remove excess stain, rinsed in running water and then counter stained with Van Gieson Solution. Sections were briefly placed in running water to remove excess stain and dehydrated rapidly through increasing strengths of alcohol finishing in histoclear. Slides were then mounted and analysed the following day.

As a result of the staining, elastic fibres were stained black, collagen was stained deep red and cytoplasm, muscle, red blood cells and fibrin were stained yellow. Sections were microscopically assessed in a blinded fashion for muscularisation of the pulmonary arteries. Pulmonary arteries (≤ 100 microns external diameter) were considered remodelled if they possessed a distinct double elastic lamina for at least half of the diameter of the vessel cross section. The percentage of remodelled vessels was calculated as number of muscularised vessels/total number of vessels x 100. All samples were analysed in a blinded fashion.

2.5 Hypoxia/SU5416 model of PH

2.5.1 Mouse 3 week model

Adult male C57Bl/6Jax mice (20-25 g body weight) were maintained in normoxic conditions (room air at ~21% O₂) or in a normobaric hypoxic chamber (10% O₂) for 21 days. Sugen-5416 (SU5416; Tocris Bioscience, Bristol, UK) suspended in CMC (0.5% (w/v) carboxyl methylcellulose sodium, 0.9% (w/v) NaCl, 0.4% (v/v) polysorbate, 0.9% (v/v) benzyl alcohol in deionised water) or vehicle was administered subcutaneously at a dose of 20 mg/kg on days 0, 7 and 14. On day 21, hemodynamic pressures were taken and tissues harvested (Figure 2.3).

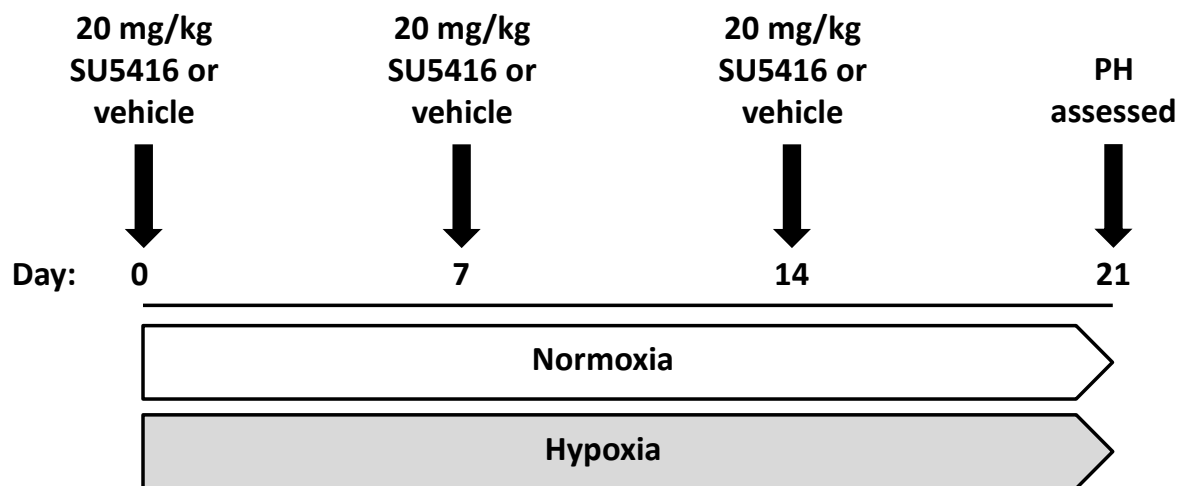
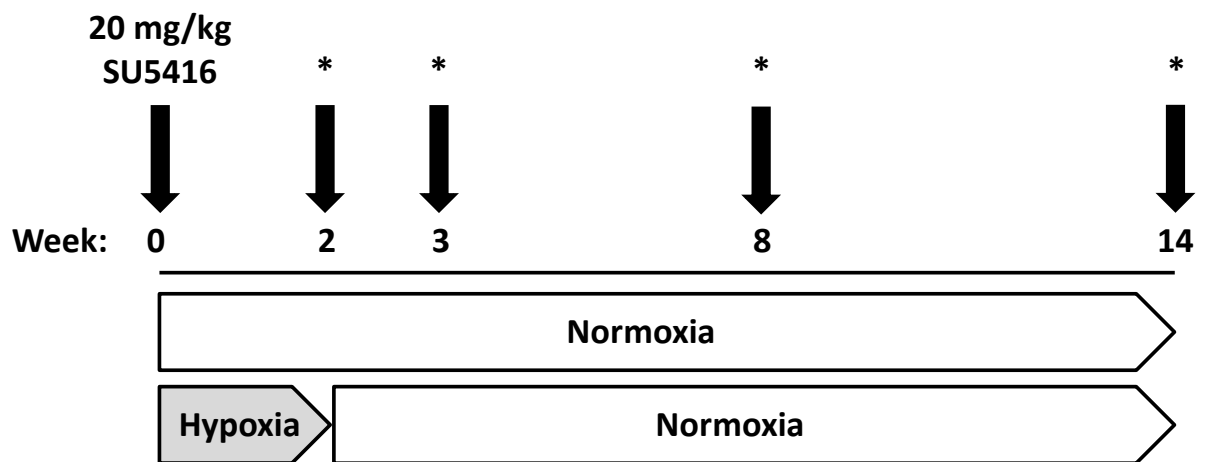


Figure 2.3 – Mouse 3 week hypoxia/SU5416 *in vivo* study design.

Male C57Bl/6Jax mice were maintained in normoxic or hypoxic conditions for 21 days. Sugen-5416 (SU5416) or vehicle was administered subcutaneously at 20 mg/kg on day 0, 7 and 14. On day 21, hemodynamic measurements were taken along with right ventricular hypertrophy assessment and tissues harvested.

2.5.2 Rat 14 week model

Adult male Wistar Kyoto rats (150-200 g body weight) were maintained in normoxic conditions (~21% O₂) or in a normobaric hypoxic chamber (10% O₂) for 14 days with subcutaneous administration of SU5416 or vehicle at a dose of 20 mg/kg on day 0. This was then immediately followed by varying lengths of time in normoxia (Figure 2.4). At each time point, a group of animals (n = 5) were tested for hemodynamic pressures and tissues were harvested.



* = PH assessed

Figure 2.4 – Rat 14 week hypoxia/SU5416 *in vivo* study design.

Male Wistar Kyoto rats were maintained in normoxic or hypoxic conditions for 14 days with SU5416 or vehicle administered subcutaneously at 20 mg/kg on day 0. This was then followed by varying lengths of time in normoxic conditions. At each time point, hemodynamic measurements were taken along with right ventricular hypertrophy assessment and tissues harvested.

2.5.3 AntimiR-145 administration

2.5.3.1 Prophylactic study

Adult male wistar kyoto rats (150-200 g body weight) were administered either antimiR-145 (supplied by miRagen Therapeutics Ltd) suspended in PBS and sterile filtered, control antimiR or PBS subcutaneously at a dose of 10 mg/kg every 14 days in a blinded study. Dosing with treatment drug began 14 days prior to SU5416 (20 mg/kg, subcutaneous injection) and normoxic (21% O₂) or normobaric hypoxic (10% O₂) exposure (Figure 2.5). Rats were then maintained in normoxic conditions for a further 21 days, after which echocardiographic indices were measured, hemodynamic pressures taken and tissues harvested.

Gleevec (imatinib mesylate) was used as a positive control for this experiment. Gleevec is a PDGF receptor inhibitor and it has previously been shown to cause reversal of the pulmonary hypertensive phenotype in rodent models of PH (Schermuly et al., 2005, Abe et al., 2011). Gleevec was administered daily at a dose of 100 mg/kg via oral gavage from day -14 to day 35.

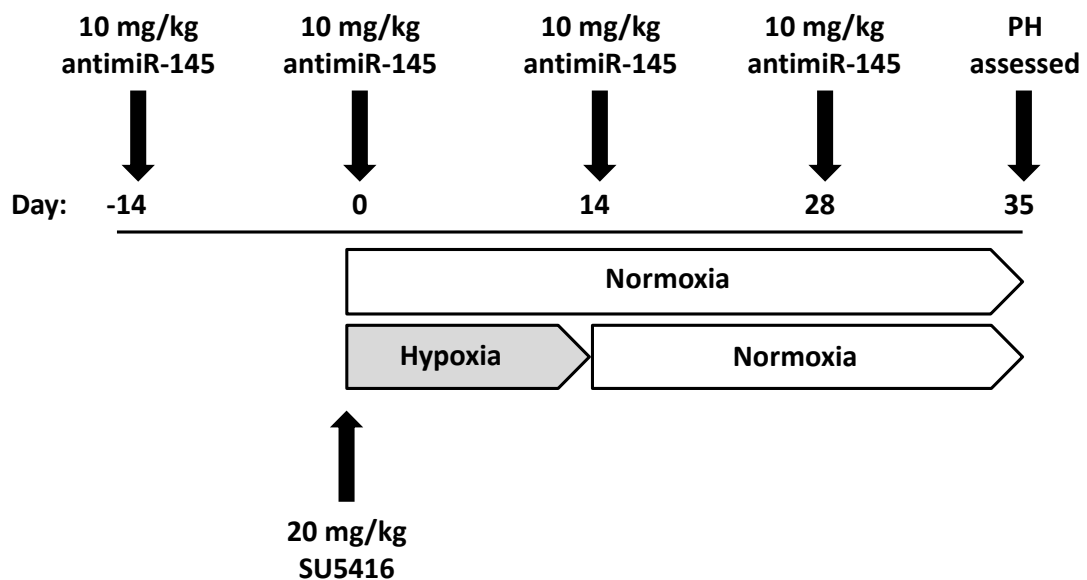


Figure 2.5 – Prophylactic antimiR-145 *in vivo* study design.

Male wistar kyoto rats were administered antimiR-145, control antimiR or PBS subcutaneously at 10 mg/kg every 14 days. 14 days after the first administration of treatment drug, rats were dosed subcutaneously with 20 mg/kg SU5416 and exposed to hypoxic or normoxic conditions for 14 days. Following this, all rats were placed in normoxic conditions for a further 21 days. On day 35, echocardiography was performed, hemodynamic measurements were taken and tissues harvested.

2.5.3.2 Therapeutic study

Adult male wistar kyoto rats (150-200 g body weight) were maintained in normoxic conditions (21% O₂) or in a normobaric hypoxic chamber (10% O₂) for 14 days with subcutaneous administration of SU5416 at a dose of 20 mg/kg on day 0 to establish experimental PH. Rats were then returned to normoxic conditions for 21 days, during which time antimiR-145, control antimiR or PBS was administered subcutaneously at a dose of 10 mg/kg every 14 days in a blinded study (Figure 2.6). On day 35, echocardiography was performed, hemodynamic pressures taken and tissue harvested.

Gleevec was used as a positive control and was administered daily at a dose of 100 mg/kg via oral gavage from day 14 to day 35.

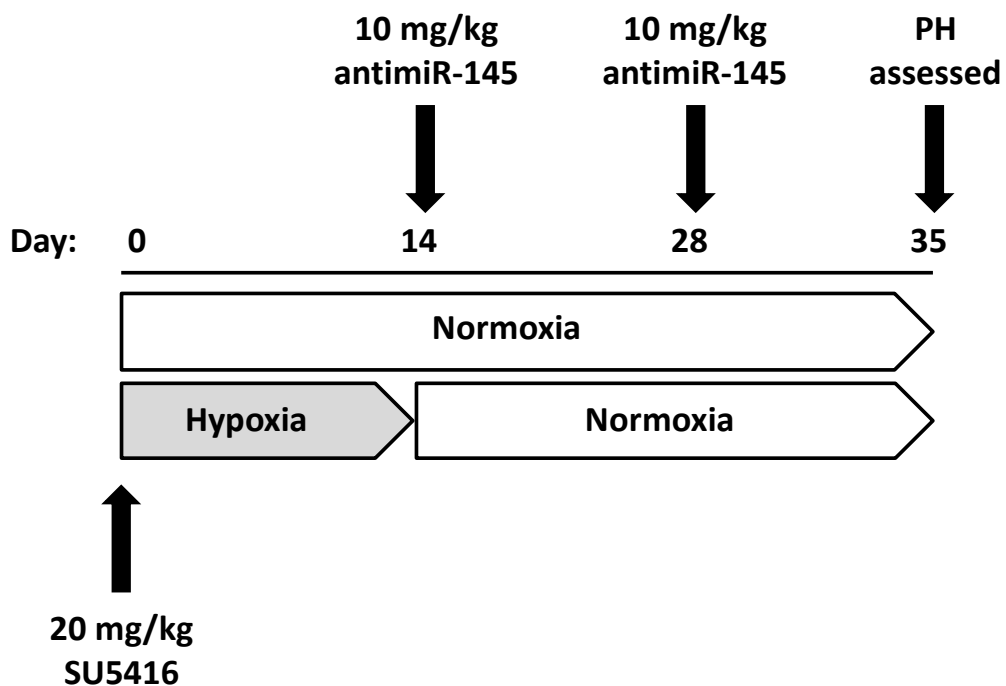


Figure 2.6 – Therapeutic antimiR-145 *in vivo* study design.

Male wistar kyoto rats were administered SU5416 subcutaneously at 20 mg/kg and exposed to normoxic or hypoxic conditions for 14 days to establish experimental PH. All rats were then returned to normoxic conditions for a further 21 days, during which time antimiR-145, control antimiR or PBS was administered subcutaneously at a dose of 10 mg/kg. On day 35, echocardiography was performed, hemodynamic pressures taken and tissues harvested.

2.5.4 Assessment of PH

Mice and rats were anaesthetised by ketamine (66 mg/kg) and medetomidine (3.3 mg/kg) via intraperitoneal injection. Animals were placed in a warming box for ~5 min and then SAP was measured non-invasively using the CODA tail cuff plethysmography method (Kent Scientific Corporation, Torrington, Connecticut).

RVP was determined in mice by catheterisation of the right ventricle via cannulation of the jugular vein using a mouse pressure-volume catheter (SPR-839; Millar, Houston, Texas). RVP was measured in rats using a rat pressure-volume catheter (SPR-869; Millar) inserted into the right ventricle via cannulation of the jugular vein. Both rat and mouse RVP were recorded using the MPVS-300 System (Millar).

2.5.4.1 RVH

RVH was calculated as described in section 2.4.3.3.

2.5.4.2 Pulmonary remodelling

Lungs were inflated, fixed in 10% formalin overnight and paraffin embedded. Sections were cut at 3 μm and staining was performed for von Willebrand Factor (vWF) and alpha-smooth muscle actin (α -SMA) by BenchMark XT (Ventana Medical Systems, Inc, Tucson, USA). Slides were examined using the DMLB microscope, digital camera and IM50 imaging software (Leica Microsystems, Milton Keynes, UK). Pulmonary arteries (10 - 100 μm diameter) were assessed for muscularisation using Image-Pro (Media Cybernetics, Rockville, Maryland), where the percentage of α -SMA staining was quantified. All samples were analysed in a blinded fashion.

2.5.4.3 Occluded vessel quantitative analysis

The percentage of occluded vessels was calculated on the same slides used for remodelling analysis (described in section 2.5.4.2) which had been stained for vWF and α -SMA. Vessels were considered occluded when the smooth muscle and endothelial cells had obliterated the lumen. For each animal, 100 vessels were

counted and each vessel was scored as occluded or non-occluded. All samples were analysed in a blinded fashion.

2.5.4.4 Echocardiography

Echocardiography was performed on rats by ultrasound using the Vivid7 Dimension (GE Healthcare, Buckinghamshire, UK) ultrasound system equipped with a 13 MHz pediatric probe. Anaesthesia was induced at 4% (v/v) sevoflurane supplemented with O₂ and then maintained at 2-3% (v/v) sevoflurane via face mask. The animal's chest was shaved and KendallTM ultrasound transmission gel (Covidien, Mansfield, USA) was applied to the chest to aid ultrasonic imaging. Animals were placed in the left lateral decubitus position on a heated mat. The probe was placed in a parasternal long axis position to visualise the pulmonary artery outflow tract. Pulsed Doppler imaging was performed to monitor blood flow through the pulmonary artery valve. From this image, heart rate, maximal flow velocity (V_{max}) and time to peak flow (acceleration time, AccT) were calculated. Mid-systolic notch was also quantified by applying a score to each wave profile, as subjects with severe PH will have a mid-systolic notch in the deceleration slope of the pulmonary artery Doppler flow profile. A score of between 0 and 3 was used with 0 having no indentation and 3 having a pronounced notch on the deceleration slope. Aortic outflow was also imaged in order to calculate systemic velocity time integral (VTI). Motion mode analysis was then used in short axis to measure aortic diameter and right ventricular wall thickness during systole and diastole. Cardiac output (CO) was derived from the values taken using the equation below:

$$CO = 0.7854 \times (\text{aortic diameter})^2 \times VTI \times \text{heart rate}$$

Analysis of echocardiographic indices was performed using Echo-PAC dimension software (GE Healthcare).

2.6 RNA extraction, purification and quantification

2.6.1 Cells

Total RNA was extracted using the QIAGEN miRNeasy mini kit including on-column DNase treatment following manufacturer's instructions. After removal of

media, cells were lysed directly by adding 700 μ l QIAzol lysis reagent and homogenised by repeated pipetting. Addition of 140 μ l chloroform to homogenised samples was followed by centrifugation at 12,000 x g for 15 min at 4°C to separate the sample into aqueous and organic phases. Protein remains in the lower organic phase and DNA partitions to the interphase while the RNA partitions to the upper aqueous phase. The RNA containing aqueous phase was extracted and added to 1.5 volumes of 100% ethanol. Samples were then applied to the RNeasy mini spin columns where the total RNA binds to the silica membrane while contaminants, such as phenol, are washed away in the subsequent wash steps. Columns were washed with 350 μ l buffer RWT for 15 sec at 8,000 x g with flow through discarded. DNA contamination can often occur during RNA extraction and this can interfere with downstream applications. Hence, digestion of DNA was performed by incubating spin columns with DNase for 15 min at room temperature. Further washing with 350 μ l buffer RWT was performed followed by two washes with 500 μ l buffer RPE to remove any traces of salts from the RNA samples. Centrifugation at full speed for 1 min was performed to dry the spin column. RNeasy spin columns were then transferred to new collection tubes and RNA was eluted using 40 μ l RNase-free water and centrifugation for 1 min at 8,000 x g. This elution step was repeated re-using the original volume of RNase-free water in order to increase RNA yield.

Total RNA was quantified using the NanoDrop 1000 Spectrophotometer (ThermoScientific). RNA quality was assessed using the A260/A280 ratio, with a ratio of ~2.0 accepted as “pure” RNA. All RNA samples were stored at -80°C.

2.6.2 Tissue

Total RNA was extracted using the QIAGEN miRNeasy mini kit including on-column DNase treatment following manufacturer’s instructions. Snap frozen tissues (~50 mg) were lysed using 700 μ l QIAzol lysis reagent and disrupted and homogenised using 5 mm stainless steel beads in the TissueLyser. Following homogenisation, 140 μ l chloroform was added to each sample and protocol followed is described in section 2.6.1.

2.6.3 Streptavidin bead samples

TRIzol® LS reagent was used to isolate RNA bound to streptavidin beads (pull down RNA) or RNA from the 10% input samples (input RNA) from the miRNA pull down experiment detailed in section 2.3.5. TRIzol® LS reagent (750 µl) was added to each sample, mixed for 1 min and then 250 µl RNase-free water was added. Chloroform (250 µl) was added, samples vortexed for 2 min and centrifuged at 12,000 x g at 4°C for 15 min. The upper aqueous phase containing the RNA was collected, 500 µl isopropanol was added along with 2 µl glycogen and samples were incubated at room temperature for 10 min. Samples were then centrifuged at 12,000 x g at 4°C for 15 min and supernatant discarded. The pellet was washed with 1 ml cold ethanol and centrifuged at 7,500 x g at 4°C for 1 min. Supernatant was decanted, samples centrifuged for a further 5 min and all ethanol removed. Pellet was left to air dry at room temperature for 5 min and then RNA was dissolved in 20 µl RNase-free water.

Total RNA was quantified using the NanoDrop 1000 Spectrophotometer. RNA quality was assessed using the A260/A280 ratio, with a ratio of ~2.0 accepted as “pure” RNA. All RNA samples were stored at -80°C.

2.6.4 Paraffin embedded tissues

RNA was extracted from formalin fixed paraffin embedded (FFPE) blocks using RecoverAll™ Total Nucleic Acid Isolation Kit (Ambion, Paisley, UK). Sections were cut to 20-30 µm and incubated with 100% xylene at 50°C for 3 min to melt the paraffin. Samples were centrifuged at maximal speed for 2 min and the tissue pellet was then washed twice with 100% ethanol to remove any excess xylene from the sample. The pellet was then air dried for 30 min at room temperature. Protease digestion was performed by incubating the samples with 4 µl protease in 100 µl digestion buffer for 15 min at 50°C and then 15 min at 80°C. For RNA isolation, 120 µl isolation additive and 275 µl 100% ethanol was added to each sample and centrifuged in a glass-fibre filter cartridge at 9,000 x g for 30 sec, where the RNA binds to the filter. The filter cartridge was washed using two wash solutions. DNase digestion for 30 min at room temperature was then performed to remove any DNA contamination. Filter cartridges were then washed thoroughly using wash solutions. Filter cartridges were then transferred

to new collection tubes and RNA was eluted in 40 μ l RNase-free water by centrifugation for 1 min at full speed. This elution step was repeated re-using the original volume of RNase-free water in order to increase RNA yield.

Total RNA was quantified using the NanoDrop 1000 Spectrophotometer. RNA quality was assessed using the A260/A280 ratio, with a ratio of \sim 2.0 accepted as “pure” RNA. All RNA samples were stored at -80°C .

2.6.5 Agilent testing RNA quality

The quality of RNA extracted from FFPE blocks is often of lower quality than that extracted from frozen samples due to cross-linking occurring between nucleic acids and proteins during the fixation process. As a result, RNA extracted from FFPE blocks using the protocol detailed in section 2.6.4 was Agilent tested to test for degradation. Total isolated RNA was analysed on a Small RNA Assay (Agilent Technologies) performed on the Agilent Bioanalyzer 2100 at the Sir Henry Wellcome Functional Genomics Facility, Microarray Unit at the University of Glasgow. The negatively charged RNA molecules are electrophoretically separated by size to produce gel images and electropherograms, allowing assessment of RNA quality. The percentage of miRNA (relative to small RNA) in the sample is also calculated using the Agilent 2100 software.

2.7 RNA expression by qRT-PCR

2.7.1 cDNA synthesis

Synthesis of cDNA from total RNA by reverse transcription is the first step in the two-step process of qRT-PCR.

2.7.1.1 miRNA expression

For the detection of miRNA expression, cDNA was synthesised using stem-loop reverse transcription primers as per the Taqman microRNA assay protocol (Applied Biosystems, Paisley, UK). Each reaction contained 250 μ M of each deoxyribonucleotide triphosphate (dNTP), 3.3 U/ μ l multiscribe reverse transcriptase, 0.25 U/ μ l RNase inhibitor, 1x RT buffer, 1x RT primer and 0.67 ng/ μ l RNA. Samples were incubated at 16°C for 30 min, 42°C for 30 min, 85°C for

5 min to inactivate the reverse transcriptase and then held at 4°C. Samples were stored at -20°C when not being used immediately.

2.7.1.2 mRNA expression

For gene expression analysis, cDNA was synthesised using the Taqman gene expression assay protocol (Applied Biosystems). Each reaction contained 5.5 mM MgCl₂, 500 μM of each dNTP, 2.5 μM random hexamers, 0.4 U/μl RNase inhibitor, 1.25 U/μl multiscribe reverse transcriptase, 1 x RT buffer and 200-1000ng RNA (same concentration of RNA used per experiment). Negative control reactions were run which did not contain multiscribe reverse transcriptase. Samples were incubated at 25°C for 10 min to maximise primer-RNA template binding followed by a 30 min incubation at 48°C to allow reverse transcription to take place. Reverse transcriptase was then inactivated at 95°C for 5 min and samples were then held at 4°C. Samples were stored at -20°C when not being used immediately.

2.7.2 Quantitative real-time polymerase chain reaction

Quantitative PCR is the second step in the two-step process of qRT-PCR. Each reaction contained 250 nM taqman probe, 1 x Taqman Universal PCR MasterMix II (containing AmpliTaq Gold[®] DNA polymerase, dNTP mixture and optimal salt conditions, no UNG; Invitrogen) and cDNA. For quantification of miRNA expression, 0.67 μl of cDNA was added to a 10 μl reaction, while for mRNA expression 1.5 μl cDNA was added to a 10 μl reaction. Technical triplicates were performed. For each probe tested, the negative reverse transcription control was run alongside a nuclease-free water control and RNA control. All qPCR experiments were performed in simplex using the 7900HT sequence detection system (Applied Biosystems). Thermal cycling conditions began with a 10 min incubation at 95°C to activate the enzyme. This was followed by 40 cycles of 15 sec at 95°C (to denature the cDNA) and then 60 sec at 60°C (to allow primer and probe to anneal to cDNA and extension of primer).

Results are shown relative to the control sample using the $-2^{\Delta\Delta Ct}$ method and expressed as relative fold change. For miRNA expression, results were normalised to U6, U87 and RNU48 for mouse, rat and human samples,

respectively. For mRNA expression, results were normalised to beta-2-microglobulin (B2M) for experiments which involved hypoxia as this gene remains unchanged in hypoxic conditions. Experiments performed in normoxic conditions were normalised to GAPDH.

2.8 Target prediction

A list of targets for each specific miRNA analysed was obtained by searching the miRNA databases miRWalk and TargetScan (<http://www.umm.uni-heidelberg.de/apps/zmf/mirwalk> and <http://www.targetscan.org>, respectively). In addition to this, literature searches were performed for each miRNA and target genes were chosen based on previous knowledge of the gene and the involvement of that gene in pathways thought to be integral in the development of PAH.

2.9 Northern blotting

Total RNA was denatured at 95°C for 5 min and 3-5 µg RNA was separated on a 15% TBE-Urea gel (Invitrogen). The RNA was then transferred onto Hybond-NX nylon membrane (GE Healthcare) using the Trans-Blot semi dry station (Bio-Rad, Hercules, USA) and immobilised onto the membrane using EDC-cross linking at 60°C for 1 h. Prehybridisation was carried out in hybridisation buffer (50% formamide, 5 x SSPE, 5 x Denhardt's solution, 0.5% SDS, 0.02 mg/ml heat denatured herring sperm DNA) at hybridisation temperature for 1 h followed by overnight incubation with 25 pmol of 5'-Digoxigenin (DIG)-labelled mercury LNATM detection probe (Exiqon, Vedbaek, Denmark). Hybridisation temperatures used were as follows: 40°C for miR-21, 55°C for miR-143, 45°C for miR-145, 50°C for miR-451 and 60°C for U6. The membranes were then washed at 50°C with a low stringency buffer containing 2 x SSC to remove unhybridised probe, followed by a high stringency wash with 0.1 x SSC to remove partially hybridised molecules. Membranes were blocked for 30 min (1% blocking reagent in maleic acid buffer) then incubated with anti-DIG antibody conjugated to alkaline phosphatase (1:5000, Roche Applied Sciences) at room temperature. Detection buffer composed of 0.1 M Tris-HCl (pH 7.5) was then added to the membranes for 3 min followed by a 5 min incubation with CDP-Star chemiluminescent substrate. CDP-Star is a chemiluminescent substrate for alkaline phosphatase

therefore allowing x-ray detection of the miRNAs which have been probed for. For normalisation purposes, membranes were stripped in boiling 1% SDS to remove hybridised probe and re-probed with the U6 control probe. Films were scanned using the Molecular Imager Chemidoc XRS+ System (Bio-Rad). Band intensities were quantified using densitometry (Quantity One software, Bio-Rad) and normalised to U6 signal for mouse and rat samples.

2.10 Protein extraction and quantification

Protein was isolated from samples by adding 25 mg snap frozen tissue to 200 μ l of ice-cold lysis buffer (20 mM Tris pH 7.5, 150 mM NaCl, 1 mM ethylene diamine tetraacetic acid (EDTA), 1 mM ethylene glycol tetraacetic acid (EGTA), 2.5 mM Na Pyrophosphate, 1 mM β -glycerophosphate, 1 mM Na_3VO_4 , 1 μ g/ml leupeptin, 1 mM phenylmethanesulfonyl fluoride (PMSF), 2 mM NaF, 1 x protease inhibitor cocktail (Roche Applied Sciences), 1:100 phosphatase inhibitor cocktail 2, 0.5% deoxycholate). Stainless steel beads were added and samples were homogenised using the TissueLyser (Qiagen). After homogenisation, samples were incubated at 4°C for 1 h with shaking, followed by centrifugation at 14,000 x g at 4°C for 40 min. Protein lysate was aspirated and stored at -80°C.

Quantification of total protein was performed using the Pierce Bicinchonic Acid (BCA) Protein Assay Kit (ThermoScientific) according to manufacturer's instructions. Protein standards of bovine serum albumin were prepared at concentrations ranging from 25 μ g/ml to 2000 μ g/ml. These reference samples were used to generate a standard curve. A working reagent was prepared by mixing reagent A and reagent B at a ratio of 50:1, respectively. Protein samples/standards (25 μ l) were then added to the working reagent (200 μ l) in a 96-well plate, mixed thoroughly, protected from light and incubated at 37°C for 30 min. Absorbance was measured at 560 nm using the Wallac 1420 Victor²™ plate reader. Samples and standards were measured in duplicate with average values taken. Protein concentration was determined using the standard curve generated by the BSA protein standards.

2.11 Western blotting

Protein samples were mixed with equal volumes of reducing loading dye (4% (v/v) SDS, 20% (v/v) glycerol, 10% (v/v) 2-mercaptoethanol, 0.004% (v/v) bromophenol blue, 125 mM Tris pH 6.8) and denatured at 95°C for 10 min. Protein (20 µg) was resolved using sodium dodecyl sulphate polyacrylamide gel electrophoresis (SDS-PAGE). A 10% polyacrylamide gel (30% (v/v) polyacrylamide (30%), 375 mM Tris pH 8.8, 0.1% (v/v) SDS, 300 µl ammonium persulphate, 30 µl TEMED) was prepared with a 4% stacking gel (13.3% (v/v) polyacrylamide (30%), 125 mM Tris pH 6.8, 0.1% (v/v) SDS, 300 µl ammonium persulphate, 30 µl TEMED). A rainbow marker (Amersham) was included on each gel as a marker of protein size. Samples were electrophoresed at 200 V in running buffer (25 mM Tris, 0.2 M glycine, 0.1% (v/v) SDS) to achieve separation of the protein.

Proteins were transferred onto Hybond P+ nitrocellulose membranes (GE Healthcare) overnight at 4°C at 90 mA in transfer buffer (25 mM Tris, 0.2 M glycine, 0.1% (v/v) SDS, 20% (v/v) methanol). Membranes were blocked in blocking buffer containing 5% (w/v) fat-free milk powder in TBS-T (140 mM NaCl, 3 mM KCl, 25 mM Tris, pH 7.4, 0.1% (v/v) Tween-20) for 2 h at room temperature with shaking. Membranes were then incubated overnight with shaking at 4°C with rabbit polyclonal Klf4 or rabbit polyclonal Klf5 antibody (Abcam, Cambridge, USA). Primary antibodies were diluted 1:500 in 1% milk in TBS-T. Membranes were then washed three times with blocking buffer at room temperature before the addition of the secondary antibody. Swine anti-rabbit horse radish peroxidase (HRP) secondary antibody was used at 1:1000 diluted in 1% milk in TBS-T and incubated with membranes for 1 h at room temperature, with shaking. Following this, membranes were washed four times in blocking buffer then four times in TBS-T, each wash lasting 15 min at room temperature with shaking. Proteins were visualised using Amersham Enhanced Chemiluminescence (ECL) Prime Western Blotting System (GE Healthcare) as per the manufacturer's instructions. Briefly, equal volumes of reagent A (containing luminol) and reagent B (containing peroxide) were mixed together and incubated with membranes for 5 min. Excess ECL-Prime was drained off the membranes and x-ray films were exposed for varying lengths of time.

For normalisation purposes, membranes were incubated at 50°C for 45 min in stripping buffer (62.5 mM Tris pH 6.8, 2% (v/v) SDS, 100 mM 2-mercaptoethanol) followed by three 10 min washes with TBS-T. Membranes were then blocked in blocking buffer for 2 h at room temperature and re-probed for alpha-tubulin (α -tubulin). Films were scanned using Molecular Imager Chemidoc XRS+ System. Band intensities were quantified using densitometry (Quantity One software) and normalised to α -tubulin signal.

2.12 Alpha-smooth muscle actin staining

Lung tissue was fixed in 10% formalin overnight and paraffin embedded. Sections were cut at 5 μ m and baked onto silane coated slides at 60°C overnight. Sections were deparaffinised by incubation in histoclear followed by rehydration by passing the sections through decreasing strengths of alcohol. Endogenous peroxidase activity was quenched by incubating slides in 20% hydrogen peroxidase for 30 min at room temperature. Blocking was carried out on the slides with 20% normal horse serum for 30 min at room temperature to reduce non-specific background staining. The sections were then incubated with rabbit polyclonal antibody against alpha-smooth muscle actin (Abcam) at a concentration of 2.67 μ g/ml in phosphate buffered saline (PBS) containing 20% horse serum for 1 h at room temperature. Serial sections were incubated with isotype matched rabbit IgG non-immune control (Invitrogen). A biotinylated anti-rat secondary antibody (Vectastain kit; Vector Laboratories, Peterborough, UK) was then added to all sections for 30 min followed by a 30 min incubation with avidin/biotinylated enzyme complex (ABC complex). Sections were then washed in PBS and staining was visualised using 3,3'-diaminobenzidine (DAB) chromogen, which produces a brown precipitate in the presence of peroxidase enzyme. Nuclei were counterstained with Harris Haematoxylin and sections were dehydrated by immersion in increasing concentrations of alcohol.

2.13 Statistical analysis

All qRT-PCR results are expressed as fold-change \pm standard error of the mean (SEM) with all other results expressed as the mean \pm SEM. Unpaired student's t-test was used when comparing two experimental groups. When more than two groups were compared, a one-way ANOVA was performed followed by a Tukey's

post hoc test or a two-way ANOVA was performed followed by a Bonferroni post hoc test, where appropriate. Statistical significance accepted at $p < 0.05$.

3 The role of miRNA-451 in PAH

3.1 Introduction

MicroRNAs have been shown to be dysregulated within various tissues during disease development (Sayed and Abdellatif, 2011, Soifer et al., 2007, Small et al., 2010). A study by Caruso and colleagues found that miR-451 was up-regulated in lung tissue from the monocrotaline and hypoxic rat models of PH (Caruso et al., 2010). MiR-451 is highly conserved across species and is located on human chromosome 17 at position 17q11.2. This miRNA exists in a cluster with miR-144, which is located approximately 100 bp upstream of miR-451 (Altuvia et al., 2005). MiR-451 differs from other miRNAs (canonical miRNA maturation pathway shown in Figure 1.6) as it is processed independent of Dicer. Processing of pri-miR-451 by Drosha forms a short hairpin pre-miR-451 of approximately 42 nt (compared to the canonical ~70 nt precursor miRNA) which is unable to be cleaved by Dicer and is therefore cleaved directed by the catalytically active Ago2 (Cifuentes et al., 2010, Yang et al., 2010). From here, mature miR-451 can be incorporated into the RISC complex allowing miR-451 to bind to target mRNA sequences resulting in target gene repression.

MiR-451 expression is high in erythrocytes and miR-451 plays a fundamental part in erythropoiesis. Microarray analysis of MEL cells found that miR-451 was the most up-regulated miRNA during erythroid maturation (Zhan et al., 2007). Studies suggest that binding of GATA-1, a transcription factor essential for erythroid development, in erythroid cells stimulates the action of RNase II to initiate transcription of the common pri-miR-144/451 cluster (Dore et al., 2008). *In vivo* studies using knockout mice have found that mice lacking miR-451 are unable to develop mature circulating red blood cells in response to stress (Patrick et al., 2010b) resulting in impaired erythroid differentiation and erythroid hyperplasia (Rasmussen et al., 2010).

As well as playing a pivotal role in erythroid differentiation and maturation, miR-451 has also been linked to many different cancer-related pathways. Microarray analysis revealed that miR-451 is the most down-regulated miRNA in non-small cell lung carcinoma (NSCLC) and ectopic expression of miR-451 in these cells suppressed cellular proliferation and colony formation via down-regulation of target gene RAB14 (Wang et al., 2011). Li and colleagues (Li et al., 2011) also reported down-regulation of miR-451 in a mouse model of notch induced T-cell

lymphoblastic leukaemia (T-ALL). Reduced miR-451 levels induced by Notch-1 resulted in derepression of the proto-oncogene *Myc* leading to accelerated tumour formation while over-expression of miR-451 suppressed *Myc* and reduced T-ALL cell growth. Similar results have been obtained in glioblastoma cells where reduced miR-451 expression was observed in the diseased state and increased expression of miR-451 reduced cell proliferation and induced apoptosis (Nan et al., 2010, Gal et al., 2008). Consistent down-regulation of miR-451 expression has been observed in various cancers and has been associated with worse prognosis in gastric cancer patients (Bandres et al., 2009). Thus providing further evidence that miR-451 is acting as a tumour suppressor. MiR-451 levels have also been found to play an important role in the development of drug resistance during cancer treatment. Tamoxifen, a selective oestrogen receptor modulator used to treat many types of oestrogen receptor positive breast cancers, down-regulates miR-451 leading to subsequent up-regulation of 14-3-3 ζ (Ywhaz), a regulator of cellular proliferation and apoptosis. Although initial treatment with tamoxifen is successful, resistance to the drug can often develop and it has been proposed that increasing miR-451 levels in addition to tamoxifen treatment may be able to prevent this drug resistance (Bergamaschi and Katzenellenbogen, 2012). In addition, over-expression of miR-451 in NSCLC cells resulted in the cells being more receptive to cisplatin treatment, the chemotherapeutic agent used to treat the majority of NSCLC cases (Bian et al., 2011). Taken together, this data suggests that miR-451 plays an important part in cancer biology, however the exact mechanisms through which this miRNA acts remain unknown.

The role of miR-451 has recently been shown in cardiac disease development. MiR-451 is down-regulated in heart tissue from heart failure patients and over-expression of the miR-144/451 cluster was protective in cardiomyocytes exposed to hypoxic stress (Zhang et al., 2010). In a similar manner, expression of the miR-451 cluster was significantly increased in preconditioned hearts compared to sham hearts and genetic knock down of miR-144/451 prevented the cardioprotective effects instigated by ischemic preconditioning. This loss of cardioprotection in mice lacking the miR-451 cluster is thought to be due to up-regulation of Rac1 in cardiomyocytes leading to increased reactive oxygen species during ischemic preconditioning (Wang et al., 2012b).

Although much scientific research has focussed on the role of miR-451 in different biological systems, the role of miR-451 in the lung during the development of pulmonary arterial hypertension is largely unknown.

3.1.1 Aim

The aims investigated in this chapter were:

- To assess the effect of over-expressing miR-451 on hPASMC proliferation and migration *in vitro*.
- To determine the effect of transiently knocking down miR-451 *in vivo* on the development of PH.
- To determine the effect of genetic ablation of miR-451 *in vivo* on the development of PH.

3.2 Results

3.2.1 *In vitro* modulation of miR-451 using Ad-miR-451

Our first aim was to modulate miR-451 *in vitro* to mimic the increased miR-451 expression observed *in vivo* in rodent models of PH (Caruso et al., 2012). Therefore an adenovirus was used to induce over-expression of miR-451 in a cell culture model. An adenovirus containing the precursor sequence for human miR-451 (human Ad-miR-451) or rat miR-451 (rat Ad-miR-451) was created to assess the effect of over-expressing miR-451 *in vitro*. For a control, Ad5 lacZ control virus was used as this contains the same backbone as that of the Ad-miR-451 viruses. These viruses were first transduced into HeLa cells for 24 hours to establish if over-expression of miR-451 was achieved in human cells. The control virus did not cause any modulation in miR-451 expression compared to control cells (Figure 3.1). Human Ad-miR-451 caused an increase of ~4 fold in mature miR-451 expression (Figure 3.1A) at the highest concentration of virus compared to control. Rat Ad-miR-451 caused ~30 fold increase in mature miR-451 levels at all concentrations tested (Figure 3.1B).

Although miR-451 expression is increased in HeLa cells, it is important to establish whether this over-expression can be reproduced in the cell type of interest. Human pulmonary artery smooth muscle cells (hPASMCs) are one of the predominant cell types within the lung vessel wall which are dysregulated during PAH, particularly within the proximal medial layer (Archer et al., 2010). Dysregulation of SMCs induces SMC migration and proliferation, distal extension of smooth muscle and leads to pulmonary vascular remodelling, increasing the severity of the disease. To assess whether the transduction protocol was effective, hPASMCs were transduced with control Ad5 lacZ virus and then exposed to 0.1% or 15% serum for 48 hours (as would be performed in a migration/proliferation assay) after which x-gal staining was performed. There was a concentration dependent increase in positive x-gal staining observed in hPASMCs transduced with Ad5 lacZ virus with more staining detected in cells exposed to 15% serum (Figure 3.2). This indicated that transduction with the Ad5 lacZ control virus was successful.

Next, we wanted to assess the effect of over-expressing miR-451 in the cell type of interest - hPASCs. Hence, the Ad-miR-451 viruses were transduced into hPASCs and expression levels of mature miR-451 were measured (Figure 3.3). However, both the human Ad-miR-451 and rat Ad-miR-451 virus failed to produce any over-expression of miR-451 in hPASCs compared to control cells.

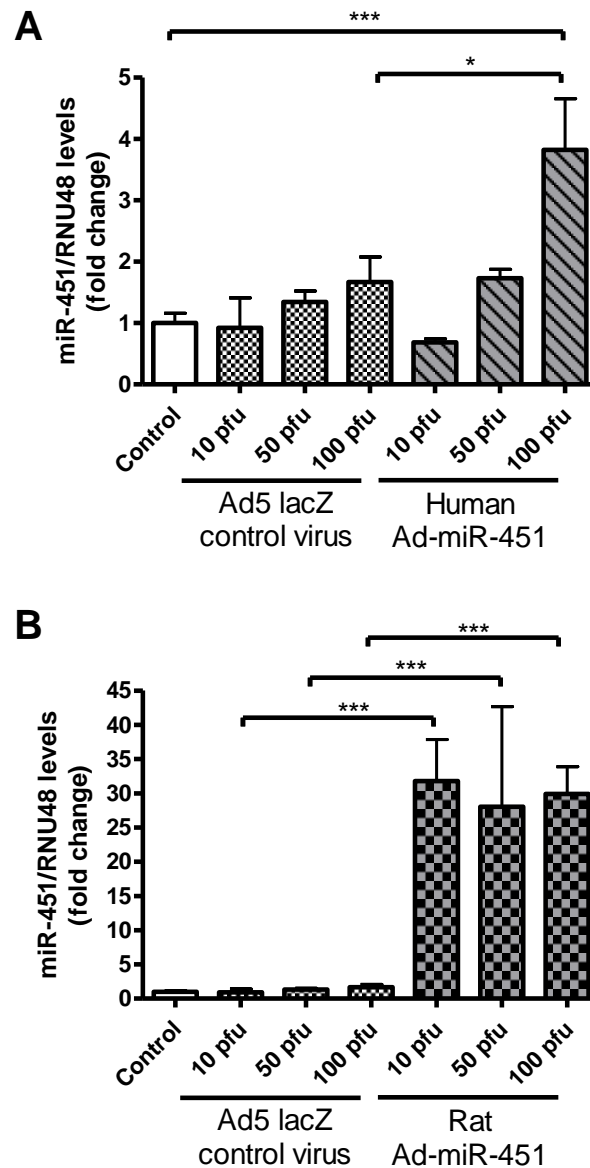


Figure 3.1 – miR-451 expression in HeLa cells transduced with adenovirus to over-express human or rat pre-miR-451.

Mature miR-451 expression in HeLa cells transduced with 10, 50 or 100 pfu of (A) human Ad-miR-451 or (B) rat Ad-miR-451 or Ad5 lacZ control virus 24h after transduction, as detected by qRT-PCR. Arbitrary value of 1 assigned to control non-transduced cells. Data expressed as fold change \pm SEM and analysed using a one-way ANOVA followed by Tukey's post hoc test. Representative graphs of two independent experiments with three technical repeats per condition. * $p < 0.05$, *** $p < 0.001$.

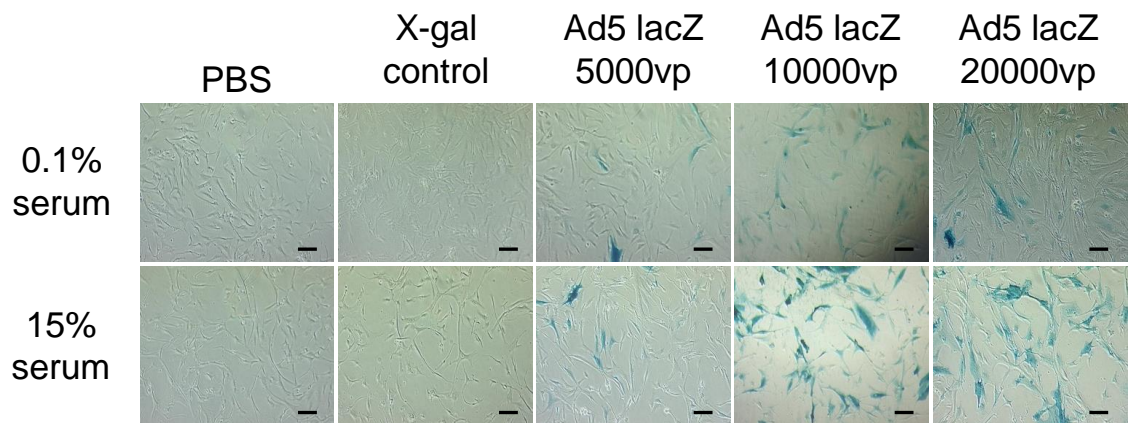


Figure 3.2 – β -galactosidase expression in hPASMCs transduced with Ad5 lacZ control virus.

hPASMCs were transduced with 5,000, 10,000 or 20,000 vp of Ad5 lacZ control virus and exposed to 0.1% or 15% serum containing media for 48 h. Cells were then fixed and stained for β -galactosidase activity. Scale bar = 100 μ m.

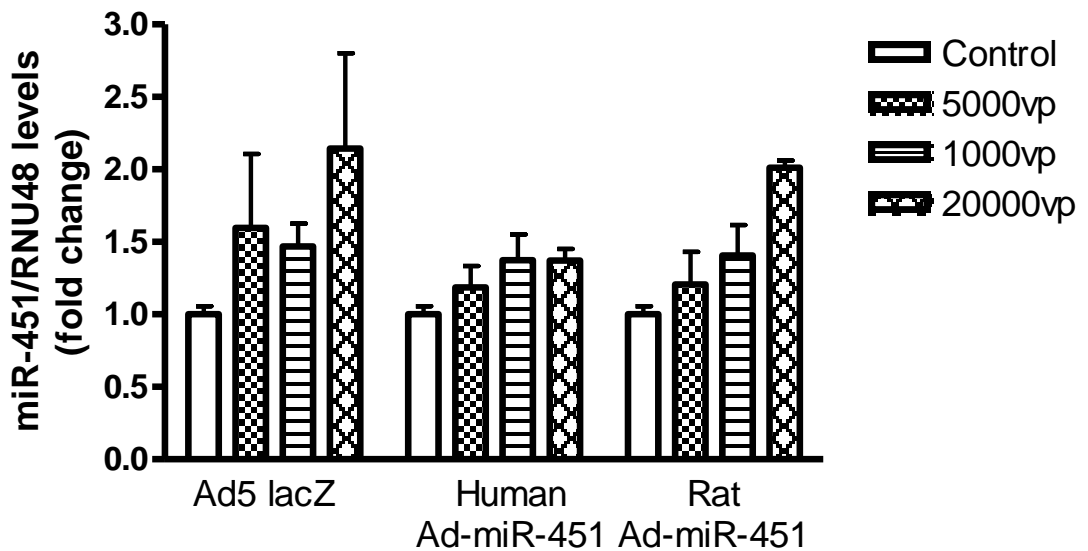


Figure 3.3 – MiR-451 expression in hPASCs transduced with adenovirus to over-express human or rat pre-miR-451.

Mature miR-451 expression in hPASCs transduced with 5,000, 10,000 or 20,000 vp of human Ad-miR-451, rat Ad-miR-451 or Ad5 lacZ control virus, quiesced for 48h and then cells lysed for RNA extraction, as detected by qRT-PCR. Arbitrary value of 1 assigned to control non-transduced cells. Data expressed as fold change \pm SEM and analysed using a one-way ANOVA followed by Tukey's post hoc test. Representative graph of two independent experiments with three technical repeats per condition.

3.2.2 Modulation of miR-451 in hPASMCs by miR-451 mimic

The adenovirus used to over-express miR-451 resulted in efficient over-expression when used in a cell line, however no over-expression of miR-451 was observed when Ad-miR-451 was transduced into primary hPASMCs. Therefore, miR-451 mimics were used to transfect hPASMCs to induce miR-451 over-expression. These miRNA mimics are double stranded chemically modified molecules which mimic endogenous miRNAs. A cy3 labelled mimic was used as a negative control and was used to visualise the transfection efficiency using three concentrations of mimic; 10 nM, 25 nM and 50 nM and quiesced in 0.1% serum containing media for 48 h. Fluorescent microscopy of cy3 labelled mimic transfected into hPASMCs shows increased dye with increasing mimic concentration and the mimic appears to be localised around the nucleus (Figure 3.4).

MiR-451 mimics were then transfected into hPASMCs at the same concentrations used for the negative control and serum starved for 48 h before lysing cells for RNA extraction. Transfection with miR-451 mimic significantly increased miR-451 expression at all concentrations compared to the control mimic and mock transfected cells (Figure 3.5A). High expression of miR-451 was observed using 10 nM of miR-451 mimic and this concentration was further examined by northern blot (Figure 3.5B, C). Northern blot analysis illustrated low miR-451 levels in control treated cells and confirmed the increase in miR-451 expression using 10 nM of miR-451 mimic. As a result, this concentration of miR mimic was used in all subsequent experiments to assess the effect of over-expressing miR-451 on hPASMCs phenotype.

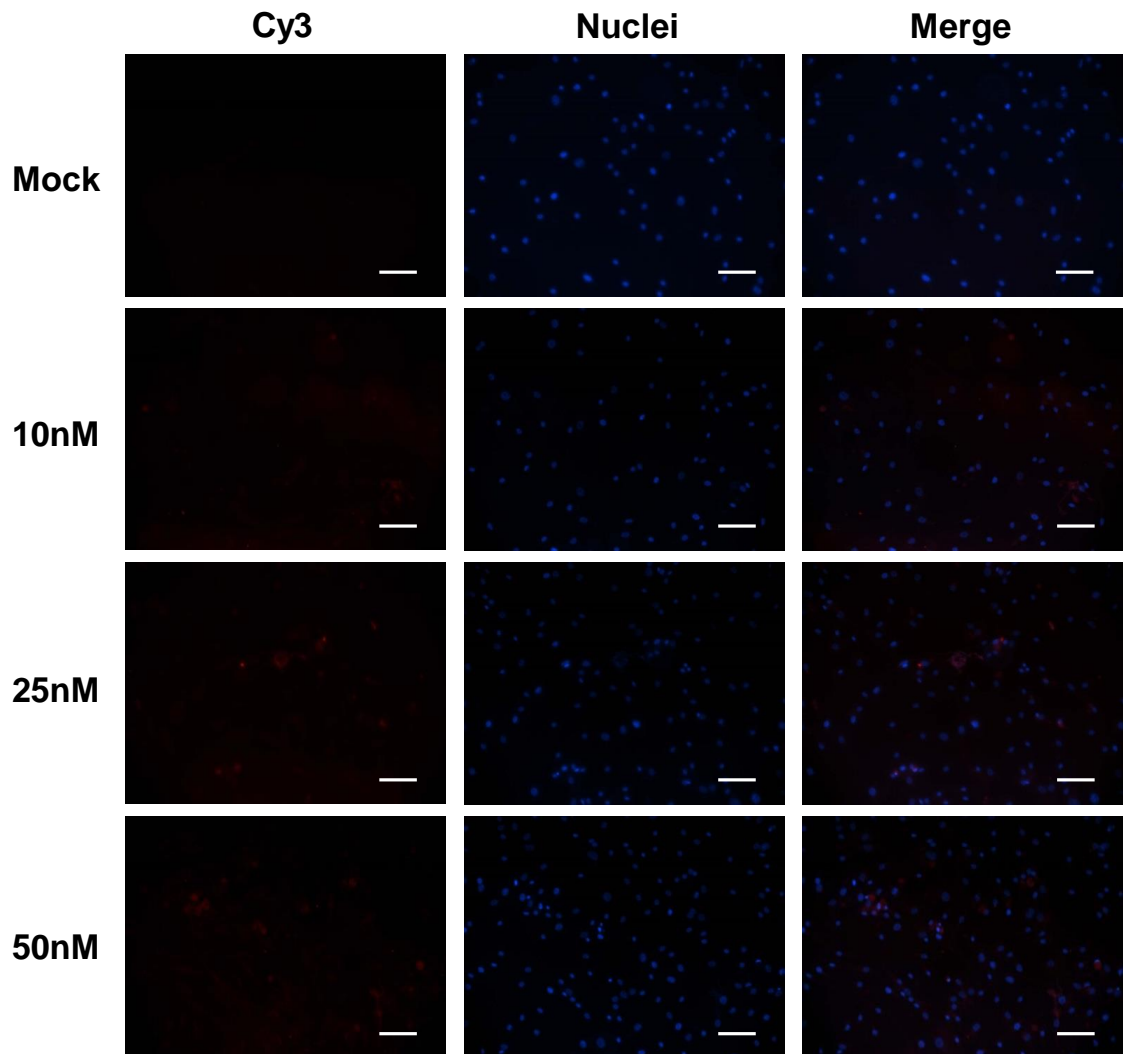


Figure 3.4 – Visualisation of cy3 labelled miR mimics in hPASMCs.

A negative control cy3 miR mimic was transfected into hPASMCs at a concentration of 10, 25 or 50 nM and quiesced for 48h. Cells were then fixed and cy3 mimic was visualised using fluorescent microscopy. Magnification X40, scale bar = 20 μm .

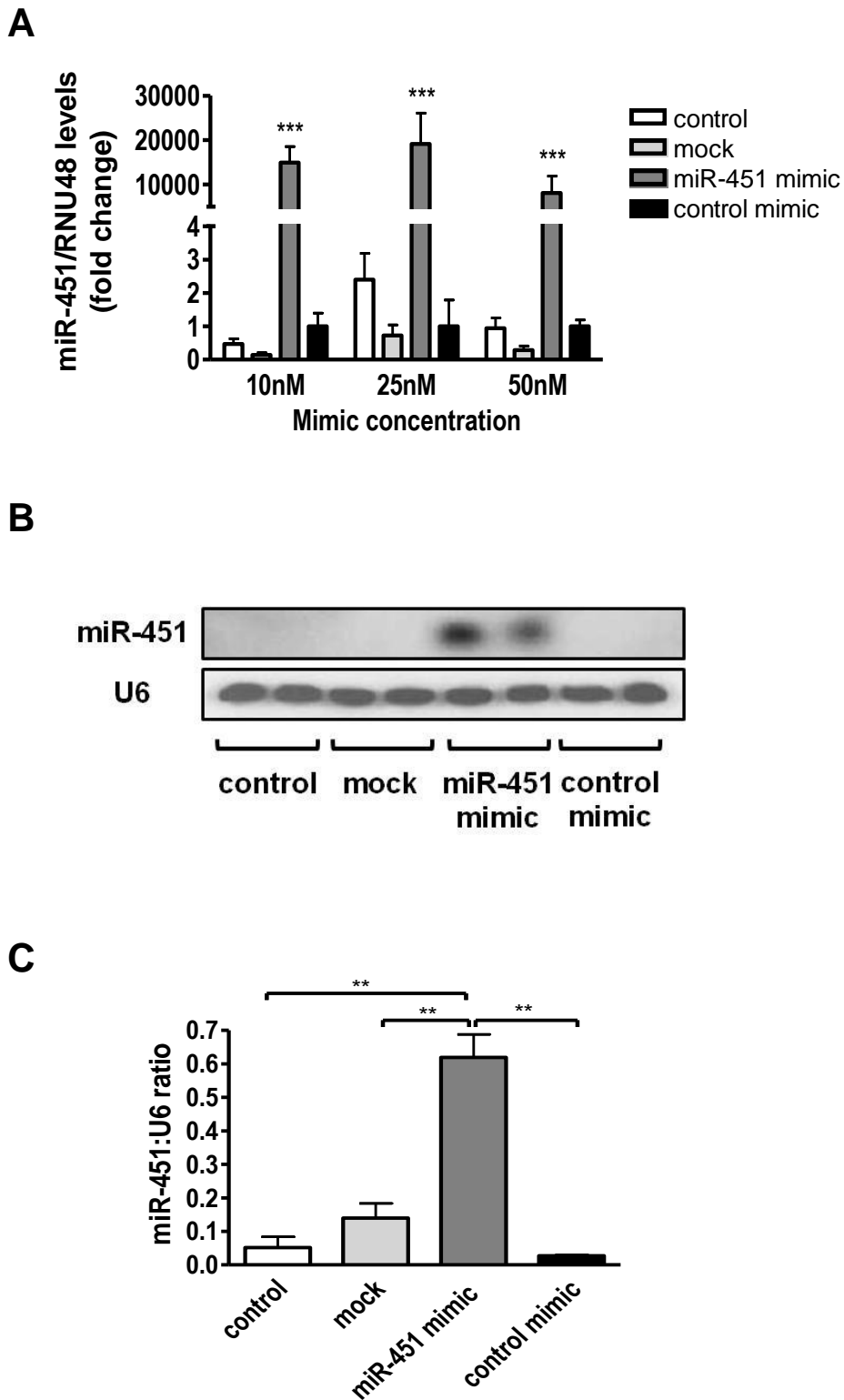


Figure 3.5 – miR-451 expression in hPASMCs over-expressing miR-451.

(A) MiR-451 expression in hPASMCs after transfection with miR mimic and quiesced for 48h, as detected by qRT-PCR. Arbitrary value of 1 assigned to control mimic. Representative graph of two independent experiments with technical triplicates, *** $p < 0.001$ vs control mimic of that concentration. Data expressed as fold change \pm SEM. (B,C) Northern blot analysis of hPASMCs using a concentration of 10 nM miR mimic, quantified by normalising the band intensity of mature miR-451 to the relative U6 signal, ** $p < 0.01$, $n = 2$ wells per condition. Data expressed as mean \pm SEM. All data analysed using a one-way ANOVA followed by Tukey's post hoc test.

3.2.3 Over-expression of miR-451 has no effect on hPASC proliferation

The effect of over-expressing miR-451 on the proliferation of hPASCs was assessed. Two methods were used to quantify proliferation; an MTS assay and a thymidine incorporation assay. Increasing concentrations of serum induced a steady increase in cellular proliferation in control and mock transfected cells as measured by thymidine incorporation (Figure 3.6A). The same pattern was observed in hPASCs transfected with 10 nM miR-451 mimic as serum did not alter proliferation rates. This was supported by the MTS assay (Figure 3.6B) where there was no significant difference between control cells and cells transfected with miR-451 mimic. Thus illustrating that miR-451 does not affect hPASC proliferation in this setting.

3.2.4 Over-expression of miR-451 promotes hPASC migration in the absence of serum

As well as assessing hPASC proliferation, cell migration was also assessed in cells over-expressing miR-451 as migration of SMCs into distal non-muscular vessels plays a critical role in PAH development (Humbert et al., 2004a). Cells transfected with control mimic stimulated with 15% serum had migrated fully to close the wound after 24 h (Figure 3.7A, C). Similarly, cells transfected with miR-451 mimic and in the presence of 15% serum were no different to control mimic cells with complete closure of the wound after 24 h. Thus indicating that over-expressing miR-451 does not inhibit serum induced migration of hPASCs under the experimental conditions tested. In the presence of 0.1% serum, cells over-expressing miR-451 showed enhanced wound closure compared to control mimic cells (Figure 3.7A, B). Therefore suggesting that miR-451 promotes hPASC migration in the absence of serum. This enhanced migratory effect by miR-451 over-expression was more obvious when analysed by microscopy than the effect observed in Figure 3.7B.

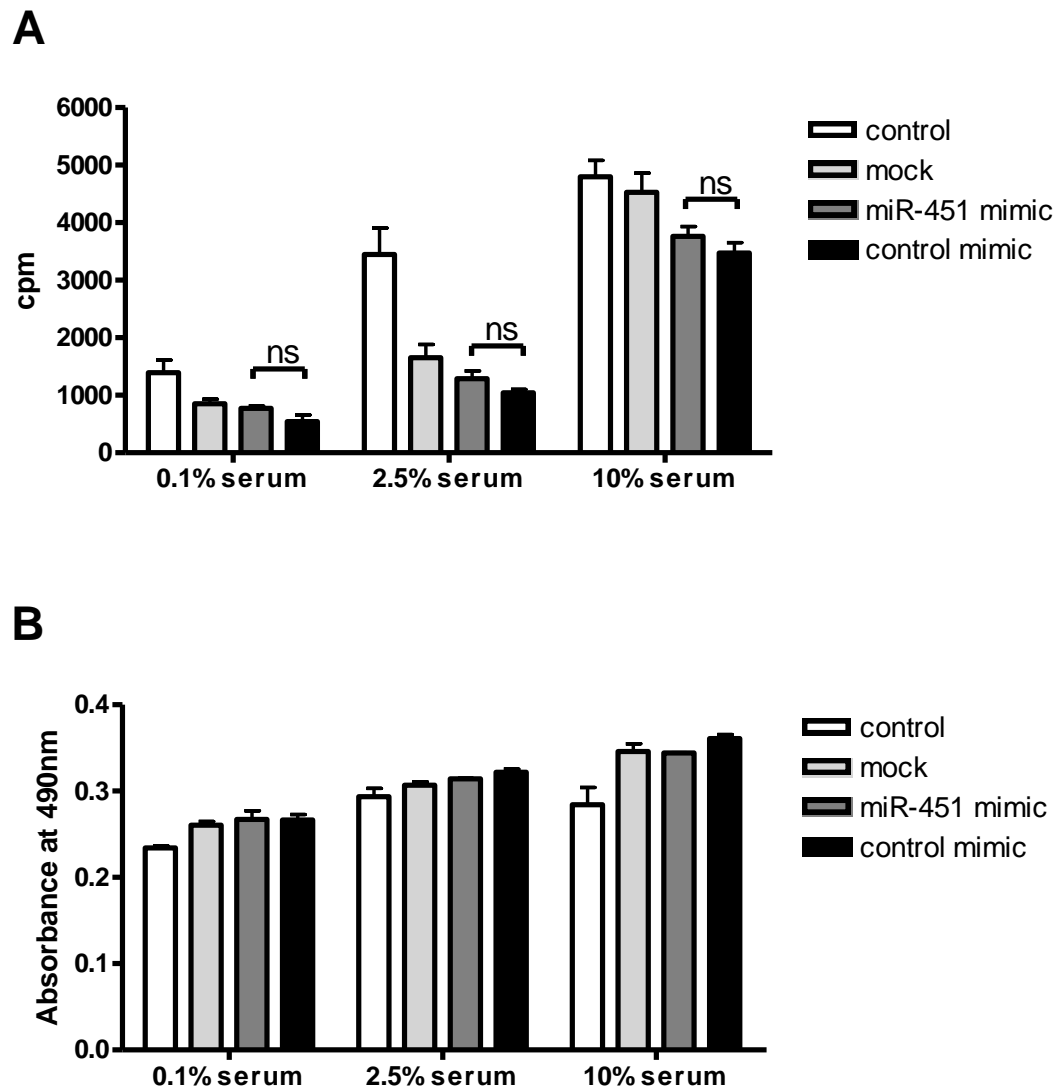


Figure 3.6 – Effect of over-expressing miR-451 on hPASMC proliferation.

Human PASMCs were transfected with 10 nM miR-451 mimic or control mimic and proliferation rates were measured 72 h later using (A) a thymidine incorporation assay and (B) MTS assay. Representative graphs of two independent experiments with four technical repeats per condition, cpm = counts per minute, ns = non-significant.

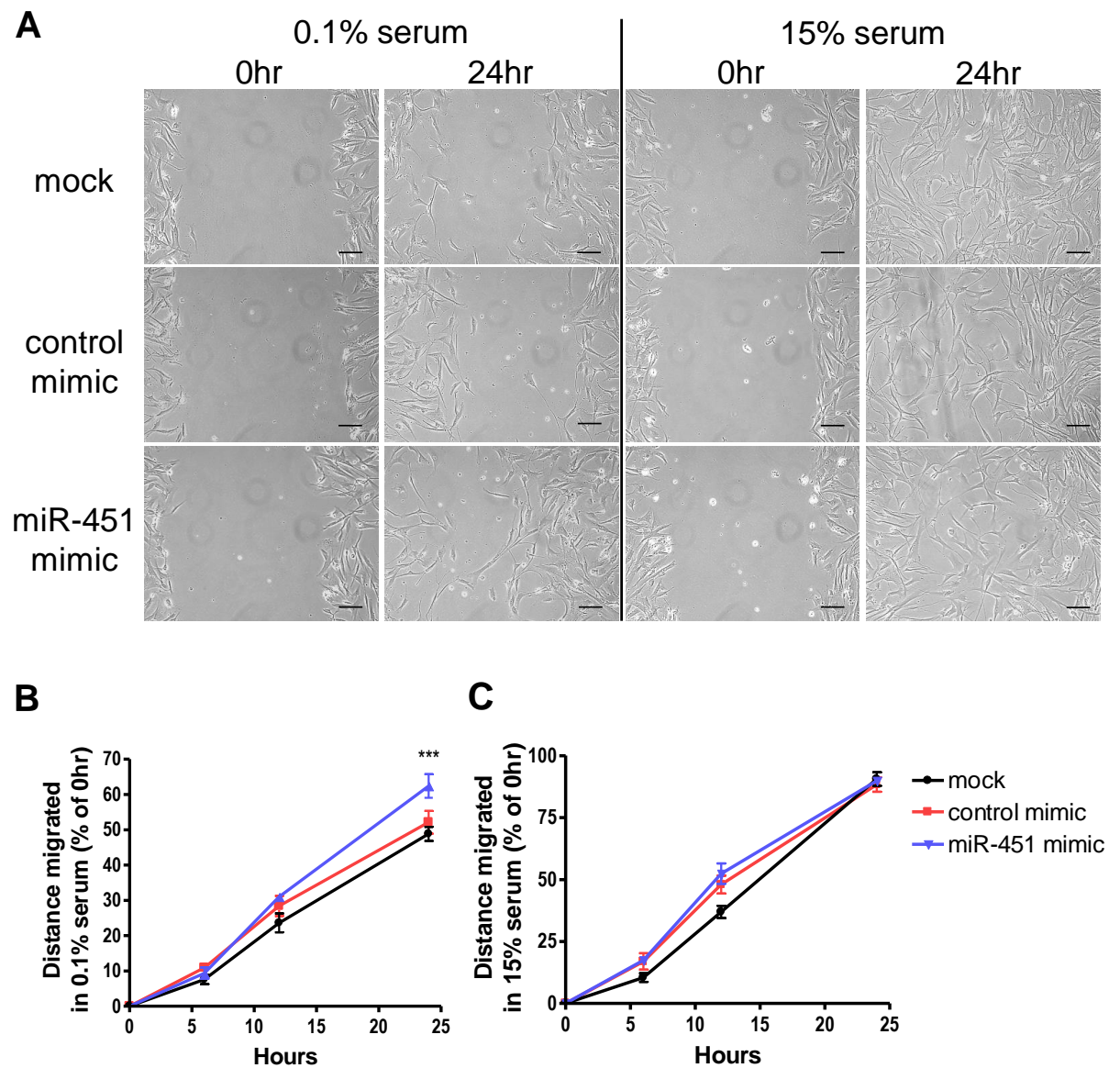


Figure 3.7 – Effect of over-expressing miR-451 on hPASMC migration.

(A) hPASMCs were transfected with 10 nM miR-451 mimic or control mimic, quiesced for 48 h and subjected to the scratch wound assay. Representative images of hPASMC scratch wound at 0 h and 24 h. Magnification X10, scale bar = 100 μ m. (B) Quantification of hPASMC migration in 0.1% serum and (C) 15% serum. Data expressed as mean \pm SEM and analysed by a one-way ANOVA followed by Tukey's post hoc test. *** $p < 0.001$ vs control mimic in 0.1% serum. Pictures and graphs are representative of three independent experiments, two wells per condition with four scratches per well.

3.2.5 Target gene analysis on hPASMCs over-expressing miR-451

To determine the pathways that may explain the increase in migration in response to miR-451 over-expression, target genes for miR-451 were analysed in cells transfected with mimic and quiesced for 48 hours. Target prediction algorithms were used along with searching the literature for putative mRNA targets for mature miR-451. Using various tissues in different disease states, previous studies have shown that miR-451 target genes include Akt1 (Wang et al., 2011, Bian et al., 2011), Rac1 (Wang et al., 2012b) and Ywhaz (Patrick et al., 2010b, Yu et al., 2010). If any of these genes were bona fide targets of miR-451, mRNA expression of the target genes would decrease significantly in cells transfected with miR-451 mimic as miR-451 levels are so high. Quantification of these genes was performed by qRT-PCR (Figure 3.8) however, none of the chosen genes were repressed in the miR-451 mimic cells compared to control mimic under these experimental conditions.

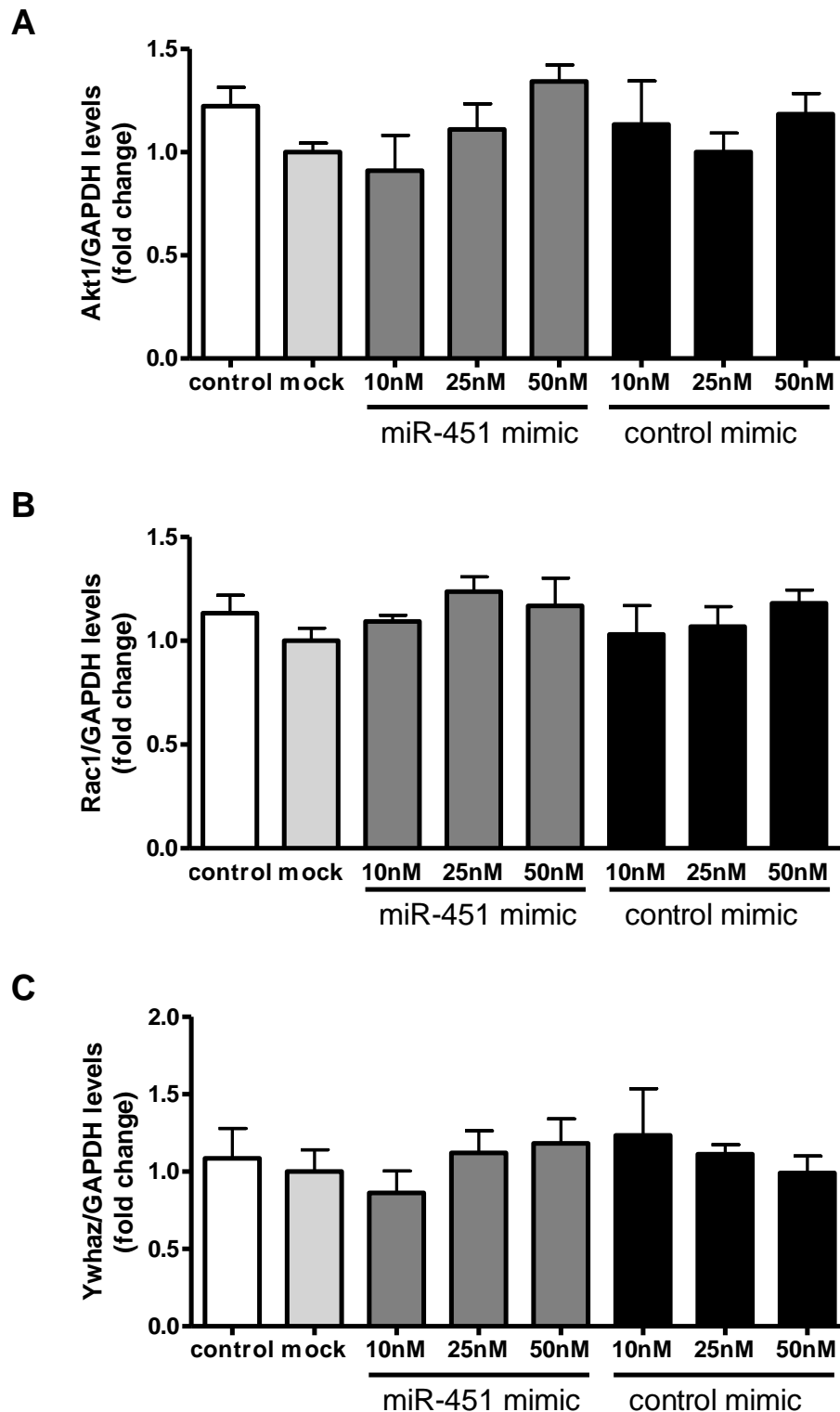


Figure 3.8 – Target gene mRNA expression in hPASCs over-expressing miR-451.

(A) Akt1, (B) Rac1 and (C) Ywhaz mRNA expression in hPASCs transfected with 10, 25 or 50 nM miR-451 or control mimic, quiesced for 48 h and then lysed for RNA extraction, as detected by qRT-PCR. Arbitrary value of 1 assigned to mock treated hPASCs. Data expressed as fold change \pm SEM and analysed by a one-way ANOVA followed by a Tukey's post hoc test, n = 3 wells per condition.

3.2.6 Transient knockdown of miR-451 *in vivo* attenuates the development of PH in the rat hypoxic model

We also assessed the role of miR-451 *in vivo*. Since previous work in our laboratory showed that miR-451 levels were increased in PH diseased animals (Caruso et al., 2010), we knocked down miR-451 *in vivo* to assess the impact of this on the development of PH. Pharmacological inhibition was achieved using an antimiR targeted to the mature miR-451. This was administered to male rats followed by 7 days hypoxic exposure. To verify the degree of knock down obtained using antimiR-451, tissues were harvested and miR-451 expression was analysed. In normoxic rats treated with control antimiR, miR-451 expression is particularly high in red blood cells (RBC). Compared to expression within the lung, the pulmonary artery, right ventricle and left ventricle plus septum have increased miR-451 expression while the testes have lower miR-451 expression (Figure 3.9A). MiR-451 expression was extremely low in all tissues treated with antimiR-451 compared to control treated tissue (Figure 3.9B) indicating that antimiR-451 reduced miR-451 levels globally. Furthermore, northern blot analysis was carried out on lung tissue from animals treated with antimiR-451. Significantly reduced levels of miR-451 compared to control were observed (Figure 3.10A, B). The knock down of miR-451 in RBCs was a concern as this miRNA plays an essential role in normal erythroid differentiation (Dore et al., 2008) and silencing miR-451 may have an impact on the outcome and interpretation of results. However, there is no known uptake mechanism in RBCs for antimiRs and from the qRT-PCR data, animals treated with antimiR-451 still have very low threshold cycle (Ct) values (and therefore high expression) for miR-451 in the RBC compartment.

As mentioned previously, miR-451 exists in a cluster with miR-144. Therefore expression levels of miR-144 were also analysed by qRT-PCR (Figure 3.11). Under basal conditions, miR-144 expression is similar to miR-451 with highest levels in RBCs (Figure 3.11A). MiR-144 expression increased in the testes and RBCs when exposed to hypoxia however, there were no differences between control and antimiR-451 treated animals in either normoxic or hypoxic conditions in any of the tissues analysed indicating that antimiR-451 is selectively down-regulating miR-451 *in vivo* (Figure 3.11B).

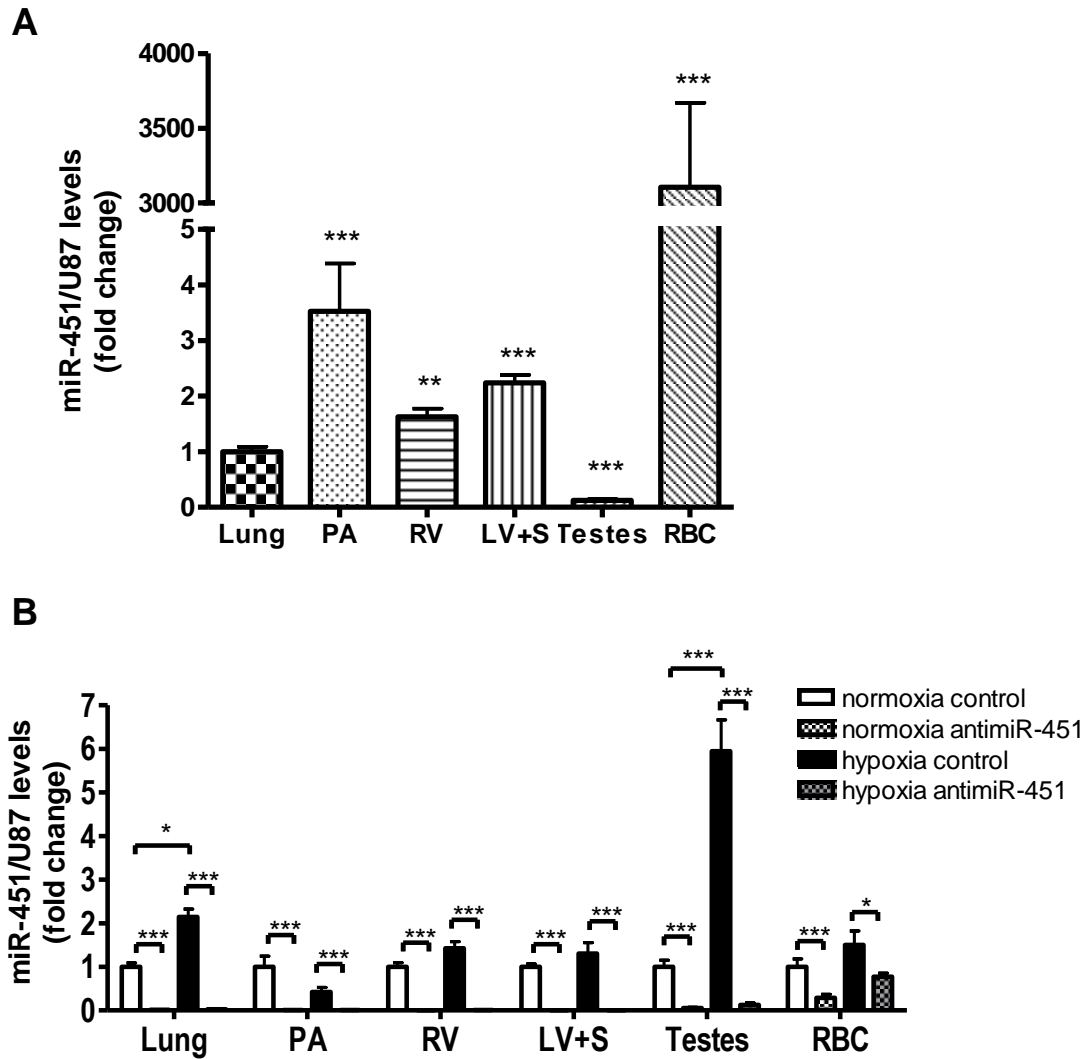


Figure 3.9 – MiR-451 expression in anti-miR-451 treated rats as detected by qRT-PCR.

(A) MiR-451 expression in tissue from male normoxic rats dosed with control anti-miR, as detected by qRT-PCR. Arbitrary value of 1 assigned to lung tissue, $n = 9$ animals per group. Data expressed as fold change \pm SEM. Data analysed by a one-way ANOVA followed by Tukey's post hoc test. (B) MiR-451 expression in tissue from male rats pre-dosed with 10 mg/kg anti-miR-451 or control anti-miR followed by 7 days exposure to normoxic or hypoxic conditions, as detected by qRT-PCR. Arbitrary value of 1 assigned to normoxic control for each tissue, $n = 9$ animals per group. Data expressed as fold change \pm SEM. Data analysed by a two-way ANOVA followed by Bonferroni post hoc test. * $p < 0.05$, ** $p < 0.01$ and *** $p < 0.001$. LV+S = left ventricle plus septum, PA = pulmonary artery, RBC = red blood cells, RV = right ventricle.

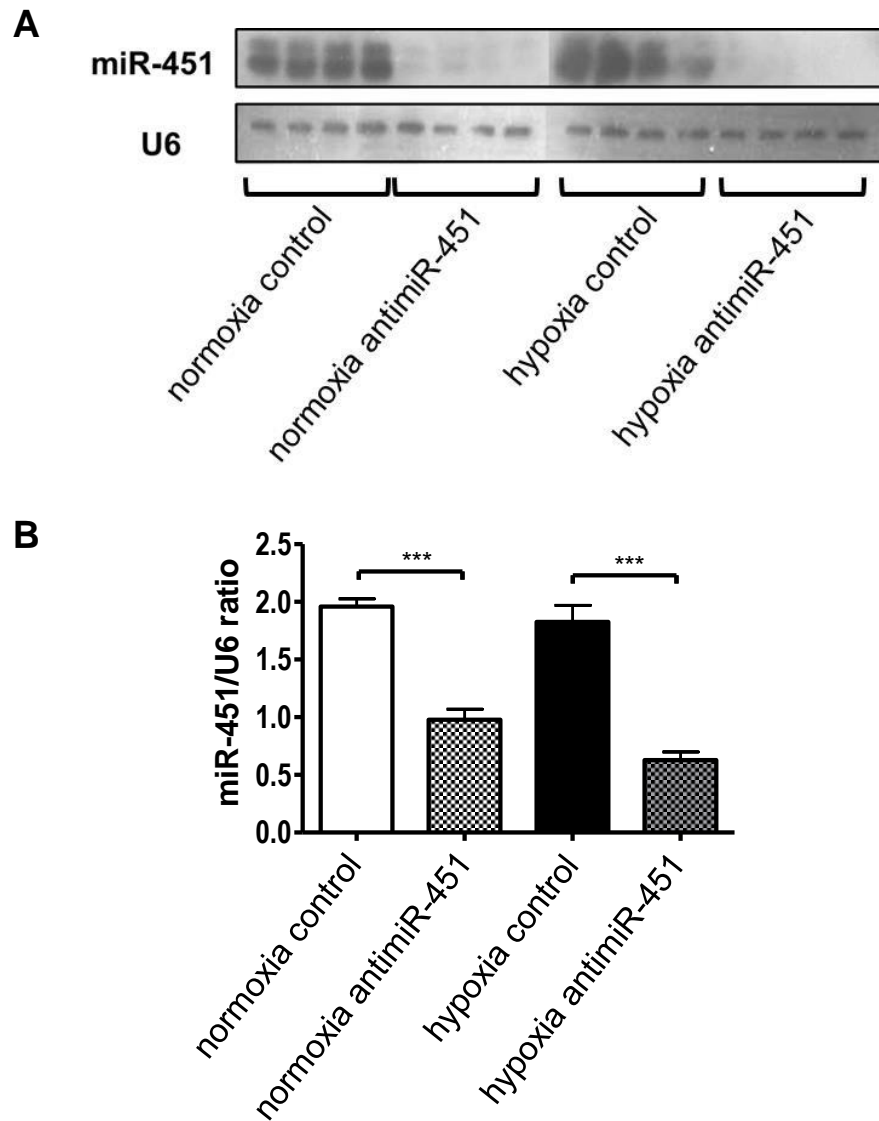


Figure 3.10 – MiR-451 expression in antimiR-451 treated animals, as detected by northern blot.

(A) Northern blot was performed on whole lung from male rats pre-dosed with 10 mg/kg antimiR-451 or control antimiR followed by 7 days exposure to normoxic or hypoxic conditions. (B) Quantification was carried out by normalising the band intensity of mature miR-451 to the relative U6 signal, $n = 4$ animals per group. Data expressed as mean \pm SEM. Data analysed by a two-way ANOVA followed by Bonferroni post hoc test, $**p < 0.01$.

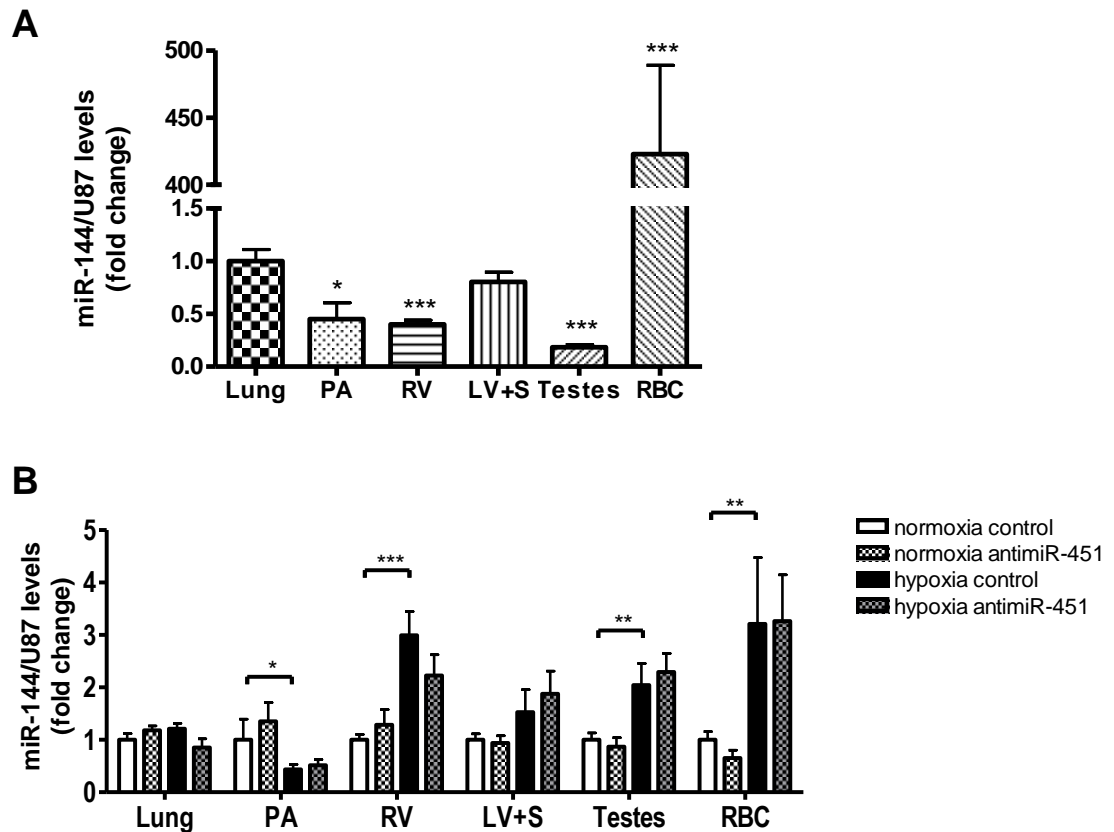


Figure 3.11 – MiR-144 expression in anti-miR-451 treated animals.

(A) MiR-144 expression in tissue from male normoxic rats dosed with control anti-miR, as detected by qRT-PCR. Arbitrary value of 1 assigned to lung tissue, $n = 9$ animals per group. Data expressed as fold change \pm SEM. Data analysed by one-way ANOVA followed by Tukey's post hoc test. (B) MiR-144 expression in tissue from male rats pre-dosed with 10 mg/kg anti-miR-451 or control anti-miR followed by 7 days exposure to normoxic or hypoxic conditions, as detected by qRT-PCR. Arbitrary value of 1 assigned to normoxic control for each tissue. Data expressed as fold change \pm SEM and analysed by a two-way ANOVA followed by a Bonferroni post hoc test. * $p < 0.05$, ** $p < 0.01$ and *** $p < 0.001$, $n = 9$ animals per group. LV+S = left ventricle plus septum, PA = pulmonary artery, RBC = red blood cells, RV = right ventricle.

The effect of silencing miR-451 on the development of PH was then analysed. Systemic arterial pressure was increased in the hypoxic rats but unchanged between control and antimiR-451 treated animals (Figure 3.12A). This increase in SAP in hypoxic conditions may be due to differences in anaesthetic levels. Heart rate was unchanged between groups (Figure 3.12B). Three of the main indices of PH were then measured to determine PH development; RVP, RVH and pulmonary remodelling. Rats exposed to hypoxic conditions along with control antimiR had a significant increase in RVP compared to normoxic control animals (56.02 ± 2.03 , 34.44 ± 2.18 mmHg, respectively) (Figure 3.13A, B). Pre-treatment with antimiR-451 prior to hypoxic exposure lowered the RVP compared to control antimiR treated animals (47.07 ± 1.36 , 56.02 ± 2.03 mmHg, respectively). Quantification of RVH illustrated no significant changes between groups (Figure 3.14A). An increase in pulmonary vascular remodelling was observed in all hypoxic groups (Figure 3.14B, C) compared to normoxic controls. Administration of antimiR-451 did not significantly reduce pulmonary remodelling. Hence pre-treatment of antimiR-451 did not alter vessel remodelling.

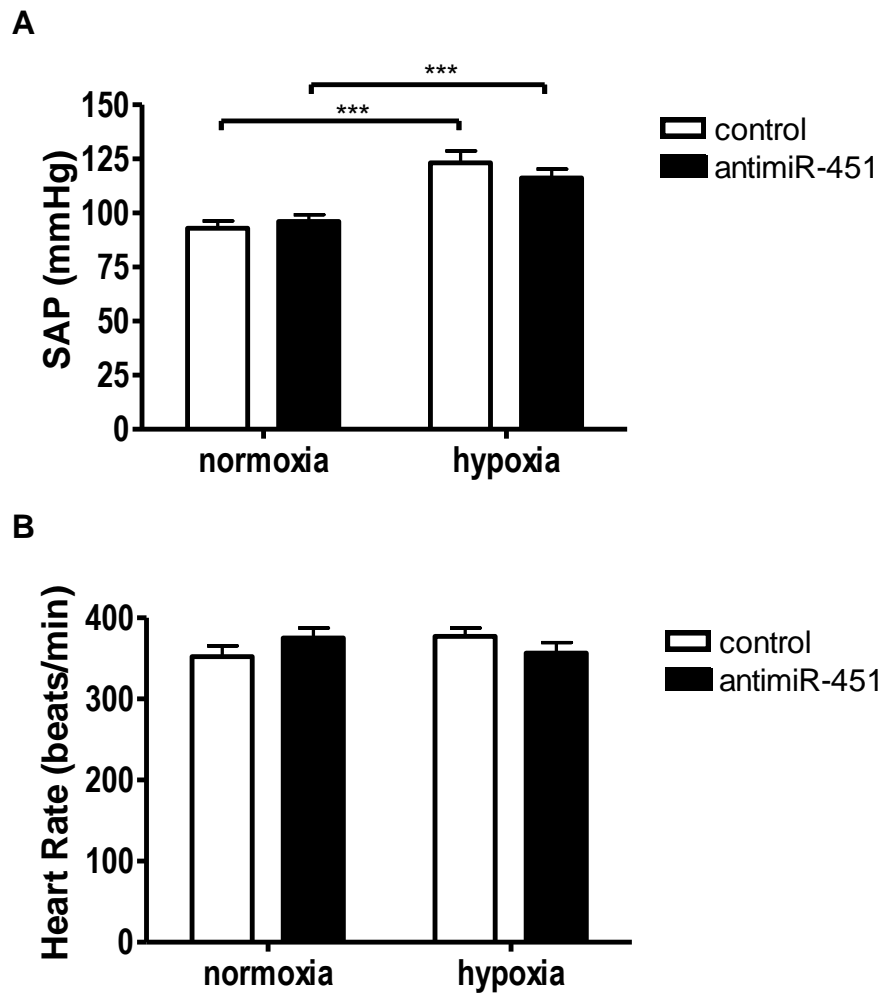


Figure 3.12 – Effect of anti-miR-451 treatment on systemic arterial pressure and heart rate.

Quantification of (A) systemic arterial pressure and (B) heart rate in male rats pre-dosed with 10 mg/kg anti-miR-451 or control anti-miR followed by 7 days exposure to normoxic or hypoxic conditions. Data are expressed as mean \pm SEM and analysed by a two-way ANOVA followed by Bonferroni post hoc test. *** $p < 0.001$, $n = 7-8$ animals per group.

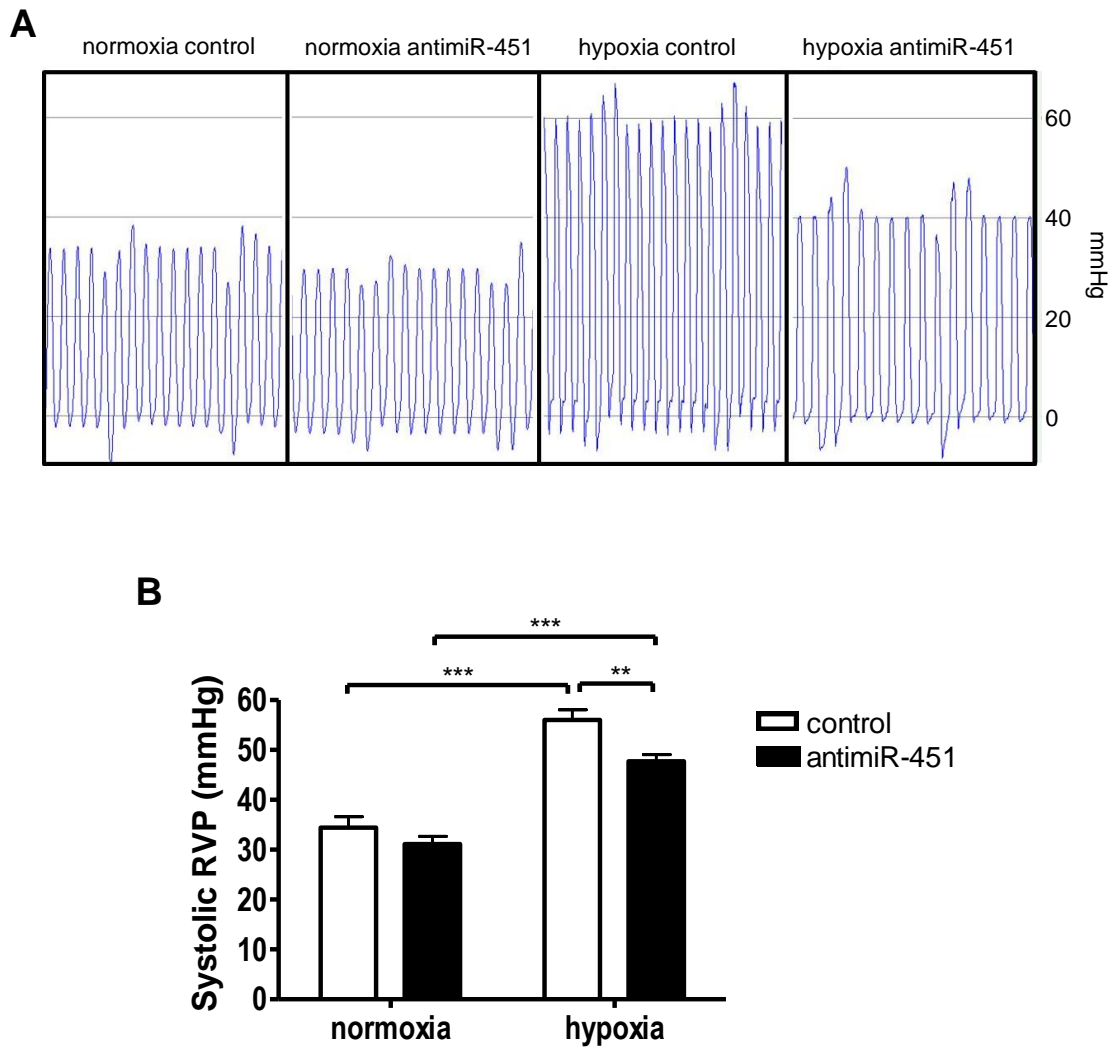


Figure 3.13 – Effect of antimiR-451 treatment on systolic right ventricular pressure.

(A) Representative recording of right ventricular pressure and (B) quantification of systolic RVP in male rats pre-dosed with 10 mg/kg antimiR-451 or control antimiR followed by 7 days exposure to normoxic or hypoxic conditions. Data represented as mean \pm SEM and analysed by a two-way ANOVA followed by Bonferroni post hoc test. ** $p < 0.01$ and *** $p < 0.001$, $n = 7-8$ animals per group.

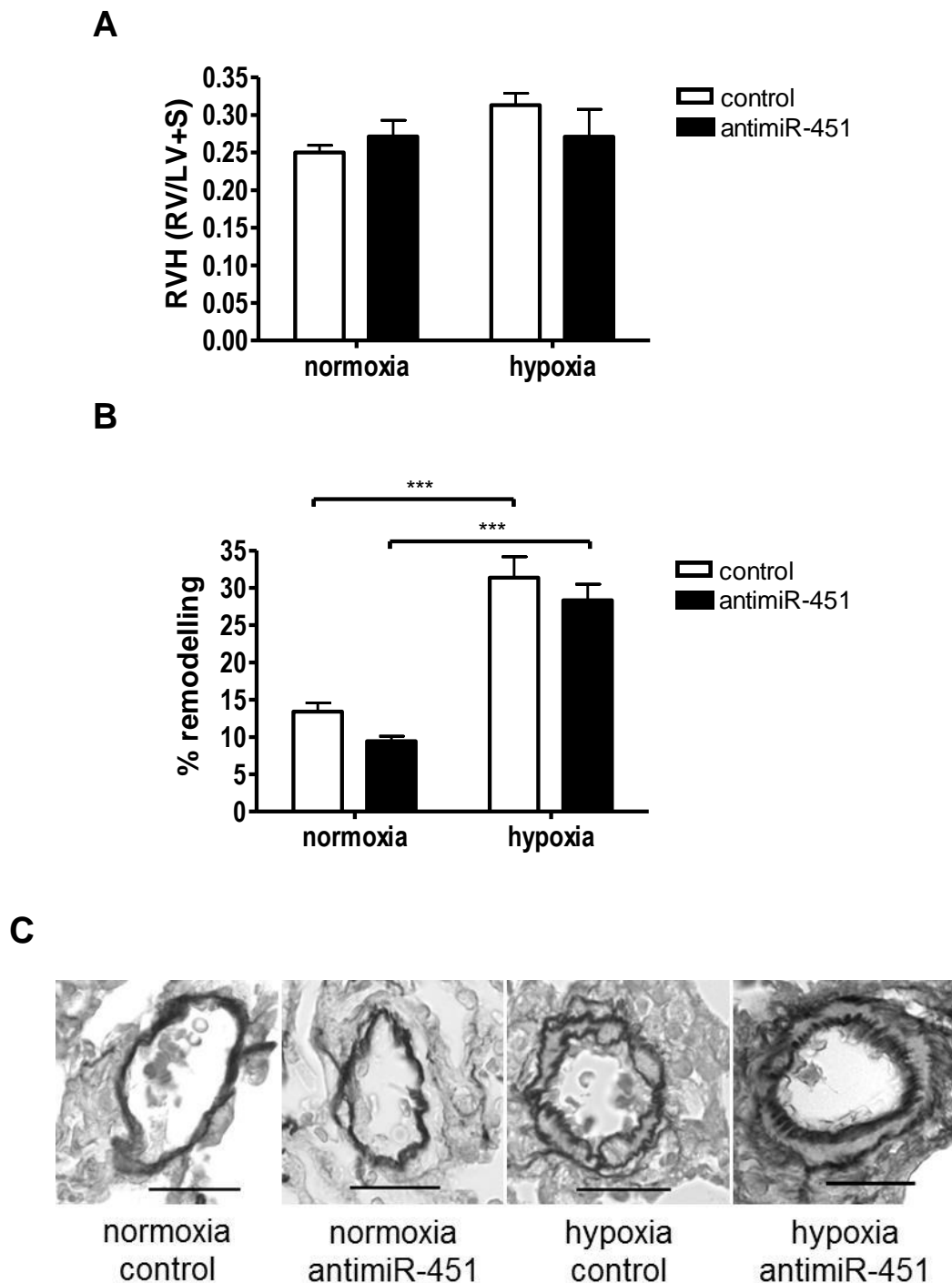


Figure 3.14 – Effect of anti-miR-451 treatment on right ventricular hypertrophy and pulmonary vascular remodelling.

Quantification of (A) right ventricular hypertrophy and (B) pulmonary vascular remodelling in male rats pre-dosed with 10 mg/kg anti-miR-451 or control anti-miR followed by 7 days exposure to normoxic or hypoxic conditions. (C) Representative images of pulmonary vessels stained with elastic van Gieson, magnification X40, scale bar = 25 μ m. Data represented as mean \pm SEM and analysed by a two-way ANOVA followed by Bonferroni post hoc test. *** $p < 0.001$, $n = 7$ animals per group for RVH and $n = 4-6$ animals per group for pulmonary vascular remodelling analysis.

3.2.7 Target gene analysis in antimiR-451 treated rats

We observed that reduced expression of miR-451 was protective in preventing the increase in RVP characteristic in hypoxic conditions. Target genes were analysed in the lungs from these animals to establish what pathways may be responsible for this effect. Similar to the target genes predicted in human tissue, Akt1 and Bcl2 (Wang et al., 2011, Bian et al., 2011), Rac1 (Wang et al., 2012b), Tbx1 (Lewis et al., 2003) and Ywhaz (Patrick et al., 2010b, Yu et al., 2010) were all predicted targets for miR-451 in rat by either target prediction algorithms or previous publications. Analysis of mRNA expression (Figure 3.15) highlighted that Akt1, Rac1 and Ywhaz were down-regulated in antimiR-451 treated animals compared to control antimiR animals. However, none of the chosen genes showed derepression in mRNA levels when miR-451 was knocked down.

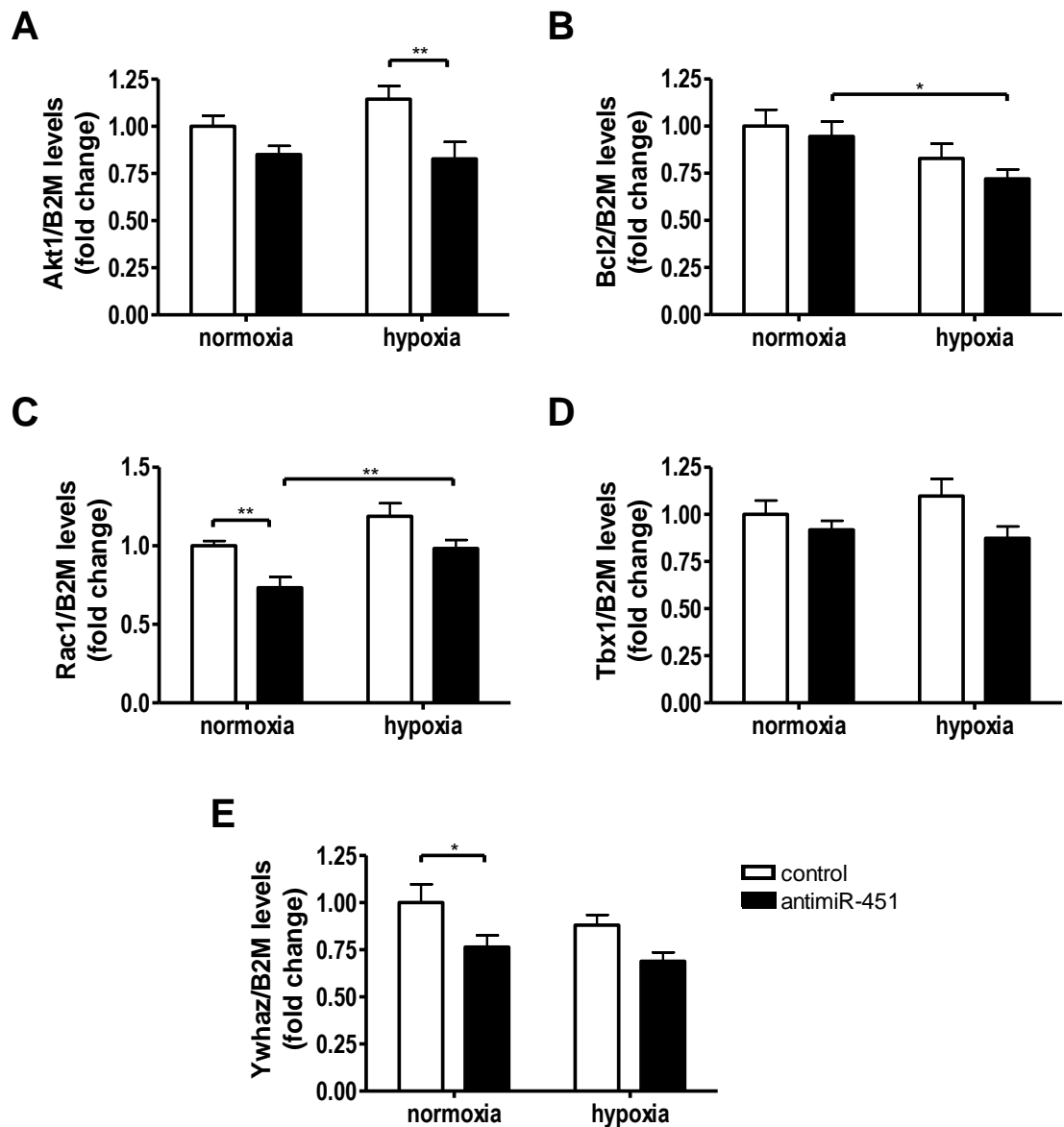


Figure 3.15 – Target gene mRNA expression in lung from anti-miR-451 treated animals.

(A) Akt1, (B) Bcl2, (C) Rac1, (D) Tbx1 and (E) Ywhaz mRNA expression in whole lung from male rats pre-dosed with 10 mg/kg anti-miR-451 or control anti-miR followed by 7 days exposure to normoxic or hypoxic conditions, as detected by qRT-PCR. Arbitrary value of 1 assigned to normoxic control group for each gene. Data represented as fold change \pm SEM and analysed by a two-way ANOVA followed by a Bonferroni post hoc test. * $p < 0.05$ and ** $p < 0.01$, $n = 9$ animals per group.

3.2.8 Genetic ablation of miR-451 in mice has no protective effect in hypoxia

From *in vitro* data, miR-451 induces PASMC migration while transient knock down of miR-451 diminishes aspects of the hypoxic response, therefore illustrating that a reduction in miR-451 levels *in vivo* attenuates the initial response to hypoxia. Hence we then sought to assess the effect of chronic knock down of miR-451 using knockout mice. MiR-451 is globally knocked out in null mice. MiR-451 knockout mice (and age matched wild type control mice) were exposed to hypoxic conditions for 14 days, after which hemodynamic measurements were taken to assess the development of PH.

Absence of miR-451 in the knockout mice was confirmed by northern blot analysis (Figure 3.16A, B) and qRT-PCR (Figure 3.16C) in lung tissue. Expression of miR-144 was also measured in the lung by qRT-PCR with levels of miR-144 unchanged between wild type and knockout mice (Figure 3.16D). Interestingly, this miRNA was significantly reduced in the lung after mice were exposed to hypoxic conditions.

Assessment of hypoxia-induced PH was then carried out. The systemic arterial pressure was variable between groups, however no consistent pattern was observed between the WT and KO mice in normoxia or hypoxia (Figure 3.17A). No difference in heart rate was observed between groups (Figure 3.17B). RVP, RVH and pulmonary remodelling all showed the expected increase in wild type mice exposed to hypoxia (Figure 3.17C - F). Knockout mice exposed to hypoxia showed the same trend in all parameters to that of wild type hypoxic mice, with no significant reduction observed in hypoxic miR-451 knockout mice.

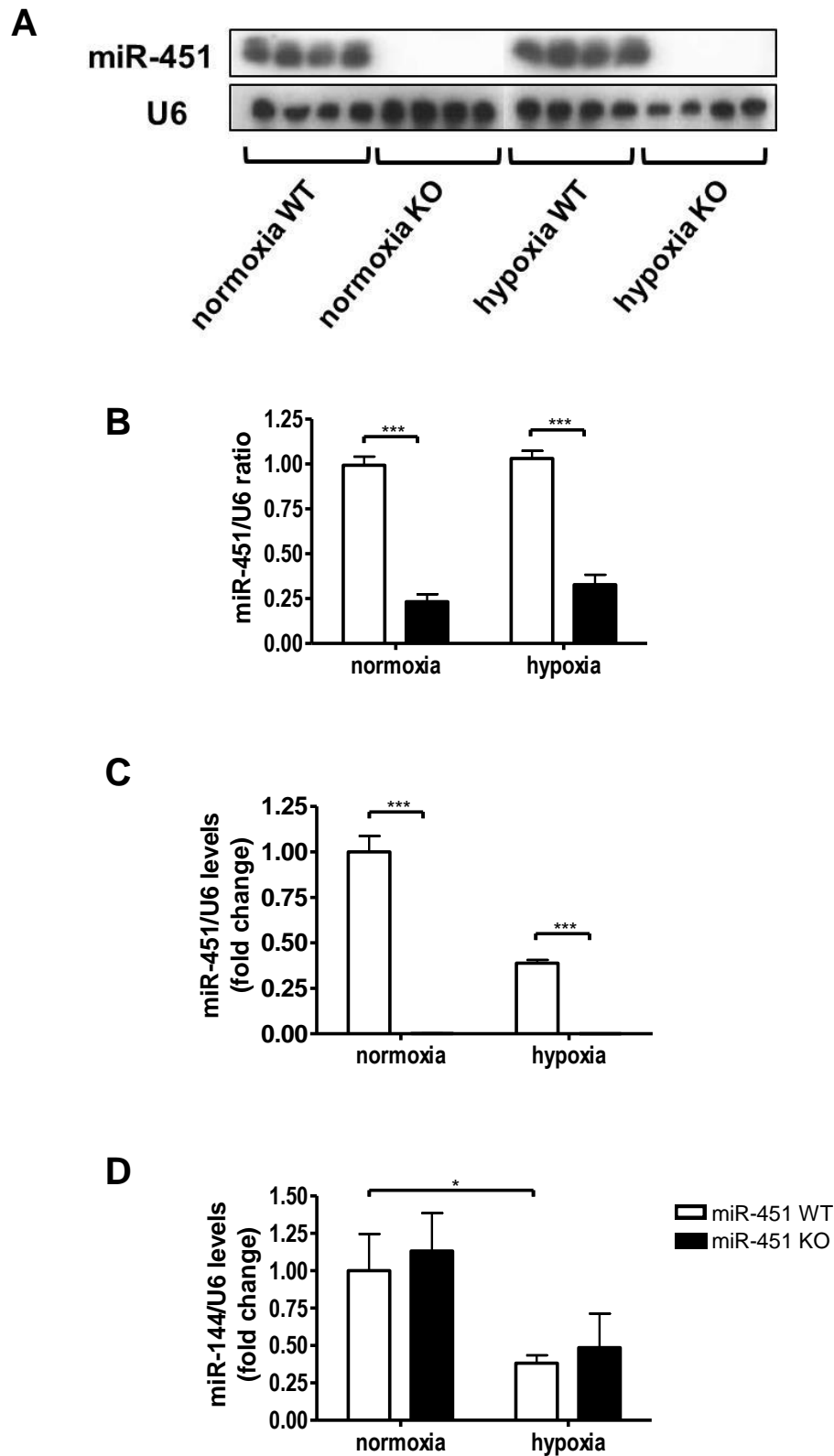


Figure 3.16 – MiR-451 and miR-144 expression in female miR-451 knockout mice.

(A, B) Northern blot was performed on RNA extracted from whole lung from female miR-451 wild type and knockout mice and quantified by normalising the band intensity of mature miR-451 to the relative U6 signal. Data expressed as mean \pm SEM, $n = 4$ animals per group. (C) MiR-451 expression and (D) miR-144 expression detected within the same samples by qRT-PCR. Arbitrary value of 1 assigned to normoxic miR-451 wild type. Data expressed as fold change \pm SEM, $n = 6$ animals per group. All data analysed by a two-way ANOVA followed by Bonferroni post hoc test. * $p < 0.05$ and *** $p < 0.001$.

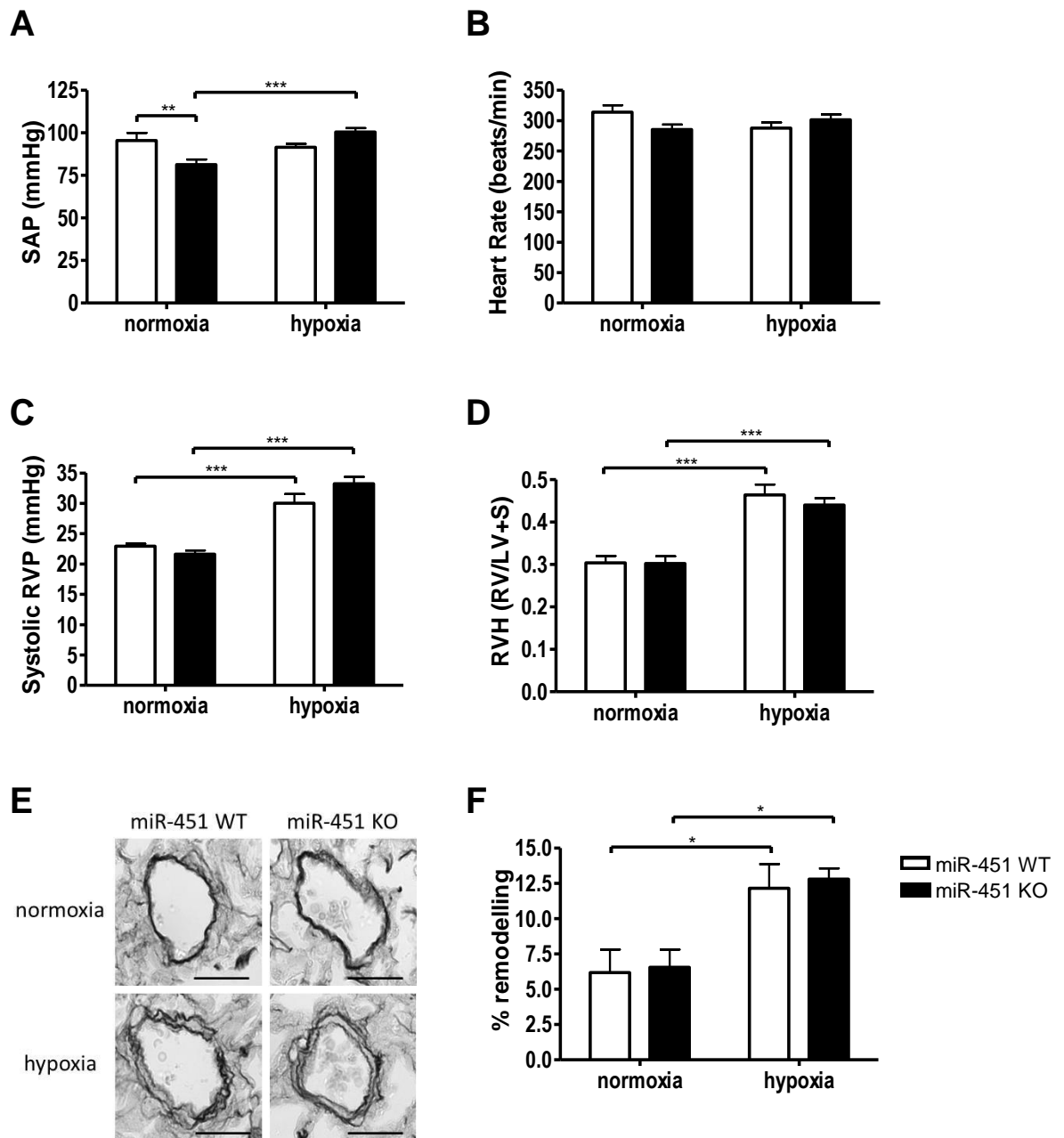


Figure 3.17 – Quantification of PH indices in female miR-451 knockout mice.

Quantification of (A) systemic arterial pressure, (B) heart rate, (C) systolic right ventricular pressure, (D) right ventricular hypertrophy and (E, F) pulmonary vascular remodelling in female miR-451 wild type and knockout mice after 14 days exposure to normoxic or hypoxic conditions. (E) Representative images of pulmonary vessels stained with elastic van gieson, magnification X40, scale bar = 25 μ m. Data represented as mean \pm SEM and analysed by a two-way ANOVA followed by Bonferroni post hoc test. * $p < 0.05$, ** $p < 0.01$ and *** $p < 0.001$, $n = 7-14$ animals per group for SAP, heart rate, systolic RVP and RVH, $n = 4-6$ animals per group for pulmonary vascular remodelling.

3.2.9 Target gene analysis in miR-451 knockout mice

Although no protective effect was detected in mice null for miR-451 and exposed to hypoxia, lung tissue was analysed for miR-451 target gene expression to determine if there were changes in any of the regulatory pathways involved in PH development and thought to be targets of miR-451 (Figure 3.18). Although a number of the target genes appear to be modulated by hypoxia, none of the chosen genes were up-regulated at the mRNA level in the absence of miR-451. *Ywhaz* was shown to be up-regulated in miR-451 knockout mice compared to wild type hypoxic mice however, this effect was only detected in hypoxic samples (Figure 3.18F).

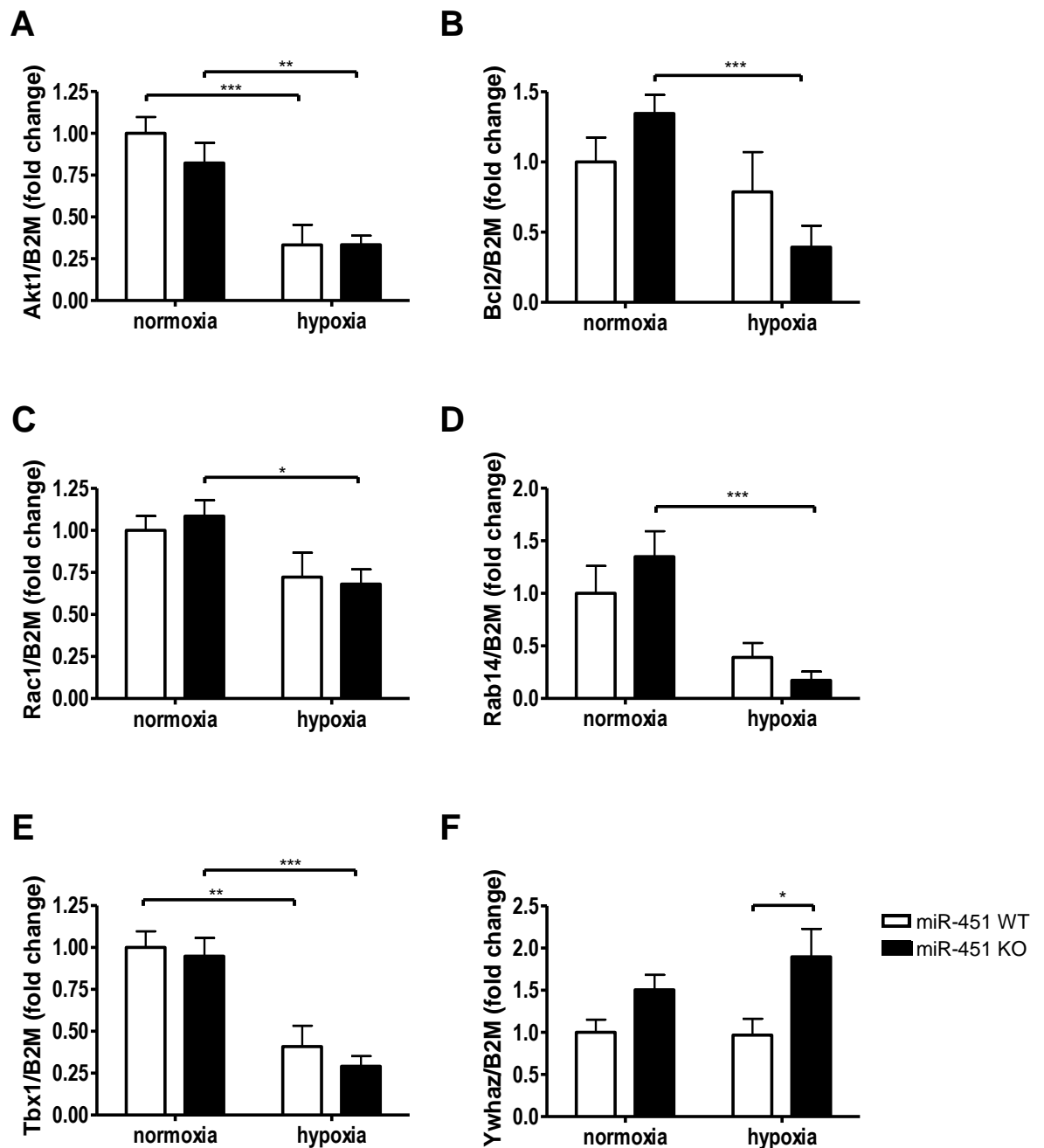


Figure 3.18 – Target gene mRNA expression in lung from female miR-451 knockout mice.

(A) Akt1, (B) Bcl2, (C) Rac1, (D) Rab14, (E) Tbx1 and (F) Ywhaz mRNA expression in whole lung from female miR-451 wild type and knockout mice after 14 days exposure to normoxic or hypoxic conditions, as detected by qRT-PCR. Arbitrary value of 1 assigned to normoxic control group for each gene. Data represented as fold change \pm SEM and analysed by a two-way ANOVA followed by a Bonferroni post hoc test. * $p < 0.05$, ** $p < 0.01$ and *** $p < 0.001$, $n = 5-7$ animals per group.

3.3 Discussion

In this chapter, both *in vitro* and *in vivo* techniques have been used to determine the role of miR-451 in the development of PH. In a cell culture model, over-expression of miR-451 promotes the migration of hPASMCs in the absence of serum but has no effect on cellular proliferation. *In vivo* data indicates that transient knockdown of miR-451 in male rats attenuates the development of PH while genetic knockout of miR-451 has no beneficial effect.

Initially, an adenovirus containing the precursor miR-451 sequence was generated as a tool to over-express miR-451 *in vitro*. Although efficient over-expression of miR-451 was achieved in a cell line, up-regulation of miR-451 was not observed in primary hPASMCs. There are many reasons which may explain why transduction of human Ad-miR-451 into hPASMCs failed to increase miR-451 expression. One possible explanation is inefficient transduction of Ad-miR-451. The virus used within this study was a serotype 5 adenovirus (species C) and the main receptor for this species of adenovirus is the coxsackie and adenovirus receptor (CAR) (Bergelson et al., 1997). It has recently been found that SMCs express very low levels of CAR, thus transduction into SMCs using Ad5 adenovirus generally requires very high titres and can result in poor transduction (Parker et al., 2013). Studies by Parker and colleagues found that SMCs have high expression levels of the species B adenovirus receptor CD46 and modification of the Ad5 adenovirus to incorporate the penton and fibre from Ad35 (a species B adenovirus) resulted in increased transduction in SMCs compared to unmodified Ad5 adenovirus (Parker et al., 2013). Utilisation of an improved adenovirus which incorporates aspects of both species B and C adenovirus may lead to increased transduction in SMCs and result in up-regulation of miR-451.

Another aspect which has to be considered when analysing these results is the fact that the recombinant adenovirus generated contained the precursor miRNA sequence. After transduction into SMCs, the precursor sequence of miR-451 would have to be processed to form the mature miR-451. As mentioned previously, pre-miR-451 is shorter than other precursor miRNAs and is processed in a dicer-independent manner via direct cleavage by Ago2 (Cifuentes et al., 2010, Yang et al., 2010). It may be possible that processing of these synthetic precursor molecules is impaired within SMCs and thus mature miRNA molecules

are not formed. This is in contrast to the miRNA mimic in which the mature form of miR-451 is transfected into the cell. As a result, the mature miRNA can be incorporated directly into RISC and illicit effects by binding to target mRNAs. This may provide a reason as to why miR-451 over-expression was observed when using the miR-451 mimic but not when transduction of Ad-miR-451 was performed.

Muscularisation of previously non-muscular arteries is one of the major characteristics which contributes to remodelling of the pulmonary vessels and can result in total occlusion of the vessel (Stenmark et al., 2009). This process is largely mediated by smooth muscle cells via dysregulation of PASMC proliferation and migration. In this study, over-expression of miR-451 using a miRNA mimic promoted the migration of hPASMCs in the absence of serum and this may play a role in the increased muscularisation during the early development of PAH. However, no effect was observed in hPASMC proliferation with over-expression of miR-451. Within the vessel layers there are various cell types and signals known to dysregulate PASMC proliferation (Morrell et al., 2001, Jalali et al., 2012). Altogether, it is most likely due to an interaction between different cell types and signalling pathways that culminate in the extensive remodelling process detected during the development of PAH. Endogenous expression of miR-451 is extremely low in hPASMCs and therefore only miR-451 mimics were used in this study. In order to further this, it would be interesting to assess the effect of knocking out miR-451 in hPASMCs by using an antimiR and assessing whether results opposite to those observed using the miR-451 mimic were obtained. However, due to the low basal miR-451 expression in hPASMCs, inhibition of miR-451 in an *in vitro* setting may not produce an effect.

Two different methods were used in this study to selectively knock down miR-451; an acute antimiR-451 approach and the use of miR-451 knockout mice. With transient loss of miR-451 in male rats exposed to 7 days hypoxia, we observed a reduction in systolic RVP compared to hypoxic controls however, this result was not observed in the RVH or remodelling data. One reason which may explain this disparity is the relatively short period of hypoxic exposure. There were no neointimal lesions present in lung sections from hypoxic rats after 7 days exposure to hypoxia. Formation of these lesions is dependent on PASMC migration and this

therefore may explain why knockdown of miR-451 did not have a beneficial effect on pulmonary remodelling in this experiment. A 7 day hypoxic exposure was chosen as previous work from our laboratory (Caruso et al., 2010) found that miR-451 levels were elevated significantly at 7 days in both the rat hypoxic and monocrotaline models of PAH. However, further studies should be performed using a more chronic hypoxic exposure model or an alternative rodent model, such as the hypoxia/SU5416 model (Taraseviciene-Stewart et al., 2001). In addition to this, it would be interesting to observe the effect of knocking down miR-451 in a non-hypoxic model of PH, such as the monocrotaline model of PH. Hypoxic exposure is known to increase haematocrit level and miR-451 also has an impact on haematocrit via regulation of erythropoiesis. Therefore the monocrotaline model of PH would allow us to investigate the role miR-451 plays in PH development without the additional complication of haematocrit modulation by hypoxic exposure.

Chronic knockout of miR-451 was studied in miR-451 knockout mice and it was found that when exposed to 14 days hypoxia, knockout mice displayed high RVP, RVH and remodelling data, similar to that of wild type hypoxic mice. One reason which may explain why minimal or no positive effect is observed as a result of knocking down miR-451 is due to blood contamination. The initial miRNA microarray by Caruso and colleagues (Caruso et al., 2010) was performed on unperfused lung tissue. Therefore blood would still be present in the samples used for analysis. As previously stated, miR-451 expression is extremely high in red blood cells and thus, the up-regulation of miR-451 observed in the hypoxic and MCT treated samples may have been detected from the blood rather than in the lung tissue itself.

The fact that transient knockdown of miR-451 reduces RVP in the acute hypoxic model of PH suggests that miR-451 may be involved in early hypoxic pulmonary vasoconstriction. The 7 day hypoxic model of PH is primarily modelling the initiation of pulmonary hypertension with prolonged vasoconstriction leading to increased pulmonary pressures. Although there will be changes within the heart, these adaptations have not had the time to develop into right ventricular hypertrophy within this acute hypoxic disease model. On the other hand, the 14 day hypoxic mouse model displays increased RVP, RVH and pulmonary

remodelling and silencing of miR-451 has no beneficial effect. Thus suggesting that miR-451 appears to play a role in initiating pulmonary vasoconstriction in response to acute hypoxic exposure.

The differences observed between the models used in this study may be due to multiple factors. Other pathways or indeed miRNAs may be compensating for the genetic loss of miR-451 in the knockout mice. MiRNAs can target hundreds of genes (Brennecke et al., 2005) and in turn, each specific gene can be modulated by many different miRNAs (Doench and Sharp, 2004). MiR-451 however has very few validated and predicted targets (Dweep et al., 2011) and thus is limited to the pathways which it can potentially modulate. As a result, other miRNAs may be activated within the lung to modulate the original miR-451 target genes and pathways under conditions of prolonged absence of miR-451. This would be consistent with the protective effect observed only with transient loss of miR-451 as the compensatory mechanisms may not have had time to fully activate and hence a reduction in systolic RVP was observed. Other studies have also found differences in results between genetic knockout and antimiR knock down of a miRNA (reviewed in (van Rooij and Olson, 2012)) as seen in this study.

The rat and mouse experiments conducted here also differ substantially in the cellular compartment in which loss of miR-451 is observed. Within the knockout mice, miR-451 is knocked out globally due to genetic deletion while in the antimiR study, miR-451 levels still remain high in the RBC compartment. This difference in miR-451 expression may also indicate a possible explanation for the results obtained. MiR-451 plays an important role in erythropoiesis and high miR-451 expression in RBCs may trigger certain pathways which are not active in the knockout mice. Therefore we cannot rule out the possibility that different modulatory systems are activated in the two knock down models. Further studies are warranted to fully understand these important issues.

In vitro data obtained from this study illustrates that miR-451 promotes hPASMC migration, thus suggesting that knocking down miR-451 could indeed reduce hPASMC migration *in vivo*. This could explain the beneficial effect observed in the antimiR-451 treated hypoxic rats. In SMCs, miR-451 has recently been suggested to target molecules involved in the AMPK signalling pathway, including MO25 α (Turczynska et al., 2013), and therefore may regulate vascular tone by

modulating actin polymerisation which is essential for both cellular migration and vasoconstriction. It would be interesting to investigate whether miR-451 targets the AMPK system in PASMCs and what effect this has on the development of PH. The protective effect may not have been observed in the hypoxic knockout mouse model due to differences in the degree of hypoxic pulmonary vasoconstriction obtained in each species. In rats, hypoxic exposure has been shown to cause sustained rho-kinase dependent vasoconstriction (Hyvelin et al., 2005). In mice, vasoconstriction is an important mechanism involved in hypoxic PH development however narrowing of the lumen also plays a critical role (Cahill et al., 2012). These studies illustrate that physiologically, rats and mice respond differently to hypoxic insult. In addition, pulmonary remodelling is more pronounced in the hypoxic rat model of PH (Stenmark et al., 2009). Thus the mouse model may not be producing sufficient stimuli to cause PASMC migration and therefore knocking out miR-451 has no beneficial effect on PH development. This highlights the importance in choice of animal model for each study. Knockout mice are of course a fundamental genetic tool which can be utilised to identify the significance of particular genes. However, the mild PH phenotype which develops in the hypoxic mouse (compared to the hypoxic rat) must be taken into consideration when designing studies and analysing results.

Another reason which may account for the differences between the two *in vivo* models is gender. PAH has a strong gender bias at the clinical level, with females being more susceptible to developing the disease (Badesch et al., 2010), however mortality is higher in males who develop the disease (Humbert et al., 2010). On the contrary, *in vitro* studies indicate oestrogens to have a protective effect in the development of PH and taken together with the clinical data gives rise to the oestrogen paradox in PH (Tofovic, 2010). Recent studies have found that there is an increase in expression of CYP1B1, the key enzyme involved in breaking down oestrogen into its metabolites, within the lung during the development of PH (White et al., 2012). An imbalance of oestrogen metabolites within the lung is thought to be detrimental and augment the PH phenotype (Tofovic, 2010, Austin et al., 2009). In addition to this, activated hormone receptors have been shown to control the maturation of miRNAs in a post-transcriptional manner. Yamagata and colleagues illustrated that oestrogen bound oestrogen receptor alpha (ER α) was able to bind to Drosha within the

nucleus and prevent the conversion of pri-miRNAs to pre-miRNAs for several miRNAs (Yamagata et al., 2009). Taken together, this data suggests that oestrogen and its metabolites are able to control the maturation of a subset of miRNAs and play an important role in PH. In the context of this project, the initial microarray performed in our laboratory (Caruso et al., 2010) studied male rats and it was found that miR-451 levels were increased in both the monocrotaline and hypoxic models of PH. Using the hypoxic model in this study, we have observed attenuated effects of knocking down miR-451 in male rats. However no effect was found in female miR-451 knockout mice. This may be due to differential miR-451 expression and modulation during disease development between the genders and further investigation is required to understand if gender is indeed a factor. This apparently gender specific effect must also be taken into consideration when planning future studies.

Target gene analysis in both the *in vivo* studies and from *in vitro* experiments did not show dysregulation of any of the selected genes when miR-451 levels were modulated. As stated above, miR-451 has relatively few predicted or validated targets and identifying bona fide targets presents a challenge. Wang and colleagues (Wang et al., 2012b) investigated the role of miR-451 in the heart and found that the miR-451 cluster targeted Rac1 in the heart. During ischaemic preconditioning, miR-451 expression was increased in the heart, therefore reducing target gene Rac1 expression. Rac1 is a critical factor involved in NADPH oxidase and during ischaemic preconditioning, repression of Rac1 reduced reactive oxygen species production. Therefore the miR-451 cluster is essential for ischaemic preconditioning mediated cardioprotection via targeting of Rac1. In a similar manner, miR-451 has been shown to decrease reactive oxygen species production during erythroid differentiation by targeting Ywhaz in erythroblasts (Patrick et al., 2010b, Yu et al., 2010). Repression of Ywhaz by miR-451 releases the inhibitory effect of Ywhaz on FoxO3, a transcription factor which regulates anti-oxidant genes. Both of these miR-451 target genes have been linked to reactive oxygen species production which is known to be upregulated in the lung during hypoxia and PAH (Frazziano et al., 2012). However, all of the studies focusing on miR-451 have been performed in different tissues and in various disease states, therefore these identified targets may not represent genuine targets for miR-451 in the lung during the

development of PH. In order to further assess target genes for miR-451, a microarray would provide a more in depth analysis of mRNA targets. Further *in vitro* techniques could be utilised in order to determine direct targets for miR-451 by pull down techniques involving immunoprecipitation with Argonaute protein (Jannot et al., 2011) or RNA-Chip (Keene et al., 2006). Similarly, a proteomics-based approach would determine the exact proteins which are being targeted when miR-451 is modulated.

Taken together, this data demonstrates that transient knock down of miR-451 reduces the increased RVP induced by acute hypoxic exposure in male rats. However, genetic ablation of miR-451 does not appear to have any beneficial effect on the development of PAH in female mice.

4 MicroRNA analysis in hypoxia/SU5416 model of PH

4.1 Introduction

Traditionally there are two main rodent models used to study PH development; exposure to chronic hypoxia and administration of the pyrrolizidine alkaloid monocrotaline. A great deal of knowledge has been gained regarding PH development using these models however, there are limitations with both. The hypoxic model only develops modest vascular remodelling while neither of the models develop the complex plexiform lesions which are characteristic of the human disease (Stenmark et al., 2009, Abe et al., 2010). As a result, a model has recently been developed which involves exposing rodents to hypoxia coupled with administration of a vascular endothelial growth factor receptor inhibitor.

Vascular endothelial growth factor is an important regulator involved in the maintenance, differentiation and function of vascular endothelial cells (Lee et al., 2007). Taraseviciene-Stewart and colleagues developed a novel rodent model of PH which blocks VEGFR2 using the inhibitor Sugden-5416 (SU5416) in combination with chronic exposure to hypoxia (Taraseviciene-Stewart et al., 2001). VEGFR2 (also known as KDR or Flk-1 receptor) is a tyrosine kinase receptor which is mainly expressed on endothelial cells and is essential for vessel development during embryogenesis (Cross and Claesson-Welsh, 2001). It was found that inhibition of VEGFR2 along with exposure to hypoxic conditions resulted in a more severe PH phenotype than that observed in hypoxia alone with increased right ventricular pressures and extensive pulmonary arterial remodelling. Blockade of VEGFR2 caused pulmonary arterial endothelial cell death and when combined with hypoxic conditions, an apoptosis-resistant population of endothelial cells were formed. These endothelial cells enter a hyperproliferative state and result in pulmonary arterial occlusion (Taraseviciene-Stewart et al., 2001, Sakao et al., 2005).

As a result of the dysfunctional endothelial cells within the hypoxia/SU5416 rodent model of PH, complex plexiform-like lesions develop in the rat, similar to those observed in human PAH disease (Abe et al., 2010). These lesions generally occur in small pulmonary arteries of <300 μm in diameter (Stenmark et al., 2009) and immunohistochemistry demonstrates that the lesions contain a high proportion of endothelial cells and display many features similar to the human plexiform lesion (Abe et al., 2010).

The hypoxia/SU5416 rodent model of PH consists of a single injection of the VEGFR2 inhibitor followed by 2-3 weeks in hypoxic conditions. It has been observed that returning the rodents to normoxic conditions for a period of time following hypoxia/SU5416 exposure causes persistence and indeed worsening of the PH phenotype and pulmonary arteriopathy (Taraseviciene-Stewart et al., 2001). This differs significantly from the mouse model of PH. The development of the hypoxia/SU5416 model in the mouse was particularly difficult due to the subtle phenotype displayed (Stenmark et al., 2009). Ciucan and colleagues (Ciucan et al., 2011) have developed a hypoxia/SU5416 murine model of PH involving weekly injections of SU5416 coupled with chronic exposure to hypoxia for 3 weeks. In contrast to the rat model, re-exposure to normoxic conditions following the hypoxia/SU5416 insult reduced the indices of PH. This suggests that the mouse hypoxia/SU5416 model of PH is less severe than the rat model.

Both the rat and mouse hypoxia/SU5416 model of PH resemble human PAH more closely than the previous models which involve a single insult. This is in accordance with the human PAH data as it is thought that the disease results from a combination of multiple 'hits' including genetic and environmental insults (Yuan and Rubin, 2005, Morrell, 2006). This may explain why the double insult of VEGF receptor blockade and chronic hypoxia results in a PH phenotype similar to that observed in human PAH patients. As a result, it is hoped that this new model will allow better translation of treatments to the clinic.

Use of the hypoxia/SU5416 model could provide essential information regarding the complex pathways involved in the advancement of PAH, in particular the development of the late stage lesions which result in vessel occlusion and vascular pruning. It is important to fully understand the molecules involved in the disease and miRNAs have been shown to be dysregulated in previous models of PH. There is a lack of data currently available on miRNA expression within pulmonary and cardiac tissue from the hypoxia/SU5416 model of PH. Hence, research into this may give an insight into the mechanistic pathways involved in the progression of PH.

4.1.1 Aim

The aims investigated in this chapter were:

- To determine lung expression of miR-21, miR-143, miR-145 and miR-451 in the hypoxia/SU5416 model of PH.
- To establish a miRNA cardiac signature in the hypoxia/SU5416 model of PH.

4.2 Results

4.2.1 Development of PH in hypoxia/SU5416 mouse model of PH

The three week hypoxia/SU5416 model of PH (Ciucan et al., 2011) was used to establish PH within the mouse (study design shown in Figure 2.3). Hemodynamic analysis confirmed that exposure to hypoxia coupled with administration of SU5416 led to the development of PH in the mouse. Systolic RVP increased significantly in both hypoxic groups compared to normoxia however, there was no further increase in pressure with the addition of SU5416 in hypoxia (Figure 4.1A). There was an increase in RVH in hypoxic mice compared to normoxic controls. RVH for the hypoxia/SU5416 group was significantly higher than hypoxia/vehicle (0.3 ± 0.011 and 0.25 ± 0.017 , respectively) (Figure 4.1B), indicating that the disease developed in the hypoxia/SU5416 treated mice was more severe than hypoxia alone. There was no difference in SAP between any groups (Figure 4.1C).

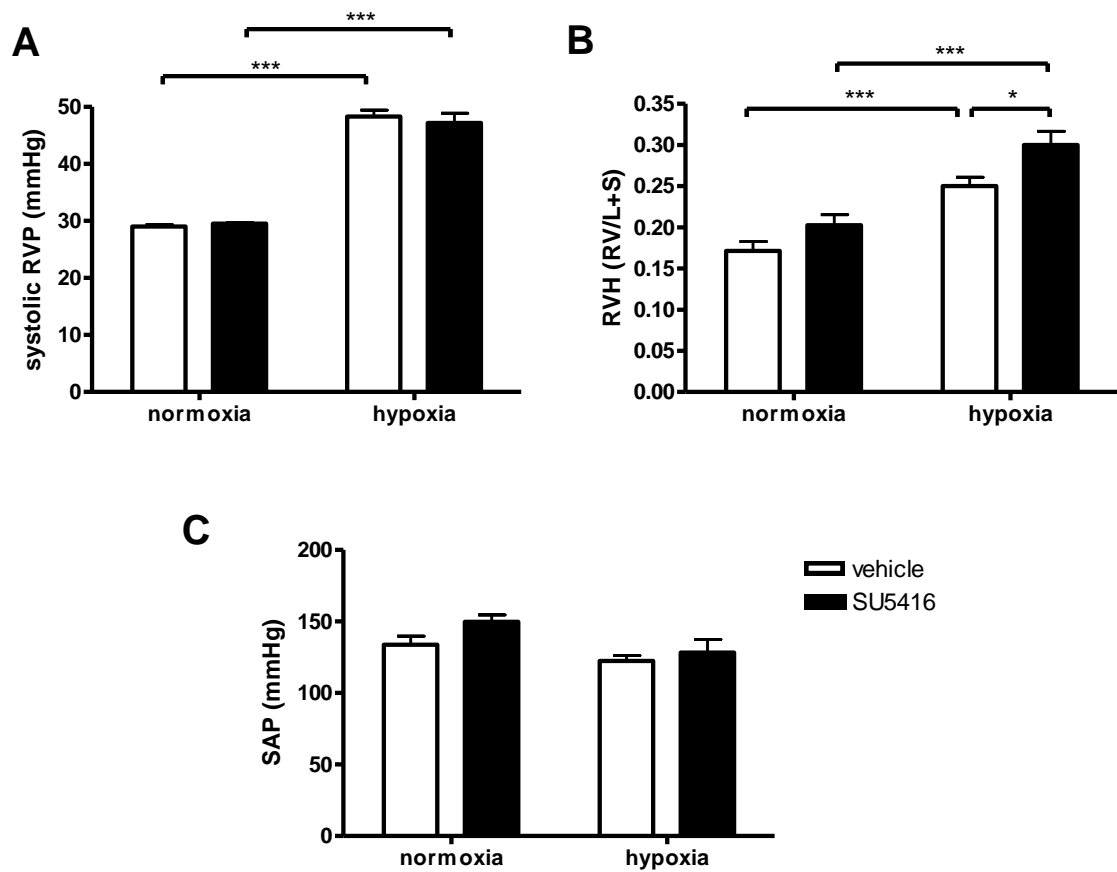


Figure 4.1 – Quantification of PH indices in hypoxia/SU5416 mouse model of PH.

Quantification of (A) systolic RVP, (B) RVH and (C) systemic arterial pressure in male C57Bl/6Jax mice after 3 weeks exposure to normoxic or hypoxic conditions, with subcutaneous administration of 20 mg/kg SU5416 or vehicle every 7 days. Data expressed as mean \pm SEM and analysed by two-way ANOVA followed by a Bonferroni post hoc test, * $p < 0.05$ and *** $p < 0.001$, $n = 6$ animals per group.

4.2.2 Lung miRNA expression profile in hypoxia/SU5416 mouse model of PH

We were interested to ascertain whether the expression of certain miRNAs was similar between the hypoxia alone and the hypoxia/SU5416 model of PH. Four miRNAs were focused on as they had previously been shown to be dysregulated within the lung during the development of PH; miR-21, miR-143, miR-145 and miR-451 (Caruso et al., 2010, Caruso et al., 2012, Sarkar et al., 2010).

MiR-21 was down regulated in normoxic conditions by SU5416 treatment (as detected by qRT-PCR - Figure 4.2A), however there was no difference in miR-21 levels between hypoxia treated mice (Figure 4.2A). Northern blot analysis for mature miR-21 did not follow this pattern as there was no difference between the groups (Figure 4.2B, C). Exposure to hypoxia caused a subtle increase in pre-miR-21 (Figure 4.2B, C) in the vehicle treated mice though this effect was not observed in the hypoxic mice treated with SU5416. There was no difference in the expression levels of miR-143 between normoxic and hypoxic animals, irrespective of SU5416 administration (Figure 4.3). MiR-145, however, displayed a modest up-regulation in hypoxia as displayed by northern blot analysis (Figure 4.4B, C) and although not significant, it trended towards an increase in hypoxia by qRT-PCR data (Figure 4.4A). Mature miR-451 expression was unchanged between groups by qRT-PCR (Figure 4.5A) however, northern blot analysis showed a decrease in miR-451 expression with SU5416 treatment which returned to normoxia/vehicle levels with exposure to hypoxia (Figure 4.5B, C). Pre-miR-451 expression was similar between all groups (Figure 4.5B, C)

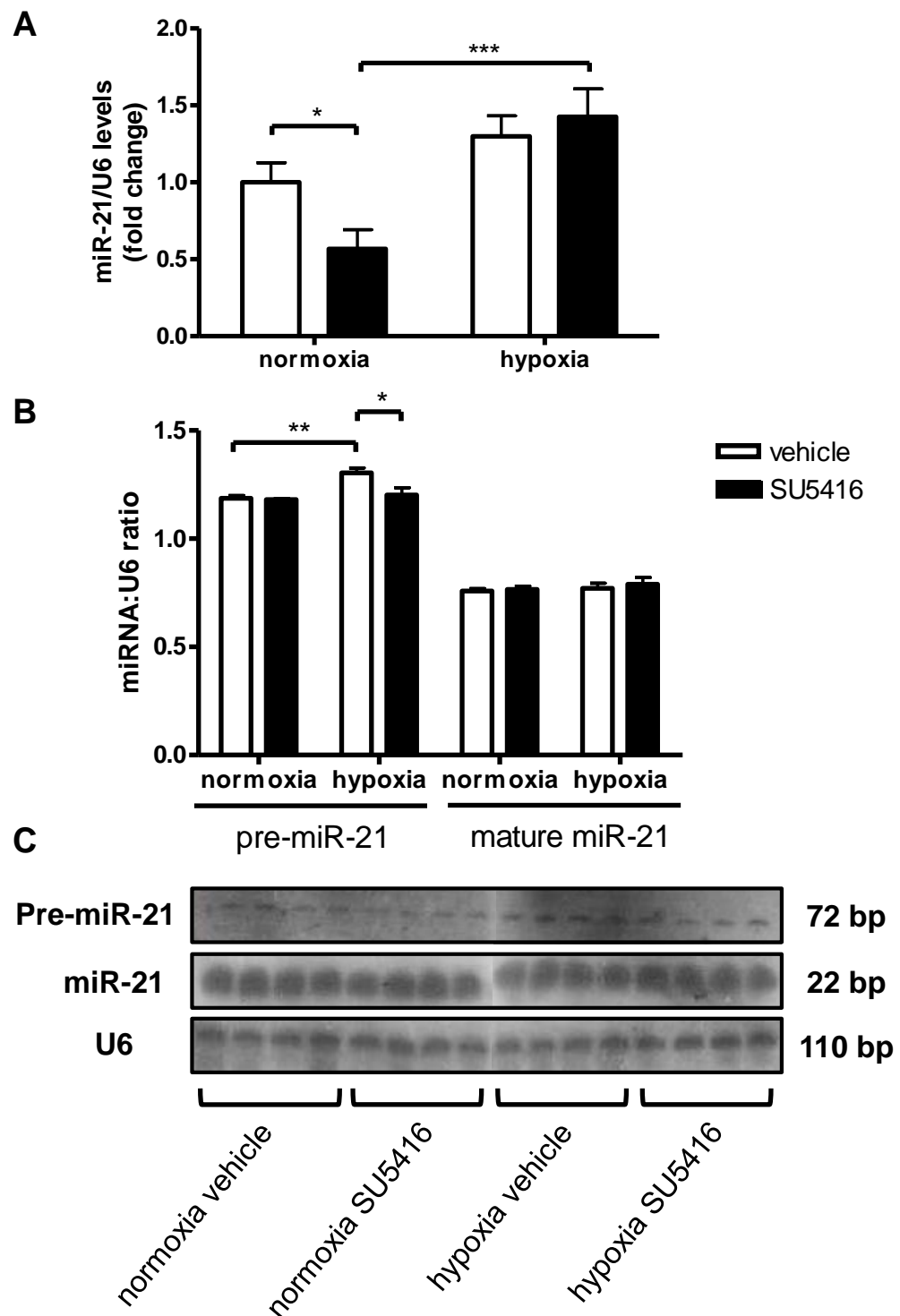


Figure 4.2 – MiR-21 expression in lung from hypoxia/SU5416 mouse model of PH.

(A) Mature miR-21 expression was detected by qRT-PCR and (B, C) mature and pre-miR-21 was detected by northern blot in whole lung from male C57Bl/6Jax mice after 3 weeks exposure to normoxic or hypoxic conditions, with subcutaneous administration of 20 mg/kg SU5416 or vehicle every 7 days. Arbitrary value of 1 assigned to normoxic vehicle for the qRT-PCR data and data expressed as fold change \pm SEM, $n = 6$ animals per group. Northern blot was quantified by normalising band intensity to the relative U6 signal and expressed as mean \pm SEM, $n = 4$ animals per group. All data analysed by two-way ANOVA followed by Bonferroni post hoc test, * $p < 0.05$ and *** $p < 0.001$.

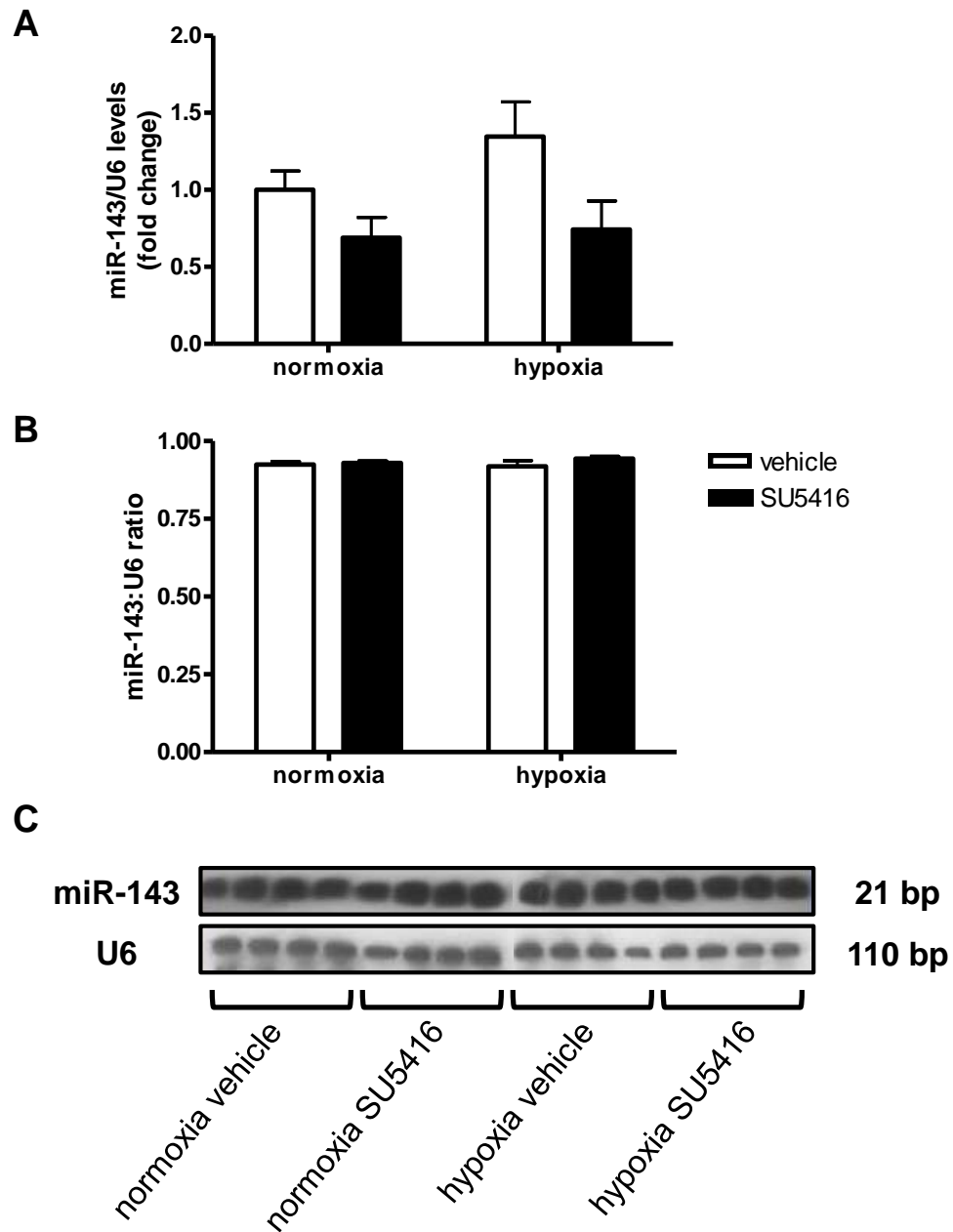


Figure 4.3 – MiR-143 expression in lung from hypoxia/SU5416 mouse model of PH.

Mature miR-143 expression was detected by (A) qRT-PCR and (B, C) northern blot in whole lung from male C57Bl/6Jax mice after 3 weeks exposure to normoxic or hypoxic conditions, with subcutaneous administration of 20 mg/kg SU5416 or vehicle every 7 days. Arbitrary value of 1 assigned to normoxic vehicle for the qRT-PCR data and data expressed as fold change \pm SEM, $n = 6$ animals per group. Northern blot was quantified by normalising band intensity of miR-143 to the relative U6 signal and expressed as mean \pm SEM, $n = 4$ animals per group. All data analysed by two-way ANOVA followed by Bonferroni post hoc test.

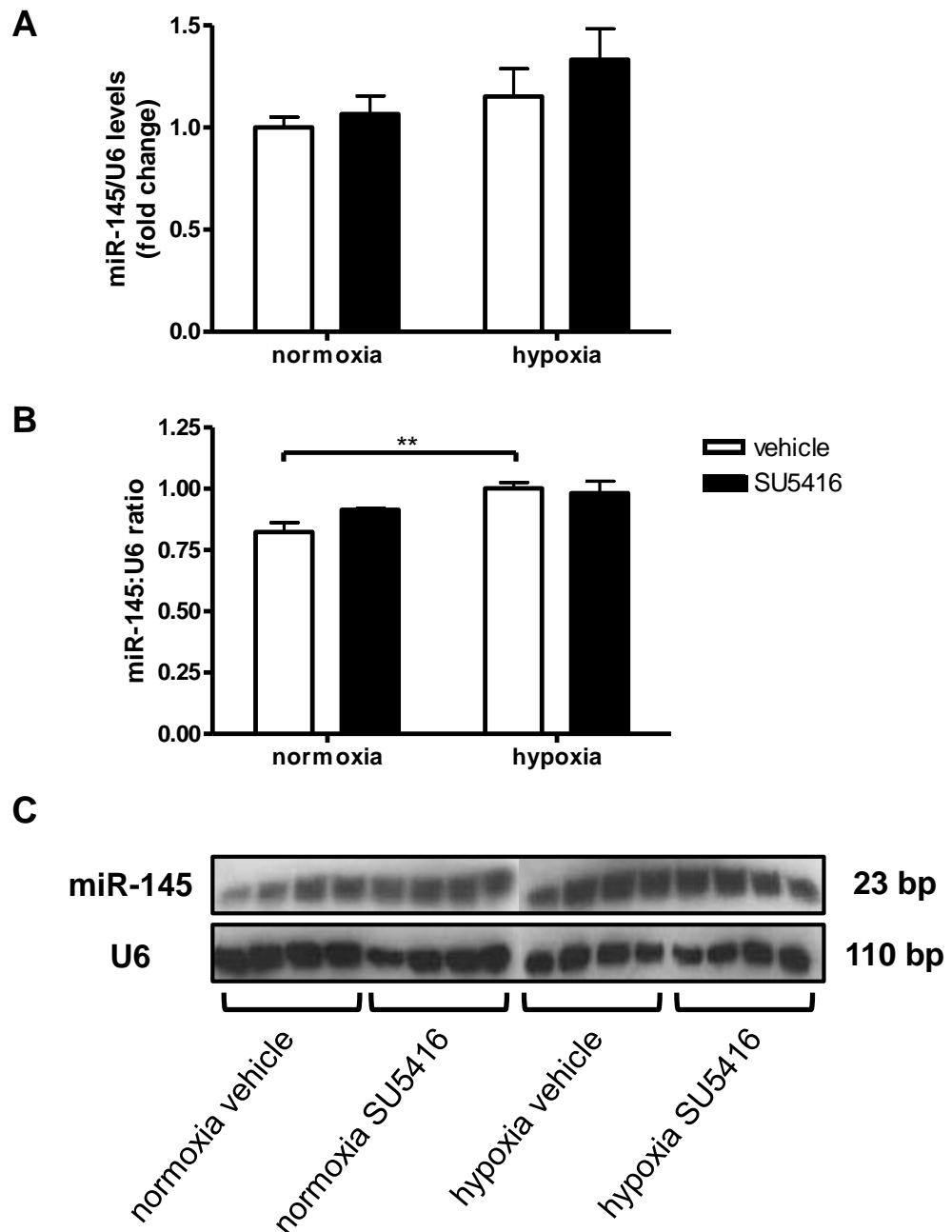


Figure 4.4 – MiR-145 expression in lung from hypoxia/SU5416 mouse model of PH.

Mature miR-145 expression was detected by (A) qRT-PCR and (B, C) northern blot in whole lung from male C57Bl/6Jax mice after 3 weeks exposure to normoxic or hypoxic conditions, with subcutaneous administration of 20 mg/kg SU5416 or vehicle every 7 days. Arbitrary value of 1 assigned to normoxic vehicle for the qRT-PCR data and data expressed as fold change \pm SEM, $n = 6$ animals per group. Northern blot was quantified by normalising band intensity of miR-145 to the relative U6 signal and expressed as mean \pm SEM, $n = 4$ animals per group. All data analysed by two-way ANOVA followed by Bonferroni post hoc test, $**p < 0.01$.

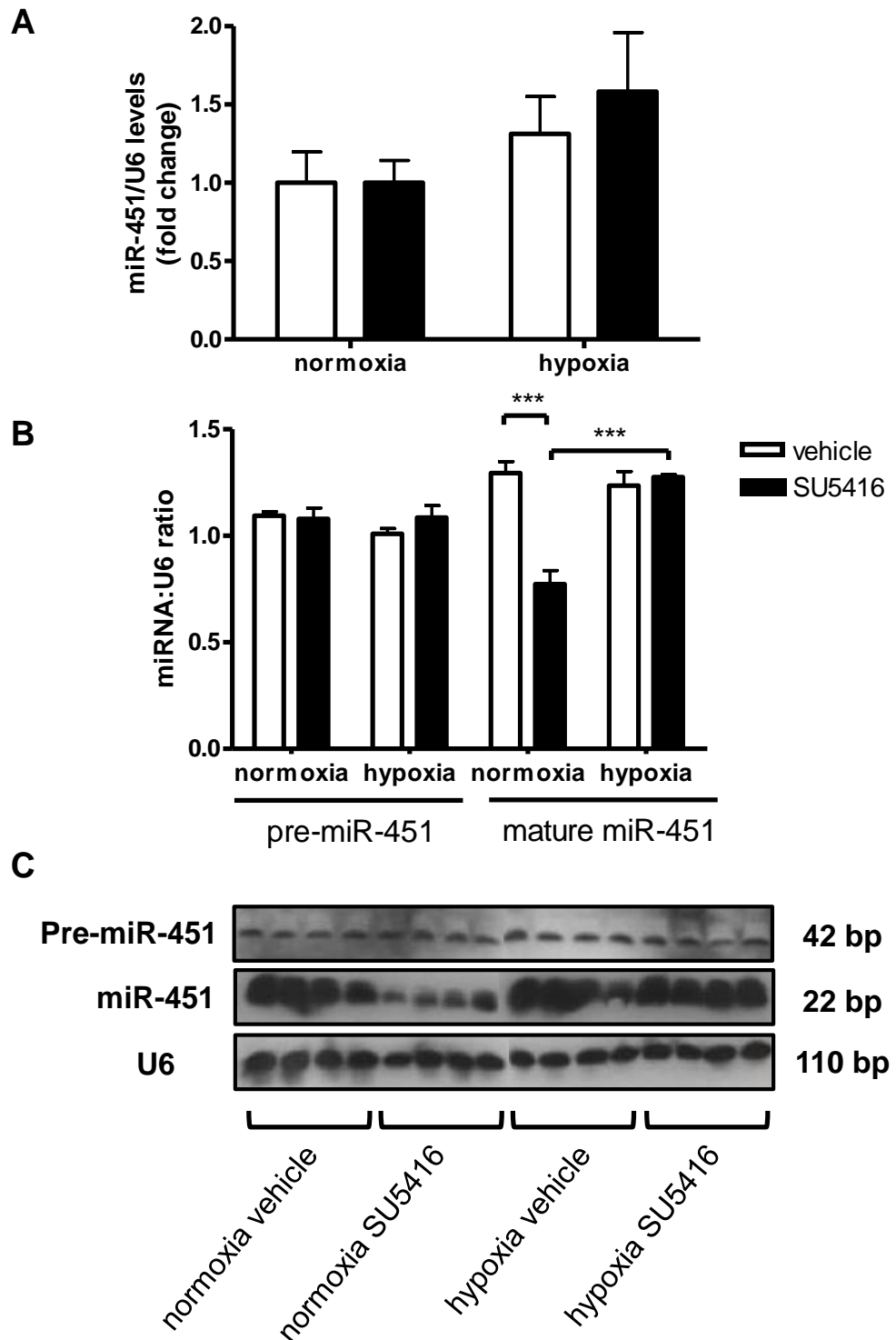


Figure 4.5 – MiR-451 expression in lung from hypoxia/SU5416 mouse model of PH.

(A) Mature miR-451 expression was detected by qRT-PCR and (B, C) mature and pre-miR-451 was detected by northern blot in whole lung from male C57Bl/6Jax mice after 3 weeks exposure to normoxic or hypoxic conditions, with subcutaneous administration of 20 mg/kg SU5416 or vehicle every 7 days. Arbitrary value of 1 assigned to normoxic vehicle for the qRT-PCR data and data expressed as fold change \pm SEM, $n = 6$ animals per group. Northern blot was quantified by normalising band intensity to the relative U6 signal and expressed as mean \pm SEM, $n = 4$ animals per group. All data analysed by two-way ANOVA followed by Bonferroni post hoc test, *** $p < 0.001$.

4.2.3 Lung miRNA expression profile in hypoxia/SU5416 rat model of PH

The hypoxia/SU5416 model was also performed in the rat to assess miRNA expression between species of the same model of PH (study design shown in Figure 2.4). Firstly, we investigated whether the rat hypoxia/SU5416 model produced exaggerated PH as would be expected. Pulmonary pressures were taken from rats which had been administered SU5416 with 2 weeks hypoxic exposure followed by 12 weeks in normoxia. This animal model was used as it had previously been shown to induce severe PH along with complex lesion structures (Abe et al., 2010). Systolic RVP was significantly increased in rats exposed to hypoxia/SU5416 compared to normoxia/SU5416 rats (117.2 ± 8.88 and 26.5 ± 1.29 mmHg, respectively) (Figure 4.6).

Severe lesions in the lung, very similar to the plexiform lesion observed in human PAH, have previously been reported in the rat hypoxia/SU5416 model of PH when exposure to normoxic conditions follows the initial hypoxia and SU5416 insult (Taraseviciene-Stewart et al., 2001, Abe et al., 2010). Alpha-smooth muscle actin staining was performed in the lung from rats exposed to normoxia or hypoxia with SU5416 followed by varying lengths of time in normoxia (Figure 4.7). At all time points normoxia/SU5416 animals had a thin layer of smooth muscle and there was a visual increase in the smooth muscle staining observed in the hypoxia/SU5416 group compared to the normoxia/SU5416 group. In the animals exposed to hypoxia/SU5416 for 2 weeks, there was a thin layer of smooth muscle surrounding the vessel which gradually increased when rats were returned to normoxia for 1 week (3 week study animals). The 8 week hypoxia/SU5416 study animals visually had a thick layer of smooth muscle encompassing the vessel while at 14 weeks, the smooth muscle had extended far into the lumen leading to complete occlusion of the vessel (Figure 4.7). These late stage lesions are comparable to the human lesions and this is in accordance with previous reports (Abe et al., 2010). Thus we were confident that the rat hypoxia/SU5416 model was indeed producing severe PH with end stage lesions.

The four specific miRNAs focused on in section 4.2.2 were chosen to analyse in the lung of this model of PH to assess the regulation of these miRNAs throughout the development of PH in the rat hypoxia/SU5416 model. Mature miRNA

expression was quantified by qRT-PCR. MiR-21 was significantly up-regulated in the lung of hypoxia/SU5416 rats at all time points compared to normoxia/vehicle 14 week group (Figure 4.8A). However, this increase in miR-21 expression only reached significance compared to time matched normoxia/SU5416 group at 14 weeks. Although miR-143 and miR-145 are transcribed together from the same primary transcript (Xin et al., 2009), qRT-PCR analysis revealed that they do not follow the same expression pattern during the development of PH. MiR-143 expression was very similar to that of miR-21 throughout the progression of disease with a significant increase in miR-143 expression in the hypoxia/SU5416 group only at 14 weeks compared to normoxia/SU5416 group (Figure 4.8B). On the other hand, miR-145 was increased in the early phase of PH development. MiR-145 was up-regulated at 2 and 3 weeks hypoxia/SU5416 compared to 14 week normoxia/vehicle, however this was only significantly increased at 3 weeks compared to normoxia/SU5416 (Figure 4.8C). MiR-451 showed a significant down-regulation at the 3 week time point in the hypoxia/SU5416 group compared to normoxia/SU5416 (Figure 4.8D).

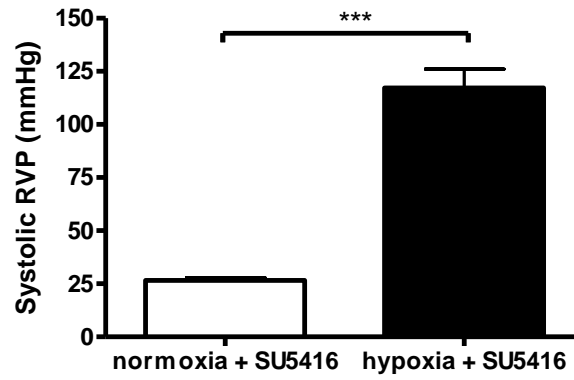


Figure 4.6 – Systolic RVP in hypoxia/SU5416 rat model of PH.

Quantification of systolic RVP in male rats exposed to normoxic or hypoxic conditions for 2 wks coupled with subcutaneous administration of 20 mg/kg SU5416 on day 0, followed by 12 weeks in normoxic conditions. Data represented as mean \pm SEM. Data analysed by unpaired t-test, *** $p < 0.001$, $n = 10$ animals per group.

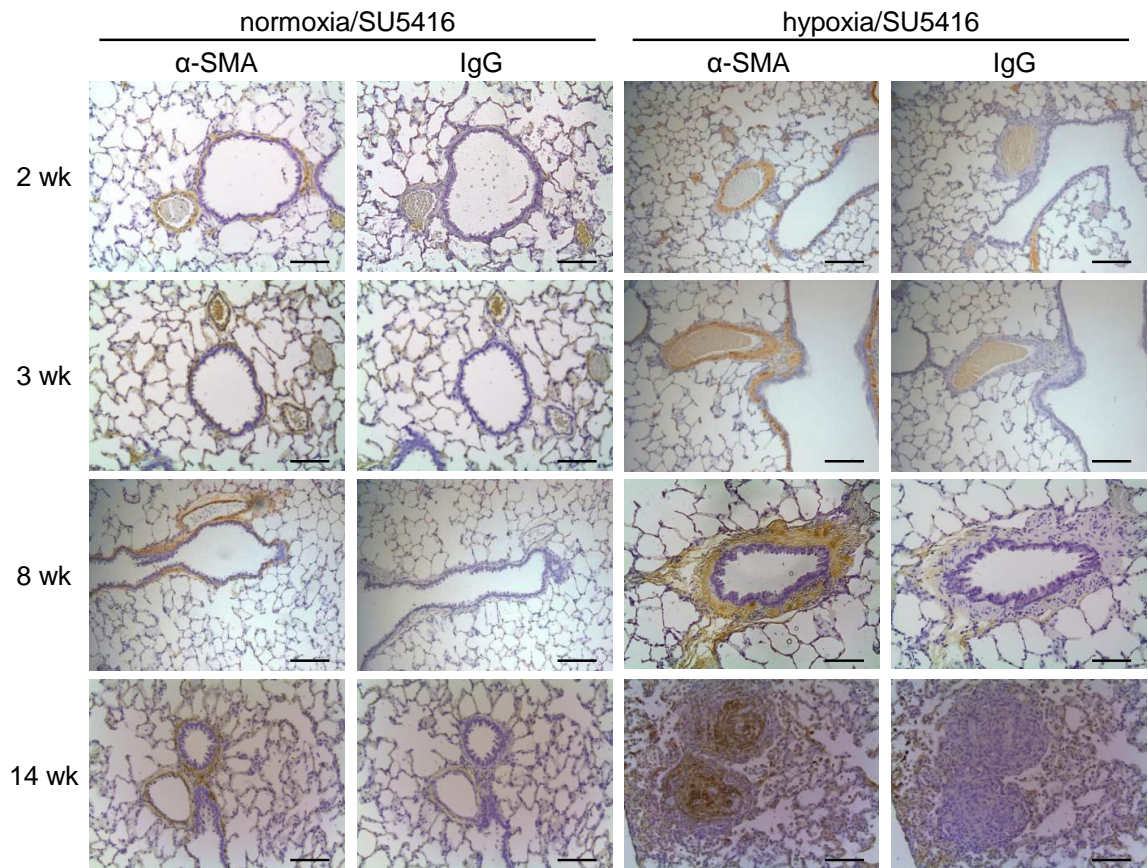


Figure 4.7 – Localisation of α -SMA in rat lung from hypoxia/SU5416 model of PH.

Representative alpha smooth muscle actin (α -SMA) staining in lung from male rats exposed to normoxic or hypoxic conditions for 2 weeks coupled with subcutaneous administration of 20 mg/kg SU5416 on day 0, followed by varying lengths of time in normoxic conditions. Total study time indicated in weeks on left hand side. Magnification X10, scale bar = 100 μ m. IgG = isotype control.

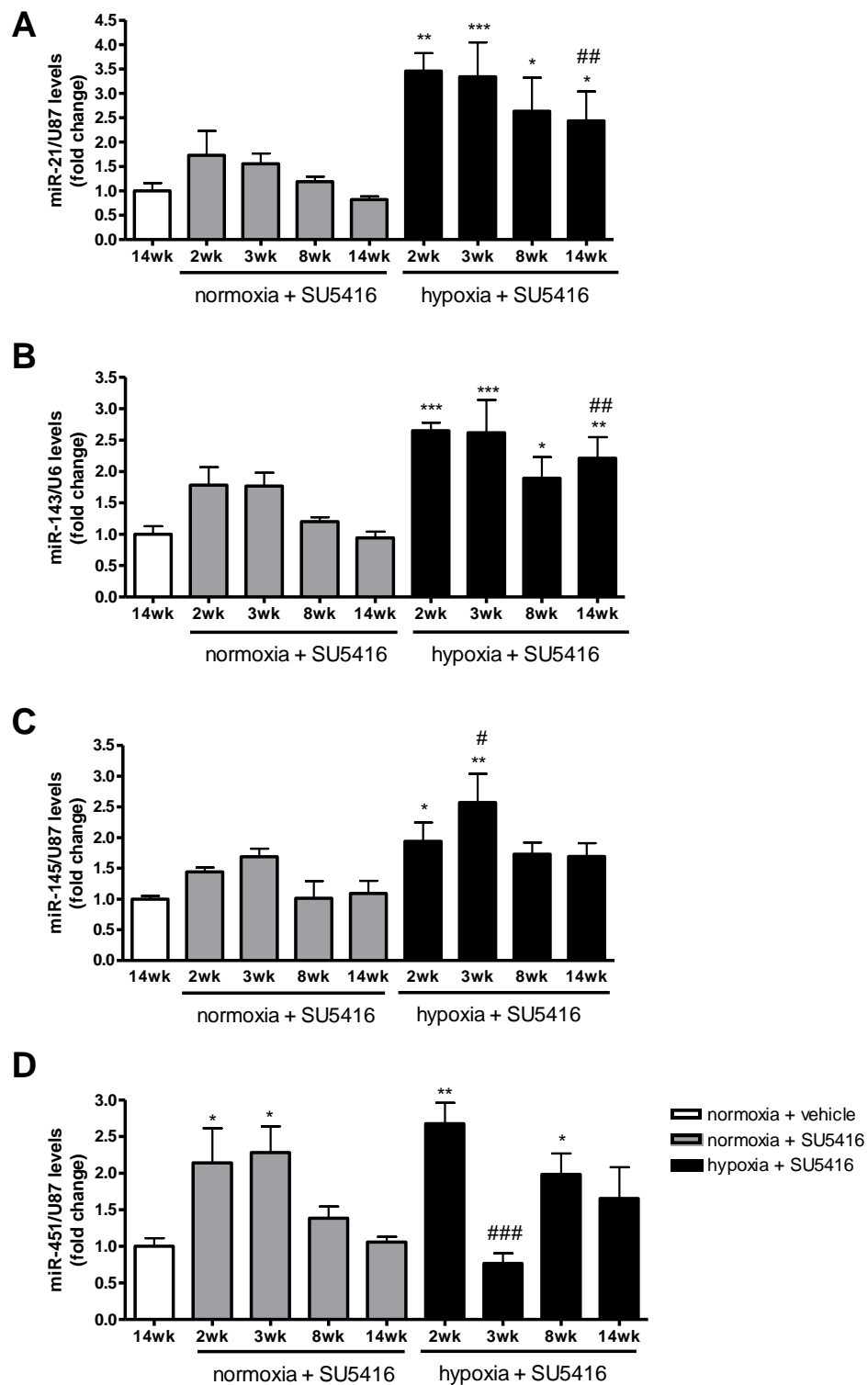


Figure 4.8 – Time course analysis of miRNA expression in lung from hypoxia/SU5416 model of PH.

Expression of mature (A) miR-21, (B) miR-143, (C) miR-145 and (D) miR-451 detected by qRT-PCR in lung from male rats exposed to normoxic or hypoxic conditions for 2 wks coupled with subcutaneous administration of 20 mg/kg SU5416 on day 0, followed by varying lengths of time in normoxic conditions. Total study time indicated on x-axis. Arbitrary value of 1 assigned to 14 wk normoxia + vehicle. Data represented as fold change \pm SEM and analysed by a one-way ANOVA followed by Tukey's post hoc test, $n = 5$ animals per group. * $p < 0.05$, ** $p < 0.01$, *** $p < 0.001$ vs 14 wk normoxia + vehicle, # $p < 0.05$, ## $p < 0.01$, ### $p < 0.001$ vs time matched normoxia + SU5416.

4.2.4 Cardiac signature in hypoxia/SU5416 model of PH

In response to injury and physiological overload, the heart activates signalling pathways to induce the expression of fetal cardiac genes and promote myocyte hypertrophy (Thum et al., 2007). Persistent activation of these pathways culminates in heart disease and can lead to heart failure. Recent work illustrated that specific miRNAs are dysregulated within the heart during disease development and the miRNA profile in cardiac tissue is well established for certain diseases (Liu and Olson, 2010, van Rooij et al., 2008). Within the heart, up-regulation of miR-21, miR-23a, miR-27a, miR-27b, miR-125, miR-195 and miR-199 was observed in mouse models of cardiac hypertrophy while miR-1, miR-29, miR-133 and miR-150 were found to be down-regulated (Care et al., 2007, van Rooij et al., 2006, Wang et al., 2012a). Cardiac contractility is primarily regulated by the expression of the myosin heavy chain (MHC) contractile proteins, α MHC and β MHC. Physiological and pathological stress alters the ratio of these proteins resulting in cardiac hypertrophy due to down-regulation of α MHC and up-regulation of β MHC. MiR-208a (known as a myomiR) is encoded within an intron of α MHC and is required for the cardiac hypertrophic response as well as expression of β MHC along with two further myomiRs, miR-208b and miR-499 (Callis et al., 2009, van Rooij et al., 2007, van Rooij et al., 2009). Furthermore, cardiac over-expression of miR-208a induces cardiac remodelling and hypertrophic growth (Callis et al., 2009). From these critical studies, miRNAs appear to play a pivotal role in cardiac disease development.

However, little is known about the regulation of miRNAs in the heart during the development of PAH. PAH is a disease which affects predominantly the right ventricle resulting in right ventricular hypertrophy and right ventricular failure. Research has shown that there is a molecular signature of both mRNA and miRNA which differs between the RV and the LV during normal physiological conditions (Drake et al., 2011). Further to this, during the development of RVH and right ventricular failure, distinct gene and miRNA expression patterns are expressed within the RV but not observed in the LV (Drake et al., 2011). It was therefore speculated that specific miRNAs would be dysregulated within the right ventricle but remain unchanged in the left ventricle during the development of PAH. Hence, the right and left ventricle were analysed separately for miRNA expression patterns. Interestingly, recent studies investigated the relationship

between the two ventricles during right heart failure. Although left ventricular size was unchanged in PAH patients, left ventricular ejection time was reduced and this was a predictor of early mortality (Hardegree et al., 2013, Sztrymf et al., 2013). Thus illustrating that the LV may undergo detrimental changes as a result of the failing RV in PAH patients.

The miRNAs chosen for analysis in the mouse heart had all been reported to be dysregulated within the heart during cardiac hypertrophy (Care et al., 2007, van Rooij et al., 2006, van Rooij et al., 2007, van Rooij et al., 2009, Wang et al., 2012a, Callis et al., 2009). Of the fourteen miRNAs analysed by qRT-PCR in the mouse 3 week hypoxia/SU5416 model, only one miRNA displayed an increase in expression during hypoxia/vehicle and hypoxia/SU5416 in the right ventricle while remaining unaffected in the left ventricle: miR-27a (Figure 4.9). Furthermore, miR-27a is increased in the right ventricle during hypoxic exposure to levels similar to those observed in the left ventricle. MiR-27b and miR-451 also showed a significant increase in the hypoxia/vehicle group selectively in the RV and although there was an increase in miR-27b expression in hypoxia/SU5416 group, this did not reach significance compared to normoxia/vehicle (Figure 4.9).

In the rat hypoxia/SU5416 model of PH, expression levels of miR-27a and miR-27b were also analysed in the heart at the 14 week time point (Figure 4.10). MiR-27a expression was unchanged between treatment groups in both the right ventricle and the left ventricle (Figure 4.10A). However, miR-27b expression was significantly up-regulated within the right ventricle and unaffected within the left ventricle (Figure 4.10B).

Since members of the miR-27 family were up-regulated in the right ventricle from both the mouse and rat hypoxia/SU5416 model of PH, expression levels were analysed in the lung from both species to determine whether this effect was cardiac specific. Both the mouse and rat model showed no dysregulation of miR-27a or miR-27b within the lung of the hypoxia/SU5416 model of PH (Figure 4.11).

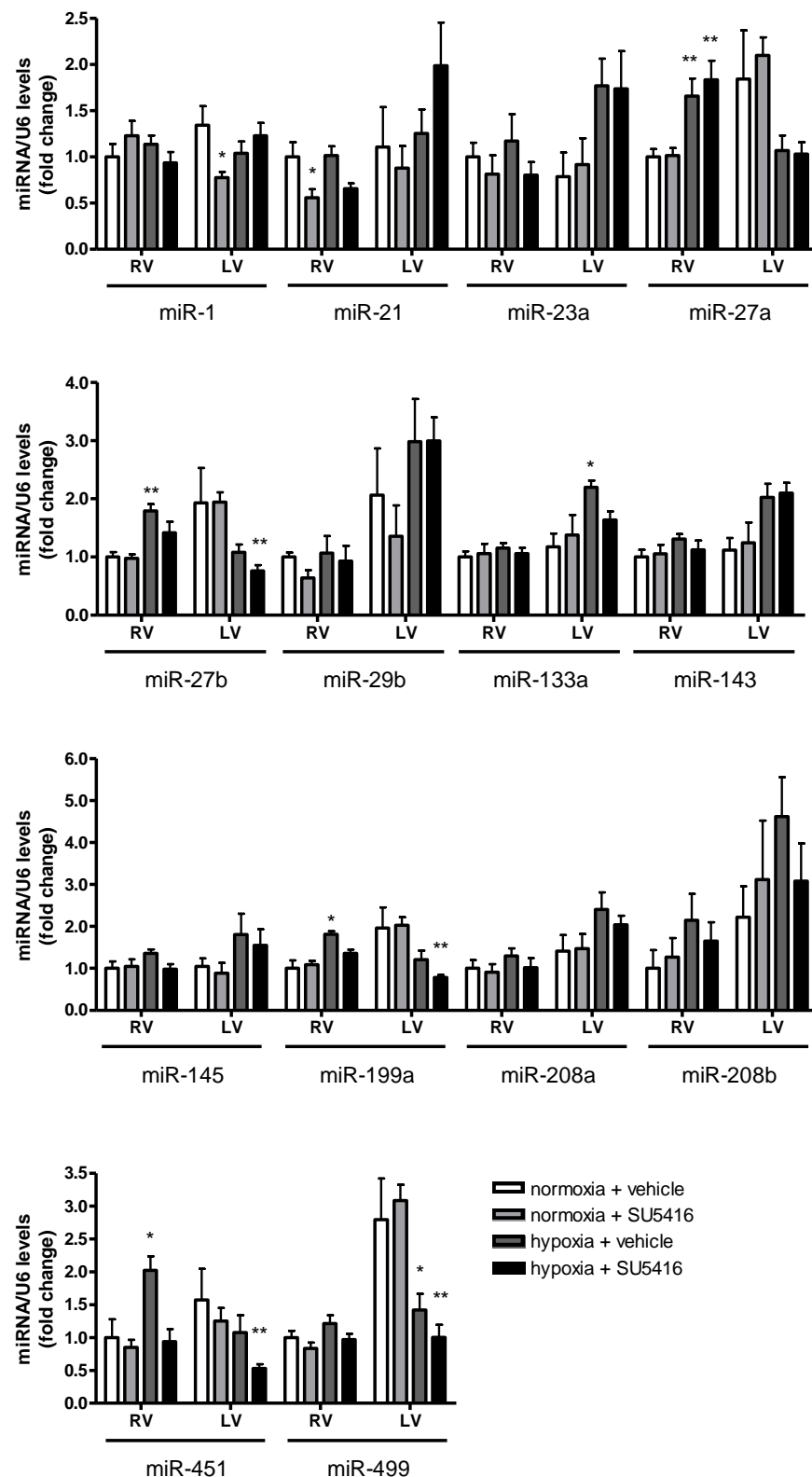


Figure 4.9 – Cardiac miRNA signature from hypoxia/SU5416 mouse model of PH.

MiRNA expression from cardiac tissue from male C57Bl/6Jax mice after 3 weeks exposure to normoxic or hypoxic conditions, with subcutaneous administration of 20 mg/kg SU5416 or vehicle every 7 days, as detected by qRT-PCR. Arbitrary value of 1 assigned to RV normoxia + vehicle for each miRNA. Data expressed as fold change \pm SEM and analysed by two-way ANOVA followed by Bonferroni post hoc test. * $p < 0.05$ and ** $p < 0.01$ vs normoxia + vehicle for that tissue and miRNA, $n = 6$ animals per group. RV = right ventricle, LV = left ventricle + septum.

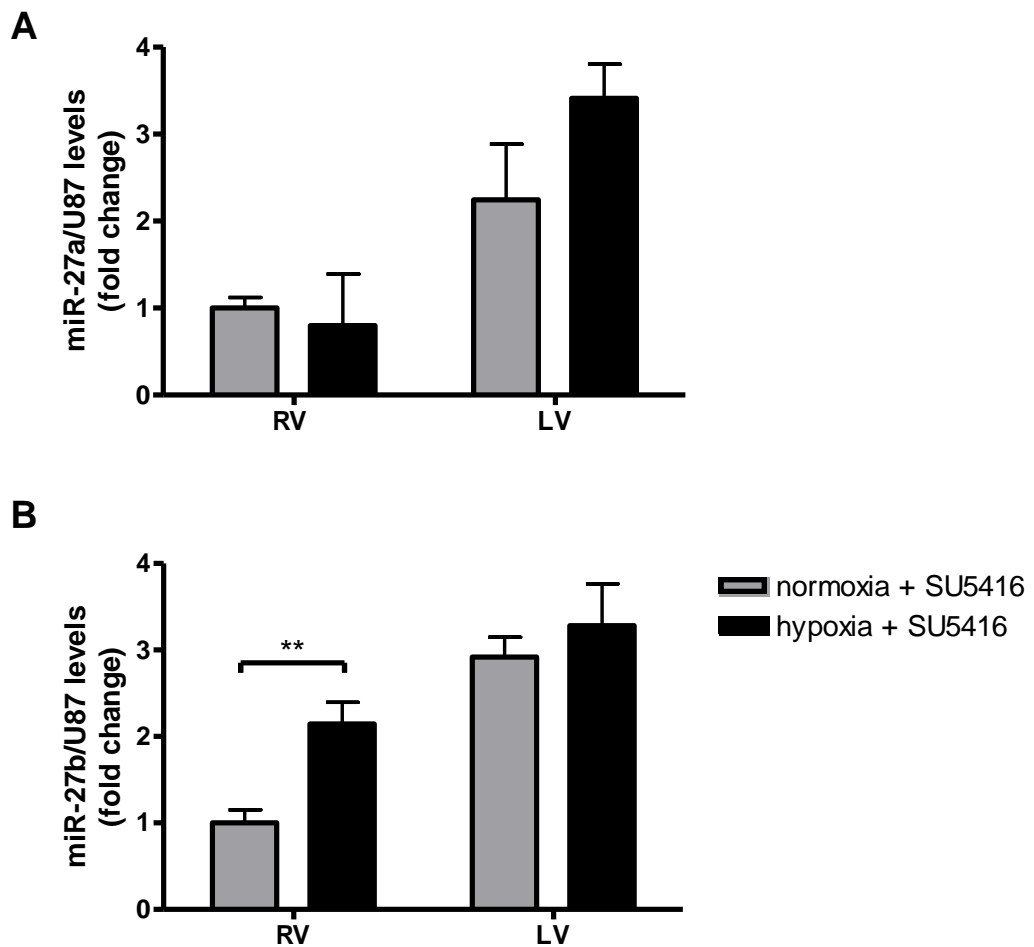


Figure 4.10 – MiR-27a and miR-27b expression in cardiac tissue from hypoxia/SU5416 rat model of PH.

(A) MiR-27a and (B) miR-27b expression in cardiac tissue from male rats exposed to normoxic or hypoxic conditions for 2 wks coupled with subcutaneous administration of 20 mg/kg SU5416 on day 0, followed by 12 weeks in normoxic conditions. Arbitrary value of 1 assigned to RV normoxia + SU5416 for each miRNA. Data expressed as fold change \pm SEM and analysed by unpaired t-test. ** $p < 0.01$ and $n = 6$ animals per group. RV = right ventricle, LV = left ventricle + septum.

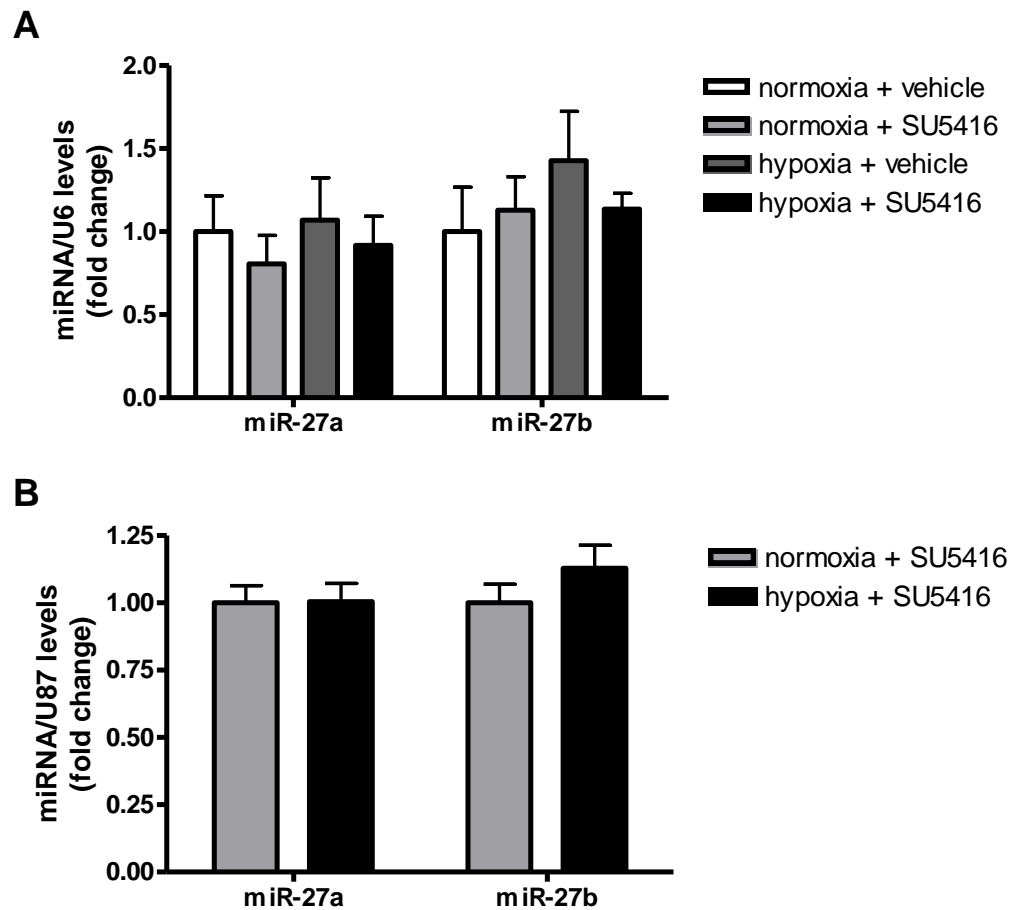


Figure 4.11 – MiR-27a and miR-27b expression in lung tissue from hypoxia/SU5416 model of PH.

(A) MiR-27a and miR-27b expression in lung tissue from male C57Bl/6Jax mice after 3 weeks exposure to normoxic or hypoxic conditions, with subcutaneous administration of 20 mg/kg SU5416 or vehicle every 7 days, as detected by qRT-PCR. Arbitrary value of 1 assigned to normoxia + vehicle for each tissue and miRNA. Data analysed by a two-way ANOVA followed by Bonferroni post hoc test. (B) MiR-27a and miR-27b expression in lung tissue from male rats exposed to normoxic or hypoxic conditions for 2 wks coupled with subcutaneous administration of 20 mg/kg SU5416 on day 0, followed by 12 weeks in normoxic conditions. Arbitrary value of 1 assigned to normoxia + SU5416 for each tissue and miRNA. Data analysed by unpaired t-test. All data expressed as fold change \pm SEM, n = 6 animals per group.

4.3 Discussion

Results from both the mouse and rat study conform to previous studies (Taraseviciene-Stewart et al., 2001, Ciuculan et al., 2011) and demonstrate that inhibition of VEGF combined with chronic hypoxia provides a robust model for studying PH pathology. Mice dosed with SU5416 and exposed to hypoxic conditions displayed increased RVP compared to normoxic mice and RVH which was greater than both normoxic mice and mice exposed to hypoxia alone. The rat hypoxia/SU5416 model exhibits a more severe PH phenotype with increased RVP and complex vascular lesions observed during the later stages of disease.

MiRNA expression analysis within the lung of the mouse hypoxia/SU5416 model showed modest variations in levels of miR-21, miR-145 and miR-451 but none of these changes were found to be consistent across qRT-PCR and northern blot analysis. Previous work has found these specific miRNAs to be dysregulated in the lung of rodents exposed to hypoxia alone or MCT insult (Caruso et al., 2010, Caruso et al., 2012, Sarkar et al., 2010), however the severity of disease differs significantly between each of the chosen models. As a result, a time course study was performed using the rat hypoxia/SU5416 model of PH to assess miRNA expression throughout the development of experimental PH within this model. MiR-21 and miR-143 expression was significantly up-regulated in hypoxia/SU5416 rats compared to normoxia/SU5416 animals at 14 weeks, indicating that these two miRNAs may play a role in the end stage of disease when lesion development occurs. In contrast, miR-145 was significantly up-regulated in the hypoxia/SU5416 rats at the early time point of 3 weeks, thus indicating that miR-145 may be involved in the detrimental pathways associated with the early progression of PH. Another reason why these miRNAs are up-regulated at different time points throughout disease development may be as a protective mechanism in an attempt to limit the excessive damage to the vessel as the disease progresses. Thus, further work into each specific miRNA is necessary within this model to understand whether these small RNAs are acting in a protective or detrimental manner in the development of PH.

PAH is a disease primarily involving the pulmonary vessels however, the impact of this disease on the heart is extensive. The increased RVP combined with RVH and vascular pruning observed in severe PH can result in right heart failure and

death (Haddad et al., 2011). The initial adaptive hypertrophy observed within the RV is primarily due to increased afterload. However, the RV cannot withstand constant pressure over-load, therefore the adaptive RVH gives rise to contractile dysfunction and eventual RV failure via various molecular pathways. Under normal conditions the heart utilises a number of substrates for metabolism, mainly fatty acids or glucose. However, metabolism during RVH is dependent on glycolysis (Sharma et al., 2004) and this metabolic shift is thought to be mediated via pyruvate dehydrogenase kinase (PDK) (Piao et al., 2010). Inhibition of PDK by dichloroacetate increased glucose oxidation and improved RV function (Piao et al., 2010) by restoration of expression and function of voltage-gated K⁺ channels (Michelakis et al., 2002b). Neurohormonal pathways are also activated during right ventricular hypertrophy due to reduced tissue perfusion. This can lead to activation of the renin-angiotensin-system (RAS) with increased angiotensin II levels (Bogaard et al., 2009). Angiotensin II exerts the majority of its effects on the heart through the angiotensin II receptor type 1 (AT₁R) by up-regulation of NAD(P)H oxidases to increase ROS production (Seshiah et al., 2002). Excessive ROS production leads to cardiac hypertrophy and contractile dysfunction (Nakamura et al., 1998, Elnakish et al., 2013). Is it fundamentally important to understand the pathways and complex interactions which occur in the heart to culminate in RV failure. One way to do that is to look at the miRNA profile of the heart and investigate which miRNAs are dysregulated within the RV during the development of PH.

Analysis of cardiac tissue from the mouse hypoxic model showed an increase in miR-451 expression selectively within the RV of the hypoxic group however this effect was not observed in the hypoxia/SU5416 group. This links back to the results obtained in chapter 3 where transient knockdown of miR-451 resulted in a reduction in RVP. As previously stated results suggest that miR-451 may be involved in acute hypoxic pulmonary vasoconstriction and therefore contribute to the increased afterload in the RV. Thus as well as playing a role in hypoxic pulmonary vasoconstriction, miR-451 may also affect RV contractility.

Cardiac miRNA analysis of the mouse and rat hypoxia/SU5416 model of PH found increased levels of miR-27a and miR-27b, respectively, selectively in the right ventricle. As well as observing no dysregulation of these miRNAs within the left

ventricle, this increase in expression was not observed in lung tissue from study animals indicating that up-regulation of miR-27 is selective to the right ventricle.

The two isoforms of the miR-27 family belong to different clusters; intergenic miR-23a/27a/24-2 cluster located on human chromosome 19 at position 19q13.13 and intronic miR-23b/27b/24-1 cluster located on human chromosome 9 at position 9q22.32. Interestingly, pri-miR-23b, pri-miR-27b and pri-miR-24-1 are transcribed independently from the same promoter however, the pre-miR-23b, pre-miR-24b and pre-miR-24-1 sequences may be transcribed together. In addition to this, members of each cluster can respond differently to various stimuli (Sun et al., 2009). MiR-27a and miR-27b are conserved across species and differ in only one nucleotide at the 3'-end. They share the same seed sequence and therefore also share most predicted targets genes (Zhou et al., 2011). Both miR-27a and miR-27b are highly expressed in vascularised tissue such as the lung, heart and endothelial cells (Zhou et al., 2011). *In vitro* studies found that inhibition of miR-27 in human umbilical vein endothelial cells (HUVECs) reduced sprout formation (Kuehbacher et al., 2007) and repressed HUVEC proliferation and migration in response to angiogenic factors (Zhou et al., 2011). In a similar manner, over-expression of miR-27a or miR-27b in HUVECs via transfection with precursor molecules resulted in a significant increase in endothelial cell sprouting and induced migration and proliferation (Urbich et al., 2012). *In vivo* data supports the cell culture experiments as silencing of miR-27 in mice using an antagomiR reduced vascularisation of implanted Matrigel (Urbich et al., 2012). In addition to this, miR-27a and miR-27b expression were found to be up-regulated in the retinal/choroidal region after laser induced injury in the choroidal neovascularisation (CNV) mouse model, a process characterised by abnormal growth of blood vessels at the back of the eye. Knock down of miR-27 using an LNA-modified antimiR immediately following the laser injury reduced CNV area significantly (Zhou et al., 2011).

Both *in vitro* and *in vivo* data indicate that miR-27 can enhance endothelial cell migration and proliferation and stimulates angiogenesis. The pro-angiogenic effects exerted by miR-27 are thought to be due in part to repression of target genes Sprouty2 and Sema6A (Zhou et al., 2011, Urbich et al., 2012). Sprouty2 is

an inhibitor of the Ras/Raf/ERK pathway as shown by repression of ERK1/2 phosphorylation (Zhou et al., 2011) and this signalling pathway is known to highly regulate the angiogenic response (Cross and Claesson-Welsh, 2001). Similarly, Sema6A is an inhibitor of angiogenesis in endothelial cells via negative regulation of the MAPK and VEGFR2 signalling pathways (Zhou et al., 2011, Dhanabal et al., 2005). Hence, repression of Sprouty2 and Sema6a by miR-27 allows the phosphorylation of key regulators of the MAPK and VEGFR2 signalling cascades and promotes angiogenesis.

Another direct target of miR-27b is myocyte-enhancer factor 2c (Mef2c) (Chinchilla et al., 2011). Mef2c is a muscle specific transcription factor which is required during embryogenesis for development of the right ventricle (Lin et al., 1997). Transgenic mice over-expressing Mef2c specifically in the heart develop hypertrophic cardiomyopathy (Xu et al., 2006) and this is thought to be due to Mef2c activating genes which can induce cardiac hypertrophy (Munoz et al., 2009). However in our study looking into the development of PH, miR-27 expression was up-regulated within the right ventricle suggesting that target gene Mef2c would be repressed. This indicates that the hypertrophic response regulated by Mef2c would also be repressed and thus targeting of Mef2c by miR-27 may not be the pathway involved in PH development within the models tested in this study.

As mentioned above, Zhou and colleagues found that miR-27 was involved in regulating VEGFR2 signalling in response to angiogenic factors through repression of target genes (Zhou et al., 2011). The rodent models of PH used within this chapter involve administration of SU5416, a VEGFR2 inhibitor. Thus, miR-27 expression may be dysregulated by blockade of VEGFR2. Therefore this experiment should be tested in other models of PH development to attain whether the results observed here are accurate or if SU5416 is having an effect on the miRNA expression.

Over time, prolonged induction of cardiac hypertrophy can eventually result in right heart dysfunction and failure. However, initial hypertrophy is an important adaptive cardiac response to stresses and requires neovascularisation to support this hypertrophic growth. Therefore angiogenesis is a key process involved in maintaining the heart in a functional state. The hypoxia/SU5416 model of PH

used in this study displays very high right ventricular pressures with very little evidence of RV failure and increased miR-27 expression in the heart (as observed within this study) may promote angiogenesis via target gene modulation to trigger this adaptive cardiac hypertrophy. Therefore focusing on whether targeting treatment towards the right heart may in fact be of benefit to PH patients would be relevant. Hence, the results shown here where miR-27 looks to be important in selectively the right ventricle shows promise and should be further investigated. It would be interesting to establish whether over-expression of miR-27a/b in the right ventricle prevents RV failure and improves RV function over a longer study period in experimental models of PH. The principle benefit of maintaining a functional RV would be to work in concert with other PH therapies (e.g. anti-remodelling treatment) to provide a better chance of survival for PAH patients.

In order to advance our knowledge regarding the role of miR-27 in the heart, *in situ* hybridisation should be performed on heart sections from rodents exposed to PH stimuli alongside healthy rodent controls. This would allow the specific localisation of miR-27 over-expression within the right ventricle. The results in this chapter highlight the expression pattern of miR-27a and miR-27b in both the rat and mouse model of PAH. Modulation of miR-27 in a cell culture model of RVH would show whether the observations displayed *in vivo* could be recapitulated in an *in vitro* setting. In order to achieve this, transfection of primary cardiomyocytes isolated from the rat right ventricle with synthetic miR-27 mimic should be carried out. Myocyte cell size and induction of fetal gene pattern (e.g. increased expression of atrial natriuretic peptide, b-type natriuretic peptide and β MHC) should be quantified to allow cardiomyocyte hypertrophy assessment. If up-regulation of miR-27 is a key molecule involved in the hypertrophic response initiated within the right ventricle, it would be expected that over-expression of miR-27 would induce myocyte enlargement and re-expression of the fetal gene program. Similarly, knockdown of miR-27 should be tested in combination with stimuli to induce hypertrophy (e.g. angiotensin II) to assess whether inhibition of miR-27 prevents the hypertrophic response. The miRNA expression data displayed within this chapter was obtained from RNA extracted from paraffin blocks for the rat samples. For future work, fresh tissue should be generated and analysed for gene and protein expression in order to

clarify the pathways regulated by increased miR-27 expression within the RV. This will give us a greater understanding of the molecular mechanisms involved in cardiac tissue during the development of PH.

5 The role of miR-145 in PAH

5.1 Introduction

Smooth muscle cells (SMCs) are one of the cell types involved in pulmonary vascular remodelling associated with PAH. Under normal physiological conditions, SMCs exist in a quiescent 'contractile' phenotype, characterised by high expression of SM-specific genes, such as SMA, calponin and SM22- α . Changes within the local environment cause these SMCs to phenotypically switch to a migratory and proliferative 'synthetic' phenotype in response to vascular injury. This phenotypic switch is essential to induce repair to the vessels (Lagna et al., 2007, Rangrez et al., 2011), after which growth factors stimulate the SMCs to return to their normal contractile phenotype. Persistent activation of the highly proliferative state can however be detrimental to the surrounding tissue and lead to disease progression (Owens et al., 2004). Many different growth factors and transcription factors are involved in this SMC phenotypic modulation and two of the key miRNAs involved in this process are thought to be miR-143 and miR-145.

MiR-145 is transcribed bicistronically along with miR-143 from human chromosome 5 at position 5q32 (Xin et al., 2009). Expression of the miR-143/miR-145 cluster is high in cardiomyocytes during the early stages of heart development but this expression is lost during the later stages of cardiogenesis. Expression of the miRNA cluster is then exclusively localized to SMCs (Xin et al., 2009, Boettger et al., 2009, Cordes et al., 2009). Activation of the miR-143/miR-145 cluster is through the conserved regulatory DNA element called a CArG box ([CC(AT)₆GG]) contained within the promoter region of the pri-miRNA cluster. Binding of serum response factor (SRF) and its cofactors myocardin (Myocd) and myocardin related transcription factors (MRTF) to the CArG box activates transcription of the miR-143/miR-145 gene cluster (Cordes et al., 2009, Lagna et al., 2007, Davis-Dusenbery et al., 2011). Members of the TGF- β super family of growth factors are known to induce SMC contractile phenotype and it has been shown that TGF- β and BMP4 achieve this through activation of miR-143/miR-145 via distinct mechanisms. TGF- β induces Myocd expression while BMP4 stimulation leads to nuclear translocation of MRTF-A (Davis-Dusenbery et al., 2011). Cofactors from both pathways can independently bind to SRF after being recruited to the CArG box and activate miR-143/miR-145 transcription (Xin et al., 2009, Lagna et al., 2007, Davis-Dusenbery et al., 2011).

Although miR-143 and miR-145 exist as a cluster, there is a lack of homology between the seed sequences of the mature miRNAs. Nevertheless, it has been found that both miRNAs potentially target many of the same genes, leading to co-operativity of this cluster in translational regulation. Activation of miR-143/miR-145 by TGF- β and BMP4 leads to down-regulation of target genes Klf4 and Klf5 resulting in increased expression of smooth muscle specific genes. Thus miR-143 and miR-145 activation induces the contractile phenotype via down-regulation of Klf4 and Klf5 and represses proliferation in SMCs (Cordes et al., 2009, Davis-Dusenbery et al., 2011, Liu et al., 2005, Cheng et al., 2009). In addition, studies have shown that Klf4 prevents expression of contractile genes by inhibiting the expression of myocardin and by decreasing SRF binding to the CArG box, both of which are critical steps in promoting the SMC contractile phenotype via miR-143/miR-145 activation (Liu et al., 2005, Davis-Dusenbery et al., 2011). Klf2 is another transcription factor which has been shown to bind to the promoter region of the miR-143/miR-145 cluster resulting in up-regulation of this miRNA cluster and stimulating cell-cell communication between endothelial cells and smooth muscle cells (Hergenreider et al., 2012). A recent study revealed that over-expression of Klf2 in HUVECs led to an up-regulation of miR-143 and miR-145 within the HUVECs but also within the extracellular vesicles released by these cells. These vesicles were then able to control the phenotype of co-cultured SMCs by down-regulating miR-143/miR-145 target genes, therefore promoting the contractile phenotype (Hergenreider et al., 2012).

Recent studies have also demonstrated activation of the miR-143/miR-145 gene cluster in an SRF-independent manner. Jagged-1 (Jag-1) induces canonical CBF1 mediated Notch signalling to form complexes which bind to the promoter region of miR-143/miR-145 independent of the CArG box and result in up-regulation of SMC contractile gene expression (Boucher et al., 2011).

Modulation of the SMC phenotype is fundamental to the development of vascular disease and many studies have reported the role of miR-143/miR-145 in this setting. Expression of this miRNA cluster is down-regulated in models of vascular stress including carotid artery ligation (Cordes et al., 2009), carotid artery balloon injury (Cheng et al., 2009), transverse aortic constriction and ApoE knockout mice (Elia et al., 2009). In addition, miR-143 and miR-145 expression is

significantly reduced in human aortic aneurysms compared to control aortas (Elia et al., 2009). Over-expression studies have used adenoviruses to modulate miR-143 or miR-145 expression *in vivo* and found reduced neo-intimal formation and increased expression of smooth muscle specific genes in the carotid artery balloon injury model (Cheng et al., 2009, Elia et al., 2009). Use of miR-143/miR-145 knockout mice support this data with increased neo-intimal formation compared to wild type mice (Boettger et al., 2009). Conversely, Xin and colleagues (Xin et al., 2009) found that miR-143, miR-145 and double knockout mice displayed reduced neo-intimal formation in response to carotid artery ligation. The divergent effects of silencing miR-143/miR-145 obtained by use of different systems and models are interesting. These contradictory results may in part be explained due to the reduced vascular tone exhibited specifically in the knockout mice, along with activation of complex mechanisms *in vivo* which are absent from the *in vitro* setting (Xin et al., 2009). These studies highlight the importance of the miR-143/miR-145 gene cluster in controlling SMC phenotype and illustrate how dysregulation of these pathways can result in cardiovascular disease.

In the setting of PAH, it has been observed that miR-145 expression was increased in the lungs and the right ventricle from the hypoxic mouse model of PH (Caruso et al., 2012). In addition, recent work established that miR-145 was up-regulated in pulmonary arteries from IPAH patients (Courboulin et al., 2011), PAH-PASMCs containing a known BMPR2 mutation and in lung tissue from IPAH and HPAH patients (Caruso et al., 2012). Expression of miR-145 was noted within the muscular regions of the lesions from IPAH and HPAH patients (Caruso et al., 2012) with greater expression of miR-145 in the concentric lesions compared to plexiform lesions (Bockmeyer et al., 2012). Furthermore, knockout of miR-145 in female mice by both genetic ablation and treatment of mice with anti-miR-145 caused a significant reduction in systolic right ventricular pressure and the number of remodelled vessels compared to control hypoxic animals. In addition, RVH was significantly reduced in female miR-145 knockout mice compared to hypoxic control mice however, RVH was unaffected by anti-miR-145 treatment (Caruso et al., 2012). Target gene analysis indicated that the Wnt signalling pathway may contain various target genes for miR-145 as increased levels of WIF1, FRZB and DAB2 (key members of the Wnt signalling pathway) were

observed in hypoxic miR-145 knockout mice (Caruso et al., 2012). In addition to this, other members of the Wnt signalling pathway have previously been shown to regulate PASMC proliferation (Sklepkiwicz et al., 2011), thus illustrating that the protective effect observed in mice void of miR-145 may potentially be due to inhibition of the Wnt/ β -Catenin canonical signalling pathway. Loss of miR-143 via anti-miR-143 treatment did not illustrate the same protective effect as miR-145 (Caruso et al., 2012).

In general terms, *in vitro* studies have demonstrated the essential role for miR-143/miR-145 in controlling SMC phenotype, while *in vivo* studies illustrate that specific knock down of miR-145 expression protects against the development of PH in mice. Investigation into the exact pathways modulated within the pulmonary vasculature by miR-145 would increase our depth of understanding of this complex disease.

5.1.1 Aim

The aims investigated in this chapter were:

- To determine the effect of silencing miR-145 both in a prevention and reversal study on the development of PH in the hypoxia/SU5416 rodent model.
- To examine the effect of genetic ablation of miR-145 *in vivo* on the development of PH and assess the role of gender in this setting.
- To identify miR-145 target genes using a miRNA pull down technique in hPASMCs *in vitro*.

5.2 Results

5.2.1 Prophylactic modulation of miR-145 in hypoxia/SU5416 model of PH

Previous work in our laboratory showed that miR-145 was up-regulated during the development of PH and silencing of this miRNA proved to be beneficial in the hypoxic mouse model of PH (Caruso et al., 2012). Thus, silencing miR-145 was investigated *in vivo* in the rat hypoxia/SU5416 model of PH using an anti-miR targeting mature miR-145. Administration of anti-miR-145 was performed two weeks prior to hypoxia/SU5416 insult and for three weeks post hypoxic exposure (Figure 5.1) to investigate the effect of prophylactic silencing of miR-145. To verify knockdown obtained using anti-miR-145, lung tissue was harvested and miR-145 expression was analysed via qRT-PCR (Figure 5.2A) and northern blot (Figure 5.2B, C). MiR-145 levels were significantly reduced in all groups treated with anti-miR-145 compared to both control anti-miR and PBS treatment groups. In order to determine the specificity of anti-miR-145, expression levels of miR-143 were also analysed as both miR-145 and miR-143 are transcribed together from a common pri-miRNA. MiR-143 levels remained unaffected by anti-miR-145 treatment in both normoxic and hypoxic conditions as detected by qRT-PCR (Figure 5.3). Although analysis into miR-143 expression was limited, anti-miR-145 appears to be specific in its action in targeting miR-145.

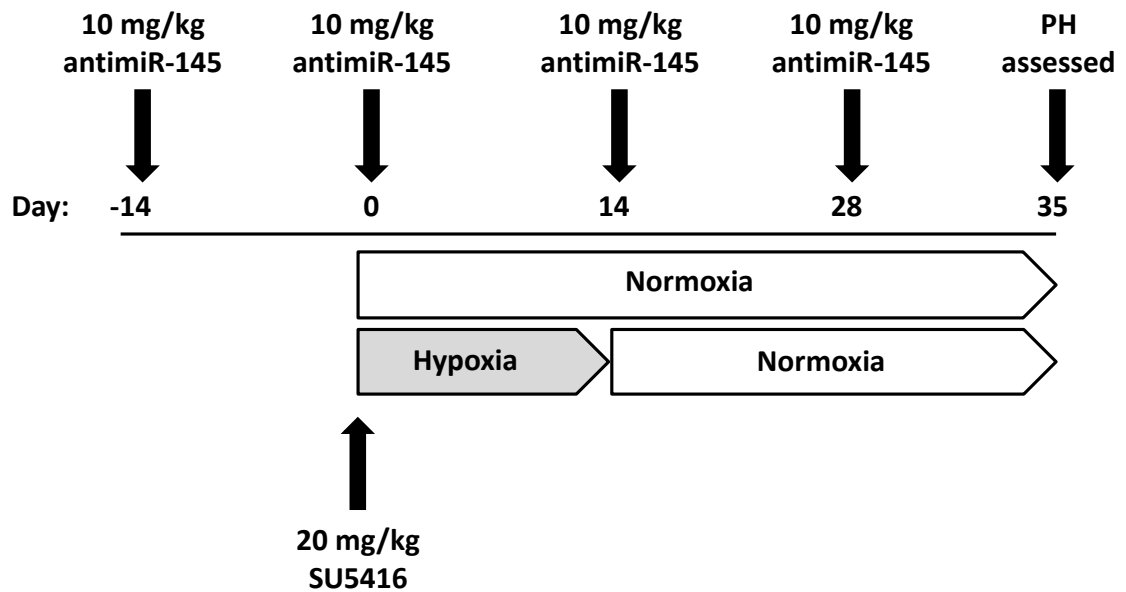


Figure 5.1 – Prophylactic antimiR-145 *in vivo* study design.

Male wistar kyoto rats were administered antimiR-145, control antimiR or PBS subcutaneously at 10 mg/kg every 14 days. 14 days after the initial administration of treatment drug, rats were dosed subcutaneously with 20 mg/kg SU5416 and exposed to hypoxic or normoxic conditions for 14 days. Following this, all rats were placed in normoxic conditions for a further 21 days. On day 35, echocardiography was performed, hemodynamic measurements were taken and tissues harvested.

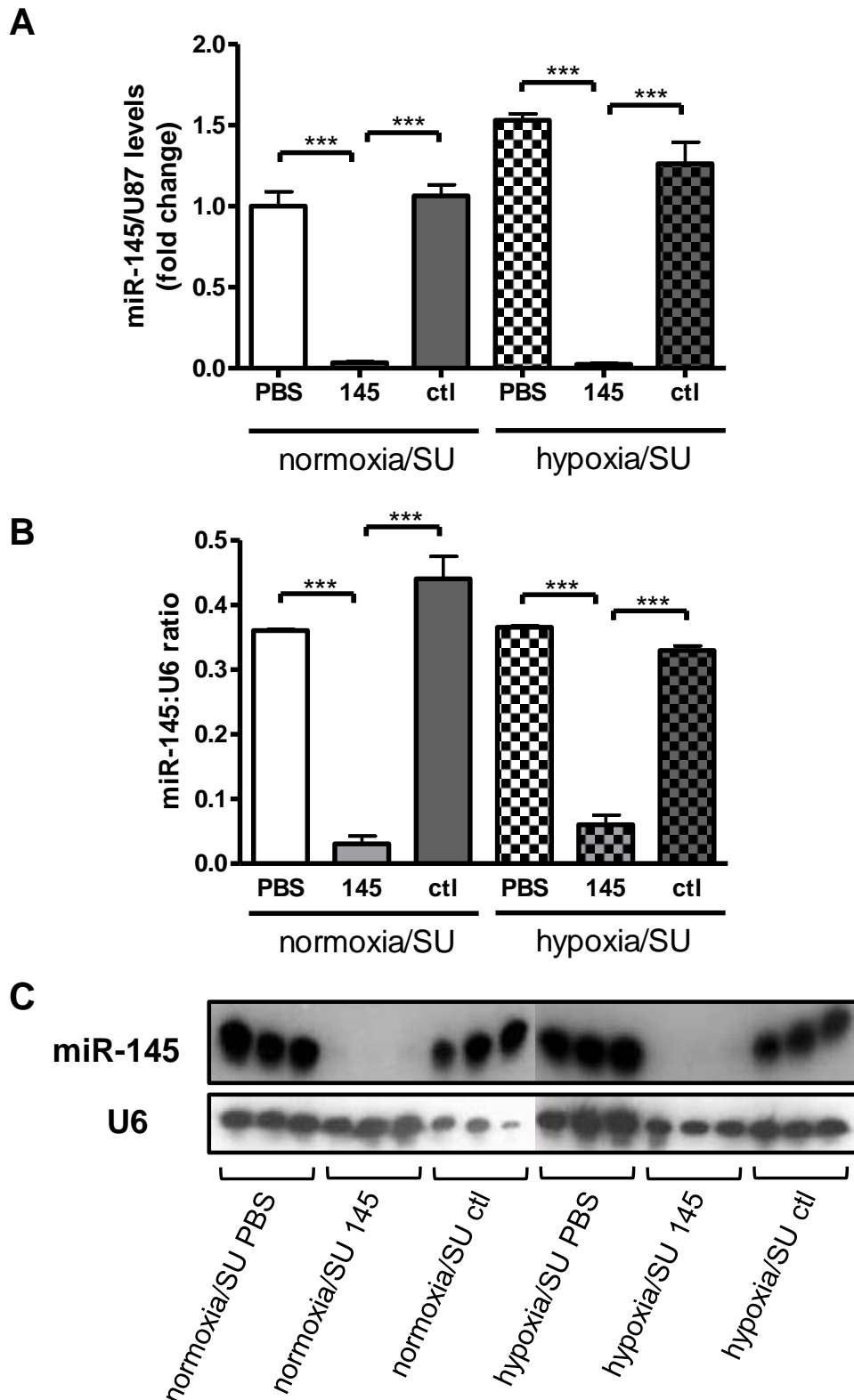


Figure 5.2 – MiR-145 expression in lung from prophylactic antimiR-145 study.

(A) Expression of miR-145 in rat whole lung tissue from prophylactic study at day 35, as detected by qRT-PCR. Arbitrary value of 1 assigned to normoxia/SU PBS group. Data expressed as fold change \pm SEM, $n = 8$ animals per group. (B) Quantification of northern blot was performed by normalising band intensity of miR-145 to the relative U6 signal (C) and expressed as mean \pm SEM, $n = 3$ animals per group. All data analysed by one-way ANOVA followed by Tukey's post hoc test, $***p < 0.001$. SU = SU5416, 145 = antimiR-145, ctl = control antimiR.

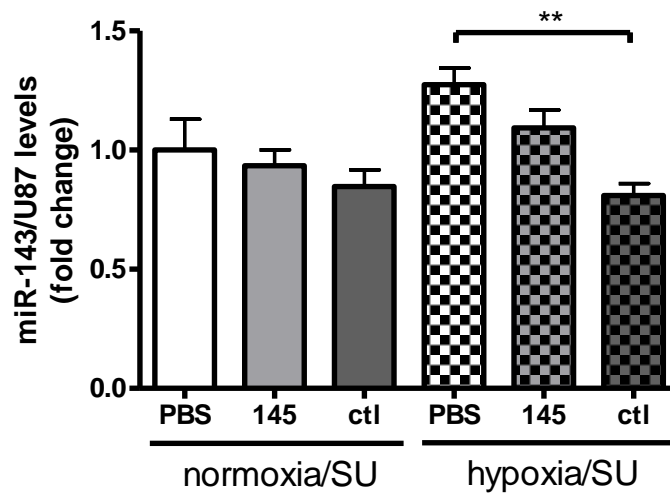


Figure 5.3 – MiR-143 expression in lung from prophylactic antiMiR-145 study.

Expression levels of miR-143 in rat whole lung tissue from prophylactic study at day 35, as detected by qRT-PCR. Arbitrary value of 1 assigned to normoxia/SU PBS group. Data expressed as fold change \pm SEM and analysed by one-way ANOVA followed by Tukey's post hoc test. ** $p < 0.01$, $n = 8$ animals per group. SU = SU5416, 145 = antiMiR-145, ctl = control antiMiR.

5.2.2 Effect of prophylactic silencing of miR-145 on the development of PH in the hypoxia/SU5416 model

The effect of silencing miR-145 on the development of PH in male rats was quantified by analysis of key indicators of disease; RVP, RVH, vessel remodelling and vessel occlusion. There was no change in systemic arterial pressure between the groups (Figure 5.4A). Rats dosed with vehicle and exposed to hypoxia/SU5416 followed by three weeks normoxic exposure displayed a significant increase in RVP compared to normoxia/SU5416 rats (140.3 ± 5.96 and 34.61 ± 1.84 mmHg, respectively) (Figure 5.4B). Gleevec, a tyrosine kinase inhibitor, was used as a positive control for this study as it had previously been reported to have anti-proliferative effects in PSMCs (Nakamura et al., 2012, Schermuly et al., 2005) and cause reversal of the pulmonary hypertensive phenotype in rodent models of PH (Abe et al., 2011, Schermuly et al., 2005). Administration of gleevec with hypoxia/SU5416 exposure prevented the dramatic increase in RVP and produced RVPs similar to that observed in normoxia/SU5416 animals. This supported previous data and indicates that the experimental conditions and reagents were working correctly. Pre-treatment with antimiR-145 and exposure to hypoxia/SU5416 however did not reduce RVP compared to control antimiR and vehicle treated hypoxia/SU5416 rats (Figure 5.4B). Similar results were obtained for RVH (Figure 5.4C), pulmonary vessel remodelling (Figure 5.5) and percentage vessel occlusion (Figure 5.6). Thus antimiR-145 treatment did not provide a protective effect in the development of PH under these experimental conditions.

Cardiac function was measured using echocardiography on day 35 of the prophylactic study. Heart rate (Figure 5.7A), pulmonary artery acceleration time (Figure 5.7B) and cardiac output (Figure 5.7D) were unchanged between normoxia/SU5416 and hypoxia/SU5416 groups. Interestingly, administration of antimiR-145 prior to hypoxia/SU5416 insult reduced the mid systolic notch observed in hypoxia/SU5416 control antimiR and vehicle treated rats in a similar manner to gleevec treatment (Figure 5.7C).

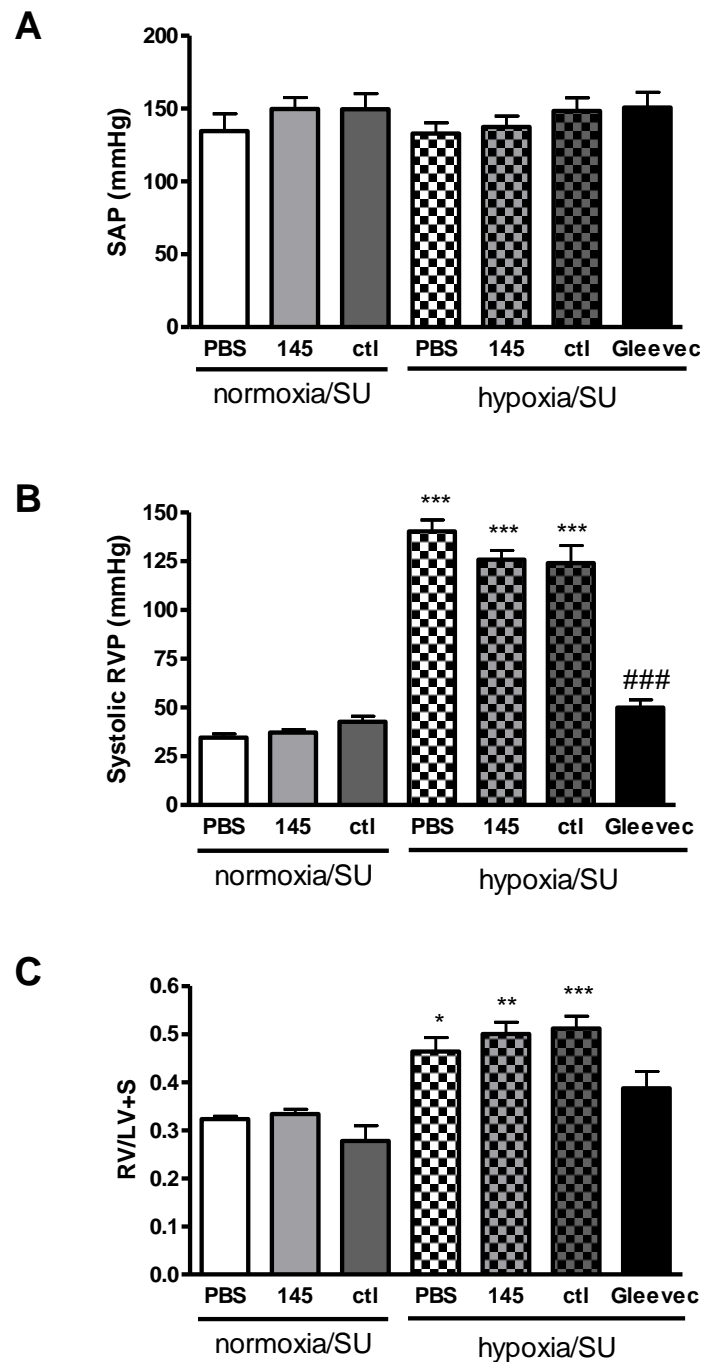


Figure 5.4 – Quantification of PH indices in prophylactic anti-miR-145 study.

Quantification of (A) SAP, (B) systolic RVP and (C) RVH in male rats from prophylactic study at day 35. Data represented as mean \pm SEM and analysed by one-way ANOVA followed by Tukey's post hoc test. * $p < 0.05$, ** $p < 0.01$ and *** $p < 0.001$ vs normoxia/SU PBS, ### $p < 0.001$ vs hypoxia/SU PBS, $n = 8-10$ animals per group for SAP and RVP ($n = 5$ animals for hypoxia/SU gleevec group), $n = 4-5$ animals per group for RVH. SU = SU5416, 145 = anti-miR-145, ctl = control anti-miR.

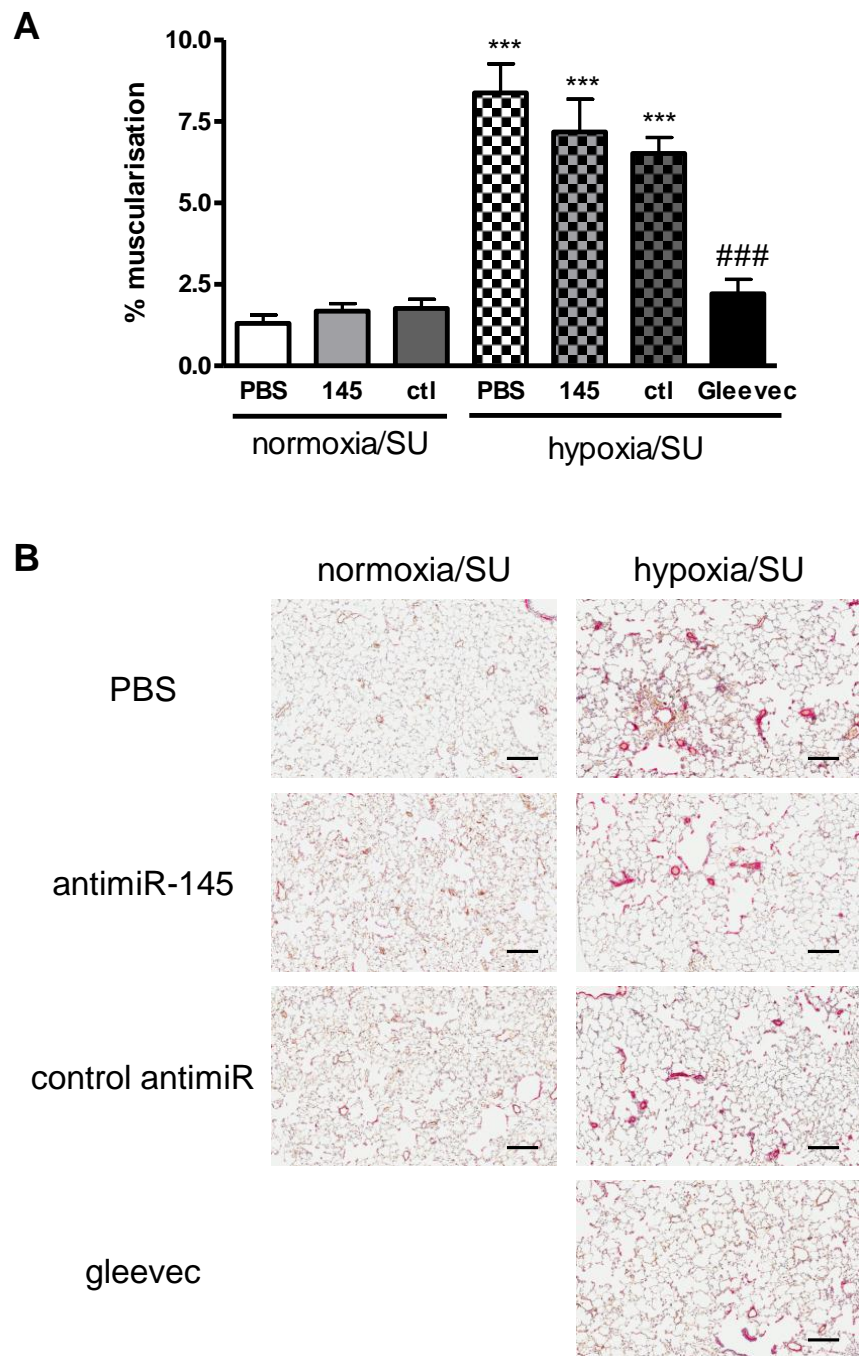


Figure 5.5 – Pulmonary remodelling in prophylactic antimiR-145 study.

(A) Quantification of pulmonary vascular remodelling in male rats from prophylactic study at day 35. Data expressed as mean \pm SEM and analysed by one-way ANOVA followed by Tukey's post hoc test. *** $p < 0.001$ vs normoxia/SU PBS and ### $p < 0.001$ vs hypoxia/SU PBS, $n = 8-10$ animals per group ($n = 5$ animals for hypoxia/SU gleevec group). (B) Representative images of lung sections stained with α -SMA (red) and von Willebrand Factor (brown), magnification X8, scale bar = 200 μm . SU = SU5416, 145 = antimiR-145, ctl = control antimiR.

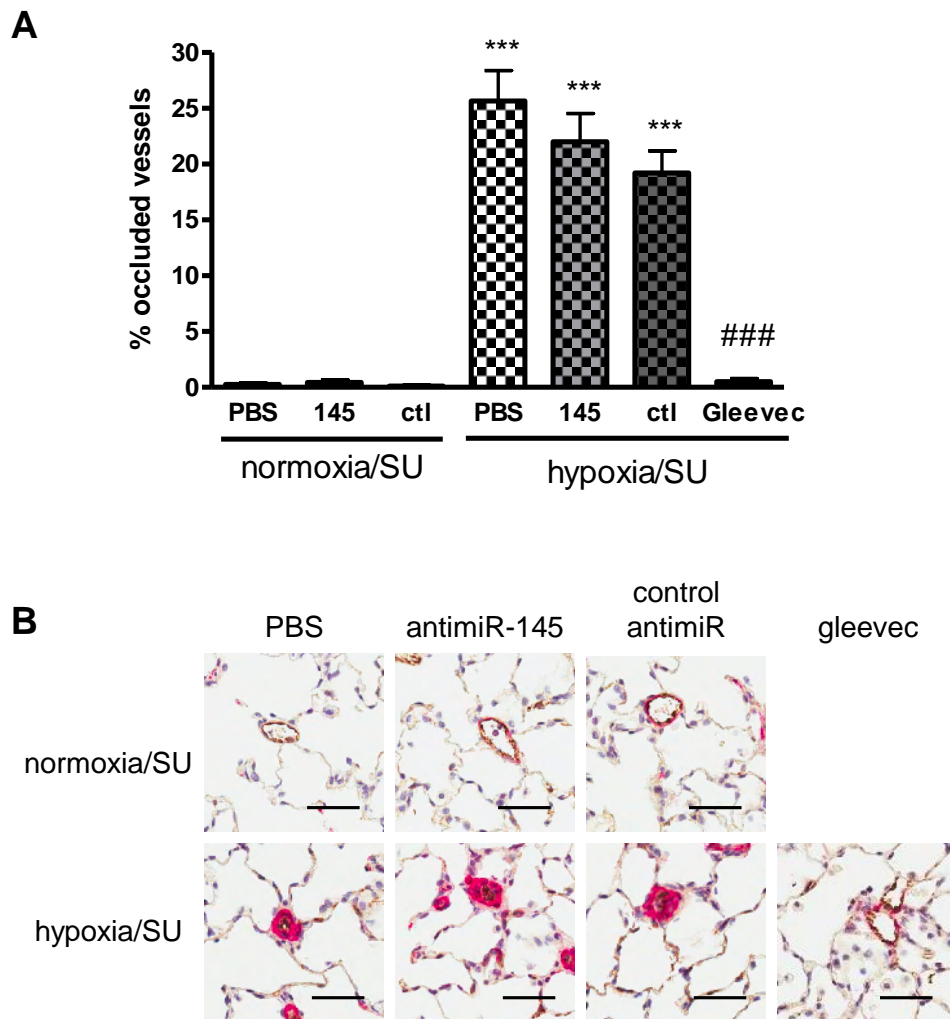


Figure 5.6 – Pulmonary occluded vessel analysis in prophylactic anti-miR-145 study.

(A) Quantification of occluded vessels in male rats from prophylactic study at day 35. Data expressed as mean \pm SEM and analysed by one-way ANOVA followed by Tukey's post hoc test. *** $p < 0.001$ vs normoxia/SU PBS and ### $p < 0.001$ vs hypoxia/SU PBS, $n = 8-10$ animals per group ($n = 5$ animals for hypoxia/SU gleevec group). (B) Representative images of pulmonary vessels stained with α -SMA (red) and von Willebrand Factor (brown), magnification X8, scale bar = 50 μ m. SU = SU5416, 145 = anti-miR-145, ctl = control anti-miR.

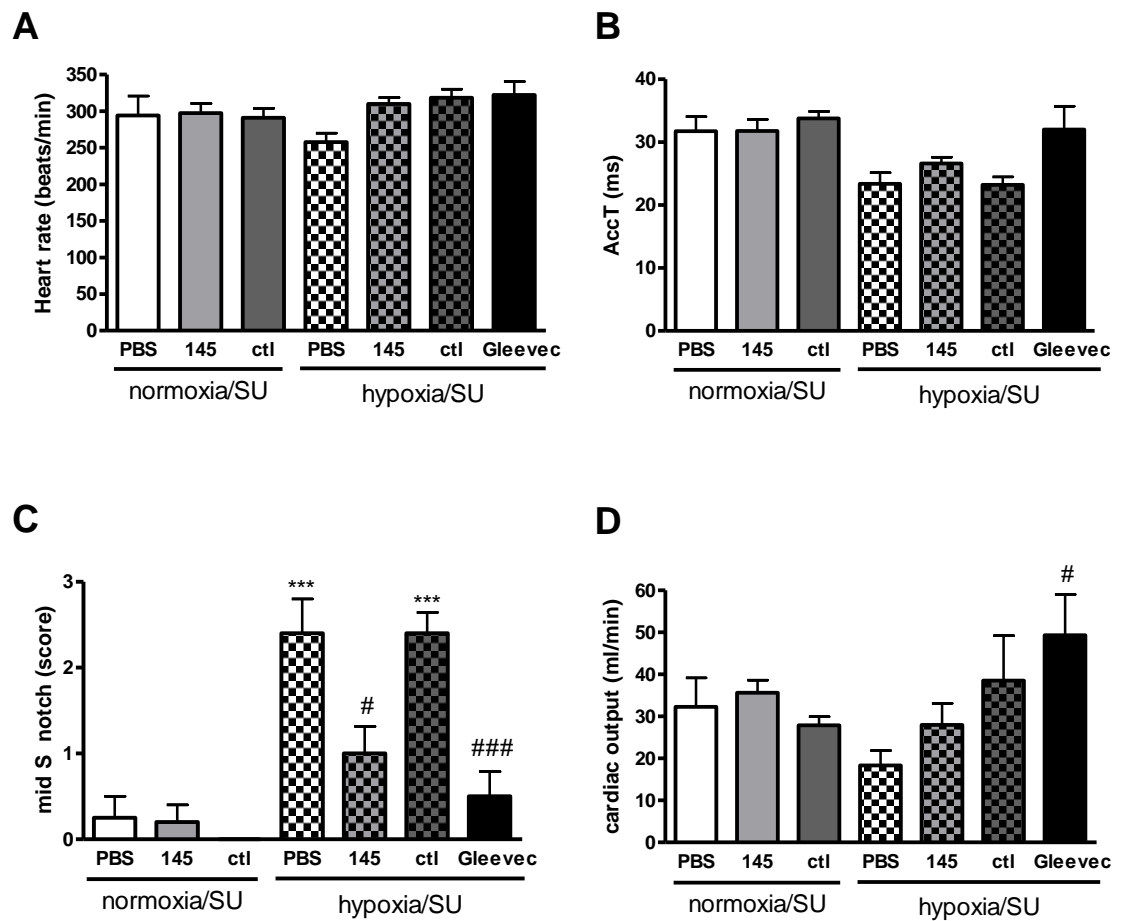


Figure 5.7 – Cardiac function parameters from prophylactic anti-miR-145 study.

Quantification of (A) heart rate, (B) pulmonary artery acceleration time (AccT), (C) mid systolic notch and (D) cardiac output calculated from echocardiography in male rats from prophylactic study at day 35. Data expressed as mean \pm SEM and analysed by one-way ANOVA followed by Tukey's post hoc test. ^{***} $p < 0.001$ vs normoxia/SU PBS, [#] $p < 0.05$ and ^{###} $p < 0.001$ vs hypoxia/SU PBS, $n = 4-5$ animals per group. SU = SU5416, 145 = anti-miR-145, ctl = control anti-miR.

5.2.3 Target gene analysis in prophylactic antimiR-145 study

MiRNA analysis (Figure 5.2) clearly shows significant knockdown of miR-145 in antimiR-145 treated rats, however, it is important to assess whether this reduction in miRNA expression results in up-regulation of target genes. A list of miR-145 targets was generated by searching the literature and from previous studies performed in our laboratory. All genes were probed for by qRT-PCR (Figure 5.8) however, none of the chosen targets were up-regulated at the mRNA level in antimiR treated animals.

Previous studies have shown that mRNA levels do not always reflect protein expression (Greenbaum et al., 2003). Therefore protein expression was analysed for Klf4 (Figure 5.9) as this is a validated target for miR-145 (Davis-Dusenbery et al., 2011, Xin et al., 2009, Cordes et al., 2009). Both at the mRNA and protein level, Klf4 expression remained unaltered by knocking down miR-145. This result demonstrates that although miR-145 expression was successfully knocked down by qRT-PCR and northern blot analysis, target gene de-repression was clearly not observed. This may explain why no effect was observed in the PH phenotype of the antimiR-145 treated hypoxia/SU5416 animals.

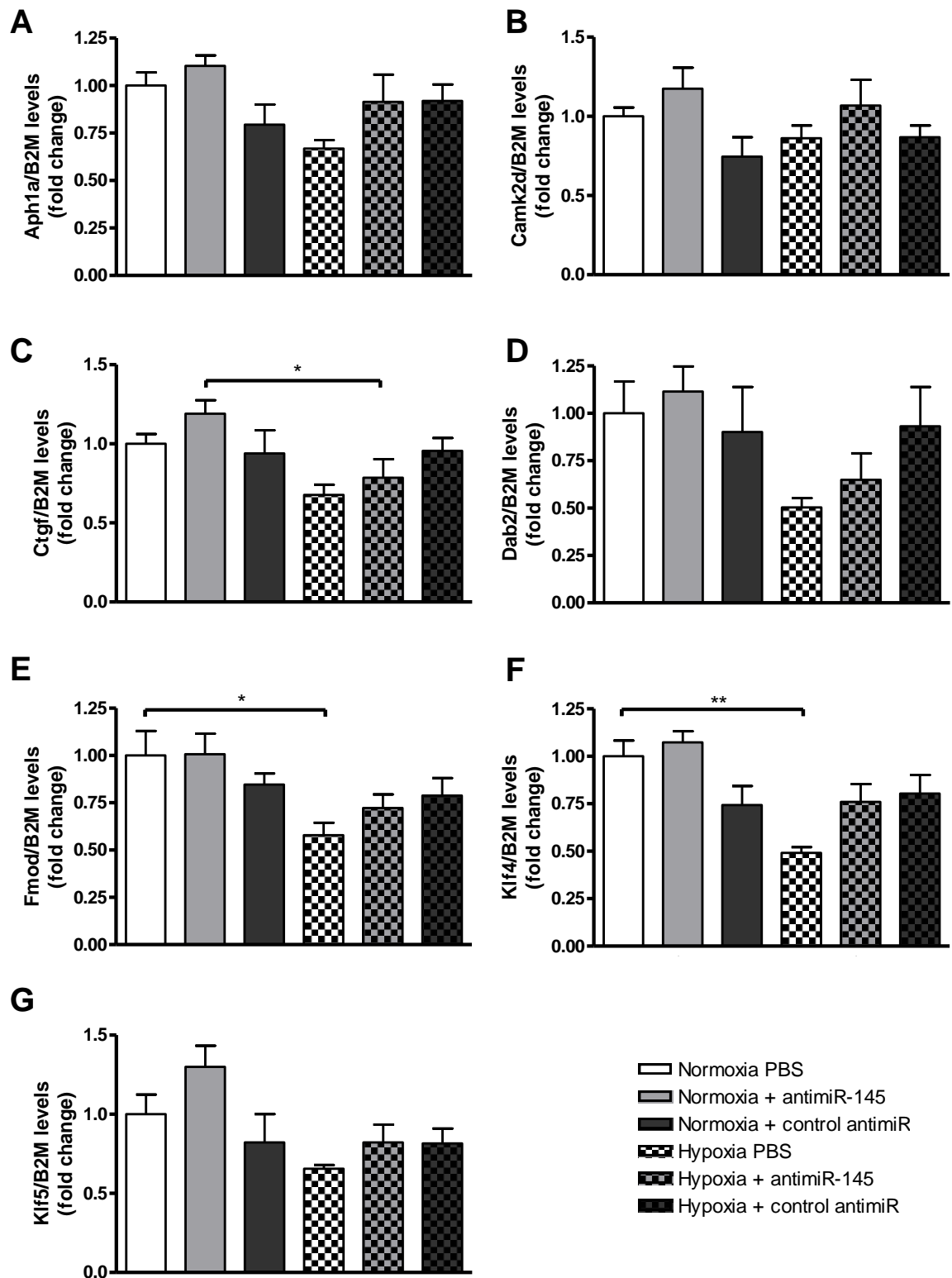


Figure 5.8 – Target gene mRNA expression from prophylactic anti-miR-145 study.

Target gene mRNA expression for (A) Aph1a, (B) Camk2d, (C) Ctgf, (D) Dab2, (E) Fmod, (F) Klf4, (G) Klf5, (H) Megf6, (I) Myocd, (J) Sema3a, (K) Smad4, (L) Smad5, (M) Sned1 and (N) Tmod1. Analysis performed in whole lung from male rats from prophylactic study at day 35, as detected by qRT-PCR. Arbitrary value of 1 assigned to normoxia/SU PBS group. Data expressed as fold change \pm SEM and analysed by one-way ANOVA followed by Tukey's post hoc test. * $p < 0.05$ and ** $p < 0.01$, $n = 8-10$ per group.

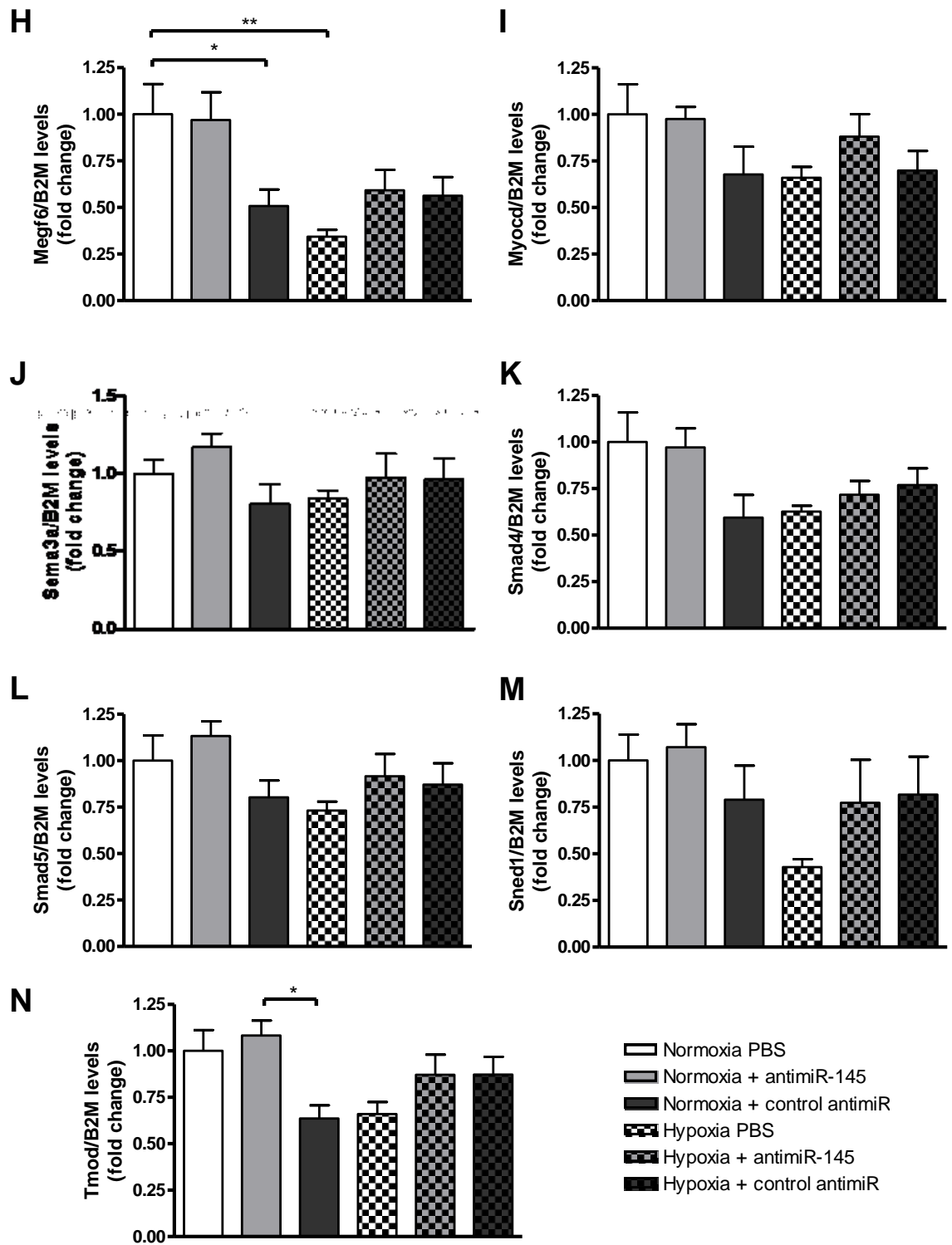


Figure 5.8 continued – Target gene mRNA expression from prophylactic anti-miR-145 study.

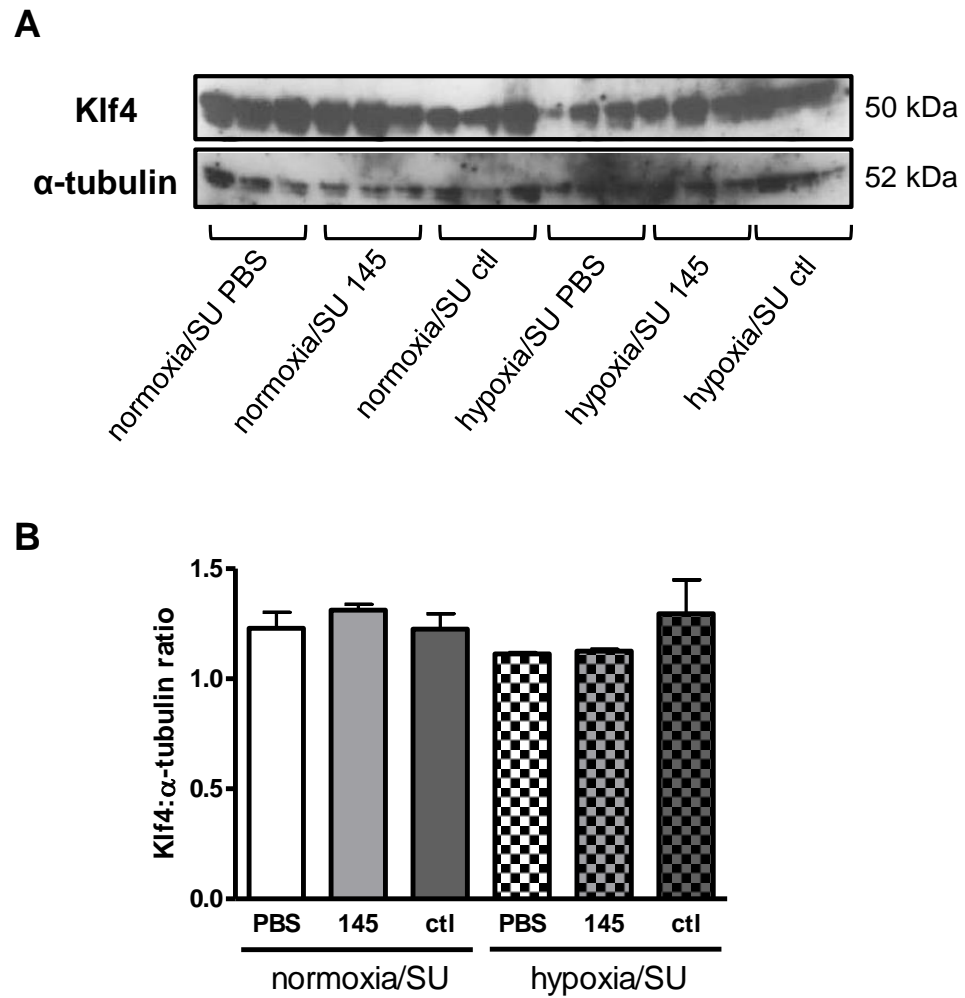


Figure 5.9 – Klf4 protein expression in lung from prophylactic anti-miR-145 study.

(A) Western blot was performed on protein extracted from whole lung from male rats from prophylactic study at day 35. (B) Quantification was performed by normalising Klf4 band intensity to the relative α -tubulin signal and expressed as mean \pm SEM, $n = 3$ animals per group. Data analysed by one-way ANOVA followed by Tukey's post hoc test. SU = SU5416, 145 = anti-miR-145, ctl = control anti-miR.

5.2.4 Therapeutic modulation of miR-145 in hypoxia/SU5416 model of PH

As well as investigating the effect of silencing miR-145 prior to hypoxia/SU5416 insult, a reversal study was also performed to determine the effect of knocking down miR-145 in male rats with established PH. This was carried out in parallel with the prophylactic study. In this therapeutic study, miR-145 levels were reduced by administration of antimiR-145 on day 14 after two weeks hypoxia/SU5416 exposure and dosing was continued for three weeks in normoxic conditions (Figure 5.10). As in the prophylactic study, miR-145 knock down in the lung was analysed using qRT-PCR (Figure 5.11A) and northern blot analysis (Figure 5.11B, C). Expression of miR-145 was significantly down-regulated in groups treated with antimiR-145 compared to control antimiR and vehicle treated groups. MiR-143 expression was also quantified (Figure 5.12) in the lung. Although miR-143 expression appeared to be up-regulated in hypoxia/SU5416 antimiR-145 group when compared to normoxia/SU5416 antimiR-145 group, there was no significant difference between control antimiR or vehicle treated animals and antimiR-145 treated animals in either normoxia/SU5416 or hypoxia/SU5416. Therefore this suggests that antimiR-145 is specifically targeting miR-145 and is not modulating miR-143 expression levels.

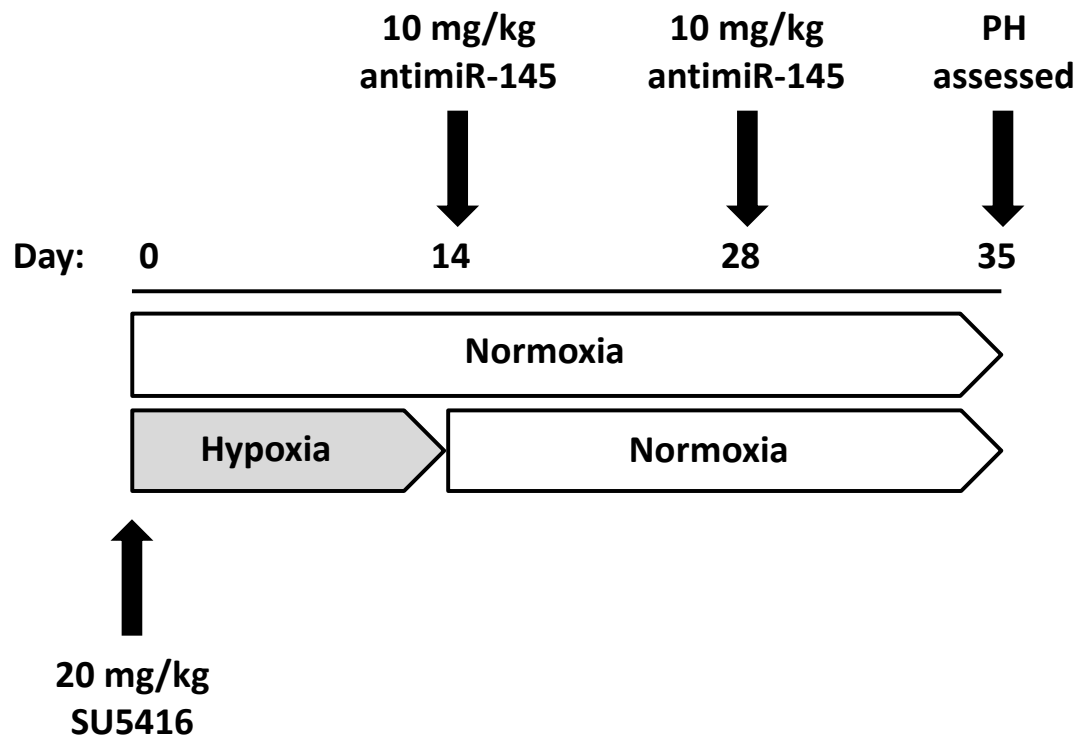


Figure 5.10 – Therapeutic antimiR-145 *in vivo* study design.

Male wistar kyoto rats were administered SU5416 subcutaneously at 20 mg/kg and exposed to normoxic or hypoxic conditions for 14 days to establish experimental PH. All rats were then returned to normoxic conditions for a further 21 days, during which time antimiR-145, control antimiR or PBS was administered subcutaneously at a dose of 10 mg/kg. On day 35, echocardiography was performed, hemodynamic pressures taken and tissues harvested.

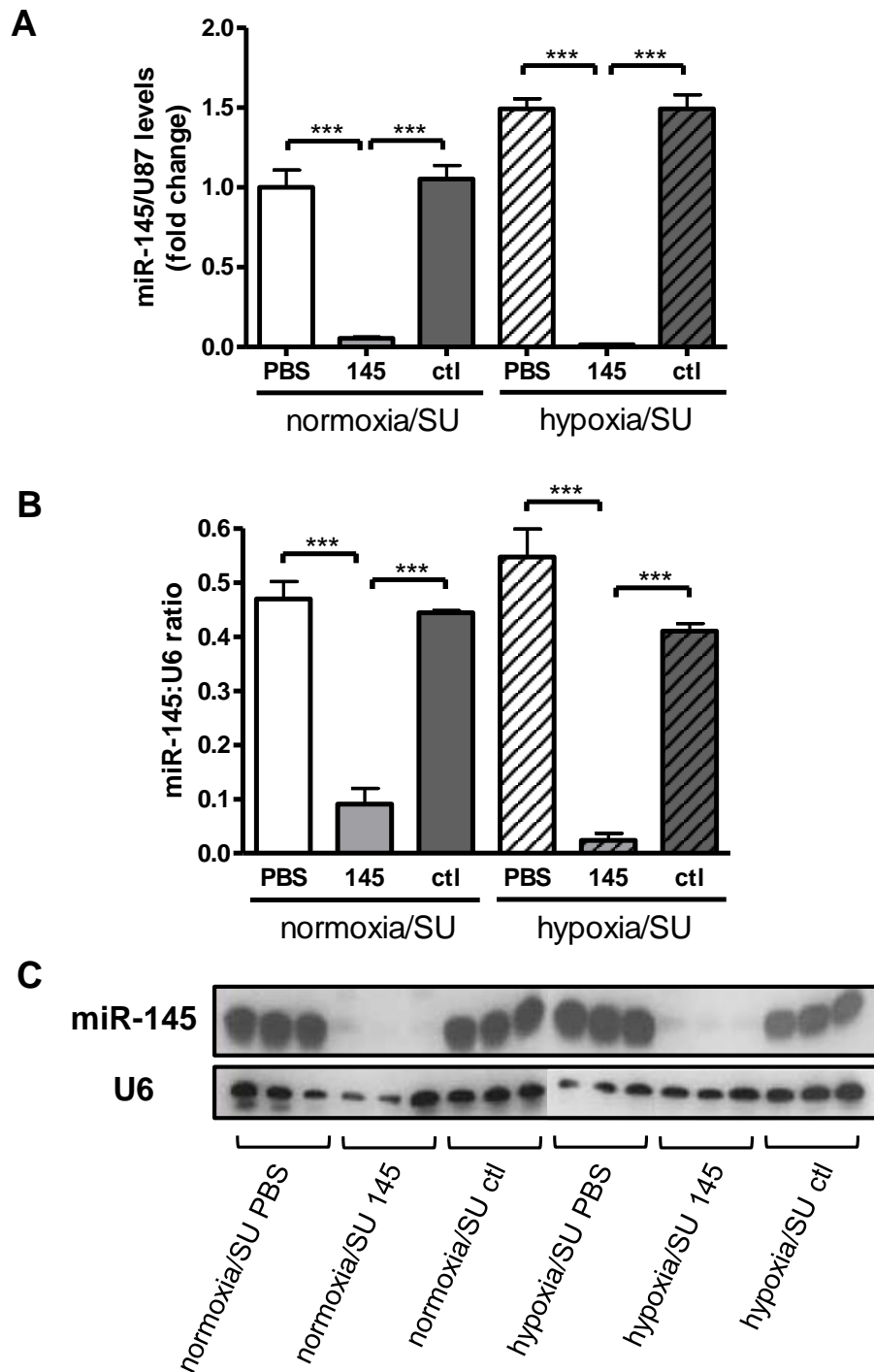


Figure 5.11 – MiR-145 expression in lung from therapeutic antiMiR-145 study.

(A) Expression of miR-145 in rat whole lung tissue from therapeutic study at day 35, as detected by qRT-PCR. Arbitrary value of 1 assigned to normoxia/SU PBS group. Data expressed as fold change \pm SEM, $n = 10$ animals per group. (B) Quantification of northern blot was performed by normalising band intensity of miR-145 to the relative U6 signal (C) and expressed as mean \pm SEM, $n = 3$ animals per group. All data analysed by one-way ANOVA followed by Tukey's post hoc test, *** $p < 0.001$. SU = SU5416, 145 = antiMiR-145, ctl = control antiMiR.

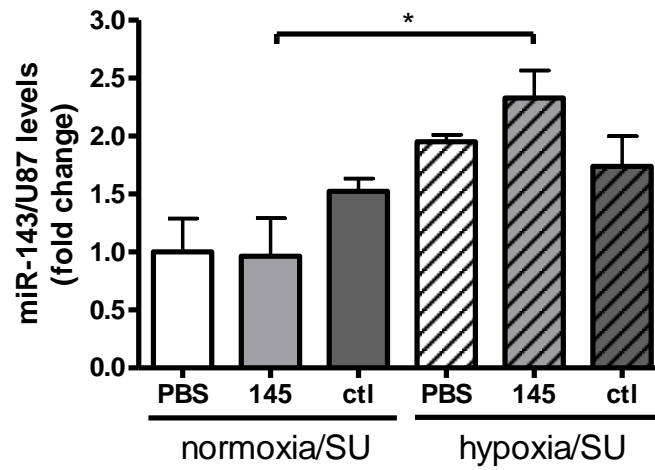


Figure 5.12 – MiR-143 expression in lung from therapeutic anti-miR-145 study.

Expression of miR-143 in rat whole lung tissue from therapeutic study at day 35, as detected by qRT-PCR. Arbitrary value of 1 assigned to normoxia/SU PBS group. Data expressed as fold change \pm SEM and analysed by one-way ANOVA followed by Tukey's post hoc test. * $p < 0.05$, $n = 10$ animals per group. SU = SU5416, 145 = anti-miR-145, ctl = control anti-miR.

5.2.5 Effect of therapeutic silencing of miR-145 in established PH

The effect of knocking down miR-145 levels was quantified by measuring the key indices of PH. Systemic arterial pressure was comparable between all groups (Figure 5.13A). Similar to the prophylactic study, exposure to hypoxia/SU5416 followed by administration of control antimiR or vehicle resulted in a significant increase in RVP compared to normoxia/SU5416 exposed animals (Figure 5.13B). Treatment with antimiR-145 after hypoxia/SU5416 exposure produced comparable RVP to animals dosed with control antimiR and vehicle. Gleevec was again used as a positive control for this study. Daily treatment with gleevec in rats with established PH reduced RVP significantly compared to all other treatment groups exposed to hypoxia/SU5416, suggesting that gleevec is reversing the PH phenotype. RVH (Figure 5.13C) and pulmonary vascular remodelling (Figure 5.14) followed a similar pattern to RVP results for all treatment groups. Interestingly, there was however a significant reduction in the percentage of occluded vessels in the antimiR-145 treated animals compared to vehicle and control antimiR treated hypoxia/SU5416 rats (Figure 5.15).

Cardiac function was measured by echocardiography and heart rate (Figure 5.16A) and pulmonary artery acceleration time (Figure 5.16B) were unchanged between groups. All groups exposed to hypoxia/SU5416 had an increased mid systolic notch, irrespective of treatment group (Figure 5.16C). Cardiac output was decreased in vehicle, antimiR-145 and control antimiR treated rats exposed to hypoxia/SU5416 compared to normoxia/SU5416 vehicle treated animals and this was reversed in gleevec treated rats (Figure 5.16D).

5.2.6 Target gene analysis in therapeutic antimiR-145 study

Target genes for miR-145 (same genes investigated in section 5.2.3) were analysed in the lung from all groups at day 35 by qRT-PCR. None of the chosen target genes were up-regulated at the mRNA level in antimiR-145 treated animals (Figure 5.17). Protein expression of Klf4, a previously validated target for miR-145, showed decreased expression in all hypoxia/SU4516 exposed animals. However, no dysregulation of Klf4 expression was observed between treatment groups (Figure 5.18).

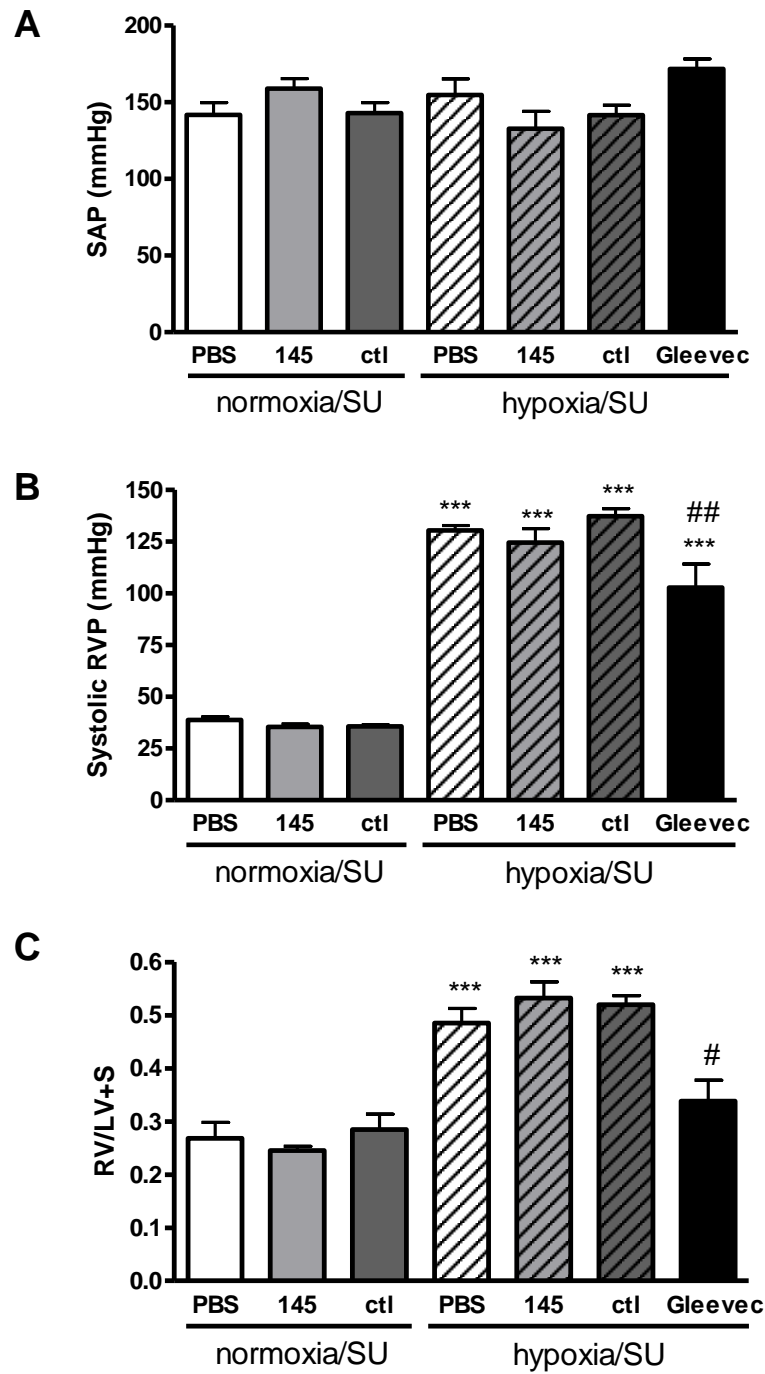


Figure 5.13 – Quantification of PH indices in therapeutic anti-miR-145 study.

Quantification of (A) SAP, (B) systolic RVP and (C) RVH in male rats from therapeutic study at day 35. Data represented as mean \pm SEM and analysed by one-way ANOVA followed by Tukey's post hoc test. $***p < 0.001$ vs normoxia/SU PBS, $\#p < 0.05$ and $##p < 0.01$ vs hypoxia/SU PBS, $n = 8-10$ animals per group for SAP and RVP ($n = 5$ animals for hypoxia/SU gleevec group), $n = 4-5$ animals per group for RVH. SU = SU5416, 145 = anti-miR-145, ctl = control anti-miR.

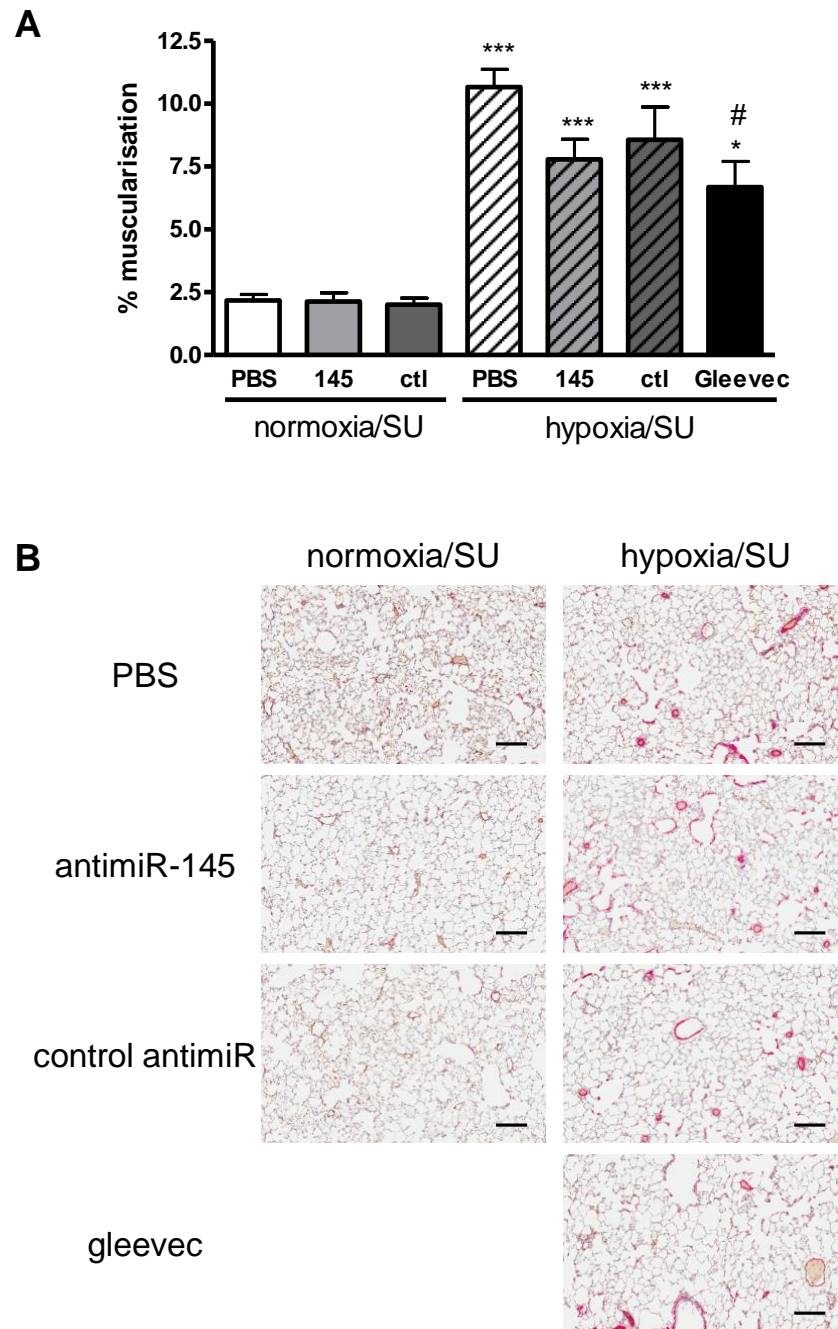


Figure 5.14 – Pulmonary remodelling in therapeutic antimiR-145 study.

(A) Quantification of pulmonary vascular remodelling in male rats from therapeutic study at day 35. Data expressed as mean \pm SEM and analysed by one-way ANOVA followed by Tukey's post hoc test. * $p < 0.05$, *** $p < 0.001$ vs normoxia/SU PBS and # $p < 0.05$ vs hypoxia/SU PBS, $n = 10$ animals per group ($n = 5$ animals for hypoxia/SU gleevec group). (B) Representative images of lung sections stained with α -SMA (red) and von Willebrand Factor (brown), magnification X8, scale bar = 200 μm . SU = SU5416, 145 = antimiR-145, ctl = control antimiR.

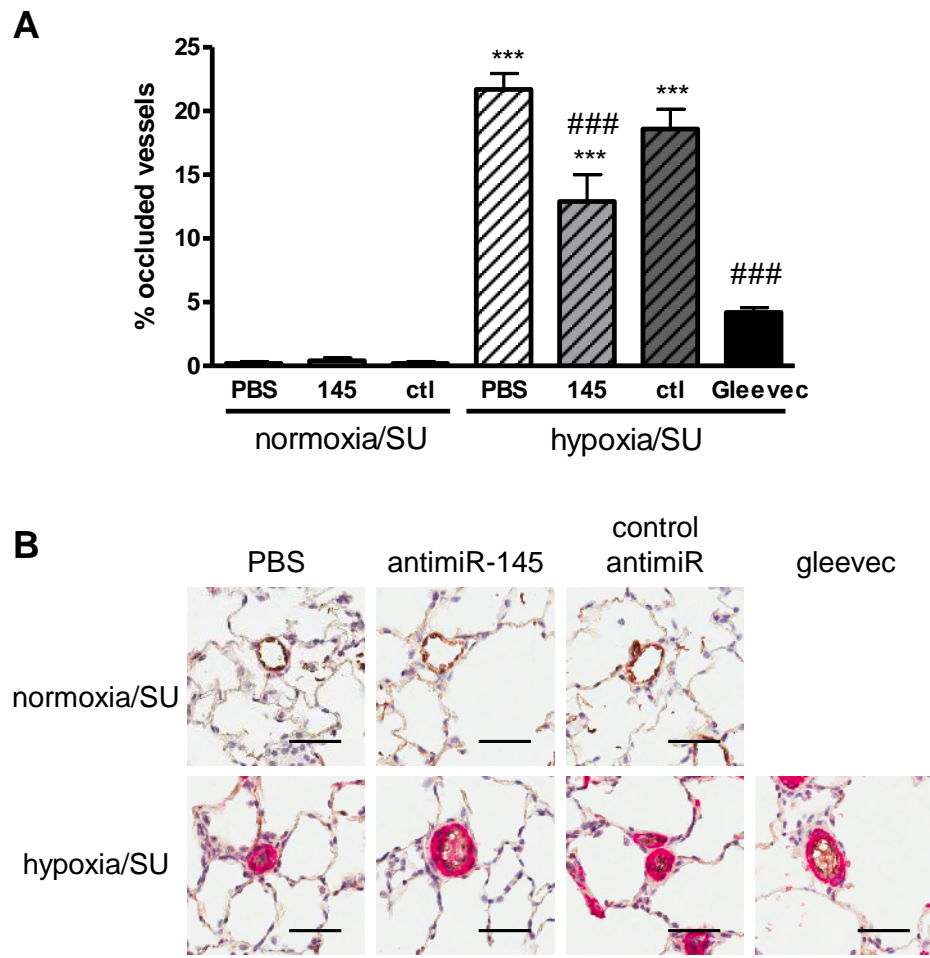


Figure 5.15 – Pulmonary occluded vessel analysis in therapeutic anti-miR-145 study.

(A) Quantification of occluded vessels in male rats from therapeutic study at day 35. Data expressed as mean \pm SEM and analysed by one-way ANOVA followed by Tukey's post hoc test. *** $p < 0.001$ vs normoxia/SU PBS and ### $p < 0.001$ vs hypoxia/SU PBS, $n = 10$ animals per group ($n = 5$ animals for hypoxia/SU gleevec group). (B) Representative images of pulmonary vessels stained with α -SMA (red) and von Willebrand Factor (brown), magnification X8, scale bar = 50 μ m. SU = SU5416, 145 = anti-miR-145, ctl = control anti-miR.

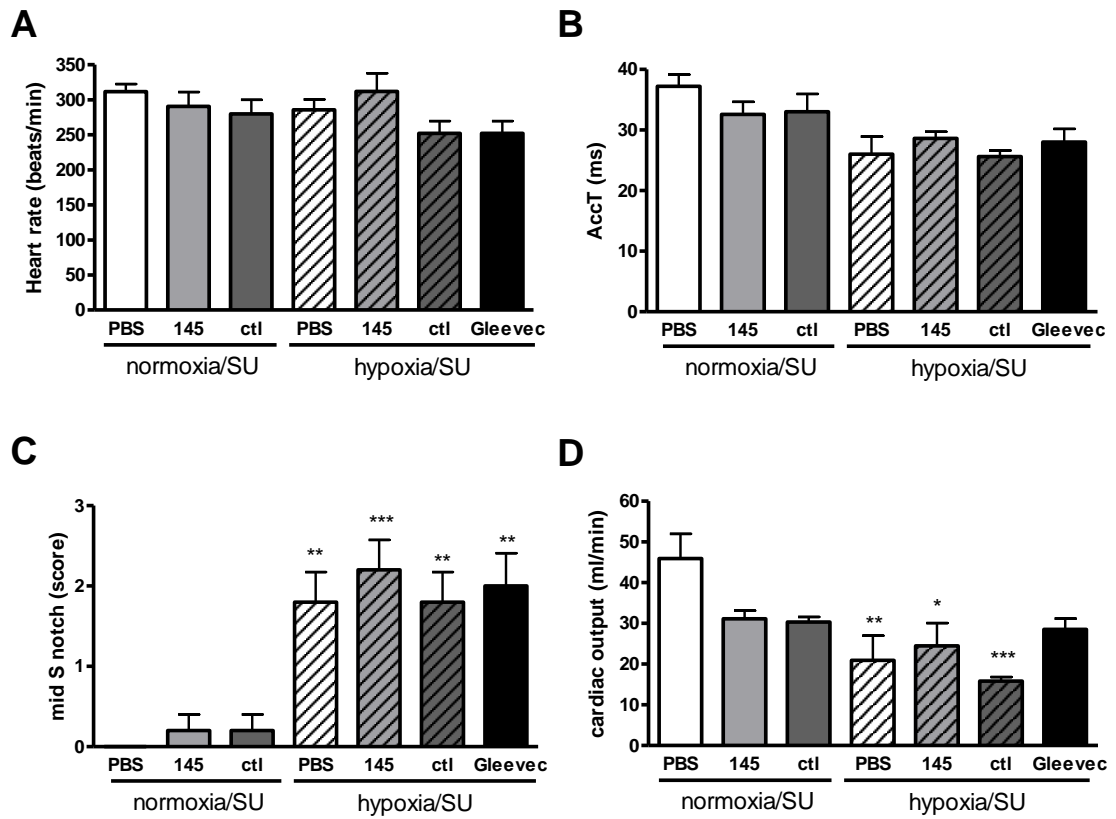


Figure 5.16 – Cardiac function parameters from therapeutic anti-miR-145 study.

Quantification of (A) heart rate, (B) pulmonary artery acceleration time (AccT), (C) mid systolic notch and (D) cardiac output calculated from echocardiography in male rats from therapeutic study at day 35. Data expressed as mean \pm SEM and analysed by one-way ANOVA followed by Tukey's post hoc test. * $p < 0.05$, ** $p < 0.01$ and *** $p < 0.001$ vs normoxia/SU PBS, $n = 5$ animals per group. SU = SU5416, 145 = anti-miR-145, ctl = control anti-miR.

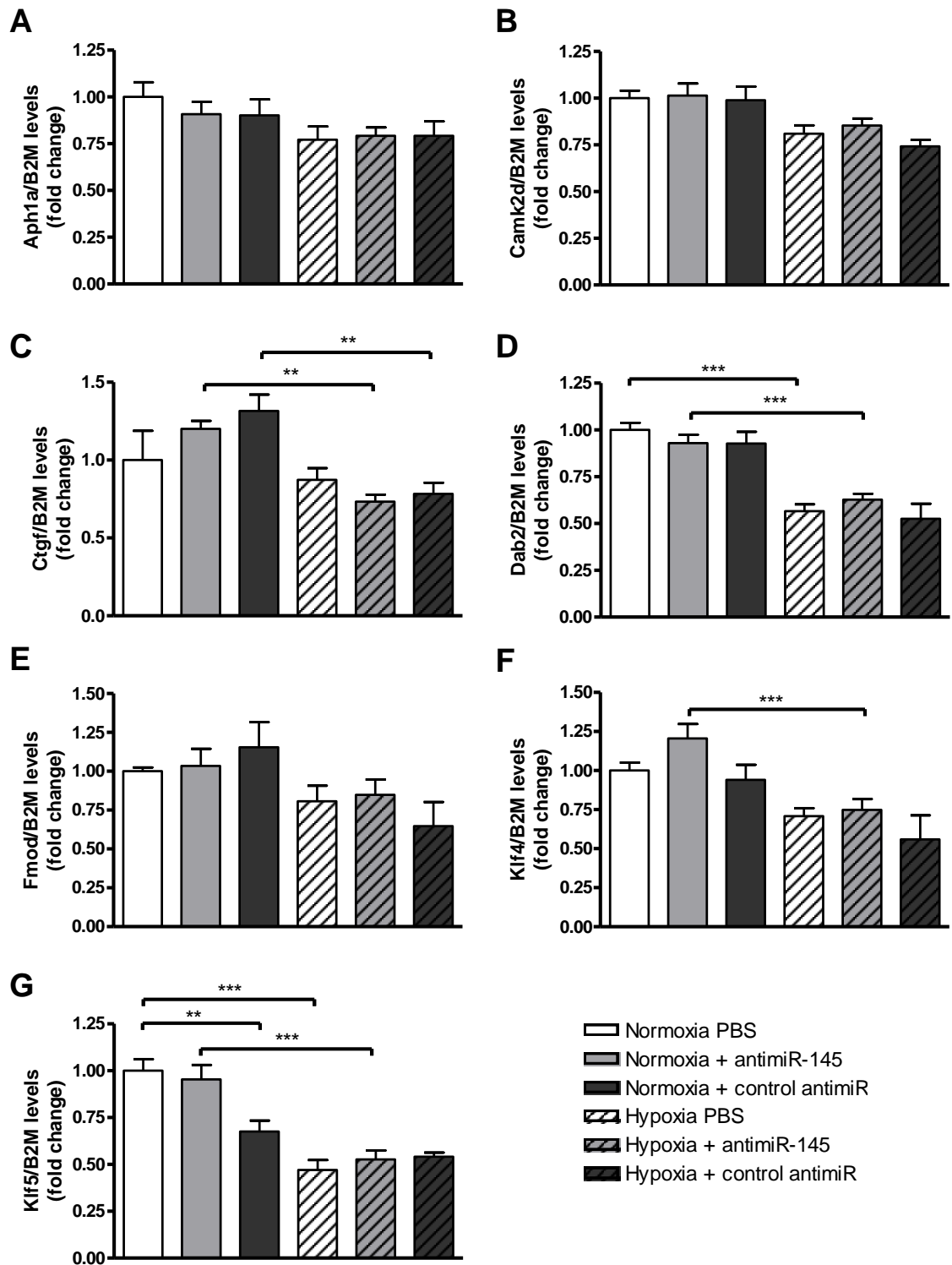


Figure 5.17 – Target gene mRNA expression from therapeutic anti-miR-145 study.

Target gene mRNA expression for (A) Aph1a, (B) Angptl4, (C) Camk2d, (D) Ctgf, (E) Dab2, (F) Fmod, (G) Kif4, (H) Kif5, (I) Megf6, (J) Myocd, (K) Sema3a, (L) Smad4, (M) Smad5, (N) Sned1 and (O) Tmod1. Analysis performed in whole lung from male rats from prophylactic study at day 35, as detected by qRT-PCR. Arbitrary value of 1 assigned to normoxia/SU PBS group. Data expressed as fold change \pm SEM and analysed by one-way ANOVA followed by Tukey's post hoc test. * $p < 0.05$, ** $p < 0.01$ and *** $p < 0.001$, $n = 8-10$ per group.

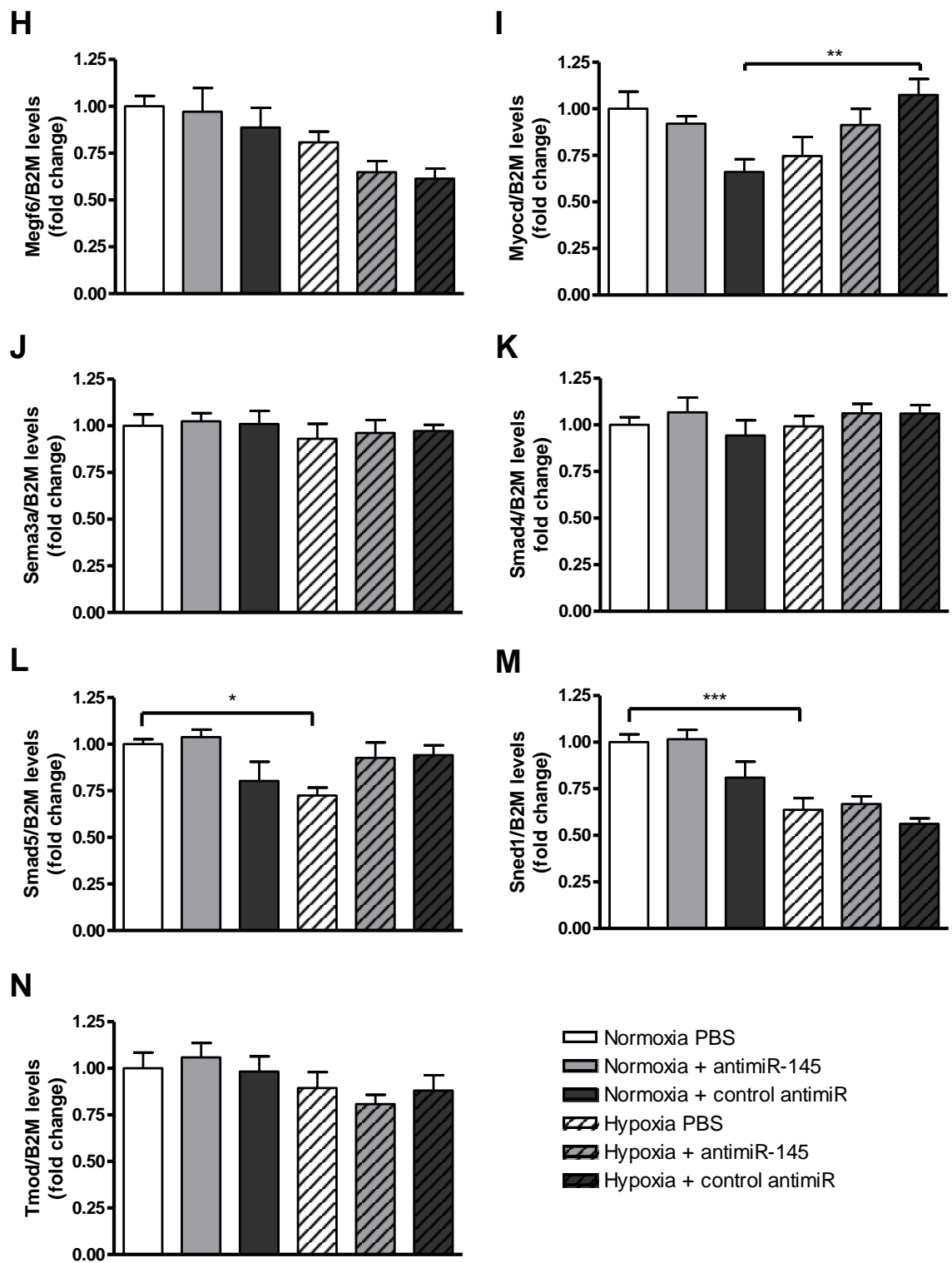


Figure 5.17 continued – Target gene mRNA expression from therapeutic anti-miR-145 study.

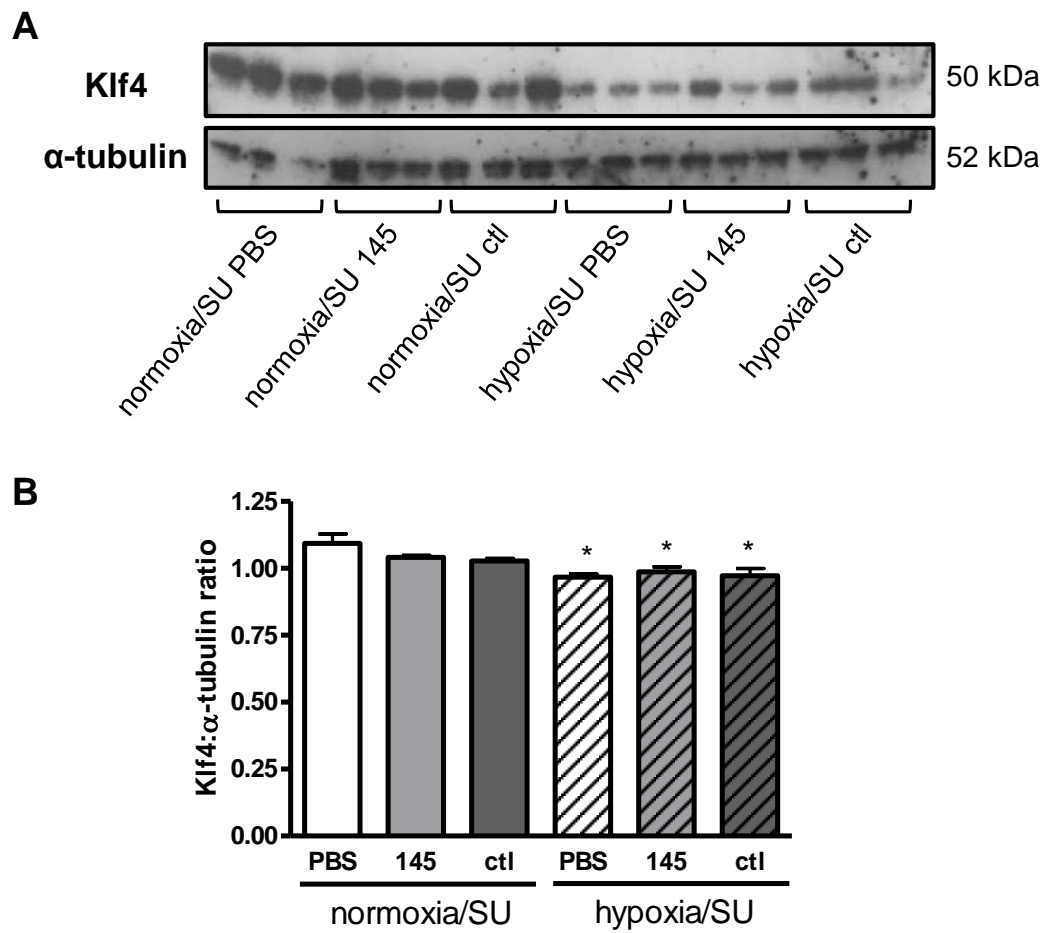


Figure 5.18 – Klf4 protein expression in lung from therapeutic antimiR-145 study.

(A) Western blot on protein extracted from whole lung from male rats from prophylactic study at day 35. (B) Quantification was performed by normalising Klf4 band intensity to the relative α -tubulin signal and expressed as mean \pm SEM, $n = 3$ animals per group. Data analysed by one-way ANOVA followed by Tukey's post hoc test, $*p < 0.05$ vs normoxia/SU PBS. SU = SU5416, 145 = antimiR-145, ctl = control antimiR.

5.2.7 Genetic ablation of miR-145 has no beneficial effect on the development of PH in male hypoxic mice

Previous work from our laboratory illustrated that genetic knockdown of miR-145 in female hypoxic mice was protective in the development of PH (Caruso et al., 2012). However, current work displayed within this chapter has shown that silencing miR-145 using an anti-miR-145 in male rats in the hypoxia/SU5416 model of PH has no beneficial effect, although this could be due to a number of reasons (see Discussion). To determine whether this difference could be due to gender differences, male miR-145 knockout mice were exposed to hypoxia for 14 days and assessed for PH parameters.

First, mice were analysed to ensure miR-145 expression was indeed silenced within the KO mice. Both northern blot analysis (Figure 5.19A, B) and qRT-PCR (Figure 5.19C) show complete loss of miR-145 expression within the lung. As stated previously, miR-145 is transcribed along with miR-143 and as a result, miR-143 expression was also quantified in the miR-145 KO mice (Figure 5.19D). MiR-143 expression was up-regulated in wild type mice exposed to hypoxia however, there was no difference in miR-143 expression between genotypes in normoxic or hypoxic conditions.

After 14 days hypoxic exposure, systemic arterial pressure was consistent across all groups (Figure 5.20A). MiR-145 WT mice showed the expected increase in RVP (Figure 5.20B), RVH (Figure 5.20C) and pulmonary remodelling (Figure 5.20D, E). This same pattern was observed in miR-145 KO mice, with significantly increased indices in hypoxic KO mice for RVP (Figure 5.20B) and RVH (Figure 5.20C) compared to normoxic KO mice. Remodelling analysis followed a similar pattern however, percentage remodelling in hypoxic miR-145 KO mice was not significantly different to that of hypoxic WT mice or normoxic miR-145 KO mice (Figure 5.20D, E).

Target gene analysis was performed on the lungs from miR-145 WT and KO mice after exposure to normoxic or hypoxic conditions for 14 days (Figure 5.21). Genes were chosen to study by searching the literature for validated targets of miR-145 in the mouse, along with using data generated from within our laboratory from previous mouse studies. Although several of the genes tested

were down-regulated in hypoxic conditions at the mRNA level (Klf4 - Figure 5.21C, Klf5 - Figure 5.21D), none of the target genes displayed the expected up-regulation in KO mice.

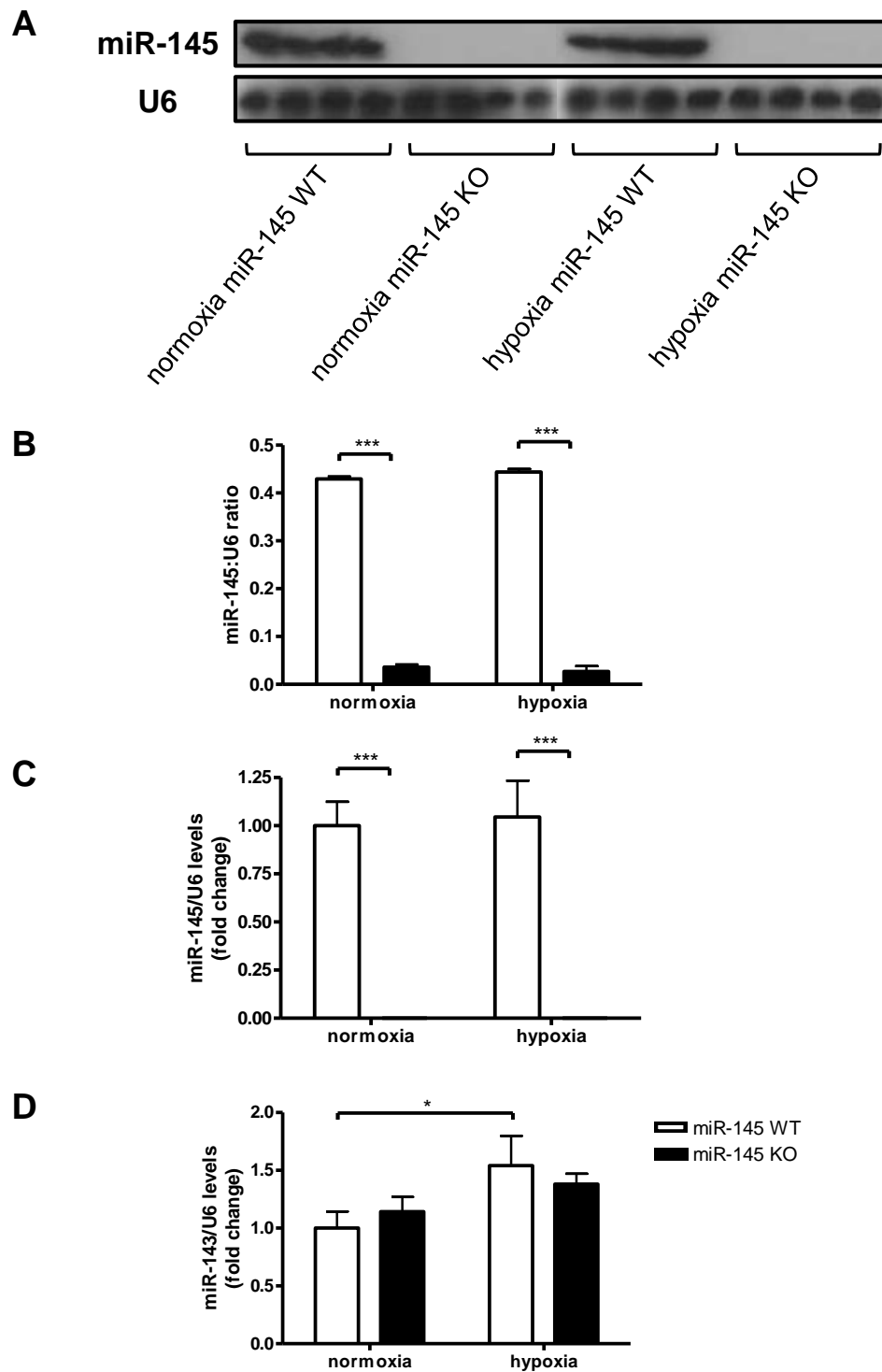


Figure 5.19 – MiR-145 and miR-143 expression in male miR-145 knockout mice.

(A) Northern blot was performed on RNA extracted from whole lung from male miR-145 wild type and knockout mice after 14 days exposure to normoxic or hypoxic conditions and quantified (B) by normalising the band intensity of miR-145 to the relative U6 signal. Data expressed as mean \pm SEM, $n = 4$ animals per group. (C) MiR-145 expression and (D) miR-143 expression detected within the same samples by qRT-PCR. Arbitrary value of 1 assigned to normoxic miR-145 wild type group. Data expressed as fold change \pm SEM, $n = 6$ animals per group. All data analysed by two-way ANOVA followed by Bonferroni post hoc test, $*p < 0.05$ and $***p < 0.001$. WT = wild type, KO = knockout.

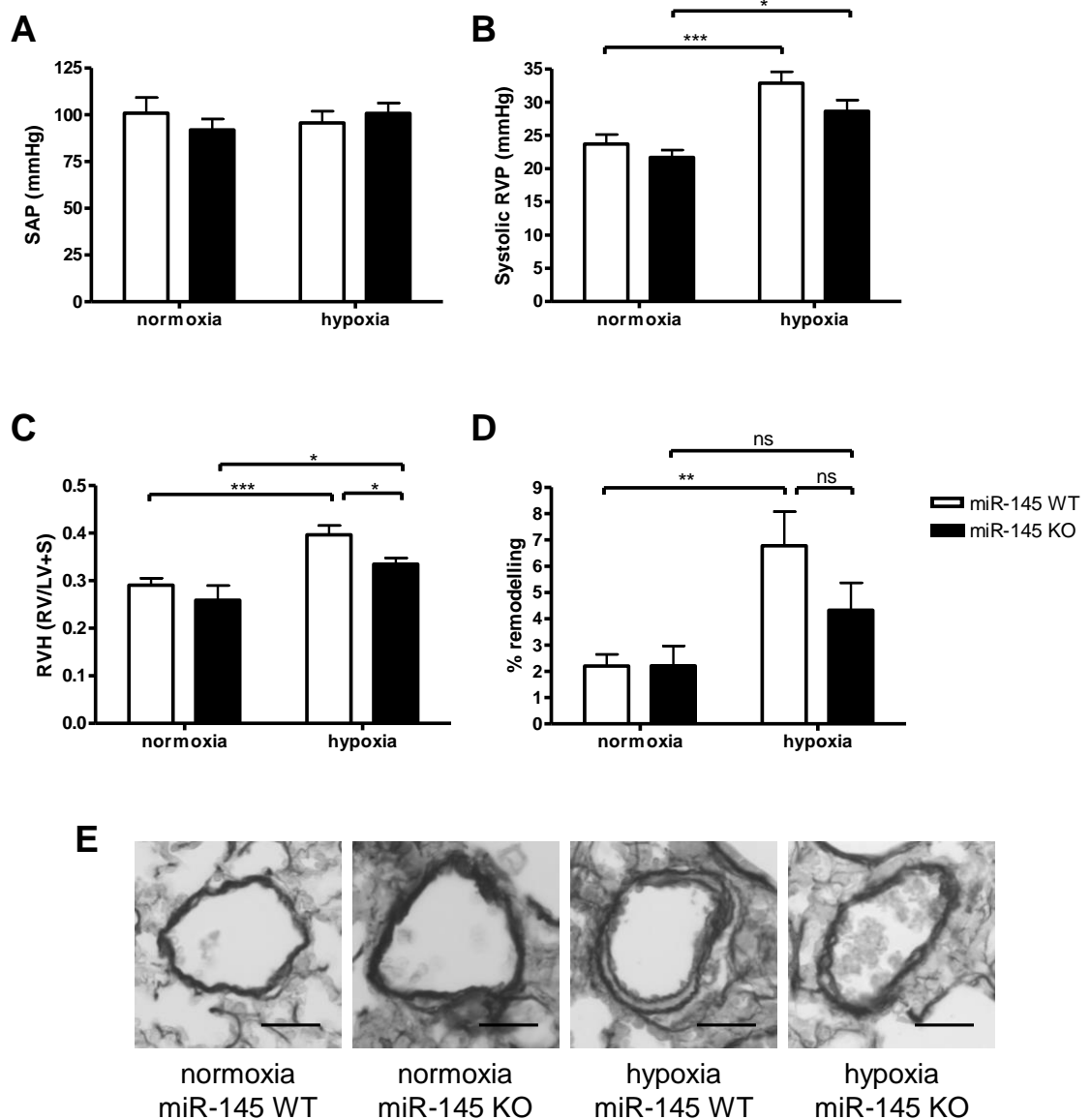


Figure 5.20 – Quantification of PH indices in male miR-145 knockout mice.

Quantification of (A) SAP, (B) systolic RVP, (C) RVH and (D) pulmonary vascular remodelling in male miR-145 wild type and knockout mice after 14 days exposure to normoxic or hypoxic conditions. (E) Representative images of pulmonary vessels stained with elastic van gieson, magnification X40, scale bar = 25 μ m. Data represented as mean \pm SEM and analysed by a two-way ANOVA followed by Bonferroni post hoc test. * $p < 0.05$, ** $p < 0.01$, *** $p < 0.001$ and ns = non-significant. For SAP, RVP and RVH, $n = 7-10$ animals per group, for pulmonary remodelling, $n = 7-8$ animals per group. WT = wild type, KO = knockout.

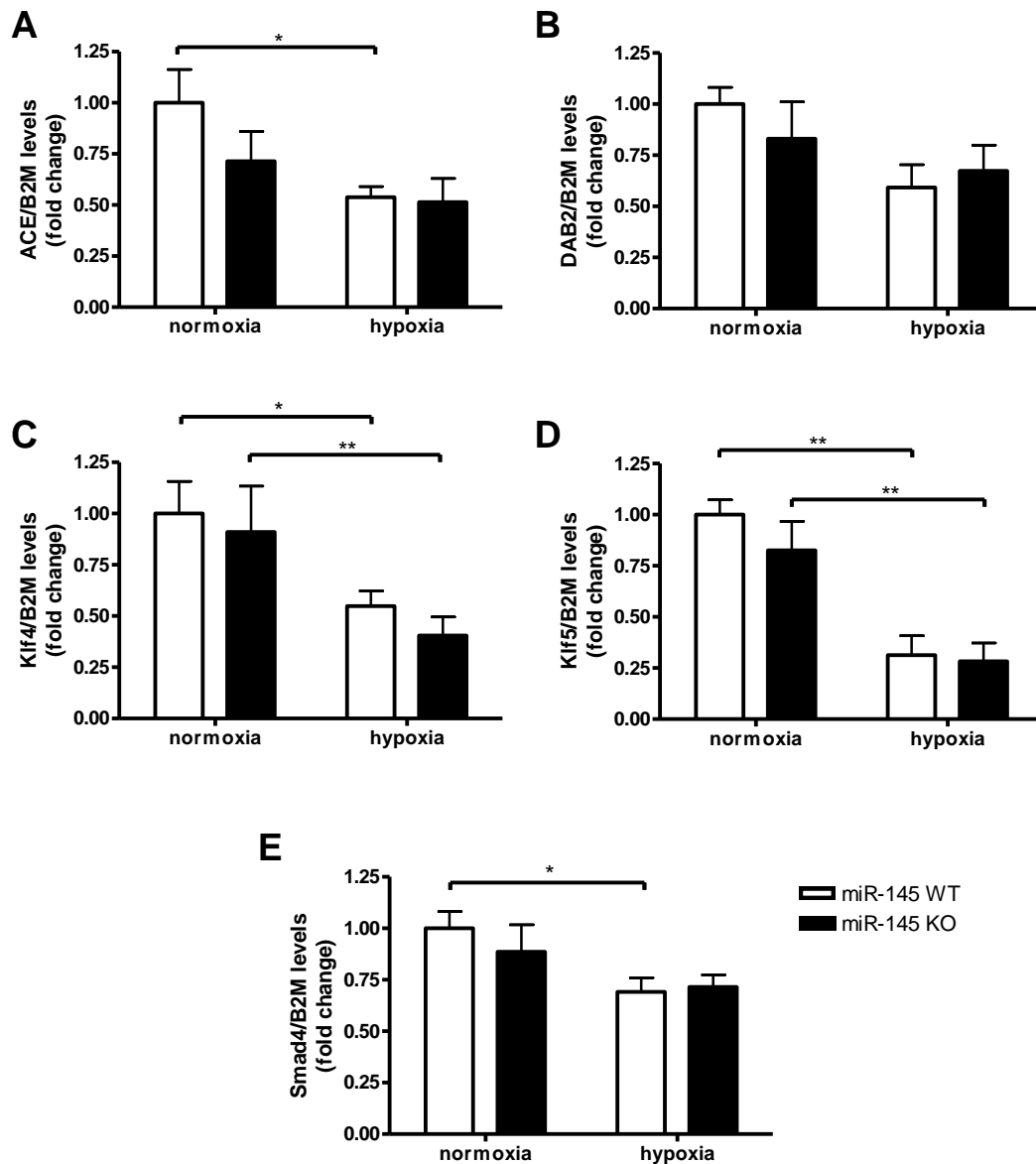


Figure 5.21 – Target gene mRNA expression in lung from male miR-145 knockout mice.

(A) ACE, (B) DAB2, (C) Klf4, (D) Klf5 and (E) Smad4 mRNA expression in whole lung from male miR-145 wild type and knockout mice after 14 days exposure to normoxic or hypoxic conditions, as detected by qRT-PCR. Arbitrary value of 1 assigned to normoxic miR-145 wild type group. Data represented as fold change \pm SEM and analysed by a two-way ANOVA followed by Bonferroni post hoc test. * $p < 0.05$ and ** $p < 0.01$, $n = 6$ animals per group. WT = wild type, KO = knockout.

5.2.8 *In vitro* analysis of miR-145 targets in hPASCs

Identification of genuine miRNA targets is a challenging task. Within this chapter, a list of candidate target genes for miR-145 was generated using target prediction algorithms TargetScan and miRWalk. These databases use specific criteria in order to determine whether mRNA sequences contain binding sites for miRNA. In order to predict miRNA targets, most computational algorithms require Watson-Crick base pairing of the miRNA seed sequence with a complementary sequence in the 3'-UTR of the mRNA, conservation of the binding site across species and also take into account the minimum free energy of the miRNA/mRNA duplex (Barbato et al., 2009, Yue et al., 2009). Original data proposed that binding of miRNA occurred selectively at the 3'UTR of target mRNA (Rajewsky, 2006) however, recent evidence has suggested that miRNAs can target sites in the 5'-UTR and in coding regions of mRNA (Lytle et al., 2007, Lee et al., 2009). As a result, target algorithms focusing exclusively on the 3'-UTR will exclude target genes where binding occurs in other regions. In addition, target prediction databases vary in criteria and small differences in criteria can produce diverse results, thus increasing the number of putative targets when several algorithms are used (Liu et al., 2012).

Consequently, an *in vitro* approach was adopted in an attempt to highlight novel miR-145 targets in biological samples. The miRNA pull down technique was used where hPASCs were transfected with biotinylated miR-145 or negative control miRNA mimic (Orom and Lund, 2007, Kang et al., 2012). RNA associated with the biotinylated miRNA mimic was isolated using streptavidin beads along with total 'input' RNA from total cell lysates (Figure 5.22). This experiment was performed twice with results kept separate in order to establish whether the same pattern of target gene expression was observed in both experiments. In order to ascertain whether the miR-145 mimic led to over-expression of miR-145, qRT-PCR was first performed on the input RNA samples (Figure 5.23A). Significant over-expression of miR-145 was produced in hPASCs transfected with 30 nM miR-145 mimic compared to cells transfected with control mimic in both experiments.

The next step was to assess target gene expression. It was expected that genuine target genes of miR-145 would be down-regulated in the input RNA

samples (due to repression by high miR-145 expression) and up-regulated in the bead extracted RNA samples (due to mimic being incorporated into the RISC, binding to the mRNA of target genes and therefore only target gene mRNA would be included in these samples). However, bead bound RNA samples were very low in concentration. Hence, qRT-PCR was performed in the first instance on the input RNA samples to assess whether the miRNA pull down technique was working effectively. Validated and predicted targets of miR-145 were chosen and quantified in input samples by qRT-PCR (Figure 5.23B-F). However, none of the chosen genes were down-regulated consistently across both experiments.

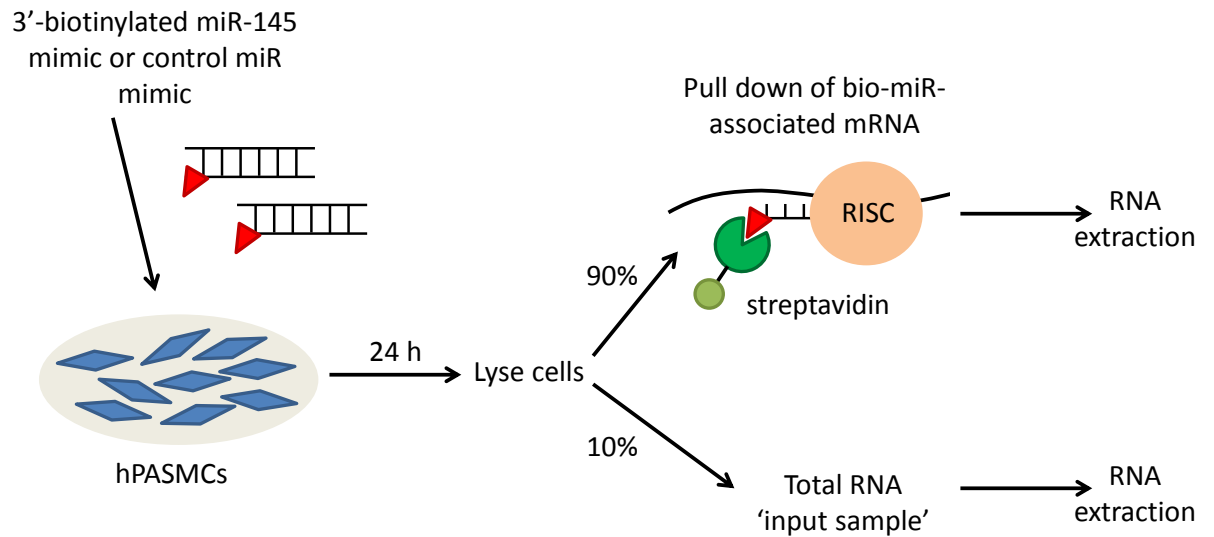


Figure 5.22 – Schematic diagram of miRNA pull down experimental set up.

hPASCs were transfected with 30 nM 3'-biotinylated miR-145 mimic or control mimic. Twenty four hours later, cells were lysed and 10% of cell lysates were removed and total 'input' RNA extracted. The remaining cell lysate was incubated with streptavidin coated magnetic beads to isolate mRNA associated with the biotinylated miRNA mimic, followed by RNA extraction.

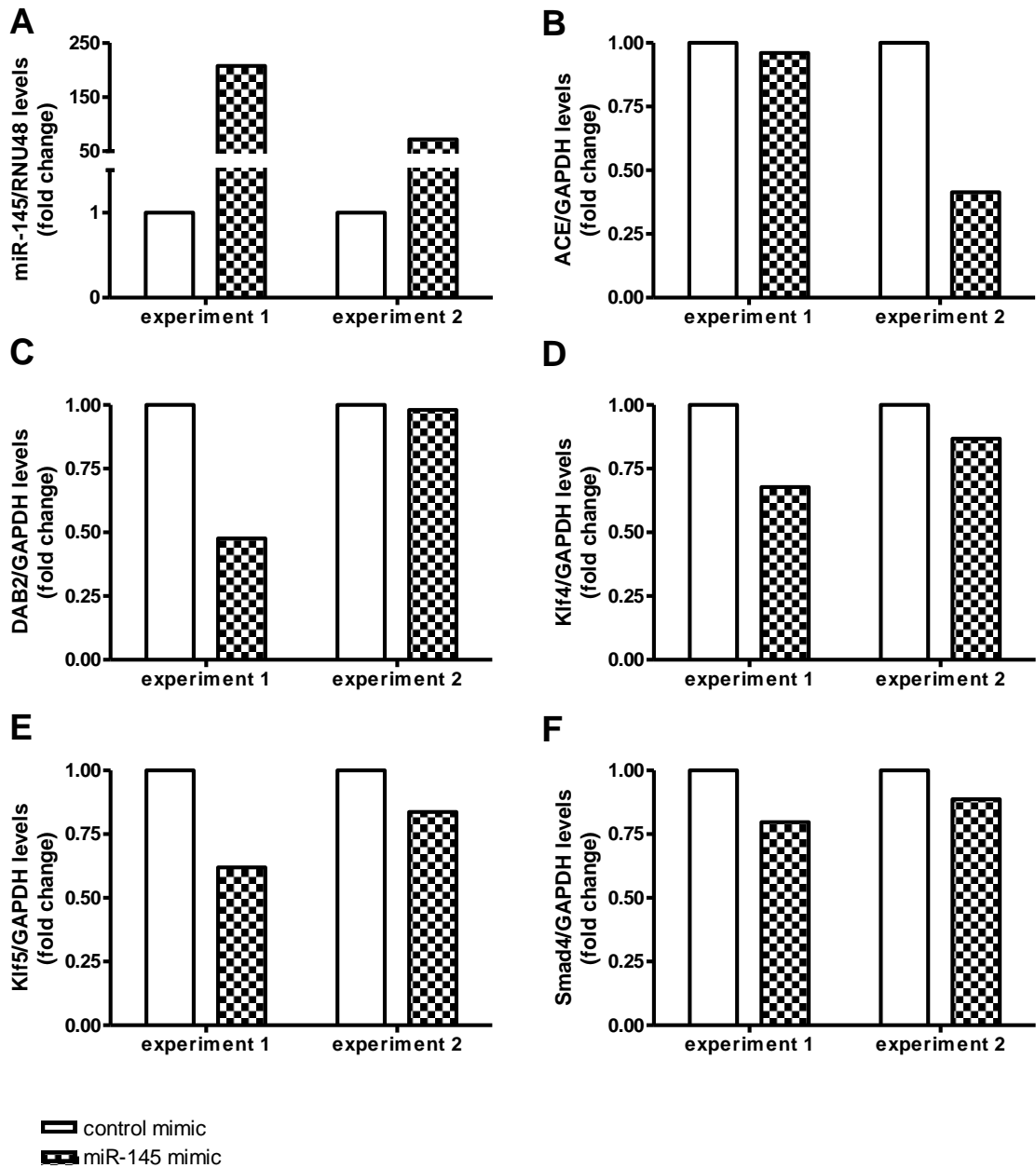


Figure 5.23 – MiR-145 and target gene mRNA expression in hPASMCs transfected with miR-145 mimic in miRNA pull-down assay.

(A) MiR-145 expression in input samples from hPASMCs transfected with 30 nM biotinylated miR-145 mimic or control mimic in miRNA pull-down assay, as detected by qRT-PCR. Target gene (B) ACE, (C) DAB2, (D) Klf4, (E) Klf5 and (F) Smad4 mRNA expression in the same input samples, as detected by qRT-PCR. Arbitrary value of 1 assigned to control mimic for each gene or miRNA in each experiment. Data expressed as fold change \pm SEM and analysed by unpaired t-test. Experiment performed twice with differing passages of hPASMCs, results for separate experiments shown.

5.3 Discussion

In this chapter we have assessed the effect of silencing miR-145 prior to the development of PH and in animals with established PH. In both the prophylactic and therapeutic study, knocking down miR-145 using an antimiR had no beneficial effect on RVP, RVH or muscularisation of pulmonary vessels in male rats exposed to hypoxia/SU5416. There was however a significant reduction in the percentage of occluded vessels in hypoxia/SU5416 animals therapeutically treated with antimiR-145. In addition, pre-treatment with antimiR-145 had beneficial cardiac effects by reducing the mid systolic notch to a similar extent as the positive control gleevec. Although antimiR-145 treatment resulted in knock down of miR-145 levels in the lung, target analysis by both qRT-PCR and western blot showed no de-repression of potential miR-145 target genes.

The reduction in occluded vessels observed in the antimiR-145 treated hypoxia/SU5416 rats in the therapeutic study is potentially very interesting as this result was not observed in the prophylactic study. MiRNAs are expressed at varying levels throughout disease development and targeting miR-145 after the disease is established appears to have more of a protective effect than silencing it prior to disease onset. The results displayed in section 4.2.3 show that miR-145 is significantly up-regulated in male rats exposed to hypoxia/SU5416 only at 3 weeks (2 weeks hypoxia/SU5416 followed by one week in normoxia) compared to normoxia/SU5416 treated rats. It may be the case that administration of antimiR-145 after hypoxia/SU5416 insult has a greater effect due to the increased expression of miR-145 shortly following hypoxia/SU5416 exposure, while silencing miR-145 in a preventative manner may allow other mechanisms to take over and thus the disease develops as normal. Further work is required to pinpoint what is happening during the reversal study and the exact mechanisms through which antimiR-145 is producing this positive effect on the pulmonary vessels.

Many different molecules and pathways are involved in the progression from pulmonary remodelling to vessel occlusion (Cool et al., 1999). Analysis of the expression of some of these molecules (e.g. nitric oxide, thromboxane A₂, serotonin, ET-1) via immunohistochemistry on lung sections from the therapeutic study may provide an indication as to which pathways are involved in the

reduced vessel occlusion in anti-miR-145 treated animals. The role of miR-145 should also be investigated in PAECs, as these cells represent the difference between the pulmonary vessels with increased SMC proliferation and hypertrophy and the obstructed vessels with endothelial cell dysfunction. *In vitro* studies in PAECs investigating the role of miR-145 on apoptosis, migration and proliferation would further our understanding of this miRNA and how it can contribute to vessel occlusion.

Cardiac parameters analysed by echocardiography were largely unchanged with anti-miR-145 treatment compared to PBS and control anti-miR treatment. However, the mid systolic notch was significantly reduced in hypoxia/SU5416 rats pre-treated with anti-miR-145 compared to hypoxia/SU5416 PBS treated rats. The reduction in mid systolic notch follows the same pattern as that observed in hypoxia/SU5416 rats dosed with gleevec. Similarly, in the therapeutic study, hypoxia/SU5416 anti-miR-145 rats had a similar mid systolic notch score as that of hypoxia/SU5416 gleevec animals, although both treatments failed to illicit any effect compared to PBS control animals. The mid systolic notch measures the degree of indent through deceleration pulmonary flow and is specific for pulmonary hypertension (Ginghina et al., 2009, Roberts and Forfia, 2011). It is interesting that treatment with anti-miR-145 appears to be following the same trend as gleevec treatment, the positive control used due to previous data showing gleevec to reduce experimental pulmonary hypertension (Schermyly et al., 2005, Abe et al., 2011). It may be the case that anti-miR-145 and gleevec share a common target which is involved in the cardiac response. In particular, a beneficial effect was only observed in both treatment groups in the prophylactic study. The difference in results between the prophylactic and therapeutic study may once again be due to activation of different pathways depending on the stage at which miR-145 was silenced.

There are several reasons which may explain why we did not observe a beneficial effect on the pulmonary pressures and vessels in the anti-miR-145 treated hypoxia/SU5416 rats in the prophylactic study and in the majority of parameters in the therapeutic study. There is significant knockdown of miR-145 expression however no modulation of miR-145 target genes was observed. Thus suggesting that the anti-miR is not working functionally within the lung

compartment and may be targeting a different area. Another reason may be due to the localisation of miR-145 within the lung and pulmonary vasculature. VEGFR2 is mainly expressed in endothelial cells and signalling through this receptor plays an important role in regulating endothelial cell maintenance and function (Lee et al., 2007). As a result, the hypoxia/SU5416 model of PH is largely characterised by endothelial dysfunction. MiR-145 on the other hand is predominantly expressed within the smooth muscle cell (Xin et al., 2009, Boettger et al., 2009, Cordes et al., 2009). Therefore silencing of a miRNA outside of the endothelial compartment may not be enough to prevent or reverse the disease in this model of PH. Recent work by Hergenreider and colleagues (Hergenreider et al., 2012) found that HUVECs stimulated by shear stress released extracellular vesicles with increased miR-143/miR-145 levels which could control the expression of target genes in co-cultured SMCs. This innovative study highlights the interaction between cell types however, it is unclear whether silencing miRNAs expressed primarily within one compartment as in the context of this study can result in the effects being observed in neighbouring cell types.

A third reason for lack of effect of anti-miR-145 treatment may be due to the fact that we are not detecting an increase in miR-145 expression as had previously been reported in the development of experimental PH and in lungs from PAH patients (Caruso et al., 2012, Courboulin et al., 2011). The fact that there is no increase in miR-145 levels between normoxia/SU5416 and hypoxia/SU5416 control animals may give an indication as to why inhibiting miR-145 had no beneficial effect on PH development. Nevertheless, the fact that miR-145 does not change between experimental conditions does not imply that the pathways involved with this miRNA are not good targets to focus on. In addition, two further issues which may contribute to the results obtained are gender and species specific. The original study performed in our laboratory which showed that knockdown of miR-145 was protective against the development of PH was performed in female mice (Caruso et al., 2012). However, the current study was carried out in male rats. Thus species or gender may explain why we are not observing a protective effect in this study with anti-miR-145 treatment.

In order to assess whether gender differences accounted for variation in results, male miR-145 WT and KO mice were exposed to normoxic or hypoxic conditions and indices of PH were assessed. Hypoxic miR-145 KO mice showed the same pattern as hypoxic WT mice with increased RVP and RVH compared to normoxic mice. Pulmonary remodelling analysis indicates that miR-145 KO mice exposed to hypoxia show a reduction in remodelling compared to WT hypoxic mice however this does not reach significance. From these results, it appears that male miR-145 KO mice are not protected against developing PH as the female miR-145 KO mice are. Thus demonstrating that the effects of silencing miR-145 *in vivo* are potentially gender specific and warrant further investigation. As in the hypoxia/SU5416 study, we did not observe an up-regulation of miR-145 in the lung of male WT mice exposed to hypoxia. Caruso and colleagues found that female hypoxic WT mice had significantly higher expression levels of miR-145 in the lung compared to normoxic WT mice (Caruso et al., 2012). This illustrates that within the lung, miR-145 expression is regulated differently between the sexes in response to hypoxic stimuli.

There has been much controversy surrounding the role of miRNAs in PAH and conflicting results have been obtained from *in vivo* experiments regarding the function of miR-145 in PH. A recent study (McLendon et al., 2013) observed a reduction in RVP in a reversal study of PH using the hypoxia/SU5416 model. Inhibition of miR-145 was achieved using intravenous injection with the oligonucleotide complexed with staramine, a lipopolyamine designed to enhance retention within the lung. However, inhalation of the miR-145 inhibitor/staramine complex did not improve PH in the same model (McLendon et al., 2013). From the same research group, studies have also found administration of antimiR-145 reversed hypoxia/SU5416 induced vascular remodelling including occlusive lesions and medial hypertrophy (Joshi et al., 2013). Taken together with the data presented in this chapter, the method used to knockdown miR-145 and administration route appears to be very important in exerting a protective effect in the development of PH.

The model used to investigate experimental PH is also an important factor which must be taken into consideration. The hypoxia/SU5416 model produces a plexogenic arteriopathy which is similar to the lesions formed in human PAH.

However, caution must be taken when using the hypoxia/SU5416 model as VEGF and VEGFR2 expression are known to be increased in PAH (Taraseviciene-Stewart et al., 2001). Therefore blockade of VEGFR2 via SU5416 may interfere with specific miRNA pathways and influence the result, irrespective of PH development. Numerous miRNAs have been reported to regulate the VEGF signalling pathway. MiR-93 and miR-200b directly target VEGF to reduce VEGF expression (Long et al., 2010, McArthur et al., 2011). Also, VEGF stimulation promotes the expression of miR-16 and miR-424 which then go on to target VEGF in a negative feedback loop thereby providing a high level of regulation (Chamorro-Jorganes et al., 2011). MiRNAs also target downstream effectors of VEGF, including phosphoinositide-3-kinase (PI3K) and MAPK/ERK (Dang et al., 2013). Inhibition of VEGF signalling via SU5416 may alter downstream signalling pathways, thus making it hard to identify target genes which are modulated by disease development or miRNA treatment as opposed to VEGF inhibition.

Target gene analysis of the miR-145 WT and KO mice using predicted and previously validated target genes did not show any dysregulation of genes in KO mice. Although Klf4 and Klf5 are down-regulated in response to hypoxia, none of the chosen genes showed the expected increase in expression in miR-145 KO mice. Compensatory mechanisms may in part explain this result. As stated previously, each gene can be regulated by many different miRNAs (Doench and Sharp, 2004). Genetic deletion of miR-145 may therefore cause other miRNAs or molecules to take over the role of miR-145. As a result, the expression of target genes is similar between the miR-145 WT and KO mice. This is in contrast to the results obtained in female miR-145 KO mice exposed to hypoxia. Caruso and colleagues (Caruso et al., 2012) found that Ctgf, Dab2, Angptl4 and Klf5 mRNA expression were up-regulated in the lung of female hypoxic KO mice and Smad4 and Smad5 were found to be up-regulated in female normoxic KO mice. In addition, Klf4 was up-regulated in female miR-145 KO mice at both the mRNA and protein level (Caruso et al., 2012). These results illustrate that there are clear differences in target gene expression between male and female mice in response to hypoxic exposure. Within this chapter, mRNA expression analysis has been used to determine gene expression. However, target gene analysis at the protein level is highly relevant as it is the protein molecules which can directly affect the PH phenotype. Furthermore, there is often a mismatch between

mRNA and protein levels (Selbach et al., 2008, Baek et al., 2008, Guo et al., 2010) and therefore analysing the protein level would allow any functional changes to be detected.

In vitro investigations into target genes of miR-145 were undertaken in hPASCs to establish novel targets. MiRNA pull down experiments were performed (Orom and Lund, 2007, Kang et al., 2012) and transfection with biotinylated miR-145 mimics resulted in significant over-expression of miR-145. The ultimate goal of this experiment was to perform a microarray with the RNA samples bound to the beads to identify genes which were up-regulated in the miR-145 mimic group compared to the negative control transfection group. However, RNA concentrations for the bead samples were extremely low and therefore input samples were analysed as a control to examine whether validated targets for miR-145 were down-regulated and hence show that the experimental set up was working correctly. Unfortunately none of the genes from the input samples were dysregulated by miR-145 mimic treatment across both repeats of the experiment. As a result, the microarray was not performed on the bead samples as it was unclear whether the transfection and experimental procedure had been successful.

There could be a number of possibilities to explain why miR-145 validated genes were not modulated in the hPASCs transfected with miR-145 mimic. Firstly, the synthetic mimic was modified with the addition of a biotin group at the 3'-end of the miRNA and although significant over-expression of miR-145 was obtained, the modification of the mimic may prevent full incorporation within RISC. Therefore when binding of the biotin labelled mimic was performed with streptavidin beads, it could simply be the mimic that is being extracted as opposed to the miRNA mimic bound to target genes via the RISC.

Another reason to explain the results obtained here could be due to the fact that basal expression of miR-145 is very high in hPASC. In this situation, RISC may be saturated with endogenous miR-145 and therefore biotinylated miR mimic is not incorporated into the complex. Consequently the miR mimic is free in the cell and when extracted with streptavidin beads, the miR mimic is not bound to anything within the cell. One way to overcome this problem would be to perform a double miRNA pull down. This involves transfecting cells with biotinylated miR-

145 mimic as in this study and then performing immunoprecipitation using an antibody against the Argonaute protein, the catalytically active component of RISC. Following this, streptavidin pull down binds specifically the miRNA mimic and then RNA extraction is carried out (Nonne et al., 2010). This two-step procedure would provide confidence that the RNA extracted was physically bound to the biotinylated miR-145 mimic/RISC complex and thus would contain direct targets for miR-145. Once again however, there are problems with this technique. Results may differ depending on the antibody used to immunoprecipitate the argonaute protein as it has been reported that AGO1 and AGO2 form RISC complexes with different miRNAs (Thomas et al., 2010). Moreover, the RNA extracted from the single pull down experiment is exceedingly low in concentration and thus with the additional AGO purification step in the two-step method, yields will be even lower. Thus the experiment would have to be extensively scaled up in order to obtain a high enough yield of pull down RNA in order to perform a screen for gene targets (e.g. a microarray) and validate the results using qRT-PCR. This would make the experiment very expensive to execute in primary cells and therefore may be more suited to cell line studies.

In summary, silencing of miR-145 using an antimiR *in vivo* both pre- and post-PH development does not provide a beneficial effect in the male rat hypoxia/SU5416 model, in the experimental settings described here. In addition, male miR-145 KO mice are not protected against the development of PH as the female miR-145 KO mice are. The results from these experiments suggest that there are complex mechanisms regulating miRNA processing within the lung during PH development and these pathways may be gender specific. Further *in vitro* investigations are required to identify novel genuine miR-145 target genes in the setting of PH and enhance our understanding of the many pathways involving miRNAs in PH development.

6 General Discussion

This thesis has concentrated on identifying the role of miRNAs during the development of PAH. MiRNAs are expressed at varying levels throughout the body in a tissue and cell specific manner, with dysregulation of miRNA expression observed during disease. Previous work within our laboratory identified several miRNAs which were modulated during the development of PAH, identifying possible therapeutic targets. This study has particularly focused on two of these miRNAs, miR-451 and miR-145, to establish the role of these miRNAs during disease progression as well as investigating the miRNA profile in pulmonary and cardiac tissue from the hypoxia/SU5416 model of PH.

MiR-451 expression has previously been reported to be up-regulated in experimental models of PH and in this study, miR-451 over-expression promoted the migration of hPASMCs in the absence of serum. Transient knockdown of miR-451 attenuated the development of PH in hypoxic rats while genetic deletion of miR-451 had no beneficial effect on the development of PH. Focussing on miR-145, another miRNA which is up-regulated during PH, prophylactic and therapeutic silencing of miR-145 in the rat hypoxia/SU5416 model demonstrated no protective effect on RVP, RVH or muscularisation of pulmonary arteries. There was however a significant reduction in the number of occluded vessels in rats with established PH treated with anti-miR-145. In addition, male miR-145 knockout mice are not protected against the development of PH as female miR-145 knockout mice are. Cardiac analysis from the hypoxia/SU5416 model of PH displayed up-regulation of miR-27a and miR-27b selectively in the right ventricle of mice and rats, respectively.

In vitro modulation of miR-451 showed that miR-451 promotes migration of hPASMCs in the absence of serum but has no effect on cellular proliferation. In this cell culture model, the focus has been on hPASMCs due to their highly proliferative and migratory response to PH stimuli (Rabinovitch, 2012, Gerthoffer, 2007). There is also a significant increase in muscularisation of small pulmonary arteries leading to remodelling of the vessels in PH patients and animals (Stenmark et al., 2009), highlighting the importance of PASMCs in the remodelling process. In addition to this, it would be of interest to assess the function of miR-451 in hPAECs as ECs also play a critical part in the cellular response to PH. Moreover, ECs are the principle cell type involved in the

formation of plexiform lesions. Investigation into the molecular basis of these lesions and the interactions between the ECs and SMCs will give us a better understanding of the processes which contribute to vessel remodelling and occlusion. Another aspect which should be explored is the effect of modulating miR-451 on apoptosis in both hPAECs and hPASMCs. Recent studies have shown that miR-451 regulates apoptosis in different systems. In NSCLC cells, miR-451 induces apoptosis by targeting RAB14 which inhibits Akt phosphorylation, increasing Bax or Bad protein levels and activating caspase 3 (Wang et al., 2011). Similarly, miR-451 promotes apoptosis in human glioblastoma cells by down-regulating the anti-apoptotic Bcl2 (Nan et al., 2010) and over-expression of miR-451 in breast cancer cells down-regulates survival factor 14-3-3 ζ to trigger apoptosis (Bergamaschi and Katzenellenbogen, 2012). This therefore suggests that miR-451 is highly involved in regulating apoptosis in numerous cell types and it would be interesting to determine if miR-451 also controls apoptosis in pulmonary cells by analysing apoptotic markers and apoptotic staining (e.g. TUNEL or caspase staining). It is unclear where miR-451 is expressed in the pulmonary vasculature other than in the red blood cells. Therefore *in situ* hybridisation would allow localisation of miR-451 within the lung and indicate a specific cell type to focus on.

The effects of knocking down miR-451 levels *in vivo* were investigated using both an antimiR and a genetic knockout approach. AntimiR-451 administration to male rats three days prior to hypoxic exposure attenuates the development of experimental PH, with a reduction in systolic RVP. The observed effect may be more pronounced if hypoxic exposure is extended to 14 or 21 days. Similarly, this result should be validated in another model of PH, for example monocrotaline-induced PH or the hypoxia/SU5416 model. If comparable results are obtained in a second model, this would validate that miR-451 inhibition conveys a protective role in the development of experimental PH. This was in contrast to miR-451 global knockout mice, where knockout mice displayed the same phenotype as wild type mice in response to hypoxic exposure. This may be due to a number of variables, such as gender, species, method used for silencing miR-451 and compensatory mechanisms which may have been active in the miR-451 knockout mice. Further investigations are required to determine which factors are responsible for the differences obtained between the two studies.

Results from this thesis, along with previous studies carried out in our laboratory demonstrate that miRNA modulation acts in a gender-specific manner. Male miR-145 knockout mice developed the same hypoxia-induced PH phenotype as wild type mice with comparable RVP and RVH values. This is in contrast to female miR-145 knockout mice which are protected against developing hypoxia-induced PH (Caruso et al., 2012). At the clinical level, PAH is a disease with gender bias with more females developing the disease (Walker et al., 2006). In contrast, experimental models of PH have shown that females develop less severe disease. This is thought to be due to the protective effect of the sex hormone oestrogen as following ovariectomy, female mice develop exacerbated RVH in response to MCT insult and this can be reversed with estradiol administration (Ahn et al., 2003). This contradiction between clinical and animal studies is known as the oestrogen paradox of PAH. The results reported here illustrate that miRNAs are regulated in distinct ways between the sexes in response to hypoxia and studies have shown that oestrogen can directly regulate miRNAs (Ferraro et al., 2012). Understanding the differences between the genders (and indeed the differences between clinical and animal studies) and the role of sex hormones on miRNA expression within the pulmonary circulation is essential if miRNAs are to be used as therapeutic targets. Gender must therefore be carefully considered when future studies are planned.

Another miRNA which had previously been shown to be up-regulated in PAH patients and experimental models of PH was miR-145 (Caruso et al., 2012, Courboulin et al., 2011), with antimiR-145 administration providing protection against hypoxia-induced PH in mice (Caruso et al., 2012). Silencing of miR-145 prior to and post hypoxia/SU5416 exposure followed by three weeks in normoxic conditions produced no beneficial effect on RVP, RVH or muscularisation of small pulmonary arteries. The percentage of occluded vessels was however reduced in the reversal study suggesting a role for miR-145 in the progression of occlusive lesions. The exact mechanisms through which miR-145 exerts an effect could be further investigated through *in vitro* studies focusing on hPASCs and hPAECs with over-expression or inhibition of miR-145. The lesions formed in the hypoxia/SU5416 model of PH are characterised by endothelial dysfunction with initial EC apoptosis, followed by proliferation of an apoptosis-resistant population of endothelial cells (Taraseviciene-Stewart et al., 2001). However,

miR-145 is predominantly expressed within smooth muscle cells therefore investigating the cross talk between these two cells types will be critical in understanding the role of miR-145 in the development of PH. The hypoxia/SU5416 model of PH can be modelled *in vitro* using an artificial capillary system where VEGF blockade is accompanied by high shear stress (Sakao et al., 2005). Analysis of apoptosis and proliferation rates in this cell culture model in the presence of miR-145 modulation would indicate in what way miR-145 is having a positive effect on the occluded vessels in the therapeutic study.

From a clinical point of view, miRNAs have the potential to be used as biomarkers for disease as well as a candidate treatment for PAH. Biomarkers are measured as an indicator of normal or pathogenic processes and recent studies have identified miR-150 as a possible biomarker for PAH. Rhodes and colleagues observed that miR-150 expression is down-regulated in plasma and circulating microvesicles from PAH patients and miR-150 plasma expression is a significant predictor of survival in patients with PAH (Rhodes et al., 2013). MiRNAs can also be used as a therapeutic agent, however the route of administration of these small RNA molecules must be carefully considered. Ideally, administration would be directly to the pulmonary circulation to minimise off target effects and maximise therapeutic effects. Local delivery to the lung can be achieved via intranasal or intratracheal delivery. Delivery of miRNA treatment to the pulmonary system via inhalation would be the most convenient route of administration clinically however, formulating inhalable miRNAs and maintaining stability during the delivery process can prove challenging.

Both miRNA therapy and gene therapy are potential treatments for PAH. However, most miRNAs target many mRNAs and direct modulation of miRNAs in the long term may produce severe off target effects *in vivo* due to the pleiotropic effect of these small RNA molecules. Therefore directing treatment at miRNA targets may reduce these adverse effects and as a result, miRNA target validation is of utmost importance. Identification of genuine miRNA target genes is therefore essential in elucidating the mechanisms through which miRNAs exert their effects in different cells and tissues. However, target identification remains a challenge. In this thesis, target analysis was negative for both miRNAs

analysed (miR-145 and miR-451). Although target genes were indeed investigated at both the mRNA and protein level, none of the chosen genes were modulated as expected after silencing of a specific miRNA. Further work needs to be done to pinpoint the exact cellular and molecular mechanisms through which this miRNA dysregulation is taking place and if it is contributing to the pathogenesis of PH through target mRNA.

One of the most problematic tasks when studying PH is the limited availability of human lung samples from PAH patients. Therefore it is critical that animal models are in place which can recapitulate the human disease. The classical models of PH (chronic hypoxia and MCT exposure) have provided us with a great deal of knowledge on the development of PH. However, neither of these models develop the severe plexogenic lesions which are characteristic of human PAH. Consequently, newer models have been established to further our understanding of these complex lesions. From the results presented, both the mouse and rat hypoxia/SU5416 model of PH produce severe PH with elevated RVP and pulmonary lesions and vessel occlusion evident in the rat model. Therefore illustrating that the hypoxia/SU5416 model of PH (rat model more so than the mouse model) develops a more severe PH phenotype than the classic models of PH and can be used in future experiments to understand the complex mechanisms involved in the development of these plexogenic lesions. Consideration must be taken when using the hypoxia/SU5416 model as VEGF and VEGFR2 expression are known to be increased in PAH (Taraseviciene-Stewart et al., 2001). Therefore although an exaggerated PH phenotype is observed in this model, it is not the best model to use if the molecules being studied interact with the VEGF signalling pathway.

Death of PAH patients is predominantly due to right ventricular hypertrophy and subsequent right ventricular failure. Therefore, a miRNA profile was established for the PAH diseased right ventricle. MiR-27a and miR-27b were up-regulated within the RV of hypoxia/SU5416 mice and rats, respectively. This response appears to be cardiac specific and may help to establish therapies to maintain and stabilise RV function. Both miR-27 family members are pro-angiogenic and a possible explanation for their up-regulation in the RV during PAH is due to an adaptive response to the increase in right ventricular pressure. Therefore the

increase in miR-27 expression may contribute to the adaptive hypertrophy observed in the RV which requires neovascularisation in order to prevent RV failure.

In conclusion, the findings presented in this thesis confirm that miRNAs are dysregulated within the lung and right ventricle during PH development. This miRNA dysregulation appears to be dependent on numerous experimental factors and therefore makes targeting specific miRNAs challenging. Investigations into these factors will provide a better understanding of miRNA modulation within the diseased model of PH. The development of newer models of PH, such as the hypoxia/SU5416 model, has given us an insight into the biological basis of the plexiform lesions characteristic of human PAH and future work using this model will further our understanding of signalling pathways involved in this complex disease.

6.1 Future Perspective

Identification of miRNA target genes allows therapeutic targeting of signalling pathways integral to the development of PAH. Microarray analysis may provide a more comprehensive overview of the target genes that are dysregulated when a miRNA is silenced (as in the case of miR-145 or miR-451). This would allow expression levels for an abundant number of genes to be analysed and candidate genes could be validated through luciferase reporter assay, western blot and qRT-PCR. As well as transcriptome analysis, proteomics is another method which could be utilised to identify novel miRNA targets. Stable-isotope labelling by amino acids in cell culture (SILAC) is a mass-spectrometry based quantitative proteomics technique used to quantify protein expression levels. SILAC is a high-throughput system allowing identification of proteins differentially expressed in diverse conditions (Thomson et al., 2011). It has been demonstrated that mRNA levels do not always correlate with protein expression (Greenbaum et al., 2003) and therefore proteomic analysis has the advantage of directly measuring the functional output of the miRNA. Performing both mRNA and protein screening will provide specific miRNA targets which can then be further validated to confirm if they are direct targets for the miRNA thus enhancing our understanding of how miRNAs modulate cellular functions.

Therapeutic targeting of the right ventricle appears a promising candidate in PH. From the results presented in this thesis, members of the miR-27 family are dysregulated selectively within the RV during disease development. Further work is required to establish whether miR-27 over-expression in PH is an adaptive response or detrimental to cardiac tissue. To test this, the effect of over-expressing miR-27a/b within the RV should be analysed in experimental models of PH and RV function and survival rates assessed. This may be of benefit as increasing RV function would decrease the severity of the disease in order for other treatments targeting, for example, the pulmonary vascular remodelling to exert a beneficial effect.

In summary, miRNAs represent a potential therapeutic target for the treatment of PAH with further work required to pinpoint the exact mechanistic pathways through which they exert their effects.

List of References

- ABE, K., TOBA, M., ALZOUBI, A., ITO, M., FAGAN, K. A., COOL, C. D., et al. 2010. Formation of plexiform lesions in experimental severe pulmonary arterial hypertension. *Circulation*, 121, 2747-54.
- ABE, K., TOBA, M., ALZOUBI, A., KOUBSKY, K., ITO, M., OTA, H., et al. 2011. Tyrosine kinase inhibitors are potent acute pulmonary vasodilators in rats. *Am J Respir Cell Mol Biol*, 45, 804-8.
- AFRAKHTE, M., MOREN, A., JOSSAN, S., ITOH, S., SAMPATH, K., WESTERMARK, B., et al. 1998. Induction of inhibitory Smad6 and Smad7 mRNA by TGF-beta family members. *Biochem Biophys Res Commun*, 249, 505-11.
- AHN, B. H., PARK, H. K., CHO, H. G., LEE, H. A., LEE, Y. M., YANG, E. K., et al. 2003. Estrogen and enalapril attenuate the development of right ventricular hypertrophy induced by monocrotaline in ovariectomized rats. *J Korean Med Sci*, 18, 641-8.
- ALTUVIA, Y., LANDGRAF, P., LITHWICK, G., ELEFANT, N., PFEFFER, S., ARAVIN, A., et al. 2005. Clustering and conservation patterns of human microRNAs. *Nucleic Acids Res*, 33, 2697-706.
- AMBARTSUMIAN, N., KLINGELHOFER, J., GRIGORIAN, M., KARLSTROM, O., SIDENIUS, N., GEORGIEV, G., et al. 1998. Tissue-specific posttranscriptional downregulation of expression of the S100A4(mts1) gene in transgenic animals. *Invasion Metastasis*, 18, 96-104.
- ARAI, H., HORI, S., ARAMORI, I., OHKUBO, H. & NAKANISHI, S. 1990. Cloning and expression of a cDNA encoding an endothelin receptor. *Nature*, 348, 730-2.
- ARCHER, S. & RICH, S. 2000. Primary pulmonary hypertension: a vascular biology and translational research "Work in progress". *Circulation*, 102, 2781-91.
- ARCHER, S. L. & MICHELAKIS, E. D. 2009. Phosphodiesterase type 5 inhibitors for pulmonary arterial hypertension. *N Engl J Med*, 361, 1864-71.
- ARCHER, S. L., WEIR, E. K. & WILKINS, M. R. 2010. Basic science of pulmonary arterial hypertension for clinicians: new concepts and experimental therapies. *Circulation*, 121, 2045-66.
- ARIAS-STELLA, J. & SALDANA, M. 1963. The Terminal Portion of the Pulmonary Arterial Tree in People Native to High Altitudes. *Circulation*, 28, 915-25.
- ARROYO, J. D., CHEVILLET, J. R., KROH, E. M., RUF, I. K., PRITCHARD, C. C., GIBSON, D. F., et al. 2011. Argonaute2 complexes carry a population of circulating microRNAs independent of vesicles in human plasma. *Proc Natl Acad Sci U S A*, 108, 5003-8.

- ATKINSON, C., STEWART, S., UPTON, P. D., MACHADO, R., THOMSON, J. R., TREMBATH, R. C., et al. 2002. Primary pulmonary hypertension is associated with reduced pulmonary vascular expression of type II bone morphogenetic protein receptor. *Circulation*, 105, 1672-8.
- AUSTIN, E. D., COGAN, J. D., WEST, J. D., HEDGES, L. K., HAMID, R., DAWSON, E. P., et al. 2009. Alterations in oestrogen metabolism: implications for higher penetrance of familial pulmonary arterial hypertension in females. *Eur Respir J*, 34, 1093-9.
- BADESCH, D. B., ABMAN, S. H., AHEARN, G. S., BARST, R. J., MCCRORY, D. C., SIMONNEAU, G., et al. 2004. Medical therapy for pulmonary arterial hypertension: ACCP evidence-based clinical practice guidelines. *Chest*, 126, 35S-62S.
- BADESCH, D. B., CHAMPION, H. C., SANCHEZ, M. A., HOEPER, M. M., LOYD, J. E., MANES, A., et al. 2009. Diagnosis and assessment of pulmonary arterial hypertension. *J Am Coll Cardiol*, 54, S55-66.
- BADESCH, D. B., RASKOB, G. E., ELLIOTT, C. G., KRICHMAN, A. M., FARBER, H. W., FROST, A. E., et al. 2010. Pulmonary arterial hypertension: baseline characteristics from the REVEAL Registry. *Chest*, 137, 376-87.
- BAEK, D., VILLEN, J., SHIN, C., CAMARGO, F. D., GYGI, S. P. & BARTEL, D. P. 2008. The impact of microRNAs on protein output. *Nature*, 455, 64-71.
- BANDRES, E., BITARTE, N., ARIAS, F., AGORRETA, J., FORTES, P., AGIRRE, X., et al. 2009. microRNA-451 regulates macrophage migration inhibitory factor production and proliferation of gastrointestinal cancer cells. *Clin Cancer Res*, 15, 2281-90.
- BARBATO, C., ARISI, I., FRIZZO, M. E., BRANDI, R., DA SACCO, L. & MASOTTI, A. 2009. Computational challenges in miRNA target predictions: to be or not to be a true target? *J Biomed Biotechnol*, 2009, 803069.
- BARST, R. J., LANGLEBEN, D., BADESCH, D., FROST, A., LAWRENCE, E. C., SHAPIRO, S., et al. 2006. Treatment of pulmonary arterial hypertension with the selective endothelin-A receptor antagonist sitaxsentan. *J Am Coll Cardiol*, 47, 2049-56.
- BARST, R. J., MCGOON, M., TORBICKI, A., SITBON, O., KROWKA, M. J., OLSCHESKI, H., et al. 2004. Diagnosis and differential assessment of pulmonary arterial hypertension. *J Am Coll Cardiol*, 43, 40S-47S.
- BARTEL, D. P. 2004. MicroRNAs: genomics, biogenesis, mechanism, and function. *Cell*, 116, 281-97.
- BEPPU, H., ICHINOSE, F., KAWAI, N., JONES, R. C., YU, P. B., ZAPOL, W. M., et al. 2004. BMPR-II heterozygous mice have mild pulmonary hypertension and

an impaired pulmonary vascular remodeling response to prolonged hypoxia. *Am J Physiol Lung Cell Mol Physiol*, 287, L1241-7.

- BEPPU, H., KAWABATA, M., HAMAMOTO, T., CHYTIL, A., MINOWA, O., NODA, T., et al. 2000. BMP type II receptor is required for gastrulation and early development of mouse embryos. *Dev Biol*, 221, 249-58.
- BERGAMASCHI, A. & KATZENELLENBOGEN, B. S. 2012. Tamoxifen downregulation of miR-451 increases 14-3-3zeta and promotes breast cancer cell survival and endocrine resistance. *Oncogene*, 31, 39-47.
- BERGELSON, J. M., CUNNINGHAM, J. A., DROGUETT, G., KURT-JONES, E. A., KRITHIVAS, A., HONG, J. S., et al. 1997. Isolation of a common receptor for Cocksackie B viruses and adenoviruses 2 and 5. *Science*, 275, 1320-3.
- BERNSTEIN, E., KIM, S. Y., CARMELL, M. A., MURCHISON, E. P., ALCORN, H., LI, M. Z., et al. 2003. Dicer is essential for mouse development. *Nat Genet*, 35, 215-7.
- BIAN, H. B., PAN, X., YANG, J. S., WANG, Z. X. & DE, W. 2011. Upregulation of microRNA-451 increases cisplatin sensitivity of non-small cell lung cancer cell line (A549). *J Exp Clin Cancer Res*, 30, 20.
- BOCKMEYER, C. L., MAEGEL, L., JANCIAUSKIENE, S., RISCHE, J., LEHMANN, U., MAUS, U. A., et al. 2012. Plexiform vasculopathy of severe pulmonary arterial hypertension and microRNA expression. *J Heart Lung Transplant*, 31, 764-72.
- BOETTGER, T., BEETZ, N., KOSTIN, S., SCHNEIDER, J., KRUGER, M., HEIN, L., et al. 2009. Acquisition of the contractile phenotype by murine arterial smooth muscle cells depends on the Mir143/145 gene cluster. *J Clin Invest*, 119, 2634-47.
- BOGAARD, H. J., ABE, K., VONK NOORDEGRAAF, A. & VOELKEL, N. F. 2009. The right ventricle under pressure: cellular and molecular mechanisms of right-heart failure in pulmonary hypertension. *Chest*, 135, 794-804.
- BOGATKEVICH, G. S., TOURKINA, E., ABRAMS, C. S., HARLEY, R. A., SILVER, R. M. & LUDWICKA-BRADLEY, A. 2003. Contractile activity and smooth muscle alpha-actin organization in thrombin-induced human lung myofibroblasts. *Am J Physiol Lung Cell Mol Physiol*, 285, L334-43.
- BOLLI, M. H., BOSS, C., BINKERT, C., BUCHMANN, S., BUR, D., HESS, P., et al. 2012. The discovery of N-[5-(4-bromophenyl)-6-[2-[(5-bromo-2-pyrimidinyl)oxy]ethoxy]-4-pyrimidinyl]-N'-p ropylsulfamide (Macitentan), an orally active, potent dual endothelin receptor antagonist. *J Med Chem*, 55, 7849-61.

- BONNET, S., ROCHEFORT, G., SUTENDRA, G., ARCHER, S. L., HAROMY, A., WEBSTER, L., et al. 2007. The nuclear factor of activated T cells in pulmonary arterial hypertension can be therapeutically targeted. *Proc Natl Acad Sci U S A*, 104, 11418-23.
- BOUCHER, J. M., PETERSON, S. M., URS, S., ZHANG, C. & LIAW, L. 2011. The miR-143/145 cluster is a novel transcriptional target of Jagged-1/Notch signaling in vascular smooth muscle cells. *J Biol Chem*, 286, 28312-21.
- BRENNECKE, J., STARK, A., RUSSELL, R. B. & COHEN, S. M. 2005. Principles of microRNA-target recognition. *PLoS Biol*, 3, e85.
- BRENNER, O. O. 1935. Pathology of the vessels of the pulmonary circulation: Part i. *Archives of Internal Medicine*, 56, 211-237.
- BROCK, M., TRENMANN, M., GAY, R. E., MICHEL, B. A., GAY, S., FISCHLER, M., et al. 2009. Interleukin-6 modulates the expression of the bone morphogenetic protein receptor type II through a novel STAT3-microRNA cluster 17/92 pathway. *Circ Res*, 104, 1184-91.
- BUCHDUNGER, E., CIOFFI, C. L., LAW, N., STOVER, D., OHNO-JONES, S., DRUKER, B. J., et al. 2000. Abl protein-tyrosine kinase inhibitor STI571 inhibits in vitro signal transduction mediated by c-kit and platelet-derived growth factor receptors. *J Pharmacol Exp Ther*, 295, 139-45.
- BUCKLEY, M. S., STAIB, R. L. & WICKS, L. M. 2013. Combination therapy in the management of pulmonary arterial hypertension. *Int J Clin Pract Suppl*, 13-23.
- BURTON, V. J., CIUCLAN, L. I., HOLMES, A. M., RODMAN, D. M., WALKER, C. & BUDD, D. C. 2011. Bone morphogenetic protein receptor II regulates pulmonary artery endothelial cell barrier function. *Blood*, 117, 333-41.
- CAHILL, E., ROWAN, S. C., SANDS, M., BANAHAN, M., RYAN, D., HOWELL, K., et al. 2012. The pathophysiological basis of chronic hypoxic pulmonary hypertension in the mouse: vasoconstrictor and structural mechanisms contribute equally. *Exp Physiol*, 97, 796-806.
- CALLIS, T. E., PANDYA, K., SEOK, H. Y., TANG, R. H., TATSUGUCHI, M., HUANG, Z. P., et al. 2009. MicroRNA-208a is a regulator of cardiac hypertrophy and conduction in mice. *J Clin Invest*, 119, 2772-86.
- CAMPION, M. E., HARDZIYENKA, M., DE BRUIN, K., VAN ECK-SMIT, B. L., DE BAKKER, J. M., VERBERNE, H. J., et al. 2010. Early inflammatory response during the development of right ventricular heart failure in a rat model. *Eur J Heart Fail*, 12, 653-8.
- CARE, A., CATALUCCI, D., FELICETTI, F., BONCI, D., ADDARIO, A., GALLO, P., et al. 2007. MicroRNA-133 controls cardiac hypertrophy. *Nat Med*, 13, 613-8.

- CARUSO, P., DEMPSIE, Y., STEVENS, H. C., MCDONALD, R. A., LONG, L., LU, R., et al. 2012. A role for miR-145 in pulmonary arterial hypertension: evidence from mouse models and patient samples. *Circ Res*, 111, 290-300.
- CARUSO, P., MACLEAN, M. R., KHANIN, R., MCCLURE, J., SOON, E., SOUTHGATE, M., et al. 2010. Dynamic changes in lung microRNA profiles during the development of pulmonary hypertension due to chronic hypoxia and monocrotaline. *Arterioscler Thromb Vasc Biol*, 30, 716-23.
- CHAMORRO-JORGANES, A., ARALDI, E., PENALVA, L. O., SANDHU, D., FERNANDEZ-HERNANDO, C. & SUAREZ, Y. 2011. MicroRNA-16 and microRNA-424 regulate cell-autonomous angiogenic functions in endothelial cells via targeting vascular endothelial growth factor receptor-2 and fibroblast growth factor receptor-1. *Arterioscler Thromb Vasc Biol*, 31, 2595-606.
- CHAN, M. C., NGUYEN, P. H., DAVIS, B. N., OHOKA, N., HAYASHI, H., DU, K., et al. 2007. A novel regulatory mechanism of the bone morphogenetic protein (BMP) signaling pathway involving the carboxyl-terminal tail domain of BMP type II receptor. *Mol Cell Biol*, 27, 5776-89.
- CHANNICK, R. N., SIMONNEAU, G., SITBON, O., ROBBINS, I. M., FROST, A., TAPSON, V. F., et al. 2001. Effects of the dual endothelin-receptor antagonist bosentan in patients with pulmonary hypertension: a randomised placebo-controlled study. *Lancet*, 358, 1119-23.
- CHEMLA, D., CASTELAIN, V., HERVE, P., LECARPENTIER, Y. & BRIMIOULLE, S. 2002. Haemodynamic evaluation of pulmonary hypertension. *Eur Respir J*, 20, 1314-31.
- CHEN, X., BA, Y., MA, L., CAI, X., YIN, Y., WANG, K., et al. 2008. Characterization of microRNAs in serum: a novel class of biomarkers for diagnosis of cancer and other diseases. *Cell Res*, 18, 997-1006.
- CHENDRIMADA, T. P., GREGORY, R. I., KUMARASWAMY, E., NORMAN, J., COOCH, N., NISHIKURA, K., et al. 2005. TRBP recruits the Dicer complex to Ago2 for microRNA processing and gene silencing. *Nature*, 436, 740-4.
- CHENG, Y., LIU, X., YANG, J., LIN, Y., XU, D. Z., LU, Q., et al. 2009. MicroRNA-145, a novel smooth muscle cell phenotypic marker and modulator, controls vascular neointimal lesion formation. *Circ Res*, 105, 158-66.
- CHENG, Y., ZHU, P., YANG, J., LIU, X., DONG, S., WANG, X., et al. 2010. Ischaemic preconditioning-regulated miR-21 protects heart against ischaemia/reperfusion injury via anti-apoptosis through its target PDCD4. *Cardiovasc Res*, 87, 431-9.
- CHIANG, H. Y., KORSHUNOV, V. A., SEROUR, A., SHI, F. & SOTTILE, J. 2009. Fibronectin is an important regulator of flow-induced vascular remodeling. *Arterioscler Thromb Vasc Biol*, 29, 1074-9.

- CHICHE, J. D., SCHLUTSMEYER, S. M., BLOCH, D. B., DE LA MONTE, S. M., ROBERTS, J. D., JR., FILIPPOV, G., et al. 1998. Adenovirus-mediated gene transfer of cGMP-dependent protein kinase increases the sensitivity of cultured vascular smooth muscle cells to the antiproliferative and proapoptotic effects of nitric oxide/cGMP. *J Biol Chem*, 273, 34263-71.
- CHINCHILLA, A., LOZANO, E., DAIMI, H., ESTEBAN, F. J., CRIST, C., ARANEGA, A. E., et al. 2011. MicroRNA profiling during mouse ventricular maturation: a role for miR-27 modulating Mef2c expression. *Cardiovasc Res*, 89, 98-108.
- CHRISTMAN, B. W., MCPHERSON, C. D., NEWMAN, J. H., KING, G. A., BERNARD, G. R., GROVES, B. M., et al. 1992. An imbalance between the excretion of thromboxane and prostacyclin metabolites in pulmonary hypertension. *N Engl J Med*, 327, 70-5.
- CIFUENTES, D., XUE, H., TAYLOR, D. W., PATNODE, H., MISHIMA, Y., CHELOUFI, S., et al. 2010. A novel miRNA processing pathway independent of Dicer requires Argonaute2 catalytic activity. *Science*, 328, 1694-8.
- CIUCLAN, L., BONNEAU, O., HUSSEY, M., DUGGAN, N., HOLMES, A. M., GOOD, R., et al. 2011. A novel murine model of severe pulmonary arterial hypertension. *Am J Respir Crit Care Med*, 184, 1171-82.
- CIUCLAN, L., HUSSEY, M. J., BURTON, V., GOOD, R., DUGGAN, N., BEACH, S., et al. 2013. Imatinib attenuates hypoxia-induced pulmonary arterial hypertension pathology via reduction in 5-hydroxytryptamine through inhibition of tryptophan hydroxylase 1 expression. *Am J Respir Crit Care Med*, 187, 78-89.
- CLOZEL, M. & GRAY, G. A. 1995. Are There Different ETB Receptors Mediating Constriction and Relaxation? *Journal of Cardiovascular Pharmacology*, 26, S262-264.
- COHEN, M. H., WILLIAMS, G., JOHNSON, J. R., DUAN, J., GOBBURU, J., RAHMAN, A., et al. 2002. Approval summary for imatinib mesylate capsules in the treatment of chronic myelogenous leukemia. *Clin Cancer Res*, 8, 935-42.
- COOL, C. D., STEWART, J. S., WERAHERA, P., MILLER, G. J., WILLIAMS, R. L., VOELKEL, N. F., et al. 1999. Three-dimensional reconstruction of pulmonary arteries in plexiform pulmonary hypertension using cell-specific markers. Evidence for a dynamic and heterogeneous process of pulmonary endothelial cell growth. *Am J Pathol*, 155, 411-9.
- COPPLE, B. L., GANEY, P. E. & ROTH, R. A. 2003. Liver inflammation during monocrotaline hepatotoxicity. *Toxicology*, 190, 155-69.
- CORBIN, J. D., BEASLEY, A., BLOUNT, M. A. & FRANCIS, S. H. 2005. High lung PDE5: a strong basis for treating pulmonary hypertension with PDE5 inhibitors. *Biochem Biophys Res Commun*, 334, 930-8.

- CORDES, K. R., SHEEHY, N. T., WHITE, M. P., BERRY, E. C., MORTON, S. U., MUTH, A. N., et al. 2009. miR-145 and miR-143 regulate smooth muscle cell fate and plasticity. *Nature*, 460, 705-10.
- COURBOULIN, A., PAULIN, R., GIGUERE, N. J., SAKSOUK, N., PERREAULT, T., MELOCHE, J., et al. 2011. Role for miR-204 in human pulmonary arterial hypertension. *J Exp Med*, 208, 535-48.
- COWAN, K. N., JONES, P. L. & RABINOVITCH, M. 2000. Elastase and matrix metalloproteinase inhibitors induce regression, and tenascin-C antisense prevents progression, of vascular disease. *J Clin Invest*, 105, 21-34.
- CROSS, M. J. & CLAESSION-WELSH, L. 2001. FGF and VEGF function in angiogenesis: signalling pathways, biological responses and therapeutic inhibition. *Trends Pharmacol Sci*, 22, 201-7.
- D'ALONZO, G. E., BARST, R. J., AYRES, S. M., BERGOFISKY, E. H., BRUNDAGE, B. H., DETRE, K. M., et al. 1991. Survival in patients with primary pulmonary hypertension. Results from a national prospective registry. *Ann Intern Med*, 115, 343-9.
- DANG, L. T., LAWSON, N. D. & FISH, J. E. 2013. MicroRNA control of vascular endothelial growth factor signaling output during vascular development. *Arterioscler Thromb Vasc Biol*, 33, 193-200.
- DAVIS-DUSENBERY, B. N., CHAN, M. C., RENO, K. E., WEISMAN, A. S., LAYNE, M. D., LAGNA, G., et al. 2011. Down-regulation of Kruppel-like factor-4 (KLF4) by microRNA-143/145 is critical for modulation of vascular smooth muscle cell phenotype by transforming growth factor-beta and bone morphogenetic protein 4. *J Biol Chem*, 286, 28097-110.
- DAVIS, B. N., HILYARD, A. C., LAGNA, G. & HATA, A. 2008. SMAD proteins control DROSHA-mediated microRNA maturation. *Nature*, 454, 56-61.
- DEMPSEY, E. C., WICK, M. J., KAROOR, V., BARR, E. J., TALLMAN, D. W., WEHLING, C. A., et al. 2009. Nephrylin null mice develop exaggerated pulmonary vascular remodeling in response to chronic hypoxia. *Am J Pathol*, 174, 782-96.
- DEMPSIE, Y., NILSEN, M., WHITE, K., MAIR, K. M., LOUGHLIN, L., AMBARTSUMIAN, N., et al. 2011. Development of pulmonary arterial hypertension in mice over-expressing S100A4/Mts1 is specific to females. *Respir Res*, 12, 159.
- DEO, M., YU, J. Y., CHUNG, K. H., TIPPENS, M. & TURNER, D. L. 2006. Detection of mammalian microRNA expression by in situ hybridization with RNA oligonucleotides. *Dev Dyn*, 235, 2538-48.
- DHANABAL, M., WU, F., ALVAREZ, E., MCQUEENEY, K. D., JEFFERS, M., MACDOUGALL, J., et al. 2005. Recombinant semaphorin 6A-1 ectodomain

- inhibits in vivo growth factor and tumor cell line-induced angiogenesis. *Cancer Biol Ther*, 4, 659-68.
- DIGNAT-GEORGE, F. & BOULANGER, C. M. 2011. The many faces of endothelial microparticles. *Arterioscler Thromb Vasc Biol*, 31, 27-33.
- DING, K., YIN, Y., CAO, K., CHRISTENSEN, G. E., LIN, C. L., HOFFMAN, E. A., et al. 2009. Evaluation of lobar biomechanics during respiration using image registration. *Med Image Comput Comput Assist Interv*, 12, 739-46.
- DOENCH, J. G. & SHARP, P. A. 2004. Specificity of microRNA target selection in translational repression. *Genes Dev*, 18, 504-11.
- DORE, L. C., AMIGO, J. D., DOS SANTOS, C. O., ZHANG, Z., GAI, X., TOBIAS, J. W., et al. 2008. A GATA-1-regulated microRNA locus essential for erythropoiesis. *Proc Natl Acad Sci U S A*, 105, 3333-8.
- DRAKE, J. I., BOGAARD, H. J., MIZUNO, S., CLIFTON, B., XIE, B., GAO, Y., et al. 2011. Molecular signature of a right heart failure program in chronic severe pulmonary hypertension. *Am J Respir Cell Mol Biol*, 45, 1239-47.
- DRESDALE, D. T., SCHULTZ, M. & MIGHTOM, R. J. 1951. Primary pulmonary hypertension. I. Clinical and hemodynamic study. *Am J Med*, 11, 686-705.
- DU, T. & ZAMORE, P. D. 2005. microPrimer: the biogenesis and function of microRNA. *Development*, 132, 4645-52.
- DUMITRASCU, R., KOEBRICH, S., DONY, E., WEISSMANN, N., SAVAI, R., PULLAMSETTI, S. S., et al. 2008. Characterization of a murine model of monocrotaline pyrrole-induced acute lung injury. *BMC Pulm Med*, 8, 25.
- DWEEP, H., STICHT, C., PANDEY, P. & GRETZ, N. 2011. miRWalk--database: prediction of possible miRNA binding sites by "walking" the genes of three genomes. *J Biomed Inform*, 44, 839-47.
- ELIA, L., QUINTAVALLE, M., ZHANG, J., CONTU, R., COSSU, L., LATRONICO, M. V., et al. 2009. The knockout of miR-143 and -145 alters smooth muscle cell maintenance and vascular homeostasis in mice: correlates with human disease. *Cell Death Differ*, 16, 1590-8.
- ELNAKISH, M. T., HASSANAIN, H. H., JANSSEN, P. M., ANGELOS, M. G. & KHAN, M. 2013. Emerging role of oxidative stress in metabolic syndrome and cardiovascular diseases: important role of Rac/NADPH oxidase. *J Pathol*, 231, 290-300.
- EULALIO, A., HUNTZINGER, E. & IZAURRALDE, E. 2008. GW182 interaction with Argonaute is essential for miRNA-mediated translational repression and mRNA decay. *Nat Struct Mol Biol*, 15, 346-53.

- EULALIO, A., MANO, M., DAL FERRO, M., ZENTILIN, L., SINAGRA, G., ZACCHIGNA, S., et al. 2012. Functional screening identifies miRNAs inducing cardiac regeneration. *Nature*, 492, 376-81.
- FDA 2008. E15 Definitions for Genomic Biomarkers, Pharmacogenomics, Pharmacogenetics, Genomic Data and Sample Coding Categories. Available: <http://www.fda.gov/downloads/Drugs/GuidanceComplianceRegulatoryInformation/Guidances/ucm073162.pdf> [Accessed 18th April 2014].
- FERRARO, L., RAVO, M., NASSA, G., TARALLO, R., DE FILIPPO, M. R., GIURATO, G., et al. 2012. Effects of oestrogen on microRNA expression in hormone-responsive breast cancer cells. *Horm Cancer*, 3, 65-78.
- FIRTH, A. L., PLATOSHYN, O., BREVNOVA, E. E., BURG, E. D., POWELL, F., HADDAD, G. H., et al. 2009. Hypoxia selectively inhibits KCNA5 channels in pulmonary artery smooth muscle cells. *Ann N Y Acad Sci*, 1177, 101-11.
- FONTANA, L., FIORI, M. E., ALBINI, S., CIFALDI, L., GIOVINAZZI, S., FORLONI, M., et al. 2008. Antagomir-17-5p abolishes the growth of therapy-resistant neuroblastoma through p21 and BIM. *Plos One*, 3, e2236.
- FRANK, D. B., LOWERY, J., ANDERSON, L., BRINK, M., REESE, J. & DE CAESTECKER, M. 2008. Increased susceptibility to hypoxic pulmonary hypertension in Bmpr2 mutant mice is associated with endothelial dysfunction in the pulmonary vasculature. *Am J Physiol Lung Cell Mol Physiol*, 294, L98-109.
- FRAZZIANO, G., CHAMPION, H. C. & PAGANO, P. J. 2012. NADPH oxidase-derived ROS and the regulation of pulmonary vessel tone. *Am J Physiol Heart Circ Physiol*, 302, H2166-77.
- FREDRIKSSON, L., LI, H. & ERIKSSON, U. 2004. The PDGF family: four gene products form five dimeric isoforms. *Cytokine & growth factor reviews*, 15, 197-204.
- FRID, M. G., BRUNETTI, J. A., BURKE, D. L., CARPENTER, T. C., DAVIE, N. J., REEVES, J. T., et al. 2006. Hypoxia-induced pulmonary vascular remodeling requires recruitment of circulating mesenchymal precursors of a monocyte/macrophage lineage. *Am J Pathol*, 168, 659-69.
- FROST, A. E., BADESCH, D. B., BARST, R. J., BENZA, R. L., ELLIOTT, C. G., FARBER, H. W., et al. 2011. The changing picture of patients with pulmonary arterial hypertension in the United States: how REVEAL differs from historic and non-US Contemporary Registries. *Chest*, 139, 128-37.
- GAL, H., PANDI, G., KANNER, A. A., RAM, Z., LITHWICK-YANAI, G., AMARIGLIO, N., et al. 2008. MIR-451 and Imatinib mesylate inhibit tumor growth of Glioblastoma stem cells. *Biochem Biophys Res Commun*, 376, 86-90.

- GALIE, N., GHOFrani, H. A., TORBICKI, A., BARST, R. J., RUBIN, L. J., BADESCH, D., et al. 2005. Sildenafil citrate therapy for pulmonary arterial hypertension. *N Engl J Med*, 353, 2148-57.
- GALIE, N., GRIGIONI, F., BACCHI-REGGIANI, L., USSIA, G., PARLANGELI, R. & CATANZARITI, P. 1996. Relation of endothelin-1 to survival in patients with primary pulmonary hypertension. *Eur J Clin Invest*, 26, 273.
- GALIE, N., MANES, A. & BRANZI, A. 2004. The endothelin system in pulmonary arterial hypertension. *Cardiovasc Res*, 61, 227-37.
- GALIE, N., MANES, A., NEGRO, L., PALAZZINI, M., BACCHI-REGGIANI, M. L. & BRANZI, A. 2009. A meta-analysis of randomized controlled trials in pulmonary arterial hypertension. *Eur Heart J*, 30, 394-403.
- GALIE, N., OLSCHIEWSKI, H., OUDIZ, R. J., TORRES, F., FROST, A., GHOFrani, H. A., et al. 2008. Ambrisentan for the treatment of pulmonary arterial hypertension: results of the ambrisentan in pulmonary arterial hypertension, randomized, double-blind, placebo-controlled, multicenter, efficacy (ARIES) study 1 and 2. *Circulation*, 117, 3010-9.
- GAMBACORTI-PASSERINI, C., ANTOLINI, L., MAHON, F. X., GUILHOT, F., DEININGER, M., FAVA, C., et al. 2011. Multicenter independent assessment of outcomes in chronic myeloid leukemia patients treated with imatinib. *J Natl Cancer Inst*, 103, 553-61.
- GERACI, M. W., GAO, B., SHEPHERD, D. C., MOORE, M. D., WESTCOTT, J. Y., FAGAN, K. A., et al. 1999. Pulmonary prostacyclin synthase overexpression in transgenic mice protects against development of hypoxic pulmonary hypertension. *J Clin Invest*, 103, 1509-15.
- GERTHOFFER, W. T. 2007. Mechanisms of vascular smooth muscle cell migration. *Circ Res*, 100, 607-21.
- GHOFrani, H. A., GALIE, N., GRIMMINGER, F., GRUNIG, E., HUMBERT, M., JING, Z. C., et al. 2013. Riociguat for the treatment of pulmonary arterial hypertension. *N Engl J Med*, 369, 330-40.
- GIAID, A., YANAGISAWA, M., LANGLEBEN, D., MICHEL, R. P., LEVY, R., SHENNIB, H., et al. 1993. Expression of endothelin-1 in the lungs of patients with pulmonary hypertension. *N Engl J Med*, 328, 1732-9.
- GINGHINA, C., MURARU, D., VLADAIA, A., JURCUT, R., POPESCU, B. A., CALIN, A., et al. 2009. Doppler flow patterns in the evaluation of pulmonary hypertension. *Rom J Intern Med*, 47, 109-21.
- GRANT, J. S., WHITE, K., MACLEAN, M. R. & BAKER, A. H. 2013. MicroRNAs in pulmonary arterial remodeling. *Cell Mol Life Sci*, 70, 4479-94.

- GREENBAUM, D., COLANGELO, C., WILLIAMS, K. & GERSTEIN, M. 2003. Comparing protein abundance and mRNA expression levels on a genomic scale. *Genome Biol*, 4, 117.
- GREENWAY, S., VAN SUYLEN, R. J., DU MARCHIE SARVAAS, G., KWAN, E., AMBARTSUMIAN, N., LUKANIDIN, E., et al. 2004. S100A4/Mts1 produces murine pulmonary artery changes resembling plexogenic arteriopathy and is increased in human plexogenic arteriopathy. *Am J Pathol*, 164, 253-62.
- GREGORY, R. I., YAN, K. P., AMUTHAN, G., CHENDRIMADA, T., DORATOTAJ, B., COOCH, N., et al. 2004. The Microprocessor complex mediates the genesis of microRNAs. *Nature*, 432, 235-40.
- GRIGORIAN, M. S., TULCHINSKY, E. M., ZAIN, S., EBRALIDZE, A. K., KRAMEROV, D. A., KRIAJEVSKA, M. V., et al. 1993. The mts1 gene and control of tumor metastasis. *Gene*, 135, 229-38.
- GRIMMINGER, F., WEIMANN, G., FREY, R., VOSWINCKEL, R., THAMM, M., BOLKOW, D., et al. 2009. First acute haemodynamic study of soluble guanylate cyclase stimulator riociguat in pulmonary hypertension. *Eur Respir J*, 33, 785-92.
- GRIMSON, A., FARH, K. K., JOHNSTON, W. K., GARRETT-ENGELE, P., LIM, L. P. & BARTEL, D. P. 2007. MicroRNA targeting specificity in mammals: determinants beyond seed pairing. *Mol Cell*, 27, 91-105.
- GUO, H., INGOLIA, N. T., WEISSMAN, J. S. & BARTEL, D. P. 2010. Mammalian microRNAs predominantly act to decrease target mRNA levels. *Nature*, 466, 835-40.
- HADDAD, F., PETERSON, T., FUH, E., KUDELKO, K. T., DE JESUS PEREZ, V., SKHIRI, M., et al. 2011. Characteristics and outcome after hospitalization for acute right heart failure in patients with pulmonary arterial hypertension. *Circ Heart Fail*, 4, 692-9.
- HAN, J., LEE, Y., YEOM, K. H., KIM, Y. K., JIN, H. & KIM, V. N. 2004. The Drosha-DGCR8 complex in primary microRNA processing. *Genes Dev*, 18, 3016-27.
- HARDEGREE, E. L., SACHDEV, A., FENSTAD, E. R., VILLARRAGA, H. R., FRANTZ, R. P., MCGOON, M. D., et al. 2013. Impaired left ventricular mechanics in pulmonary arterial hypertension: identification of a cohort at high risk. *Circ Heart Fail*, 6, 748-55.
- HARRIS, K. S., ZHANG, Z., MCMANUS, M. T., HARFE, B. D. & SUN, X. 2006. Dicer function is essential for lung epithelium morphogenesis. *Proc Natl Acad Sci U S A*, 103, 2208-13.

- HATA, A., LAGNA, G., MASSAGUE, J. & HEMMATI-BRIVANLOU, A. 1998. Smad6 inhibits BMP/Smad1 signaling by specifically competing with the Smad4 tumor suppressor. *Genes Dev*, 12, 186-97.
- HAYASHI, H., ABDOLLAH, S., QIU, Y., CAI, J., XU, Y. Y., GRINNELL, B. W., et al. 1997. The MAD-related protein Smad7 associates with the TGFbeta receptor and functions as an antagonist of TGFbeta signaling. *Cell*, 89, 1165-73.
- HE, L., THOMSON, J. M., HEMANN, M. T., HERNANDO-MONGE, E., MU, D., GOODSON, S., et al. 2005. A microRNA polycistron as a potential human oncogene. *Nature*, 435, 828-33.
- HERGENREIDER, E., HEYDT, S., TREGUER, K., BOETTGER, T., HORREVOETS, A. J., ZEIHNER, A. M., et al. 2012. Atheroprotective communication between endothelial cells and smooth muscle cells through miRNAs. *Nat Cell Biol*, 14, 249-56.
- HERGET, J., SUGGETT, A. J., LEACH, E. & BARER, G. R. 1978. Resolution of pulmonary hypertension and other features induced by chronic hypoxia in rats during complete and intermittent normoxia. *Thorax*, 33, 468-73.
- HIRATA, Y., EMORI, T., EGUCHI, S., KANNO, K., IMAI, T., OHTA, K., et al. 1993. Endothelin receptor subtype B mediates synthesis of nitric oxide by cultured bovine endothelial cells. *J Clin Invest*, 91, 1367-73.
- HISLOP, A. & REID, L. 1973. Pulmonary arterial development during childhood: branching pattern and structure. *Thorax*, 28, 129-35.
- HOEPER, M. M., BARST, R. J., BOURGE, R. C., FELDMAN, J., FROST, A. E., GALIE, N., et al. 2013. Imatinib mesylate as add-on therapy for pulmonary arterial hypertension: results of the randomized IMPRES study. *Circulation*, 127, 1128-38.
- HONG, K. H., LEE, Y. J., LEE, E., PARK, S. O., HAN, C., BEPPU, H., et al. 2008. Genetic ablation of the BMP2 gene in pulmonary endothelium is sufficient to predispose to pulmonary arterial hypertension. *Circulation*, 118, 722-30.
- HOSHIKAWA, Y., NANA-SINKAM, P., MOORE, M. D., SOTTO-SANTIAGO, S., PHANG, T., KEITH, R. L., et al. 2003. Hypoxia induces different genes in the lungs of rats compared with mice. *Physiol Genomics*, 12, 209-19.
- HOSHIKAWA, Y., VOELKEL, N. F., GESELL, T. L., MOORE, M. D., MORRIS, K. G., ALGER, L. A., et al. 2001. Prostacyclin Receptor-dependent Modulation of Pulmonary Vascular Remodeling. *American Journal of Respiratory and Critical Care Medicine*, 164, 314-318.
- HU, Y., ZHANG, Z., TORSNEY, E., AFZAL, A. R., DAVISON, F., METZLER, B., et al. 2004. Abundant progenitor cells in the adventitia contribute to

- atherosclerosis of vein grafts in ApoE-deficient mice. *J Clin Invest*, 113, 1258-65.
- HUANG, J., WOLK, J. H., GEWITZ, M. H. & MATHEW, R. 2010. Progressive endothelial cell damage in an inflammatory model of pulmonary hypertension. *Exp Lung Res*, 36, 57-66.
- HUANG, W., YEN, R. T., MCLAURINE, M. & BLEDSOE, G. 1996. Morphometry of the human pulmonary vasculature. *J Appl Physiol* (1985), 81, 2123-33.
- HUEZ, S., BRIMIOULLE, S., NAEIJE, R. & VACHIERY, J. L. 2004. Feasibility of routine pulmonary arterial impedance measurements in pulmonary hypertension. *Chest*, 125, 2121-8.
- HUMBERT, M., MONTI, G., BRENOT, F., SITBON, O., PORTIER, A., GRANGEOT-KEROS, L., et al. 1995. Increased interleukin-1 and interleukin-6 serum concentrations in severe primary pulmonary hypertension. *American Journal of Respiratory and Critical Care Medicine*, 151, 1628-1631.
- HUMBERT, M., MORRELL, N. W., ARCHER, S. L., STENMARK, K. R., MACLEAN, M. R., LANG, I. M., et al. 2004a. Cellular and molecular pathobiology of pulmonary arterial hypertension. *J Am Coll Cardiol*, 43, 13S-24S.
- HUMBERT, M., SITBON, O., CHAOUAT, A., BERTOCCHI, M., HABIB, G., GRESSIN, V., et al. 2010. Survival in patients with idiopathic, familial, and anorexigen-associated pulmonary arterial hypertension in the modern management era. *Circulation*, 122, 156-63.
- HUMBERT, M., SITBON, O., CHAOUAT, A., BERTOCCHI, M., HABIB, G., GRESSIN, V., et al. 2006. Pulmonary arterial hypertension in France: results from a national registry. *Am J Respir Crit Care Med*, 173, 1023-30.
- HUMBERT, M., SITBON, O. & SIMONNEAU, G. 2004b. Treatment of pulmonary arterial hypertension. *N Engl J Med*, 351, 1425-36.
- HURDMAN, J., CONDLIFFE, R., ELLIOT, C. A., DAVIES, C., HILL, C., WILD, J. M., et al. 2012. ASPIRE registry: assessing the Spectrum of Pulmonary hypertension Identified at a REferral centre. *Eur Respir J*, 39, 945-55.
- HYVELIN, J. M., HOWELL, K., NICHOL, A., COSTELLO, C. M., PRESTON, R. J. & MCLOUGHLIN, P. 2005. Inhibition of Rho-kinase attenuates hypoxia-induced angiogenesis in the pulmonary circulation. *Circ Res*, 97, 185-91.
- IMAMURA, T., TAKASE, M., NISHIHARA, A., OEDA, E., HANAI, J., KAWABATA, M., et al. 1997. Smad6 inhibits signalling by the TGF-beta superfamily. *Nature*, 389, 622-6.

- IZIKKI, M., GUIGNABERT, C., FADEL, E., HUMBERT, M., TU, L., ZADIGUE, P., et al. 2009. Endothelial-derived FGF2 contributes to the progression of pulmonary hypertension in humans and rodents. *J Clin Invest*, 119, 512-23.
- JALALI, S., RAMANATHAN, G. K., PARTHASARATHY, P. T., ALJUBRAN, S., GALAM, L., YUNUS, A., et al. 2012. Mir-206 regulates pulmonary artery smooth muscle cell proliferation and differentiation. *Plos One*, 7, e46808.
- JANNOT, G., VASQUEZ-RIFO, A. & SIMARD, M. J. 2011. Argonaute pull-down and RISC analysis using 2'-O-methylated oligonucleotides affinity matrices. *Methods Mol Biol*, 725, 233-49.
- JANSSEN, H. L., REESINK, H. W., LAWITZ, E. J., ZEUZEM, S., RODRIGUEZ-TORRES, M., PATEL, K., et al. 2013. Treatment of HCV infection by targeting microRNA. *N Engl J Med*, 368, 1685-94.
- JELASKA, A., STREHLOW, D. & KORN, J. H. 1999. Fibroblast heterogeneity in physiological conditions and fibrotic disease. *Springer Semin Immunopathol*, 21, 385-95.
- JIANG, Y. L., DAI, A. G., LI, Q. F. & HU, R. C. 2006. Transforming growth factor-beta1 induces transdifferentiation of fibroblasts into myofibroblasts in hypoxic pulmonary vascular remodeling. *Acta Biochim Biophys Sin (Shanghai)*, 38, 29-36.
- JIN, Y., WANG, C., LIU, X., MU, W., CHEN, Z., YU, D., et al. 2011. Molecular characterization of the microRNA-138-Fos-like antigen 1 (FOSL1) regulatory module in squamous cell carcinoma. *J Biol Chem*, 286, 40104-9.
- JING, Z. C., PARIKH, K., PULIDO, T., JERJES-SANCHEZ, C., WHITE, R. J., ALLEN, R., et al. 2013. Efficacy and safety of oral treprostinil monotherapy for the treatment of pulmonary arterial hypertension: a randomized, controlled trial. *Circulation*, 127, 624-33.
- JOPLING, C. L., YI, M., LANCASTER, A. M., LEMON, S. M. & SARNOW, P. 2005. Modulation of hepatitis C virus RNA abundance by a liver-specific MicroRNA. *Science*, 309, 1577-81.
- JOSHI, S. R., MCLENDON, J. M., MATAR, M., FEWELL, J., OKA, M., MCMURTRY, I. F., et al. 2013. Treatment with anti-microRNA-145 in an experimental model of occlusive pulmonary arterial hypertension reverses vascular remodeling [Abstract]. *Am J Respir Crit Care Med*, 187, A2095.
- KANG, H., DAVIS-DUSENBERY, B. N., NGUYEN, P. H., LAL, A., LIEBERMAN, J., VAN AELST, L., et al. 2012. Bone morphogenetic protein 4 promotes vascular smooth muscle contractility by activating microRNA-21 (miR-21), which down-regulates expression of family of dedicator of cytokinesis (DOCK) proteins. *J Biol Chem*, 287, 3976-86.

- KAY, J. M., HARRIS, P. & HEATH, D. 1967. Pulmonary hypertension produced in rats by ingestion of *Crotalaria spectabilis* seeds. *Thorax*, 22, 176-9.
- KEENE, J. D., KOMISAROW, J. M. & FRIEDERSDORF, M. B. 2006. RIP-Chip: the isolation and identification of mRNAs, microRNAs and protein components of ribonucleoprotein complexes from cell extracts. *Nat Protoc*, 1, 302-7.
- KLOOSTERMAN, W. P., WIENHOLDS, E., KETTING, R. F. & PLASTERK, R. H. 2004. Substrate requirements for let-7 function in the developing zebrafish embryo. *Nucleic Acids Res*, 32, 6284-91.
- KOS, A., OLDE LOOHUIS, N. F., WIECZOREK, M. L., GLENNON, J. C., MARTENS, G. J., KOLK, S. M., et al. 2012. A potential regulatory role for intronic microRNA-338-3p for its host gene encoding apoptosis-associated tyrosine kinase. *Plos One*, 7, e31022.
- KOTA, J., CHIVUKULA, R. R., O'DONNELL, K. A., WENTZEL, E. A., MONTGOMERY, C. L., HWANG, H. W., et al. 2009. Therapeutic microRNA delivery suppresses tumorigenesis in a murine liver cancer model. *Cell*, 137, 1005-17.
- KRETZSCHMAR, M., LIU, F., HATA, A., DOODY, J. & MASSAGUE, J. 1997. The TGF-beta family mediator Smad1 is phosphorylated directly and activated functionally by the BMP receptor kinase. *Genes Dev*, 11, 984-95.
- KRUTZFELDT, J., KUWAJIMA, S., BRAICH, R., RAJEEV, K. G., PENA, J., TUSCHL, T., et al. 2007. Specificity, duplex degradation and subcellular localization of antagomirs. *Nucleic Acids Res*, 35, 2885-92.
- KUEHBACHER, A., URBICH, C., ZEIHNER, A. M. & DIMMELER, S. 2007. Role of Dicer and Drosha for endothelial microRNA expression and angiogenesis. *Circ Res*, 101, 59-68.
- KUHR, F. K., SMITH, K. A., SONG, M. Y., LEVITAN, I. & YUAN, J. X. 2012. New mechanisms of pulmonary arterial hypertension: role of Ca(2)(+) signaling. *Am J Physiol Heart Circ Physiol*, 302, H1546-62.
- KULSHRESHTHA, R., FERRACIN, M., WOJCIK, S. E., GARZON, R., ALDER, H., AGOSTO-PEREZ, F. J., et al. 2007. A microRNA signature of hypoxia. *Mol Cell Biol*, 27, 1859-67.
- KUMARSWAMY, R., VOLKMANN, I. & THUM, T. 2011. Regulation and function of miRNA-21 in health and disease. *RNA Biol*, 8, 706-13.
- LAGNA, G., KU, M. M., NGUYEN, P. H., NEUMAN, N. A., DAVIS, B. N. & HATA, A. 2007. Control of phenotypic plasticity of smooth muscle cells by bone morphogenetic protein signaling through the myocardin-related transcription factors. *J Biol Chem*, 282, 37244-55.

- LALICH, J. J. & EHRHART, L. A. 1962. Monocrotaline-induced pulmonary arteritis in rats. *J Atheroscler Res*, 2, 482-92.
- LANE, K. B., MACHADO, R. D., PAUCIULO, M. W., THOMSON, J. R., PHILLIPS, J. A., 3RD, LOYD, J. E., et al. 2000. Heterozygous germline mutations in *BMP2*, encoding a TGF-beta receptor, cause familial primary pulmonary hypertension. *Nat Genet*, 26, 81-4.
- LEE, I., AJAY, S. S., YOOK, J. I., KIM, H. S., HONG, S. H., KIM, N. H., et al. 2009. New class of microRNA targets containing simultaneous 5'-UTR and 3'-UTR interaction sites. *Genome Res*, 19, 1175-83.
- LEE, S., CHEN, T. T., BARBER, C. L., JORDAN, M. C., MURDOCK, J., DESAI, S., et al. 2007. Autocrine VEGF signaling is required for vascular homeostasis. *Cell*, 130, 691-703.
- LEWIS, B. P., SHIH, I. H., JONES-RHOADES, M. W., BARTEL, D. P. & BURGE, C. B. 2003. Prediction of mammalian microRNA targets. *Cell*, 115, 787-98.
- LI, X., SANDA, T., LOOK, A. T., NOVINA, C. D. & VON BOEHMER, H. 2011. Repression of tumor suppressor miR-451 is essential for NOTCH1-induced oncogenesis in T-ALL. *J Exp Med*, 208, 663-75.
- LIAO, D. F., JIN, Z. G., BAAS, A. S., DAUM, G., GYGI, S. P., AEBERSOLD, R., et al. 2000. Purification and identification of secreted oxidative stress-induced factors from vascular smooth muscle cells. *J Biol Chem*, 275, 189-96.
- LIN, Q., SCHWARZ, J., BUCANA, C. & OLSON, E. N. 1997. Control of mouse cardiac morphogenesis and myogenesis by transcription factor MEF2C. *Science*, 276, 1404-7.
- LING, Y., JOHNSON, M. K., KIELY, D. G., CONDLIFFE, R., ELLIOT, C. A., GIBBS, J. S., et al. 2012. Changing demographics, epidemiology, and survival of incident pulmonary arterial hypertension: results from the pulmonary hypertension registry of the United Kingdom and Ireland. *Am J Respir Crit Care Med*, 186, 790-6.
- LIU, B., LI, J. & CAIRNS, M. J. 2012. Identifying miRNAs, targets and functions. *Brief Bioinform*.
- LIU, J., CARMELL, M. A., RIVAS, F. V., MARSDEN, C. G., THOMSON, J. M., SONG, J. J., et al. 2004. Argonaute2 is the catalytic engine of mammalian RNAi. *Science*, 305, 1437-41.
- LIU, N. & OLSON, E. N. 2010. MicroRNA regulatory networks in cardiovascular development. *Dev Cell*, 18, 510-25.
- LIU, S., PREMONT, R. T., KONTOS, C. D., HUANG, J. & ROCKEY, D. C. 2003. Endothelin-1 activates endothelial cell nitric-oxide synthase via

heterotrimeric G-protein betagamma subunit signaling to protein kinase B/Akt. *J Biol Chem*, 278, 49929-35.

- LIU, Y., SINHA, S., MCDONALD, O. G., SHANG, Y., HOOFNAGLE, M. H. & OWENS, G. K. 2005. Kruppel-like factor 4 abrogates myocardin-induced activation of smooth muscle gene expression. *J Biol Chem*, 280, 9719-27.
- LONG, J., WANG, Y., WANG, W., CHANG, B. H. & DANESH, F. R. 2010. Identification of microRNA-93 as a novel regulator of vascular endothelial growth factor in hyperglycemic conditions. *J Biol Chem*, 285, 23457-65.
- LONG, L., MACLEAN, M. R., JEFFERY, T. K., MORECROFT, I., YANG, X., RUDARAKANCHANA, N., et al. 2006. Serotonin increases susceptibility to pulmonary hypertension in BMPR2-deficient mice. *Circ Res*, 98, 818-27.
- LOW, F. N. 1953. The pulmonary alveolar epithelium of laboratory mammals and man. *Anat Rec*, 117, 241-63.
- LUCAS, K. A., PITARI, G. M., KAZEROUNIAN, S., RUIZ-STEWART, I., PARK, J., SCHULZ, S., et al. 2000. Guanylyl cyclases and signaling by cyclic GMP. *Pharmacol Rev*, 52, 375-414.
- LYTLE, J. R., YARIO, T. A. & STEITZ, J. A. 2007. Target mRNAs are repressed as efficiently by microRNA-binding sites in the 5' UTR as in the 3' UTR. *Proc Natl Acad Sci U S A*, 104, 9667-72.
- MACCHIA, A., MARCHIOLI, R., MARFISI, R., SCARANO, M., LEVANTESI, G., TAVAZZI, L., et al. 2007. A meta-analysis of trials of pulmonary hypertension: a clinical condition looking for drugs and research methodology. *Am Heart J*, 153, 1037-47.
- MACHADO, R. D., ALDRED, M. A., JAMES, V., HARRISON, R. E., PATEL, B., SCHWALBE, E. C., et al. 2006. Mutations of the TGF-beta type II receptor BMPR2 in pulmonary arterial hypertension. *Hum Mutat*, 27, 121-32.
- MACHADO, R. D., PAUCIULO, M. W., THOMSON, J. R., LANE, K. B., MORGAN, N. V., WHEELER, L., et al. 2001. BMPR2 haploinsufficiency as the inherited molecular mechanism for primary pulmonary hypertension. *Am J Hum Genet*, 68, 92-102.
- MARTIN, C. A. & DORF, M. E. 1991. Differential regulation of interleukin-6, macrophage inflammatory protein-1, and JE/MCP-1 cytokine expression in macrophage cell lines. *Cell Immunol*, 135, 245-58.
- MASSAGUE, J. & CHEN, Y. G. 2000. Controlling TGF-beta signaling. *Genes Dev*, 14, 627-44.

- MATSUMOTO, H., SUZUKI, N., ONDA, H. & FUJINO, M. 1989. Abundance of endothelin-3 in rat intestine, pituitary gland and brain. *Biochem Biophys Res Commun*, 164, 74-80.
- MCARTHUR, K., FENG, B., WU, Y., CHEN, S. & CHAKRABARTI, S. 2011. MicroRNA-200b regulates vascular endothelial growth factor-mediated alterations in diabetic retinopathy. *Diabetes*, 60, 1314-23.
- MCCULLOCH, K. M., DOCHERTY, C. C., MORECROFT, I. & MACLEAN, M. R. 1996. EndothelinB receptor-mediated contraction in human pulmonary resistance arteries. *Br J Pharmacol*, 119, 1125-30.
- MCLAUGHLIN, V. V., GAINE, S. P., BARST, R. J., OUDIZ, R. J., BOURGE, R. C., FROST, A., et al. 2003. Efficacy and safety of treprostinil: an epoprostenol analog for primary pulmonary hypertension. *J Cardiovasc Pharmacol*, 41, 293-9.
- MCLAUGHLIN, V. V. & MCGOON, M. D. 2006. Pulmonary arterial hypertension. *Circulation*, 114, 1417-31.
- MCLAUGHLIN, V. V., OUDIZ, R. J., FROST, A., TAPSON, V. F., MURALI, S., CHANNICK, R. N., et al. 2006. Randomized study of adding inhaled iloprost to existing bosentan in pulmonary arterial hypertension. *Am J Respir Crit Care Med*, 174, 1257-63.
- MCLAUGHLIN, V. V., SHILLINGTON, A. & RICH, S. 2002. Survival in primary pulmonary hypertension: the impact of epoprostenol therapy. *Circulation*, 106, 1477-82.
- MCLENDON, J. M., JOSHI, S. R., MATAR, M., FEWELL, J. G., OKA, M., MCMURTRY, I., et al. 2013. Targeted pulmonary delivery of a microRNA-145 inhibitor reverses severe pulmonary arterial hypertension in rats [Abstract]. *Am J Respir Crit Care Med*, 187, A2093.
- MEIER, B., RADEKE, H. H., SELLE, S., YOUNES, M., SIES, H., RESCH, K., et al. 1989. Human fibroblasts release reactive oxygen species in response to interleukin-1 or tumour necrosis factor-alpha. *Biochem J*, 263, 539-45.
- MEISTER, G., LANDTHALER, M., PATKANIOWSKA, A., DORSETT, Y., TENG, G. & TUSCHL, T. 2004. Human Argonaute2 mediates RNA cleavage targeted by miRNAs and siRNAs. *Mol Cell*, 15, 185-97.
- MERKLINGER, S. L., WAGNER, R. A., SPIEKERKOETTER, E., HINEK, A., KNUTSEN, R. H., KABIR, M. G., et al. 2005. Increased fibulin-5 and elastin in S100A4/Mts1 mice with pulmonary hypertension. *Circ Res*, 97, 596-604.
- MEYRICK, B., GAMBLE, W. & REID, L. 1980. Development of Crotalaria pulmonary hypertension: hemodynamic and structural study. *American Journal of Physiology-Heart and Circulatory Physiology*, 239, H692-H702.

- MEYRICK, B. & REID, L. 1979. Hypoxia and incorporation of 3H-thymidine by cells of the rat pulmonary arteries and alveolar wall. *Am J Pathol*, 96, 51-70.
- MEYRICK, B. & REID, L. 1980. Endothelial and subintimal changes in rat hilar pulmonary artery during recovery from hypoxia. A quantitative ultrastructural study. *Laboratory investigation; a journal of technical methods and pathology*, 42, 603.
- MICHELAKIS, E., TYMCHAK, W., LIEN, D., WEBSTER, L., HASHIMOTO, K. & ARCHER, S. 2002a. Oral sildenafil is an effective and specific pulmonary vasodilator in patients with pulmonary arterial hypertension: comparison with inhaled nitric oxide. *Circulation*, 105, 2398-403.
- MICHELAKIS, E. D., MCMURTRY, M. S., WU, X. C., DYCK, J. R., MOUDGIL, R., HOPKINS, T. A., et al. 2002b. Dichloroacetate, a metabolic modulator, prevents and reverses chronic hypoxic pulmonary hypertension in rats: role of increased expression and activity of voltage-gated potassium channels. *Circulation*, 105, 244-50.
- MOLEDINA, S., DE BRUYN, A., SCHIEVANO, S., OWENS, C. M., YOUNG, C., HAWORTH, S. G., et al. 2011. Fractal branching quantifies vascular changes and predicts survival in pulmonary hypertension: a proof of principle study. *Heart*, 97, 1245-9.
- MONCADA, S. & VANE, J. R. 1981. Prostacyclin: its biosynthesis, actions and clinical potential. *Philos Trans R Soc Lond B Biol Sci*, 294, 305-29.
- MONTANI, D., BERGOT, E., GUNTHER, S., SAVALE, L., BERGERON, A., BOURDIN, A., et al. 2012. Pulmonary arterial hypertension in patients treated by dasatinib. *Circulation*, 125, 2128-37.
- MORRELL, N. W. 2006. Pulmonary hypertension due to BMPR2 mutation: a new paradigm for tissue remodeling? *Proc Am Thorac Soc*, 3, 680-6.
- MORRELL, N. W., YANG, X., UPTON, P. D., JOURDAN, K. B., MORGAN, N., SHEARES, K. K., et al. 2001. Altered growth responses of pulmonary artery smooth muscle cells from patients with primary pulmonary hypertension to transforming growth factor-beta(1) and bone morphogenetic proteins. *Circulation*, 104, 790-5.
- MUNOZ, J. P., COLLAO, A., CHIONG, M., MALDONADO, C., ADASME, T., CARRASCO, L., et al. 2009. The transcription factor MEF2C mediates cardiomyocyte hypertrophy induced by IGF-1 signaling. *Biochem Biophys Res Commun*, 388, 155-60.
- NAGENDRAN, J., ARCHER, S. L., SOLIMAN, D., GURTU, V., MOUDGIL, R., HAROMY, A., et al. 2007. Phosphodiesterase type 5 is highly expressed in the hypertrophied human right ventricle, and acute inhibition of phosphodiesterase type 5 improves contractility. *Circulation*, 116, 238-48.

- NAKAMURA, K., AKAGI, S., OGAWA, A., KUSANO, K. F., MATSUBARA, H., MIURA, D., et al. 2012. Pro-apoptotic effects of imatinib on PDGF-stimulated pulmonary artery smooth muscle cells from patients with idiopathic pulmonary arterial hypertension. *Int J Cardiol*, 159, 100-6.
- NAKAMURA, K., FUSHIMI, K., KOUCHI, H., MIHARA, K., MIYAZAKI, M., OHE, T., et al. 1998. Inhibitory effects of antioxidants on neonatal rat cardiac myocyte hypertrophy induced by tumor necrosis factor-alpha and angiotensin II. *Circulation*, 98, 794-9.
- NAKAO, A., AFRAKHTE, M., MOREN, A., NAKAYAMA, T., CHRISTIAN, J. L., HEUCHEL, R., et al. 1997. Identification of Smad7, a TGFbeta-inducible antagonist of TGF-beta signalling. *Nature*, 389, 631-5.
- NAN, Y., HAN, L., ZHANG, A., WANG, G., JIA, Z., YANG, Y., et al. 2010. MiRNA-451 plays a role as tumor suppressor in human glioma cells. *Brain Res*, 1359, 14-21.
- NAPH 2013. National Audit of Pulmonary Hypertension 2013. Fourth annual report: key findings from the National Audit of Pulmonary Hypertension for the United Kingdom, Channel Islands, Gibraltar and Isle of Man. Report for the audit period April 2012 to March 2013. Available: <http://www.hscic.gov.uk/catalogue/PUB13318/nati-pulm-hype-audi-2013-rep.pdf>.
- NASIM, M. T., OGO, T., CHOWDHURY, H. M., ZHAO, L., CHEN, C. N., RHODES, C., et al. 2012. BMPR-II deficiency elicits pro-proliferative and anti-apoptotic responses through the activation of TGFbeta-TAK1-MAPK pathways in PAH. *Hum Mol Genet*, 21, 2548-58.
- NEWMAN, J. H., TREMBATH, R. C., MORSE, J. A., GRUNIG, E., LOYD, J. E., ADNOT, S., et al. 2004. Genetic basis of pulmonary arterial hypertension: current understanding and future directions. *J Am Coll Cardiol*, 43, 33S-39S.
- NEWMAN, J. H., WHEELER, L., LANE, K. B., LOYD, E., GADDIPATI, R., PHILLIPS, J. A., 3RD, et al. 2001. Mutation in the gene for bone morphogenetic protein receptor II as a cause of primary pulmonary hypertension in a large kindred. *N Engl J Med*, 345, 319-24.
- NISHIHARA, A., WATABE, T., IMAMURA, T. & MIYAZONO, K. 2002. Functional heterogeneity of bone morphogenetic protein receptor-II mutants found in patients with primary pulmonary hypertension. *Mol Biol Cell*, 13, 3055-63.
- NONNE, N., AMEYAR-ZAZOUA, M., SOUIDI, M. & HAREL-BELLAN, A. 2010. Tandem affinity purification of miRNA target mRNAs (TAP-Tar). *Nucleic Acids Res*, 38, e20.

- OHTA-OGO, K., HAO, H., ISHIBASHI-UEDA, H., HIROTA, S., NAKAMURA, K., OHE, T., et al. 2012. CD44 expression in plexiform lesions of idiopathic pulmonary arterial hypertension. *Pathol Int*, 62, 219-25.
- OROM, U. A. & LUND, A. H. 2007. Isolation of microRNA targets using biotinylated synthetic microRNAs. *Methods*, 43, 162-5.
- OROM, U. A., NIELSEN, F. C. & LUND, A. H. 2008. MicroRNA-10a binds the 5'UTR of ribosomal protein mRNAs and enhances their translation. *Mol Cell*, 30, 460-71.
- OWEN, N. E. 1985. Prostacyclin can inhibit DNA synthesis in vascular smooth muscle cells. *Prostaglandins, leukotrienes, and lipoxins*. Springer.
- OWENS, G. K., KUMAR, M. S. & WAMHOFF, B. R. 2004. Molecular regulation of vascular smooth muscle cell differentiation in development and disease. *Physiol Rev*, 84, 767-801.
- PARIKH, V. N., JIN, R. C., RABELLO, S., GULBAHCE, N., WHITE, K., HALE, A., et al. 2012. MicroRNA-21 integrates pathogenic signaling to control pulmonary hypertension: results of a network bioinformatics approach. *Circulation*, 125, 1520-32.
- PARKER, A. L., WHITE, K. M., LAVERY, C. A., CUSTERS, J., WADDINGTON, S. N. & BAKER, A. H. 2013. Pseudotyping the adenovirus serotype 5 capsid with both the fibre and penton of serotype 35 enhances vascular smooth muscle cell transduction. *Gene Ther*.
- PATRICK, D. M., MONTGOMERY, R. L., QI, X., OBAD, S., KAUPPINEN, S., HILL, J. A., et al. 2010a. Stress-dependent cardiac remodeling occurs in the absence of microRNA-21 in mice. *J Clin Invest*, 120, 3912-6.
- PATRICK, D. M., ZHANG, C. C., TAO, Y., YAO, H., QI, X., SCHWARTZ, R. J., et al. 2010b. Defective erythroid differentiation in miR-451 mutant mice mediated by 14-3-3zeta. *Genes Dev*, 24, 1614-9.
- PAULIN, R., COURBOULIN, A., MELOCHE, J., MAINGUY, V., DUMAS DE LA ROQUE, E., SAKSOUK, N., et al. 2011a. Signal transducers and activators of transcription-3/pim1 axis plays a critical role in the pathogenesis of human pulmonary arterial hypertension. *Circulation*, 123, 1205-15.
- PAULIN, R., MELOCHE, J., JACOB, M. H., BISSERIER, M., COURBOULIN, A. & BONNET, S. 2011b. Dehydroepiandrosterone inhibits the Src/STAT3 constitutive activation in pulmonary arterial hypertension. *Am J Physiol Heart Circ Physiol*, 301, H1798-809.
- PEÑALOZA, D., SIME, F., BANCHERO, N., GAMBOA, R., CRUZ, J. & MARTICORENA, E. 1963. Pulmonary hypertension in healthy men born and living at high altitudes. *The American Journal of Cardiology*, 11, 150-157.

- PERROS, F., DORFMULLER, P., MONTANI, D., HAMMAD, H., WAELPUT, W., GIRERD, B., et al. 2012. Pulmonary lymphoid neogenesis in idiopathic pulmonary arterial hypertension. *Am J Respir Crit Care Med*, 185, 311-21.
- PERROS, F., MONTANI, D., DORFMULLER, P., DURAND-GASSELIN, I., TCHERAKIAN, C., LE PAVEC, J., et al. 2008. Platelet-derived growth factor expression and function in idiopathic pulmonary arterial hypertension. *Am J Respir Crit Care Med*, 178, 81-8.
- PIAO, L., FANG, Y. H., CADETE, V. J., WIETHOLT, C., URBONIENE, D., TOTH, P. T., et al. 2010. The inhibition of pyruvate dehydrogenase kinase improves impaired cardiac function and electrical remodeling in two models of right ventricular hypertrophy: resuscitating the hibernating right ventricle. *J Mol Med (Berl)*, 88, 47-60.
- PIETRA, G. G., CAPRON, F., STEWART, S., LEONE, O., HUMBERT, M., ROBBINS, I. M., et al. 2004. Pathologic assessment of vasculopathies in pulmonary hypertension. *J Am Coll Cardiol*, 43, 25S-32S.
- PILLAI, R. S., ARTUS, C. G. & FILIPOWICZ, W. 2004. Tethering of human Ago proteins to mRNA mimics the miRNA-mediated repression of protein synthesis. *RNA*, 10, 1518-25.
- PITTMAN, R. N. 2011. *Regulation of Tissue Oxygenation*, Morgan & Claypool Life Sciences, San Rafael (CA).
- PLATOSHYN, O., GOLOVINA, V. A., BAILEY, C. L., LIMSUWAN, A., KRICK, S., JUHASZOVA, M., et al. 2000. Sustained membrane depolarization and pulmonary artery smooth muscle cell proliferation. *Am J Physiol Cell Physiol*, 279, C1540-9.
- PLATOSHYN, O., YU, Y., GOLOVINA, V. A., MCDANIEL, S. S., KRICK, S., LI, L., et al. 2001. Chronic hypoxia decreases K(V) channel expression and function in pulmonary artery myocytes. *Am J Physiol Lung Cell Mol Physiol*, 280, L801-12.
- POLACH, K. J., MATAR, M., RICE, J., SLOBODKIN, G., SPARKS, J., CONGO, R., et al. 2012. Delivery of siRNA to the mouse lung via a functionalized lipopolyamine. *Mol Ther*, 20, 91-100.
- POLLOCK, D. M., KEITH, T. L. & HIGHSMITH, R. F. 1995. Endothelin receptors and calcium signaling. *FASEB J*, 9, 1196-204.
- POST, J. M., HUME, J. R., ARCHER, S. L. & WEIR, E. K. 1992. Direct role for potassium channel inhibition in hypoxic pulmonary vasoconstriction. *Am J Physiol*, 262, C882-90.

- PULIDO, T., ADZERIKHO, I., CHANNICK, R. N., DELCROIX, M., GALIE, N., GHOFRANI, H. A., et al. 2013. Macitentan and morbidity and mortality in pulmonary arterial hypertension. *N Engl J Med*, 369, 809-18.
- PULLAMSETTI, S. S., DOEBELE, C., FISCHER, A., SAVAI, R., KOJONAZAROV, B., DAHAL, B. K., et al. 2012. Inhibition of microRNA-17 improves lung and heart function in experimental pulmonary hypertension. *Am J Respir Crit Care Med*, 185, 409-19.
- RABINOVITCH, M. 2007. Pathobiology of pulmonary hypertension. *Annu Rev Pathol*, 2, 369-99.
- RABINOVITCH, M. 2012. Molecular pathogenesis of pulmonary arterial hypertension. *J Clin Invest*, 122, 4306-13.
- RABINOVITCH, M., GAMBLE, W., NADAS, A. S., MIETTINEN, O. S. & REID, L. 1979. Rat pulmonary circulation after chronic hypoxia: hemodynamic and structural features. *Am J Physiol*, 236, H818-27.
- RAJEWSKY, N. 2006. microRNA target predictions in animals. *Nat Genet*, 38 Suppl, S8-13.
- RANGREZ, A. Y., MASSY, Z. A., METZINGER-LE MEUTH, V. & METZINGER, L. 2011. miR-143 and miR-145: molecular keys to switch the phenotype of vascular smooth muscle cells. *Circ Cardiovasc Genet*, 4, 197-205.
- RASMUSSEN, K. D., SIMMINI, S., ABREU-GOODGER, C., BARTONICEK, N., DI GIACOMO, M., BILBAO-CORTES, D., et al. 2010. The miR-144/451 locus is required for erythroid homeostasis. *J Exp Med*, 207, 1351-8.
- REID, M., LAME, M., MORIN, D., WILSON, D. & SEGALL, H. 1998. Involvement of cytochrome P450 3A in the metabolism and covalent binding of 14C-monocrotaline in rat liver microsomes. *Journal of biochemical and molecular toxicology*, 12, 157-166.
- RHOADES, M. W., REINHART, B. J., LIM, L. P., BURGE, C. B., BARTEL, B. & BARTEL, D. P. 2002. Prediction of plant microRNA targets. *Cell*, 110, 513-20.
- RHODES, C. J., WHARTON, J., BOON, R. A., ROEXE, T., TSANG, H., WOJCIAK-STOTHARD, B., et al. 2013. Reduced microRNA-150 is associated with poor survival in pulmonary arterial hypertension. *Am J Respir Crit Care Med*, 187, 294-302.
- RICH, S., DANTZKER, D. R., AYRES, S. M., BERGOFSKY, E. H., BRUNDAGE, B. H., DETRE, K. M., et al. 1987. Primary pulmonary hypertension. A national prospective study. *Ann Intern Med*, 107, 216-23.

- ROBERTS, J. D. & FORFIA, P. R. 2011. Diagnosis and assessment of pulmonary vascular disease by Doppler echocardiography. *Pulm Circ*, 1, 160-81.
- ROTH, R., DOTZLAF, L., BARANYI, B., KUO, C.-H. & HOOK, J. 1981. Effect of monocrotaline ingestion on liver, kidney, and lung of rats. *Toxicology and applied pharmacology*, 60, 193-203.
- RUBIN, L. J. 2004. Diagnosis and management of pulmonary arterial hypertension: ACCP evidence-based clinical practice guidelines. *Chest*, 126, 7S-10S.
- RUBIN, L. J., BADESCH, D. B., BARST, R. J., GALIE, N., BLACK, C. M., KEOGH, A., et al. 2002. Bosentan therapy for pulmonary arterial hypertension. *N Engl J Med*, 346, 896-903.
- RYAN, J., TIVNAN, A., FAY, J., BRYAN, K., MEEHAN, M., CREEVEY, L., et al. 2012a. MicroRNA-204 increases sensitivity of neuroblastoma cells to cisplatin and is associated with a favourable clinical outcome. *Br J Cancer*, 107, 967-76.
- RYAN, J. J., THENAPPAN, T., LUO, N., HA, T., PATEL, A. R., RICH, S., et al. 2012b. The WHO classification of pulmonary hypertension: A case-based imaging compendium. *Pulm Circ*, 2, 107-21.
- SACCONI, A., BIAGIONI, F., CANU, V., MORI, F., DI BENEDETTO, A., LORENZON, L., et al. 2012. miR-204 targets Bcl-2 expression and enhances responsiveness of gastric cancer. *Cell Death Dis*, 3, e423.
- SAKAMOTO, S., AOKI, K., HIGUCHI, T., TODAKA, H., MORISAWA, K., TAMAKI, N., et al. 2009. The NF90-NF45 complex functions as a negative regulator in the microRNA processing pathway. *Mol Cell Biol*, 29, 3754-69.
- SAKAO, S., TARASEVICIENE-STEWART, L., LEE, J. D., WOOD, K., COOL, C. D. & VOELKEL, N. F. 2005. Initial apoptosis is followed by increased proliferation of apoptosis-resistant endothelial cells. *FASEB J*, 19, 1178-80.
- SAKURAI, T., YANAGISAWA, M., TAKUWA, Y., MIYAZAKI, H., KIMURA, S., GOTO, K., et al. 1990. Cloning of a cDNA encoding a non-isopeptide-selective subtype of the endothelin receptor. *Nature*, 348, 732-5.
- SANCHEZ, L. S., DE LA MONTE, S. M., FILIPPOV, G., JONES, R. C., ZAPOL, W. M. & BLOCH, K. D. 1998. Cyclic-GMP-binding, cyclic-GMP-specific phosphodiesterase (PDE5) gene expression is regulated during rat pulmonary development. *Pediatr Res*, 43, 163-8.
- SARKAR, J., GOU, D., TURAKA, P., VIKTOROVA, E., RAMCHANDRAN, R. & RAJ, J. U. 2010. MicroRNA-21 plays a role in hypoxia-mediated pulmonary artery smooth muscle cell proliferation and migration. *Am J Physiol Lung Cell Mol Physiol*, 299, L861-71.

- SAVAI, R., PULLAMSETTI, S. S., KOLBE, J., BIENIEK, E., VOSWINCKEL, R., FINK, L., et al. 2012. Immune and inflammatory cell involvement in the pathology of idiopathic pulmonary arterial hypertension. *Am J Respir Crit Care Med*, 186, 897-908.
- SAVALE, L., TU, L., RIDEAU, D., IZZIKI, M., MAITRE, B., ADNOT, S., et al. 2009. Impact of interleukin-6 on hypoxia-induced pulmonary hypertension and lung inflammation in mice. *Respir Res*, 10, 6.
- SAYED, D. & ABDELLATIF, M. 2011. MicroRNAs in development and disease. *Physiol Rev*, 91, 827-87.
- SCHELLER, J., CHALARIS, A., SCHMIDT-ARRAS, D. & ROSE-JOHN, S. 2011. The pro- and anti-inflammatory properties of the cytokine interleukin-6. *Biochim Biophys Acta*, 1813, 878-88.
- SCHERMULY, R. T., DONY, E., GHOFRANI, H. A., PULLAMSETTI, S., SAVAI, R., ROTH, M., et al. 2005. Reversal of experimental pulmonary hypertension by PDGF inhibition. *J Clin Invest*, 115, 2811-21.
- SCHERMULY, R. T., KREISSELMEIER, K. P., GHOFRANI, H. A., YILMAZ, H., BUTROUS, G., ERMERT, L., et al. 2004. Chronic sildenafil treatment inhibits monocrotaline-induced pulmonary hypertension in rats. *Am J Respir Crit Care Med*, 169, 39-45.
- SEFERIAN, A. & SIMONNEAU, G. 2013. Therapies for pulmonary arterial hypertension: where are we today, where do we go tomorrow? *Eur Respir Rev*, 22, 217-26.
- SELBACH, M., SCHWANHAUSSER, B., THIERFELDER, N., FANG, Z., KHANIN, R. & RAJEWSKY, N. 2008. Widespread changes in protein synthesis induced by microRNAs. *Nature*, 455, 58-63.
- SEO, B., OEMAR, B. S., SIEBENMANN, R., VON SEGESSER, L. & LUSCHER, T. F. 1994. Both ETA and ETB receptors mediate contraction to endothelin-1 in human blood vessels. *Circulation*, 89, 1203-8.
- SESHIAH, P. N., WEBER, D. S., ROCIC, P., VALPPU, L., TANIYAMA, Y. & GRIENGLING, K. K. 2002. Angiotensin II stimulation of NAD(P)H oxidase activity: upstream mediators. *Circ Res*, 91, 406-13.
- SHARMA, S., TAEGTMEYER, H., ADROGUE, J., RAZEGHI, P., SEN, S., NGUMBELA, K., et al. 2004. Dynamic changes of gene expression in hypoxia-induced right ventricular hypertrophy. *Am J Physiol Heart Circ Physiol*, 286, H1185-92.
- SHI-WEN, X., CHEN, Y., DENTON, C. P., EASTWOOD, M., RENZONI, E. A., BOUGHARIOS, G., et al. 2004. Endothelin-1 promotes myofibroblast induction through the ETA receptor via a rac/phosphoinositide 3-kinase/Akt-

dependent pathway and is essential for the enhanced contractile phenotype of fibrotic fibroblasts. *Mol Biol Cell*, 15, 2707-19.

- SHI, W., CHEN, H., SUN, J., CHEN, C., ZHAO, J., WANG, Y. L., et al. 2004. Overexpression of Smurf1 negatively regulates mouse embryonic lung branching morphogenesis by specifically reducing Smad1 and Smad5 proteins. *Am J Physiol Lung Cell Mol Physiol*, 286, L293-300.
- SHI, Y., PATEL, S., NICULESCU, R., CHUNG, W., DESROCHERS, P. & ZALEWSKI, A. 1999. Role of matrix metalloproteinases and their tissue inhibitors in the regulation of coronary cell migration. *Arterioscler Thromb Vasc Biol*, 19, 1150-5.
- SHIMADA, K., TAKAHASHI, M. & TANZAWA, K. 1994. Cloning and functional expression of endothelin-converting enzyme from rat endothelial cells. *J Biol Chem*, 269, 18275-8.
- SIMONNEAU, G., BARST, R. J., GALIE, N., NAEIJE, R., RICH, S., BOURGE, R. C., et al. 2002. Continuous subcutaneous infusion of treprostinil, a prostacyclin analogue, in patients with pulmonary arterial hypertension: a double-blind, randomized, placebo-controlled trial. *Am J Respir Crit Care Med*, 165, 800-4.
- SIMONNEAU, G., GATZOULIS, M. A., ADATIA, I., CELERMAJER, D., DENTON, C., GHOFRANI, A., et al. 2013. Updated clinical classification of pulmonary hypertension. *J Am Coll Cardiol*, 62, D34-41.
- SIMONNEAU, G., ROBBINS, I. M., BEGHETTI, M., CHANNICK, R. N., DELCROIX, M., DENTON, C. P., et al. 2009. Updated clinical classification of pulmonary hypertension. *J Am Coll Cardiol*, 54, S43-54.
- SITBON, O., HUMBERT, M., NUNES, H., PARENT, F., GARCIA, G., HERVE, P., et al. 2002. Long-term intravenous epoprostenol infusion in primary pulmonary hypertension: prognostic factors and survival. *J Am Coll Cardiol*, 40, 780-8.
- SKLEPKIEWICZ, P., SCHERMULY, R. T., TIAN, X., GHOFRANI, H. A., WEISSMANN, N., SEDDING, D., et al. 2011. Glycogen synthase kinase 3beta contributes to proliferation of arterial smooth muscle cells in pulmonary hypertension. *Plos One*, 6, e18883.
- SKOG, J., WURDINGER, T., VAN RIJN, S., MEIJER, D. H., GAINCHE, L., SENA-ESTEVEZ, M., et al. 2008. Glioblastoma microvesicles transport RNA and proteins that promote tumour growth and provide diagnostic biomarkers. *Nat Cell Biol*, 10, 1470-6.
- SMALL, E. M., FROST, R. J. & OLSON, E. N. 2010. MicroRNAs add a new dimension to cardiovascular disease. *Circulation*, 121, 1022-32.

- SOIFER, H. S., ROSSI, J. J. & SAETROM, P. 2007. MicroRNAs in disease and potential therapeutic applications. *Mol Ther*, 15, 2070-9.
- SOMLYO, A. P. & SOMLYO, A. V. 1994. Smooth muscle: excitation-contraction coupling, contractile regulation, and the cross-bridge cycle. *Alcohol Clin Exp Res*, 18, 138-43.
- SONG, J. J., SMITH, S. K., HANNON, G. J. & JOSHUA-TOR, L. 2004. Crystal structure of Argonaute and its implications for RISC slicer activity. *Science*, 305, 1434-7.
- SONG, Y., JONES, J. E., BEPPU, H., KEANEY, J. F., JR., LOSCALZO, J. & ZHANG, Y. Y. 2005. Increased susceptibility to pulmonary hypertension in heterozygous BMPR2-mutant mice. *Circulation*, 112, 553-62.
- STEINER, M. K., SYRKINA, O. L., KOLLIPUTI, N., MARK, E. J., HALES, C. A. & WAXMAN, A. B. 2009. Interleukin-6 overexpression induces pulmonary hypertension. *Circ Res*, 104, 236-44, 28p following 244.
- STENMARK, K. R., DAVIE, N., FRID, M., GERASIMOVSKAYA, E. & DAS, M. 2006a. Role of the adventitia in pulmonary vascular remodeling. *Physiology (Bethesda)*, 21, 134-45.
- STENMARK, K. R., FAGAN, K. A. & FRID, M. G. 2006b. Hypoxia-induced pulmonary vascular remodeling: cellular and molecular mechanisms. *Circ Res*, 99, 675-91.
- STENMARK, K. R., FASULES, J., HYDE, D. M., VOELKEL, N. F., HENSON, J., TUCKER, A., et al. 1987. Severe pulmonary hypertension and arterial adventitial changes in newborn calves at 4,300 m. *Journal of Applied Physiology*, 62, 821-830.
- STENMARK, K. R., GERASIMOVSKAYA, E., NEMENOFF, R. A. & DAS, M. 2002. Hypoxic activation of adventitial fibroblasts: role in vascular remodeling. *Chest*, 122, 326S-334S.
- STENMARK, K. R., MEYRICK, B., GALIE, N., MOOI, W. J. & MCMURTRY, I. F. 2009. Animal models of pulmonary arterial hypertension: the hope for etiological discovery and pharmacological cure. *Am J Physiol Lung Cell Mol Physiol*, 297, L1013-32.
- STEWART, D. J., LEVY, R. D., CERNACEK, P. & LANGLEBEN, D. 1991. Increased plasma endothelin-1 in pulmonary hypertension: marker or mediator of disease? *Ann Intern Med*, 114, 464-9.
- SUN, F., WANG, J., PAN, Q., YU, Y., ZHANG, Y., WAN, Y., et al. 2009. Characterization of function and regulation of miR-24-1 and miR-31. *Biochem Biophys Res Commun*, 380, 660-5.

- SZTRYMF, B., GUNTHER, S., ARTAUD-MACARI, E., SAVALE, L., JAIS, X., SITBON, O., et al. 2013. Left ventricular ejection time in acute heart failure complicating precapillary pulmonary hypertension. *Chest*, 144, 1512-20.
- TAGANOV, K. D., BOLDIN, M. P., CHANG, K. J. & BALTIMORE, D. 2006. NF-kappaB-dependent induction of microRNA miR-146, an inhibitor targeted to signaling proteins of innate immune responses. *Proc Natl Acad Sci U S A*, 103, 12481-6.
- TAKAHASHI, H., GOTO, N., KOJIMA, Y., TSUDA, Y., MORIO, Y., MURAMATSU, M., et al. 2006. Downregulation of type II bone morphogenetic protein receptor in hypoxic pulmonary hypertension. *Am J Physiol Lung Cell Mol Physiol*, 290, L450-8.
- TANZER, A. & STADLER, P. F. 2004. Molecular evolution of a microRNA cluster. *J Mol Biol*, 339, 327-35.
- TARASEVICIENE-STEWART, L., KASAHARA, Y., ALGER, L., HIRTH, P., MC MAHON, G., WALTENBERGER, J., et al. 2001. Inhibition of the VEGF receptor 2 combined with chronic hypoxia causes cell death-dependent pulmonary endothelial cell proliferation and severe pulmonary hypertension. *FASEB J*, 15, 427-38.
- TEICHERT-KULISZEWSKA, K., KUTRYK, M. J., KULISZEWSKI, M. A., KAROUBI, G., COURTMAN, D. W., ZUCCO, L., et al. 2006. Bone morphogenetic protein receptor-2 signaling promotes pulmonary arterial endothelial cell survival: implications for loss-of-function mutations in the pathogenesis of pulmonary hypertension. *Circ Res*, 98, 209-17.
- THOMAS, M., LIEBERMAN, J. & LAL, A. 2010. Desperately seeking microRNA targets. *Nat Struct Mol Biol*, 17, 1169-74.
- THOMPSON, K. & RABINOVITCH, M. 1996. Exogenous leukocyte and endogenous elastases can mediate mitogenic activity in pulmonary artery smooth muscle cells by release of extracellular-matrix bound basic fibroblast growth factor. *J Cell Physiol*, 166, 495-505.
- THOMSON, D. W., BRACKEN, C. P. & GOODALL, G. J. 2011. Experimental strategies for microRNA target identification. *Nucleic Acids Res*, 39, 6845-53.
- THOMSON, J. R., MACHADO, R. D., PAUCIUOLO, M. W., MORGAN, N. V., HUMBERT, M., ELLIOTT, G. C., et al. 2000. Sporadic primary pulmonary hypertension is associated with germline mutations of the gene encoding BMPR-II, a receptor member of the TGF-beta family. *J Med Genet*, 37, 741-5.
- THUM, T., GALUPPO, P., WOLF, C., FIEDLER, J., KNEITZ, S., VAN LAAKE, L. W., et al. 2007. MicroRNAs in the human heart: a clue to fetal gene reprogramming in heart failure. *Circulation*, 116, 258-67.

- THUM, T., GROSS, C., FIEDLER, J., FISCHER, T., KISSLER, S., BUSSEN, M., et al. 2008. MicroRNA-21 contributes to myocardial disease by stimulating MAP kinase signalling in fibroblasts. *Nature*, 456, 980-4.
- TIJSEN, A. J., CREEMERS, E. E., MOERLAND, P. D., DE WINDT, L. J., VAN DER WAL, A. C., KOK, W. E., et al. 2010. MiR423-5p as a circulating biomarker for heart failure. *Circ Res*, 106, 1035-9.
- TODOROVICH-HUNTER, L., JOHNSON, D., RANGER, P., KEELEY, F. & RABINOVITCH, M. 1988. Altered elastin and collagen synthesis associated with progressive pulmonary hypertension induced by monocrotaline. A biochemical and ultrastructural study. *Laboratory investigation; a journal of technical methods and pathology*, 58, 184.
- TOFOVIC, S. P. 2010. Estrogens and development of pulmonary hypertension: interaction of estradiol metabolism and pulmonary vascular disease. *J Cardiovasc Pharmacol*, 56, 696-708.
- TRABUCCHI, M., BRIATA, P., GARCIA-MAYORAL, M., HAASE, A. D., FILIPOWICZ, W., RAMOS, A., et al. 2009. The RNA-binding protein KSRP promotes the biogenesis of a subset of microRNAs. *Nature*, 459, 1010-4.
- TU, L., DEWACHTER, L., GORE, B., FADEL, E., DARTEVELLE, P., SIMONNEAU, G., et al. 2011. Autocrine fibroblast growth factor-2 signaling contributes to altered endothelial phenotype in pulmonary hypertension. *Am J Respir Cell Mol Biol*, 45, 311-22.
- TUDER, R. M., COOL, C. D., GERACI, M. W., WANG, J., ABMAN, S. H., WRIGHT, L., et al. 1999. Prostacyclin synthase expression is decreased in lungs from patients with severe pulmonary hypertension. *Am J Respir Crit Care Med*, 159, 1925-32.
- TUDER, R. M., GROVES, B., BADESCH, D. B. & VOELKEL, N. F. 1994. Exuberant endothelial cell growth and elements of inflammation are present in plexiform lesions of pulmonary hypertension. *Am J Pathol*, 144, 275-85.
- TURCZYNSKA, K. M., BHATTACHARIYA, A., SALL, J., GORANSSON, O., SWARD, K., HELLSTRAND, P., et al. 2013. Stretch-sensitive down-regulation of the miR-144/451 cluster in vascular smooth muscle and its role in AMP-activated protein kinase signaling. *Plos One*, 8, e65135.
- URBICH, C., KALUZA, D., FROMEL, T., KNAU, A., BENNEWITZ, K., BOON, R. A., et al. 2012. MicroRNA-27a/b controls endothelial cell repulsion and angiogenesis by targeting semaphorin 6A. *Blood*, 119, 1607-16.
- VALADI, H., EKSTROM, K., BOSSIOS, A., SJOSTRAND, M., LEE, J. J. & LOTVALL, J. O. 2007. Exosome-mediated transfer of mRNAs and microRNAs is a novel mechanism of genetic exchange between cells. *Nat Cell Biol*, 9, 654-9.

- VAN ROOIJ, E., MARSHALL, W. S. & OLSON, E. N. 2008. Toward microRNA-based therapeutics for heart disease: the sense in antisense. *Circ Res*, 103, 919-28.
- VAN ROOIJ, E. & OLSON, E. N. 2007. MicroRNAs: powerful new regulators of heart disease and provocative therapeutic targets. *J Clin Invest*, 117, 2369-76.
- VAN ROOIJ, E. & OLSON, E. N. 2012. MicroRNA therapeutics for cardiovascular disease: opportunities and obstacles. *Nat Rev Drug Discov*, 11, 860-72.
- VAN ROOIJ, E., QUIAT, D., JOHNSON, B. A., SUTHERLAND, L. B., QI, X., RICHARDSON, J. A., et al. 2009. A family of microRNAs encoded by myosin genes governs myosin expression and muscle performance. *Dev Cell*, 17, 662-73.
- VAN ROOIJ, E., SUTHERLAND, L. B., LIU, N., WILLIAMS, A. H., MCANALLY, J., GERARD, R. D., et al. 2006. A signature pattern of stress-responsive microRNAs that can evoke cardiac hypertrophy and heart failure. *Proc Natl Acad Sci U S A*, 103, 18255-60.
- VAN ROOIJ, E., SUTHERLAND, L. B., QI, X., RICHARDSON, J. A., HILL, J. & OLSON, E. N. 2007. Control of stress-dependent cardiac growth and gene expression by a microRNA. *Science*, 316, 575-9.
- VICKERS, K. C., PALMISANO, B. T., SHOUCRI, B. M., SHAMBUREK, R. D. & REMALEY, A. T. 2011. MicroRNAs are transported in plasma and delivered to recipient cells by high-density lipoproteins. *Nat Cell Biol*, 13, 423-33.
- VOELKEL, N. F., GOMEZ-ARROYO, J., ABBATE, A., BOGAARD, H. J. & NICOLLS, M. R. 2012. Pathobiology of pulmonary arterial hypertension and right ventricular failure. *Eur Respir J*, 40, 1555-65.
- VOELKEL, N. F. & TUDER, R. M. 2000. Hypoxia-induced pulmonary vascular remodeling: a model for what human disease? *J Clin Invest*, 106, 733-8.
- VOLK, N. & SHOMRON, N. 2011. Versatility of MicroRNA biogenesis. *Plos One*, 6, e19391.
- VON SEGGERN, D. J., KEHLER, J., ENDO, R. I. & NEMEROW, G. R. 1998. Complementation of a fibre mutant adenovirus by packaging cell lines stably expressing the adenovirus type 5 fibre protein. *J Gen Virol*, 79 (Pt 6), 1461-8.
- WALKER, A. M., LANGLEBEN, D., KORELITZ, J. J., RICH, S., RUBIN, L. J., STROM, B. L., et al. 2006. Temporal trends and drug exposures in pulmonary hypertension: an American experience. *Am Heart J*, 152, 521-6.

- WANG, G. K., ZHU, J. Q., ZHANG, J. T., LI, Q., LI, Y., HE, J., et al. 2010. Circulating microRNA: a novel potential biomarker for early diagnosis of acute myocardial infarction in humans. *Eur Heart J*, 31, 659-66.
- WANG, J., SONG, Y., ZHANG, Y., XIAO, H., SUN, Q., HOU, N., et al. 2012a. Cardiomyocyte overexpression of miR-27b induces cardiac hypertrophy and dysfunction in mice. *Cell Res*, 22, 516-27.
- WANG, J., WEIGAND, L., FOXSON, J., SHIMODA, L. A. & SYLVESTER, J. T. 2007. Ca²⁺ signaling in hypoxic pulmonary vasoconstriction: effects of myosin light chain and Rho kinase antagonists. *Am J Physiol Lung Cell Mol Physiol*, 293, L674-85.
- WANG, K., ZHANG, S., MARZOLF, B., TROISCH, P., BRIGHTMAN, A., HU, Z., et al. 2009. Circulating microRNAs, potential biomarkers for drug-induced liver injury. *Proc Natl Acad Sci U S A*, 106, 4402-7.
- WANG, R., WANG, Z. X., YANG, J. S., PAN, X., DE, W. & CHEN, L. B. 2011. MicroRNA-451 functions as a tumor suppressor in human non-small cell lung cancer by targeting ras-related protein 14 (RAB14). *Oncogene*, 30, 2644-58.
- WANG, X., ZHU, H., ZHANG, X., LIU, Y., CHEN, J., MEDVEDOVIC, M., et al. 2012b. Loss of the miR-144/451 cluster impairs ischaemic preconditioning-mediated cardioprotection by targeting Rac-1. *Cardiovasc Res*, 94, 379-90.
- WEST, J., FAGAN, K., STEUDEL, W., FOUTY, B., LANE, K., HARRAL, J., et al. 2004. Pulmonary hypertension in transgenic mice expressing a dominant-negative BMPRII gene in smooth muscle. *Circ Res*, 94, 1109-14.
- WEST, J., HARRAL, J., LANE, K., DENG, Y., ICKES, B., CRONA, D., et al. 2008. Mice expressing BMPRII^{R899X} transgene in smooth muscle develop pulmonary vascular lesions. *Am J Physiol Lung Cell Mol Physiol*, 295, L744-55.
- WHARTON, J., STRANGE, J. W., MOLLER, G. M., GROWCOTT, E. J., REN, X., FRANKLYN, A. P., et al. 2005. Antiproliferative effects of phosphodiesterase type 5 inhibition in human pulmonary artery cells. *Am J Respir Crit Care Med*, 172, 105-13.
- WHITE, K., DEMPSIE, Y., NILSEN, M., WRIGHT, A. F., LOUGHLIN, L. & MACLEAN, M. R. 2011a. The serotonin transporter, gender, and 17beta oestradiol in the development of pulmonary arterial hypertension. *Cardiovasc Res*, 90, 373-82.
- WHITE, K., JOHANSEN, A. K., NILSEN, M., CIUCLAN, L., WALLACE, E., PATON, L., et al. 2012. Activity of the estrogen-metabolizing enzyme cytochrome P450 1B1 influences the development of pulmonary arterial hypertension. *Circulation*, 126, 1087-98.

- WHITE, K., LOUGHLIN, L., MAQBOOL, Z., NILSEN, M., MCCLURE, J., DEMPSIE, Y., et al. 2011b. Serotonin transporter, sex, and hypoxia: microarray analysis in the pulmonary arteries of mice identifies genes with relevance to human PAH. *Physiol Genomics*, 43, 417-37.
- WILLIAMS, A. E., MOSCHOS, S. A., PERRY, M. M., BARNES, P. J. & LINDSAY, M. A. 2007. Maternally imprinted microRNAs are differentially expressed during mouse and human lung development. *Dev Dyn*, 236, 572-80.
- WILSON, D. W., SEGALL, H. J., PAN, L. C. & DUNSTON, S. K. 1989. Progressive inflammatory and structural changes in the pulmonary vasculature of monocrotaline-treated rats. *Microvasc Res*, 38, 57-80.
- WOJCIAK-STOTHARD, B., ZHAO, L., OLIVER, E., DUBOIS, O., WU, Y., KARDASSIS, D., et al. 2012. Role of RhoB in the regulation of pulmonary endothelial and smooth muscle cell responses to hypoxia. *Circ Res*, 110, 1423-34.
- WOODS, K., THOMSON, J. M. & HAMMOND, S. M. 2007. Direct regulation of an oncogenic micro-RNA cluster by E2F transcription factors. *J Biol Chem*, 282, 2130-4.
- WRANA, J. L., ATTISANO, L., WIESER, R., VENTURA, F. & MASSAGUE, J. 1994. Mechanism of activation of the TGF- β receptor. *Nature*, 370, 341-347.
- XIN, M., SMALL, E. M., SUTHERLAND, L. B., QI, X., MCANALLY, J., PLATO, C. F., et al. 2009. MicroRNAs miR-143 and miR-145 modulate cytoskeletal dynamics and responsiveness of smooth muscle cells to injury. *Genes Dev*, 23, 2166-78.
- XU, J., GONG, N. L., BODI, I., ARONOW, B. J., BACKX, P. H. & MOLKENTIN, J. D. 2006. Myocyte enhancer factors 2A and 2C induce dilated cardiomyopathy in transgenic mice. *J Biol Chem*, 281, 9152-62.
- YAMAGATA, K., FUJIYAMA, S., ITO, S., UEDA, T., MURATA, T., NAITOU, M., et al. 2009. Maturation of microRNA is hormonally regulated by a nuclear receptor. *Mol Cell*, 36, 340-7.
- YAN, L. X., HUANG, X. F., SHAO, Q., HUANG, M. Y., DENG, L., WU, Q. L., et al. 2008. MicroRNA miR-21 overexpression in human breast cancer is associated with advanced clinical stage, lymph node metastasis and patient poor prognosis. *RNA*, 14, 2348-60.
- YANAGISAWA, M., KURIHARA, H., KIMURA, S., TOMOBE, Y., KOBAYASHI, M., MITSUI, Y., et al. 1988. A novel potent vasoconstrictor peptide produced by vascular endothelial cells. *Nature*, 332, 411-5.
- YANG, J. S., MAURIN, T., ROBINE, N., RASMUSSEN, K. D., JEFFREY, K. L., CHANDWANI, R., et al. 2010. Conserved vertebrate mir-451 provides a

- platform for Dicer-independent, Ago2-mediated microRNA biogenesis. *Proc Natl Acad Sci U S A*, 107, 15163-8.
- YANG, S., BANERJEE, S., FREITAS, A., CUI, H., XIE, N., ABRAHAM, E., et al. 2012. miR-21 regulates chronic hypoxia-induced pulmonary vascular remodeling. *Am J Physiol Lung Cell Mol Physiol*, 302, L521-9.
- YANG, X., LONG, L., SOUTHWOOD, M., RUDARAKANCHANA, N., UPTON, P. D., JEFFERY, T. K., et al. 2005. Dysfunctional Smad signaling contributes to abnormal smooth muscle cell proliferation in familial pulmonary arterial hypertension. *Circ Res*, 96, 1053-63.
- YEN, R. T. & SOBIN, S. S. 1988. Elasticity of arterioles and venules in postmortem human lungs. *J Appl Physiol (1985)*, 64, 611-9.
- YI, R., QIN, Y., MACARA, I. G. & CULLEN, B. R. 2003. Exportin-5 mediates the nuclear export of pre-microRNAs and short hairpin RNAs. *Genes Dev*, 17, 3011-6.
- YU, D., DOS SANTOS, C. O., ZHAO, G., JIANG, J., AMIGO, J. D., KHANDROS, E., et al. 2010. miR-451 protects against erythroid oxidant stress by repressing 14-3-3zeta. *Genes Dev*, 24, 1620-33.
- YU, Y., SWEENEY, M., ZHANG, S., PLATOSHYN, O., LANDSBERG, J., ROTHMAN, A., et al. 2003. PDGF stimulates pulmonary vascular smooth muscle cell proliferation by upregulating TRPC6 expression. *Am J Physiol Cell Physiol*, 284, C316-30.
- YUAN, J. X. & RUBIN, L. J. 2005. Pathogenesis of pulmonary arterial hypertension: the need for multiple hits. *Circulation*, 111, 534-8.
- YUAN, X. J., WANG, J., JUHASZOVA, M., GAINE, S. P. & RUBIN, L. J. 1998. Attenuated K⁺ channel gene transcription in primary pulmonary hypertension. *Lancet*, 351, 726-7.
- YUE, D., LIU, H. & HUANG, Y. 2009. Survey of Computational Algorithms for MicroRNA Target Prediction. *Curr Genomics*, 10, 478-92.
- ZAMPETAKI, A., KIECHL, S., DROZDOV, I., WILLEIT, P., MAYR, U., PROKOPI, M., et al. 2010. Plasma microRNA profiling reveals loss of endothelial miR-126 and other microRNAs in type 2 diabetes. *Circ Res*, 107, 810-7.
- ZAMPETAKI, A. & MAYR, M. 2012. Analytical challenges and technical limitations in assessing circulating miRNAs. *Thromb Haemost*, 108, 592-8.
- ZERNECKE, A., BIDZHEKOV, K., NOELS, H., SHAGDARSUREN, E., GAN, L., DENECKE, B., et al. 2009. Delivery of microRNA-126 by apoptotic bodies induces CXCL12-dependent vascular protection. *Sci Signal*, 2, ra81.

- ZHAN, M., MILLER, C. P., PAPAYANNOPOULOU, T., STAMATOYANNOPOULOS, G. & SONG, C. Z. 2007. MicroRNA expression dynamics during murine and human erythroid differentiation. *Exp Hematol*, 35, 1015-25.
- ZHANG, B., SHEN, M., XU, M., LIU, L. L., LUO, Y., XU, D. Q., et al. 2012. Role of macrophage migration inhibitory factor in the proliferation of smooth muscle cell in pulmonary hypertension. *Mediators Inflamm*, 2012, 840737.
- ZHANG, S., FANTOZZI, I., TIGNO, D. D., YI, E. S., PLATOSHYN, O., THISTLETHWAITE, P. A., et al. 2003. Bone morphogenetic proteins induce apoptosis in human pulmonary vascular smooth muscle cells. *Am J Physiol Lung Cell Mol Physiol*, 285, L740-54.
- ZHANG, X., WANG, X., ZHU, H., ZHU, C., WANG, Y., PU, W. T., et al. 2010. Synergistic effects of the GATA-4-mediated miR-144/451 cluster in protection against simulated ischemia/reperfusion-induced cardiomyocyte death. *J Mol Cell Cardiol*, 49, 841-50.
- ZHAO, L., MASON, N. A., MORRELL, N. W., KOJONAZAROV, B., SADYKOV, A., MARIPOV, A., et al. 2001. Sildenafil inhibits hypoxia-induced pulmonary hypertension. *Circulation*, 104, 424-8.
- ZHOU, Q., GALLAGHER, R., UFRET-VINCENY, R., LI, X., OLSON, E. N. & WANG, S. 2011. Regulation of angiogenesis and choroidal neovascularization by members of microRNA-23-27-24 clusters. *Proc Natl Acad Sci U S A*, 108, 8287-92.
- ZHU, H., KAVSAK, P., ABDOLLAH, S., WRANA, J. L. & THOMSEN, G. H. 1999. A SMAD ubiquitin ligase targets the BMP pathway and affects embryonic pattern formation. *Nature*, 400, 687-93.
- ZINCARELLI, C., SOLTYS, S., RENGO, G. & RABINOWITZ, J. E. 2008. Analysis of AAV serotypes 1-9 mediated gene expression and tropism in mice after systemic injection. *Mol Ther*, 16, 1073-80.

Appendices

Appendix 1

J.S. Grant, K. White, M.R. MacLean & A.H. Baker (2013). MicroRNAs in pulmonary arterial remodelling. *Cell Mol Life Sci*, **70**, 4479-94.

Appendix 2

J.S. Grant, I. Morecroft, Y. Dempsie, E. van Rooij, M.R. MacLean & A.H. Baker. Transient but not genetic loss of miR-451 is protective in the development of pulmonary arterial hypertension. *Pulm Circ*, accepted for publication November 2013.